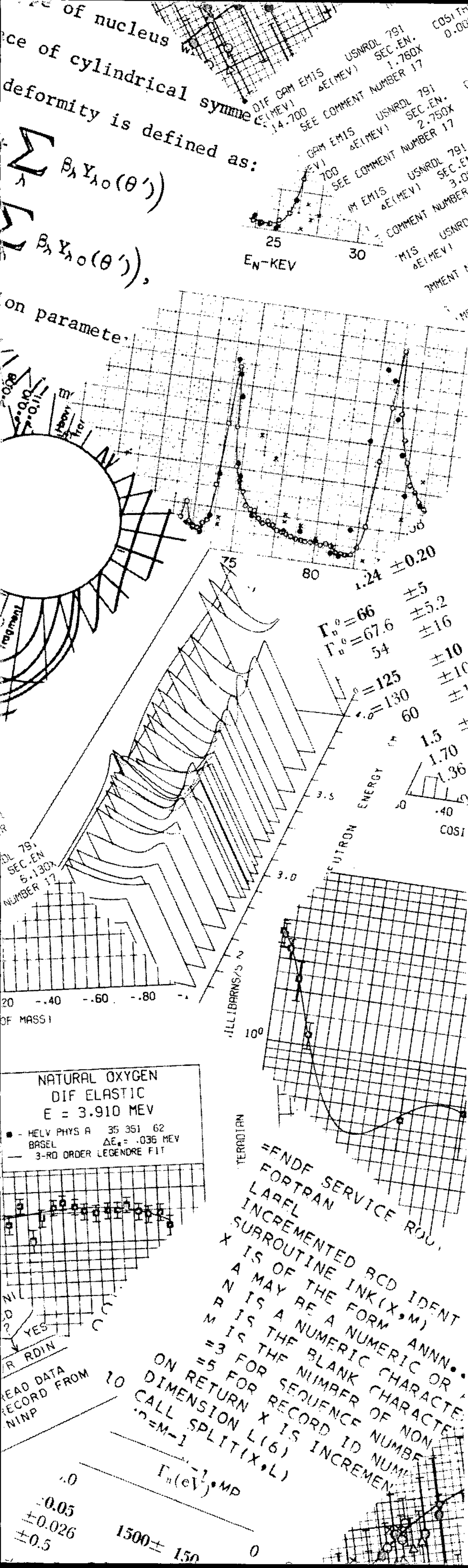

BNL-NCS-27800
DOE/NDC-19/U
NEANDC(US)-207/U
INDC(USA)-83/U
Informal Report
Limited Distribution

REPORTS TO THE DOE NUCLEAR DATA COMMITTEE

Compiled by
NATIONAL NUCLEAR DATA CENTER
for the
U.S. Department of Energy
Nuclear Data Committee

May 1980

BROOKHAVEN NATIONAL LABORATORY
ASSOCIATED UNIVERSITIES, INC.
UPTON, NEW YORK 11973

national nuclear data center

BNL-NCS-27800
DOE/NDC-19/U

REPORTS TO THE DOE NUCLEAR DATA COMMITTEE

May 1980

Compiled by
NATIONAL NUCLEAR DATA CENTER
for the
U.S. Department of Energy
Nuclear Data Committee

NATIONAL NUCLEAR DATA CENTER

BROOKHAVEN NATIONAL LABORATORY

ASSOCIATED UNIVERSITIES, INC.

UNDER CONTRACT NO. DE-AC02-76CH00016 WITH THE

UNITED STATES DEPARTMENT OF ENERGY

The material contained in this report is in the form submitted by the various contributors.

PREFACE

The reports in this document were submitted to the Department of Energy, Nuclear Data Committee (DOE-NDC) in May, 1980. The reporting laboratories are those having a substantial effort in measuring neutron and nuclear cross sections of relevance to the U.S. applied nuclear energy program.

The authors of the Status Report contributions are responsible for collecting and editing individual contributions from their laboratory and are not necessarily the sole authors of the contributions. The scientists responsible for the work described in each individual contribution are listed at the beginning of the contribution.

The material contained in these reports is to be regarded as comprised of informal statements of recent developments and preliminary data. Persons wishing to make use of these data should contact the individual experimenter for further details. The data which appear in this document should be quoted only by permission of the contributor and should be referenced as private communication, and not by this document number. Appropriate subjects are listed as follows:

1. Microscopic neutron cross sections relevant to the nuclear energy program, including shielding. Inverse reactions where pertinent are included.

2. Charged-particle cross sections, where they are relevent to "1" above, and where relevant to developing and testing nuclear models.

3. Gamma-ray production, radioactive decay, and theoretical developments in nuclear structure which are applicable to nuclear energy programs.

4. Proton and alpha-particle cross sections, at energies of up to 1 GeV, which are of interest to the space program.

These reports cannot be regarded as a complete summary of the nuclear research efforts in the U.S. A number of laboratories, whose research is less programmatically oriented do not submit reports; neither do the submitted reports reflect all the work related to nuclear data in progress at the submitting laboratory.

This compilation has been produced almost completely from master copies prepared by the individual contributors listed in the Table of Contents.

The CINDA-type index and CPND-type index, which follow the Table of Contents, were prepared by Gail Wyant and Thomas Burrows, respectively, of the National Nuclear Data Center, Brookhaven National Laboratory, Upton, New York.

TABLE OF CONTENTS

TABLE OF CONTENTS (cont.)

Element S	A	Quantity	Energy (eV) Min	Max	Type	Documentation Ref	Vol	Page	Date	Lab	Comments
H	001	TOTAL XSECT	6.0+4	8.0+7	Expt	DOE-NDC-19		83	580	LRL	Phillips+LINAC.NDG.TBP PL/B.
H	001	TOTAL XSECT	2.0+6	8.0+7	Expt	DOE-NDC-19		131	580	ORL	Larson+TRNS.CFD OPTMDL CS.NDG.TBP.
H	001	TOTAL XSECT	2.0+6	8.0+7	Expt	DOE-NDC-19		130	580	ORL	Larson+TRNS.SEVERAL THICKNESSES.NDG.
H	002	TOTAL XSECT	6.0+4	8.0+7	Expt	DOE-NDC-19		83	580	LRL	Phillips+LINAC.NDG.SEE UCRL-77783.
H	002	DIFF ELASTIC	9.0+6	1.1+7	Exth	DOE-NDC-19		151	580	OHO	Kulkarni+DIFF MEAS.TH CALC TBD.NDG.
H	002	N,GAMMA	Maxw		Expt	DOE-NDC-19		70	580	LAS	Bendt+MEAS RESOLVES DISCREP.NDG.
H	002	N2N REACTION	1.1+7	2.5+7	Exth	DOE-NDC-19		151	580	OHO	Kulkarni+DIFF MEAS.TH CALC TBD.NDG.
H	002	GAMMA,N	NDG		Expt	DOE-NDC-19		83	580	LRL	Berman+(G,N),(G,2N) CS MEAS.NDG.
H	003	TOTAL XSECT	1.0-2	1.1+1	Theo	DOE-NDC-19		72	580	LAS	Hale+CHG INDEP R-MATRIX ANAL.CFD.NDG
H	003	TOTAL XSECT	6.0+4	8.0+7	Expt	DOE-NDC-19		83	580	LRL	Phillips+GRPH.CFD OTH.0 E CS CALC.
H	003	TOTAL XSECT	5.0+4	1.0+8	Expt	DOE-NDC-19		69	580	LRL	Seagrave.CFD R-MATRIX.NDG.TBP PR/C.
H	003	ELASTIC SCAT	NDG		Expt	DOE-NDC-19		69	580	LRL	Seagrave.ZERO E CS,SCT LENGTHS.TBP
H	003	GAMMA,N	NDG		Expt	DOE-NDC-19		102	580	LRL	Berman.ATLAS TBP IN ND/A.
H	003	GAMMA,N	7.0+6	2.5+7	Expt	DOE-NDC-19		83	580	LRL	Berman+(G,N),(G,2N) CS MEAS.NDG.
HE	003	ELASTIC SCAT	NDG		Theo	DOE-NDC-19		72	580	LAS	Hale+CHG INDEP R-MATRIX ANAL.CFD.NDG
HE	003	GAMMA,N	NDG		Expt	DOE-NDC-19		102	580	LRL	Berman.ATLAS TBP IN ND/A.
HE	004	GAMMA,N	NDG		Expt	DOE-NDC-19		102	580	LRL	Berman.ATLAS TBP IN ND/A.
LI	006	TOTAL XSECT	5.0+5	4.8+6	Expt	DOE-NDC-19		1	580	ANL	Guenther+NDG.TBP ANL-NDM-52.
LI	006	ELASTIC SCAT	7.0+6	1.4+7	Expt	DOE-NDC-19		163	580	TNL	Beyerle+TOF.CFD ENDF.NDG.SEE NSE 69.
LI	006	DIFF ELASTIC	1.5+6	4.0+6	Expt	DOE-NDC-19		1	580	ANL	Guenther+NDG.TBP ANL-NDM-52.
LI	006	DIFF ELASTIC	6.0+6	1.4+7	Expt	DOE-NDC-19		70	580	LAS	Drake+3ES.E,ANGDISTS.GRPHS.TBP.
LI	006	DIFF ELASTIC	2.3+6	4.1+6	Expt	DOE-NDC-19		145	580	OHO	Knox+5 ES.ANAL COMPLETE.CFD OTH.NDG
LI	006	DIFF ELASTIC	7.0+6	1.4+7	Expt	DOE-NDC-19		163	580	TNL	Beyerle+TOF.CFD ENDF.NDG.SEE NSE 69.
LI	006	DIFF ELASTIC		4.0+6	Expt	DOE-NDC-19		178	580	YAL	Chiu+GLOBAL ANAL REFINED.TBP NP/A.
LI	006	DIFF INELAST	3.5+6	4.0+6	Expt	DOE-NDC-19		1	580	ANL	Guenther+NDG.TBP ANL-NDM-52.
LI	006	DIFF INELAST	6.0+6	1.4+7	Expt	DOE-NDC-19		70	580	LAS	Drake+3ES.E,ANGDISTS.GRPHS.TBP.
LI	006	DIFF INELAST	NDG		Expt	DOE-NDC-19		145	580	OHO	Knox+ANAL TBC.NDG.

Element S	A	Quantity	Energy (eV) Min	Max	Type	Documentation Ref	Vol	Page	Date	Lab	Comments
LI	006	DIFF INELAST	7.0+6	1.4+7	Expt	DOE-NDC-19		163	580	TNL	Beyerle+TOF.CFD ENDF.NDG.SEE NSE 69.
LI	006	DIFF INELAST		4.0+6	Expt	DOE-NDC-19		178	580	YAL	Chiu+GLOBAL ANAL REFINED.TBP NP/A.
LI	006	N,TRITON	1.0+0	1.0+3	Expt	DOE-NDC-19		115	580	NBS	Czirr+B10(N,A)/LIG(N,T).GRPHS.CFD.
LI	007	ELASTIC SCAT	7.0+6	1.4+7	Expt	DOE-NDC-19		163	580	TNL	Beyerle+TOF.CFD ENDF.NDG.SEE NSE 69.
LI	007	DIFF ELASTIC	6.0+6	1.4+7	Expt	DOE-NDC-19		70	580	LAS	Drake+3ES.E,ANGDISTS.GRPHS.TBP.
LI	007	DIFF ELASTIC	2.3+6	4.1+6	Expt	DOE-NDC-19		145	580	OHO	Knox+5 ES.ANAL COMPLETE.CFD OTH.NDG
LI	007	DIFF ELASTIC		8.0+6	Exth	DOE-NDC-19		150	580	OHO	Knox+ORMAP CODE.NDG.TBP.
LI	007	DIFF ELASTIC	7.0+6	1.4+7	Expt	DOE-NDC-19		163	580	TNL	Beyerle+TOF.CFD ENDF.NDG.SEE NSE 69.
LI	007	DIFF INELAST	6.0+6	1.4+7	Expt	DOE-NDC-19		70	580	LAS	Drake+3ES.E,ANGDISTS.GRPHS.TBP.
LI	007	DIFF INELAST	NDG		Expt	DOE-NDC-19		145	580	OHO	Knox+ANAL TBC.NDG.
LI	007	DIFF INELAST		8.0+6	Exth	DOE-NDC-19		150	580	OHO	Knox+ORMAP CODE.NDG.TBP.
LI	007	DIFF INELAST	7.0+6	1.4+7	Expt	DOE-NDC-19		163	580	TNL	Beyerle+TOF.CFD ENDF.NDG.SEE NSE 69.
LI	007	INELST GAMMA	4.8+5	5.0+6	Expt	DOE-NDC-19		129	580	ORL	Olsen+478KEV G PROD.CFD ENDF/4.NDG.
LI	007	N,N PROTON	1.4+7	1.5+7	Expt	DOE-NDC-19		87	580	LRL	Haight+ES,ANGDIST CHG PARTICLES.NDG
LI	007	N,DEUTERON	1.4+7	1.5+7	Expt	DOE-NDC-19		87	580	LRL	Haight+ES,ANGDIST CHG PARTICLES.NDG
LI	007	N,N TRITON	1.4+7	1.5+7	Expt	DOE-NDC-19		87	580	LRL	Haight+ES,ANGDIST CHG PARTICLES.NDG
B	010	DIFF ELASTIC	8.0+6	1.4+7	Expt	DOE-NDC-19		163	580	TNL	Beyerle+OPTMDL ANAL.TBLS.GRPHS.
B	010	N,ALPHA REAC	1.0+0	1.0+3	Expt	DOE-NDC-19		115	580	NBS	Czirr+B10(N,A)/LIG(N,T).GRPHS.CFD.
B	010	N,ALPHA REAC	5.0-1	1.0+3	Expt	DOE-NDC-19		117	580	NBS	Carlson+GRPH.CS FOR BF3 VS SOLID B10
B	011	DIFF ELASTIC	4.8+6	7.6+6	Expt	DOE-NDC-19		145	580	OHO	Koehler+7ES.ANGDISTS.ANAL TBD.NDG.
B	011	DIFF ELASTIC	2.6+6	8.0+6	Exth	DOE-NDC-19		150	580	OHO	Knox+ORMAP CODE.NDG.TBP NP/A.
B	011	DIFF ELASTIC	8.0+6	1.4+7	Expt	DOE-NDC-19		163	580	TNL	Beyerle+OPTMDL ANAL.TBLS.GRPHS.
B	011	DIFF INELAST	2.6+6	8.0+6	Exth	DOE-NDC-19		150	580	OHO	Knox+ORMAP CODE.NDG.TBP NP/A.
B	011	DIFF INELAST	4.8+6	7.6+6	Expt	DOE-NDC-19		145	580	OHO	Koehler+7ES.ANGDISTS.ANAL TBD.NDG.
B	CMP	N,ALPHA REAC	5.0-1	1.0+3	Expt	DOE-NDC-19		117	580	NBS	Carlson+GRPH.CS FOR BF3 VS SOLID B10
C	012	TOTAL XSECT	2.0+6	8.0+7	Expt	DOE-NDC-19		131	580	ORL	Larson+TRNS.CFD OPTMDL CS.NDG.TBP.
C	012	TOTAL XSECT	2.0+6	8.0+7	Expt	DOE-NDC-19		130	580	ORL	Larson+TRNS.SEVERAL THICKNESSES.NDG.

Element S	A	Quantity	Energy (eV) Min	Max	Type	Documentation Ref	Vol	Page	Date	Lab	Comments
C	012	N,GAMMA	Maxw		Expt	DOE-NDC-19		70	580	LAS	Bendt+CS MEAS.NDG
C	012	N,PROTON	1.4+7	1.5+7	Expt	DOE-NDC-19		87	580	LRL	Haight+ES,ANGDIST CHG PARTICLES.NDG
C	012	N,DEUTERON	1.4+7	1.5+7	Expt	DOE-NDC-19		87	580	LRL	Haight+ES,ANGDIST CHG PARTICLES.NDG
C	012	N,ALPHA REAC	1.4+7	1.5+7	Expt	DOE-NDC-19		87	580	LRL	Haight+ES,ANGDIST CHG PARTICLES.NDG
C	013	DIFF ELASTIC	1.3+6	6.0+6	Expt	DOE-NDC-19		150	580	OHO	Lane+9 ANGS.R-MATRIX ANAL.NDG.TBP.
C	013	DIFF ELASTIC	5.7+6	8.3+6	Expt	DOE-NDC-19		145	580	OHO	Koehler+6ES.ANGDISTS.ANAL TBD.NDG.
C	013	DIFF INELAST	5.7+6	8.3+6	Expt	DOE-NDC-19		145	580	OHO	Koehler+6ES.ANGDISTS.ANAL TBD.NDG.
C	013	GAMMA,N	6.5+6	9.3+6	Expt	DOE-NDC-19		13	580	ANL	Aolt+ANGDIST 2 ANGS.R-MATRIX.NDG.
C	013	GAMMA,N	NDG		Expt	DOE-NDC-19		85	580	LRL	Berman+LINAC.(G,N),(G,2N).NDG.
N	014	SPECT N,GAMM		1.0+3	Expt	DOE-NDC-19		51	580	INL	Greenwood+G RAY ES.TBL.
O	016	ELASTIC SCAT	9.2+6	1.4+7	Expt	DOE-NDC-19		167	580	TNL	Beyerle+OPTMDL ANAL.TBLS.GRPHS.
O	016	DIFF ELASTIC	2.4+7		Expt	DOE-NDC-19		146	580	OHO	Grabmayr+TOF.LANE MDL ANAL.NDG.TBP.
O	016	DIFF ELASTIC	9.2+6	1.4+7	Expt	DOE-NDC-19		167	580	TNL	Beyerle+OPTMDL ANAL.TBLS.GRPHS.
O	016	DIFF INELAST	2.4+7		Expt	DOE-NDC-19		146	580	OHO	Grabmayr+TOF.LANE MDL ANAL.NDG.TBP.
O	017	GAMMA,N	8.0+6	4.0+7	Expt	DOE-NDC-19		85	580	LRL	Berman+LINAC.(G,N),(G,2N).NDG.
O	017	GAMMA,N	NDG		Expt	DOE-NDC-19		102	580	LRL	Berman.ATLAS TBP IN ND/A.
O	018	DIFF ELASTIC	2.4+7		Expt	DOE-NDC-19		146	580	OHO	Grabmayr+TOF.LANE MDL ANAL.NDG.TBP.
O	018	DIFF INELAST	2.4+7		Expt	DOE-NDC-19		146	580	OHO	Grabmayr+TOF.LANE MDL ANAL.NDG.TBP.
F	019	N,PROTON	1.4+7	1.5+7	Expt	DOE-NDC-19		87	580	LRL	Haight+ES,ANGDIST CHG PARTICLES.NDG
F	019	N,DEUTERON	1.4+7	1.5+7	Expt	DOE-NDC-19		87	580	LRL	Haight+ES,ANGDIST CHG PARTICLES.NDG
F	019	N,ALPHA REAC	1.4+7	1.5+7	Expt	DOE-NDC-19		87	580	LRL	Haight+ES,ANGDIST CHG PARTICLES.NDG
NE		N,GAMMA	NDG		Expt	DOE-NDC-19		129	580	ORL	Macklin+MEAS COMPLETED.NDG.
NA	023	SPECT N,GAMM		1.0+3	Expt	DOE-NDC-19		51	580	INL	Greenwood+G RAY ES.NDG.
MG	024	POLARIZATION	5.0+4	5.0+5	Expt	DOE-NDC-19		178	580	YAL	Kruk+MEAS STARTED.TBC.NDG
AL	027	TOTAL XSECT	2.0+6	8.0+7	Expt	DOE-NDC-19		131	580	ORL	Larson+TRNS.CFD OPTMDL CS.NDG.TBP.
AL	027	TOTAL XSECT	2.0+6	8.0+7	Expt	DOE-NDC-19		130	580	ORL	Larson+TRNS.SEVERAL THICKNESSES.NDG.
SI		TOTAL XSECT	2.0+6	8.0+7	Expt	DOE-NDC-19		131	580	ORL	Larson+TRNS.CFD OPTMDL CS.NDG.TBP.

Element S	A	Quantity	Energy (eV) Min	Max	Type	Documentation Ref	Vol	Page	Date	Lab	Comments
SI		TOTAL XSECT	2.0+6	8.0+7	Expt	DOE-NDC-19		130	580	ORL	Larson+TRNS.SEVERAL THICKNESSES.NDG.
SI	028	POLARIZATION	5.0+4	5.0+5	Expt	DOE-NDC-19		178	580	YAL	Kruk+MEAS STARTED.TBC.NDG
S		TOTAL XSECT	2.5+3	1.1+6	Expt	DOE-NDC-19		130	580	ORL	Johnson+ANAL FOR SINGLE-LVL PARS.NDG
S		RESON PARAM	2.5+3	1.1+6	Expt	DOE-NDC-19		130	580	ORL	Johnson+TOT.SINGLE-LVL PAR ANAL.NDG
S		STRNGTH FUNC	0.0+0	1.1+6	Expt	DOE-NDC-19		130	580	ORL	Johnson+TOT.SINGLE-LVL PAR ANAL.NDG
S	032	POLARIZATION	5.0+4	5.0+5	Expt	DOE-NDC-19		178	580	YAL	Kruk+MEAS STARTED.TBC.NDG
S	032	ABSORPTION	2.5-2		Expt	DOE-NDC-19		58	580	INL	Smith. EFFECT UPON CF-252 NU.
AR		N,GAMMA	NDG		Expt	DOE-NDC-19		129	580	ORL	Macklin+MEAS COMPLETED.NDG.
K		SPECT N,GAMM	2.0+3		Expt	DOE-NDC-19		28	580	BNL	Engler+TOF.THR E ALSO.ANAL TBP.NDG.
K	039	SPECT N,GAMM	2.0+3		Expt	DOE-NDC-19		28	580	BNL	Engler+TOF.THR E ALSO.ANAL TBP.NDG.
CA		TOTAL XSECT	2.0+6	8.0+7	Expt	DOE-NDC-19		131	580	ORL	Larson+TRNS.CFD OPTMDL CS.NDG.TBP.
CA		TOTAL XSECT	2.0+6	8.0+7	Expt	DOE-NDC-19		130	580	ORL	Larson+TRNS.SEVERAL THICKNESSES.NDG.
SC	045	SPECT N,GAMM	2.5-2		Expt	DOE-NDC-19		28	580	BNL	Liou+POL NS.GRPHS.TBP NP/A.
SC	045	SPECT N,GAMM	4.6+2	4.3+3	Expt	DOE-NDC-19		28	580	BNL	Liou+4 RES.PRIMARY.SECONDARY.NDG.TBP
CR		TOTAL XSECT	1.5+6	4.0+6	Expt	DOE-NDC-19		1	580	ANL	Guenther+BROAD RESOL.CFD EVAL.NDG
CR		TOTAL XSECT	2.0+6	8.0+7	Expt	DOE-NDC-19		131	580	ORL	Larson+TRNS.CFD OPTMDL CS.NDG.TBP.
CR		TOTAL XSECT	2.0+6	8.0+7	Expt	DOE-NDC-19		130	580	ORL	Larson+TRNS.SEVERAL THICKNESSES.NDG.
CR		DIFF ELASTIC	1.5+6	4.0+6	Expt	DOE-NDC-19		1	580	ANL	Guenther+BROAD RESOL.CFD EVAL.GRPH.
CR		DIFF INELAST	1.5+6	4.0+6	Expt	DOE-NDC-19		1	580	ANL	Guenther+BROAD RESOL.CFD EVAL.GRPH.
CR		SPECT N,GAMM	NDG		Expt	DOE-NDC-19		28	580	BNL	Kopecky+TOF.CR 52 STUDY.NDG
CR	052	SPECT N,GAMM	1.6+3		Expt	DOE-NDC-19		28	580	BNL	Kopecky+TOF.26 G-RAYS OBS.NDG
CR	052	N,PROTON	5.3+6	9.0+6	Exth	DOE-NDC-19		7	580	ANL	Smith+GRPH.EXCIT FN CALC TO 20MEV.
CR	052	RESON PARAM	1.6+3		Expt	DOE-NDC-19		28	580	BNL	Kopecky+TOF.SPIN,PI FOR 1626 EV RES.
FE		TOTAL XSECT	2.0+6	8.0+7	Expt	DOE-NDC-19		131	580	ORL	Larson+TRNS.CFD OPTMDL CS.NDG.TBP.
FE		TOTAL XSECT	2.0+6	8.0+7	Expt	DOE-NDC-19		130	580	ORL	Larson+TRNS.SEVERAL THICKNESSES.NDG.
FE		DIFF INELAST	7.5+6	1.2+7	Expt	DOE-NDC-19		170	580	TNL	Beyerle+3 ES.TOF.5 ANGS.DBL DIF.GRPH
FE	054	EVALUATION	3.0+6	4.0+7	Eval	DOE-NDC-19		77	580	LAS	Arthur+HF,PRE-EQUIL,H-F.NDG.

Element S	A	Quantity	Energy (eV) Min	Max	Type	Documentation Ref	Vol	Page	Date	Lab	Comments
FE	054	DIFF ELASTIC	8.0+6	1.2+7	Expt	DOE-NDC-19		175	580	TNL	Beyerle+ANGDISTS.OPTMDL ANAL.GRPHS.
FE	056	EVALUATION	3.0+6	4.0+7	Eval	DOE-NDC-19		77	580	LAS	Arthur+HF,PRE-EQUIL,H-F.GRPHS.
FE	056	DIFF ELASTIC	8.0+6	1.2+7	Expt	DOE-NDC-19		175	580	TNL	Beyerle+ANGDISTS.OPTMDL ANAL.GRPHS.
NI		TOTAL XSECT	1.0+6	5.0+6	Expt	DOE-NDC-19		1	580	ANL	Guenther+E AVG CS CFD.NDG.TBC.
NI		TOTAL XSECT	2.0+6	8.0+7	Expt	DOE-NDC-19		131	580	ORL	Larson+TRNS.CFD OPTMDL CS.NDG.TBP.
NI		TOTAL XSECT	2.0+6	8.0+7	Expt	DOE-NDC-19		130	580	ORL	Larson+TRNS.SEVERAL THICKNESSES.NDG.
NI		DIFF ELASTIC	1.0+6	5.0+6	Expt	DOE-NDC-19		1	580	ANL	Guenther+NDG.TBC.
NI		DIFF INELAST	1.0+6	5.0+6	Expt	DOE-NDC-19		1	580	ANL	Guenther+NDG.TBC.
NI		DIFF INELAST	7.5+6	1.2+7	Expt	DOE-NDC-19		170	580	TNL	Beyerle+3 ES.TOF.5 ANGS.DBL DIF.GRPH
NI	058	TOTAL XSECT	1.0+6	5.0+6	Expt	DOE-NDC-19		1	580	ANL	Guenther+NDG.TBC.
NI	058	DIFF ELASTIC	1.0+6	5.0+6	Expt	DOE-NDC-19		1	580	ANL	Guenther+NDG.TBC.
NI	058	DIFF ELASTIC	1.1+7	2.4+7	Expt	DOE-NDC-19		147	580	OHO	Yamanouti+TOF.2 ES.OPTMDL ANAL.NDG.
NI	058	DIFF INELAST	1.0+6	5.0+6	Expt	DOE-NDC-19		1	580	ANL	Guenther+NDG.TBC.
NI	058	DIFF INELAST	1.1+7	2.4+7	Expt	DOE-NDC-19		147	580	OHO	Yamanouti+TOF.2 ES.OPTMDL ANAL.NDG.
NI	058	N,PROTON	8.0+6	1.1+7	Expt	DOE-nDC-19		152	580	OHO	Randers-Pehrson+3ANGS,2ES.NDG
NI	060	DIFF ELASTIC	1.1+7	2.4+7	Expt	DOE-NDC-19		147	580	OHO	Yamanouti+TOF.2 ES.OPTMDL ANAL.NDG.
NI	060	DIFF INELAST	1.1+7	2.4+7	Expt	DOE-NDC-19		147	580	OHO	Yamanouti+TOF.2 ES.OPTMDL ANAL.NDG.
CU		TOTAL XSECT	1.5+6	4.0+6	Expt	DOE-NDC-19		2	580	ANL	Guenther+50KEV INTERVAL.NDG.ANAL TBD
CU		TOTAL XSECT	2.0+6	8.0+7	Expt	DOE-NDC-19		131	580	ORL	Larson+TRNS.CFD OPTMDL CS.NDG.TBP.
CU		TOTAL XSECT	2.0+6	8.0+7	Expt	DOE-NDC-19		130	580	ORL	Larson+TRNS.SEVERAL THICKNESSES.NDG.
CU		DIFF ELASTIC	1.5+6	4.0+6	Expt	DOE-NDC-19		2	580	ANL	Guenther+50KEV INTERVAL.NDG.ANAL TBD
CU		DIFF INELAST	1.5+6	4.0+6	Expt	DOE-NDC-19		2	580	ANL	Guenther+50KEV INTERVAL.NDG.ANAL TBD
CU		DIFF INELAST	7.5+6	1.2+7	Expt	DOE-NDC-19		170	580	TNL	Beyerle+3 ES.TOF.5 ANGS.DBL DIF.GRPH
CU	063	DIFF ELASTIC	8.0+6	1.2+7	Expt	DOE-NDC-19		175	580	TNL	Beyerle+ANGDISTS.OPTMDL ANAL.GRPHS.
CU	063	N,ALPHA REAC	3.0+6	1.0+7	Expt	DOE-NDC-19		7	580	ANL	Winkler+INTEGRAL/DIFF DISCREPANCY.
CU	065	DIFF ELASTIC	8.0+6	1.2+7	Expt	DOE-NDC-19		175	580	TNL	Beyerle+ANGDISTS.OPTMDL ANAL.GRPHS.
ZN	066	N,PROTON	4.2+6	1.0+7	Expt	DOE-NDC-19		3	580	ANL	Smith+ACT.NDG.SPEC AVG CS FOR U235.

Element S	A	Quantity	Energy (eV) Min	Max	Type	Documentation Ref	Vol	Page	Date	Lab	Comments
SE		SPECT N,GAMM	2.7+1	2.0+3	Expt	DOE-NDC-19		27	580	BNL	Engler+THR E ALSO.ISOTOPE G-RAYS.
SE	074	SPECT N,GAMM	2.7+1	2.7+2	Expt	DOE-NDC-19		27	580	BNL	Engler+THR E ALSO.PRIMARY G-RAYS GVN
SE	076	SPECT N,GAMM	3.8+2		Expt	DOE-NDC-19		27	580	BNL	Engler+THR E ALSO.PRIMARY G-RAYS GVN
SE	077	SPECT N,GAMM	1.1+2	3.4+2	Expt	DOE-NDC-19		27	580	BNL	Engler+THR E ALSO.PRIMARY G-RAYS GVN
SE	080	SPECT N,GAMM	2.0+3		Expt	DOE-NDC-19		27	580	BNL	Engler+THR E ALSO.PRIMARY G-RAYS GVN
KR	086	N,GAMMA	NDG		Expt	DOE-NDC-19		129	580	ORL	Macklin+MEAS COMPLETED.NDG.
RB		SPECT N,GAMM	2.0+3		Expt	DOE-NDC-19		28	580	BNL	Engler+TOF.THR E ALSO.ANAL TBP.NDG.
RB	085	SPECT N,GAMM	2.0+3		Expt	DOE-NDC-19		28	580	BNL	Engler+TOF.THR E ALSO.ANAL TBP.NDG.
RB	087	SPECT N,GAMM	2.0+3		Expt	DOE-NDC-19		28	580	BNL	Engler+TOF.THR E ALSO.ANAL TBP.NDG.
SR	087	SPECT N,GAMM	2.0+3	2.4+4	Expt	DOE-NDC-19		24	580	BNL	Stelts+CAPT SPEC.NDG.ANAL TBC.
SR	087	SPECT N,GAMM	Maxw		Expt	DOE-NDC-19		24	580	BNL	Stelts+CAPT SPEC.NDG.ANAL TBC.
SR	087	STRNGTH FUNC	NDG		Expt	DOE-NDC-19		24	580	BNL	Stelts+CAPT SPEC.NDG.ANAL TBC.
Y	088	N,PROTON	NDG		Expt	DOE-NDC-19		85	580	LRL	Grimes+INV.SR-88(P,N) GRPH,ANAL TBC
Y	089	TOTAL XSECT	5.0+4	4.5+6	Expt	DOE-NDC-19		3	580	ANL	Poenitz+FOR OPTMDL PARS.NDG.ANAL TBD
ZR		TOTAL XSECT	5.0+4	4.5+6	Expt	DOE-NDC-19		3	580	ANL	Poenitz+FOR OPTMDL PARS.NDG.ANAL TBD
ZR	090	N,PROTON	1.4+7	1.5+7	Expt	DOE-NDC-19		87	580	LRL	Haight+ES,ANGDIST CHG PARTICLES.NDG.
ZR	090	N,DEUTERON	1.4+7	1.5+7	Expt	DOE-NDC-19		87	580	LRL	Haight+ES,ANGDIST CHG PARTICLES.NDG.
ZR	090	N,ALPHA REAC	1.4+7	1.5+7	Expt	DOE-NDC-19		87	580	LRL	Haight+ES,ANGDIST CHG PARTICLES.NDG.
NB	093	TOTAL XSECT	5.0+4	4.5+6	Expt	DOE-NDC-19		3	580	ANL	Poenitz+FOR OPTMDL PARS.NDG.ANAL TBD
NB	093	N,GAMMA	Maxw		Theo	DOE-NDC-19		97	580	LRL	Gardner+GDR CALC OF SPEC CFD EXPT.
NB	093	SPECT N,GAMM	Maxw		Theo	DOE-NDC-19		97	580	LRL	Gardner+GDR CALC OF SPEC CFD EXPT.
MO		TOTAL XSECT	5.0+4	4.5+6	Expt	DOE-NDC-19		3	580	ANL	Poenitz+FOR OPTMDL PARS.NDG.ANAL TBD
MO	092	N,PROTON	1.4+7	1.5+7	Expt	DOE-NDC-19		87	580	LRL	Haight+ES,ANGDIST CHG PARTICLES.NDG.
MO	092	N,DEUTERON	1.4+7	1.5+7	Expt	DOE-NDC-19		87	580	LRL	Haight+ES,ANGDIST CHG PARTICLES.NDG.
MO	092	N,ALPHA REAC	1.4+7	1.5+7	Expt	DOE-NDC-19		87	580	LRL	Haight+ES,ANGDIST CHG PARTICLES.NDG.
MO	094	N,PROTON	1.4+7		Expt	DOE-NDC-19		87	580	LRL	Haight+90 DEG P SPEC GRPH.
MO	094	N,DEUTERON	1.4+7	1.5+7	Expt	DOE-NDC-19		87	580	LRL	Haight+ES,ANGDIST CHG PARTICLES.NDG.

Element S	A	Quantity	Energy (eV) Min	Max	Type	Documentation Ref	Vol	Page	Date	Lab	Comments
MO	094	N,ALPHA REAC	1.4+7	1.5+7	Expt	DOE-NDC-19		87	580	LRL	Haight+ES,ANGDIST CHG PARTICLES.NDG.
MO	095	N,PROTON	1.4+7	1.5+7	Expt	DOE-NDC-19		87	580	LRL	Haight+ES,ANGDIST CHG PARTICLES.NDG.
MO	095	N,DEUTERON	1.4+7	1.5+7	Expt	DOE-NDC-19		87	580	LRL	Haight+ES,ANGDIST CHG PARTICLES.NDG.
MO	095	N,ALPHA REAC	1.4+7	1.5+7	Expt	DOE-NDC-19		87	580	LRL	Haight+ES,ANGDIST CHG PARTICLES.NDG.
MO	096	N,PROTON	1.4+7	1.5+7	Expt	DOE-NDC-19		87	580	LRL	Haight+ES,ANGDIST CHG PARTICLES.NDG.
MO	096	N,DEUTERON	1.4+7	1.5+7	Expt	DOE-NDC-19		87	580	LRL	Haight+ES,ANGDIST CHG PARTICLES.NDG.
MO	096	N,ALPHA REAC	1.4+7	1.5+7	Expt	DOE-NDC-19		87	580	LRL	Haight+ES,ANGDIST CHG PARTICLES.NDG.
RU	100	N,GAMMA	2.6+3	5.9+5	Expt	DOE-NDC-19		129	580	ORL	Macklin+ORELA.NDG.TBP IN NSE.
RU	101	N,GAMMA	2.6+3	6.9+5	Expt	DOE-NDC-19		129	580	ORL	Macklin+ORELA.NDG.TBP IN NSE.
RU	102	N,GAMMA	2.6+3	5.9+5	Expt	DOE-NDC-19		129	580	ORL	Macklin+ORELA.NDG.TBP IN NSE.
RU	102	SPECT N,GAMM	NDG		Expt	DOE-NDC-19		30	580	BNL	Casten+AVG RES CAPT SPEC.NDG.
RU	104	N,GAMMA	2.6+3	6.9+5	Expt	DOE-NDC-19		129	580	ORL	Macklin+ORELA.NDG.TBP IN NSE.
RH	103	TOTAL XSECT	5.0+5	4.0+6	Expt	DOE-NDC-19		3	580	ANL	Poenitz+REL AU.GRPH.SEE 79 BOLOGNA.
RH	103	TOTAL XSECT	5.0+4	4.5+6	Expt	DOE-NDC-19		3	580	ANL	Poenitz+FOR OPTMDL PARS.NDG.ANAL TBD
PD		TOTAL XSECT	5.0+5	4.0+6	Expt	DOE-NDC-19		3	580	ANL	Poenitz+REL AU.GRPH.SEE 79 BOLOGNA.
PD		TOTAL XSECT	5.0+4	4.5+6	Expt	DOE-NDC-19		3	580	ANL	Poenitz+FOR OPTMDL PARS.NDG.ANAL TBD
PD	108	SPECT N,GAMM	NDG		Expt	DOE-NDC-19		30	580	BNL	Casten+AVG RES CAPT SPEC.NDG.
AG		TOTAL XSECT	5.0+4	4.5+6	Expt	DOE-NDC-19		3	580	ANL	Poenitz+FOR OPTMDL PARS.NDG.ANAL TBD
AG	107	RESON PARAM	1.6+3		Expt	DOE-NDC-19		22	580	BNL	Liou+EFFECTIVE TEMP,DEBYE TEMP.GRPHS
AG	107	RESON PARAM	1.6+3		Expt	DOE-NDC-19		22	580	BNL	Liou+EFFECTIVE TEMP,DEBYE TEMP.TBL.
AG	CMP	N,GAMMA	1.6+3		Expt	DOE-NDC-19		22	580	BNL	Liou+EFFECTIVE TEMP,DEBYE TEMP.GRPHS
AG	CMP	N,GAMMA	1.6+3		Expt	DOE-NDC-19		22	580	BNL	Liou+EFFECTIVE TEMP,DEBYE TEMP.TBL.
CD		TOTAL XSECT	5.0+4	4.5+6	Expt	DOE-NDC-19		3	580	ANL	Poenitz+FOR OPTMDL PARS.NDG.ANAL TBD
IN		TOTAL XSECT	5.0+4	4.5+6	Expt	DOE-NDC-19		3	580	ANL	Poenitz+FOR OPTMDL PARS.NDG.ANAL TBD
IN	115	N,GAMMA	NDG		Expt	DOE-NDC-19		110	580	MHG	Grady+NDG.EXPT TBD.
SN		TOTAL XSECT	5.0+4	4.5+6	Expt	DOE-NDC-19		3	580	ANL	Poenitz+FOR OPTMDL PARS.NDG.ANAL TBD
SN	112	N,GAMMA	2.4+4		Expt	DOE-NDC-19		17	580	BNL	Bradley+ACT.24 KEV CS GVN,30KEV DRVD

Element S	A	Quantity	Energy (eV) Min	Max	Type	Documentation Ref	Vol Page	Date	Lab	Comments
SB		TOTAL XSECT	5.0+4	4.5+6	Expt	DOE-NDC-19	3	580	ANL	Poenitz+FOR OPTMDL PARS.NDG.ANAL TBD
TE		TOTAL XSECT	5.0+4	4.5+6	Expt	DOE-NDC-19	3	580	ANL	Poenitz+FOR OPTMDL PARS.NDG.ANAL TBD
XE	131	SPECT N,GAMM	NDG		Expt	DOE-NDC-19	30	580	BNL	Casten+AVG RES CAPT SPEC.NDG.
BA	130	N,GAMMA	2.4+4		Expt	DOE-NDC-19	17	580	BNL	Bradley+ACT.24 KEV CS GVN,30KEV DRVD
BA	135	SPECT N,GAMM	NDG		Expt	DOE-NDC-19	30	580	BNL	Casten+AVG RES CAPT SPEC.NDG.
CE	140	TOTAL XSECT	2.5+6	6.0+7	Expt	DOE-NDC-19	39	580	LRL	Camarda+OPTMDL CALC TBD.NDG.
CE	142	TOTAL XSECT	2.5+6	6.0+7	Expt	DOE-NDC-19	39	580	LRL	Camarda+CE142/CE140 RATIO.NDG.
PR	141	TOTAL XSECT	2.5+6	6.0+7	Expt	DOE-NDC-19	39	580	LRL	Camarda+PR141/CE140 RATIO.NDG.
ND		TOTAL XSECT	5.0+5	4.0+6	Expt	DOE-NDC-19	3	580	ANL	Poenitz+REL AU.GRPH.SEE 79 BOLOGNA.
ND	146	N,GAMMA	2.4+4		Expt	DOE-NDC-19	17	580	BNL	Bradley+ACT.24 KEV CS GVN,30KEV DRVD
ND	148	N,GAMMA	2.4+4		Expt	DOE-NDC-19	17	580	BNL	Bradley+ACT.24 KEV CS GVN,30KEV DRVD
SM		TOTAL XSECT	5.0+5	4.0+6	Expt	DOE-NDC-19	3	580	ANL	Poenitz+REL AU.GRPH.SEE 79 BOLOGNA.
SM	151	SPECT N,GAMM	NDG		Expt	DOE-NDC-19	52	580	INL	Greenwood. NDG. ANAL TBC.
SM	154	SPECT N,GAMM	2.0+3	2.4+4	Expt	DOE-NDC-19	19	580	BNL	Stelts+51 DRVD FROM CAPT SPEC.NDG.
SM	154	STRNGTH FUNC	2.0+3	2.4+4	Expt	DOE-NDC-19	19	580	BNL	Stelts+51 DRVD FROM CAPT SPEC.
ER	167	SPECT N,GAMM	2.0+3	2.4+4	Expt	DOE-NDC-19	19	580	BNL	Stelts+51 DRVD FROM CAPT SPEC.NDG.
ER	167	SPECT N,GAMM	NDG		Expt	DOE-NDC-19	30	580	BNL	Casten+AVG RES CAPT SPEC.NDG.
ER	167	STRNGTH FUNC	2.0+3	2.4+4	Expt	DOE-NDC-19	19	580	BNL	Stelts+51 DRVD FROM CAPT SPEC.
TA	181	TOTAL XSECT	4.0+4	4.8+6	Expt	DOE-NDC-19	4	580	ANL	Poenitz+NDG.SEE 79 KNOX.TBP NSE.
TA	181	TOTAL XSECT	4.0+4	4.8+6	Expt	DOE-NDC-19	4	580	ANL	Poenitz+NDG.SEE 79 KNOX.TBP NSE.
W	182	TOTAL XSECT		1.0+6	Expt	DOE-NDC-19	4	580	ANL	Poenitz+RES SELF SHIELD EFFECT.NDG.
W	184	TOTAL XSECT		1.0+6	Expt	DOE-NDC-19	4	580	ANL	Poenitz+RES SELF SHIELD EFFECT.NDG.
W	186	TOTAL XSECT		1.0+6	Expt	DOE-NDC-19	4	580	ANL	Poenitz+RES SELF SHIELD EFFECT.NDG.
W	186	N,GAMMA	2.4+4		Expt	DOE-NDC-19	17	580	BNL	Bradley+ACT.24 KEV CS GVN,30KEV DRVD
OS	186	N,GAMMA	5.0-1	1.5+5	Expt	DOE-NDC-19	91	580	LRL	Berman+TOF.LINAC.5 PCT ACCR.NDG
OS	187	N,GAMMA	5.0-1	1.5+5	Expt	DOE-NDC-19	91	580	LRL	Berman+TOF.LINAC.5 PCT ACCR.NDG
OS	188	N,GAMMA	5.0-1	1.5+5	Expt	DOE-NDC-19	91	580	LRL	Berman+TOF.LINAC.5 PCT ACCR.NDG

Element S	A	Quantity	Energy (eV) Min	Max	Type	Documentation Ref	Vol	Page	Date	Lab	Comments
OS	189	N,GAMMA	5.0-1	1.5+5	Expt	DOE-NDC-19		91	580	LRL	Berman+TOF.LINAC.5 PCT ACCR.NDG
OS	190	N,GAMMA	2.4+4		Expt	DOE-NDC-19		17	580	BNL	Bradley+ACT.24 KEV CS GVN,30KEV DRVD
OS	190	N,GAMMA	5.0-1	1.5+5	Expt	DOE-NDC-19		91	580	LRL	Berman+TOF.LINAC.5 PCT ACCR.NDG
OS	190	SPECT N,GAMM	NDG		Expt	DOE-NDC-19		30	580	BNL	Casten+AVG RES CAPT,DOUBLE CAPT.NDG.
OS	192	N,GAMMA	2.4+4		Expt	DOE-NDC-19		17	580	BNL	Bradley+ACT.24 KEV CS GVN,30KEV DRVD
OS	192	N,GAMMA	5.0-1	1.5+5	Expt	DOE-NDC-19		91	580	LRL	Berman+TOF.LINAC.5 PCT ACCR.NDG
PT	192	SPECT N,GAMM	NDG		Expt	DOE-NDC-19		30	580	BNL	Casten+AVG RES CAPT SPEC.NDG.
PT	194	SPECT N,GAMM	NDG		Expt	DOE-NDC-19		30	580	BNL	Casten+AVG RES CAPT SPEC.NDG.
PT	195	SPECT N,GAMM	NDG		Expt	DOE-NDC-19		30	580	BNL	Casten+AVG RES CAPT SPEC.NDG.
AU	197	TOTAL XSECT	4.0+4	4.8+6	Expt	DOE-NDC-19		4	580	ANL	Poenitz+NDG.SEE 79 KNOX.TBP NSE.
AU	197	TOTAL XSECT	2.0+6	8.0+7	Expt	DOE-NDC-19		131	580	ORL	Larson+TRNS.CFD OPTMDL CS.NDG.TBP.
AU	197	TOTAL XSECT	2.0+6	8.0+7	Expt	DOE-NDC-19		130	580	ORL	Larson+TRNS.SEVERAL THICKNESSES.NDG.
AU	197	N,GAMMA	Fast		Expt	DOE-NDC-19		124	580	NBS	Gilliam.ISNF.AU197NG/U235 NF GVN.
PB		TOTAL XSECT	2.0+6	8.0+7	Expt	DOE-NDC-19		131	580	ORL	Larson+TRNS.CFD OPTMDL CS.NDG.TBP.
PB		TOTAL XSECT	2.0+6	8.0+7	Expt	DOE-NDC-19		130	580	ORL	Larson+TRNS.SEVERAL THICKNESSES.NDG.
PB		DIFF INELAST	7.5+6	1.2+7	Expt	DOE-NDC-19		170	580	TNL	Beyerle+3 ES.TOF.5 ANGS.DBL DIF.GRPH
BI	209	EVALUATION	1.0-5	2.0+7	Eval	DOE-NDC-19		5	580	ANL	Smith+EVAL IN ENDF FORMAT.NDG.
BI	209	EVALUATION	1.0-5	2.0+7	Eval	DOE-NDC-19		102	580	ANL	Howerton+EVAL IN ENDF/B FORMAT.NDG.
BI	209	TOTAL XSECT	1.2+6	4.5+6	Expt	DOE-NDC-19		5	580	ANL	Smith+BROAD RESOL.1 PCT.ACCR.NDG.
BI	209	DIFF ELASTIC	1.5+6	4.0+6	Expt	DOE-NDC-19		5	580	ANL	Smith+20-160 DEG.NDG.
BI	209	POLARIZATION	2.0+6	4.0+6	Expt	DOE-NDC-19		178	580	YAL	Ahmed+ASYM.ANAL TBD.NDG.
BI	209	DIFF INELAST		4.0+6	Expt	DOE-NDC-19		5	580	ANL	Smith+
RA	226	FISSION	3.0+6	5.0+6	Comp	DOE-NDC-19		113	580	NBS	Behrens.57 ISOTOPES.NF VS A.TBP ANS.
AC	227	FISSION	3.0+6	5.0+6	Comp	DOE-NDC-19		113	580	NBS	Behrens.57 ISOTOPES.NF VS A.TBP ANS.
TH	228	FISSION	3.0+6	5.0+6	Comp	DOE-NDC-19		113	580	NBS	Behrens.57 ISOTOPES.NF VS A.TBP ANS.
TH	229	FISS YIELD	2.5-2		Expt	DOE-NDC-19		9	580	ANL	Gindler+TBL PCT FISS YLDS.
TH	230	SPECT N,GAMM	NDG		Expt	DOE-NDC-19		30	580	BNL	Casten+AVG RES CAPT SPEC.NDG.

Element S	A	Quantity	Energy (eV) Min	Max	Type	Documentation Ref	Vol Page	Date	Lab	Comments
TH	230	FISSION	Tr	1.0+7	Expt	DOE-NDC-19	9	580	ANL	Meadows.REL U235.GRPH.CFD ENDF.
TH	230	FISSION	3.0+6	5.0+6	Comp	DOE-NDC-19	113	580	NBS	Behrens.57 ISOTOPES.NF VS A.TBP ANS.
TH	231	FISSION	3.0+6	5.0+6	Comp	DOE-NDC-19	113	580	NBS	Behrens.57 ISOTOPES.NF VS A.TBP ANS.
TH	232	TOTAL XSECT	4.0+4	4.8+6	Expt	DOE-NDC-19	4	580	ANL	Poenitz+NDG.SEE 79 KNOX.TBP NSE.
TH	232	DIFF INELAST	1.5+6	2.0+6	Expt	DOE-NDC-19	5	580	ANL	Guenther+NDG.ANAL TBD.
TH	232	DIFF INELAST	1.5+6	2.0+6	Expt	DOE-NDC-19	5	580	ANL	Guenther+NDG.ANAL TBD.
TH	232	DIFF INELAST	7.0+5	2.0+6	Expt	DOE-NDC-19	103	580	LTI	Beghian+TOF.FROM DNG DATA.NDG.
TH	232	DIFF INELAST	9.0+5	1.4+6	Expt	DOE-NDC-19	104	580	LTI	Kegel+TOF.15 KEV RESLN.NDG.TBC
TH	232	DIFF INELAST	NDG		Theo	DOE-NDC-19	107	580	LTI	Sheldon.COMPD NUCL+DIRECT INT.NDG.
TH	232	N,GAMMA	2.3+4		Expt	DOE-NDC-19	110	580	MHG	Grady+MEAS UNDERWAY.NDG.
TH	232	N,GAMMA	1.0+2	5.0+4	Expt	DOE-NDC-19	130	580	ORL	Perez+TOF.CFD ENDF/B-V.NDG.
TH	232	N,GAMMA	8.0-3	1.0+1	Expt	DOE-NDC-19	155	580	RPI	Little+CAPT YLDS.PRELIM.TBC.
TH	232	FISSION	Tr	1.0+7	Expt	DOE-NDC-19	9	580	ANL	Meadows.REL U235.GRPH.CFD ENDF.
TH	232	FISSION	3.0+6	5.0+6	Comp	DOE-NDC-19	113	580	NBS	Behrens.57 ISOTOPES.NF VS A.TBP ANS.
TH	232	FISSION	Fiss		Expt	DOE-NDC-19	124	580	NBS	Gilliam+SPEC AVG CS RATIO WITH U-235
TH	232	NU(BAR)	1.0+4	2.0+7	Expt	DOE-NDC-19	94	580	LRL	Howe+PRELIM RESULTS.NDG
TH	232	F NEUT DELAY	1.0+6	1.4+7	Theo	DOE-NDC-19	80	580	LAS	England+2 ES.NDG.SPEC CALC TBC.NDG
TH	232	F NEUT DELAY	NDG		Exth	DOE-NDC-19	101	580	LRL	Waldo+BETA-DELAY YLDS MEAS,CALC.TBL
PA	229	FISSION	3.0+6	5.0+6	Comp	DOE-NDC-19	113	580	NBS	Behrens.57 ISOTOPES.NF VS A.TBP ANS.
PA	230	FISSION	3.0+6	5.0+6	Comp	DOE-NDC-19	113	580	NBS	Behrens.57 ISOTOPES.NF VS A.TBP ANS.
PA	231	TOTAL XSECT	1.0-2	1.0+2	Expt	DOE-NDC-19	132	580	ORL	Dabbs+TRNS.RES PAR ANAL.NDG
PA	231	SPECT N,GAMM	NDG		Expt	DOE-NDC-19	30	580	BNL	Casten+AVG RES CAPT SPEC.NDG.
PA	231	FISSION	3.0+6	5.0+6	Comp	DOE-NDC-19	113	580	NBS	Behrens.57 ISOTOPES.NF VS A.TBP ANS.
PA	231	FISSION	4.0-1	1.2+7	Expt	DOE-NDC-19	133	580	ORL	Plattard+TRIPLE HUMP BARRIER.TBP.
PA	231	RESON PARAM	1.0-2	1.0+2	Expt	DOE-NDC-19	132	580	ORL	Dabbs+TRNS.RES PAR ANAL.NDG
PA	232	FISSION	3.0+6	5.0+6	Comp	DOE-NDC-19	113	580	NBS	Behrens.57 ISOTOPES.NF VS A.TBP ANS.
U	230	FISSION	3.0+6	5.0+6	Comp	DOE-NDC-19	113	580	NBS	Behrens.57 ISOTOPES.NF VS A.TBP ANS.

Element S	A	Quantity	Energy (eV) Min	Max	Type	Documentation Ref	Vol	Page	Date	Lab	Comments
U	231	FISSION	3.0+6	5.0+6	Comp	DOE-NDC-19		113	580	NBS	Behrens.57 ISOTOPES.NF VS A.TBP ANS.
U	232	FISSION	3.0+6	5.0+6	Comp	DOE-NDC-19		113	580	NBS	Behrens.57 ISOTOPES.NF VS A.TBP ANS.
U	232	F NEUT DELAY	NDG		Exth	DOE-NDC-19		101	580	LRL	Waldo+BETA-DELAY YLDS MEAS,CALC.TBL
U	233	TOTAL XSECT	4.0+4	4.8+6	Expt	DOE-NDC-19		4	580	ANL	Poenitz+NDG.SEE 79 KNOX.TBP NSE.
U	233	DIFF INELAST	1.5+6	2.0+6	Expt	DOE-NDC-19		5	580	ANL	Guenther+NDG.ANAL TBD.
U	233	DIFF INELAST	1.5+6	2.0+6	Expt	DOE-NDC-19		5	580	ANL	Guenther+NDG.ANAL TBD.
U	233	FISSION	2.3+4	9.6+5	Expt	DOE-NDC-19		110	580	MHG	Grady+5 ES.ANAL TBD.NDG.
U	233	FISSION	1.4+7		Expt	DOE-NDC-19		111	580	MHG	Mahdavi+MEAS TBD.NDG.
U	233	FISSION	3.0+6	5.0+6	Comp	DOE-NDC-19		113	580	NBS	Behrens.57 ISOTOPES.NF VS A.TBP ANS.
U	233	FISSION	Fiss		Expt	DOE-NDC-19		124	580	NBS	Gilliam+SPEC AVG CS RATIO WITH U-235
U	233	F NEUT DELAY	1.0+6	1.4+7	Theo	DOE-NDC-19		80	580	LAS	England+THR E ALSO.SPEC CALC TBC.NDG
U	233	F NEUT DELAY	NDG		Exth	DOE-NDC-19		101	580	LRL	Waldo+BETA-DELAY YLDS MEAS,CALC.TBL
U	233	SPECT FISS N	5.5+5		Expt	DOE-NDC-19		9	580	ANL	Smith+TOF.REL CF252.PROMPT NS.GRPH.
U	233	FISS YIELD	NDG		Expt	DOE-NDC-19		110	580	MHG	Grady+ANISOTROPY MEAS TBD.NDG.
U	234	FISSION	3.0+6	5.0+6	Comp	DOE-NDC-19		113	580	NBS	Behrens.57 ISOTOPES.NF VS A.TBP ANS.
U	235	TOTAL XSECT	4.0+4	4.8+6	Expt	DOE-NDC-19		4	580	ANL	Poenitz+NDG.SEE 79 KNOX.TBP NSE.
U	235	FISSION	Tr	1.0+7	Expt	DOE-NDC-19		9	580	ANL	Meadows.TH 230,232 REL U.GRPHS.
U	235	FISSION	1.0-3	2.0+7	Expt	DOE-NDC-19		94	580	LRL	White+CM245 REL U235.NDG.
U	235	FISSION	1.4+7		Expt	DOE-NDC-19		111	580	MHG	Mahdavi+MEAS TBD.NDG.
U	235	FISSION	2.0+5	1.2+6	Expt	DOE-NDC-19		112	580	NBS	Wasson+TOF.NDG.
U	235	FISSION	3.0+6	5.0+6	Comp	DOE-NDC-19		113	580	NBS	Behrens.57 ISOTOPES.NF VS A.TBP ANS.
U	235	FISSION	1.4+7		Expt	DOE-NDC-19		112	580	NBS	Wasson+ASSOC PARTICLE TECH.TBD.NDG.
U	235	FISSION	Fiss		Expt	DOE-NDC-19		124	580	NBS	Gilliam+RATIO WITH U233,TH232,PU240.
U	235	FISSION	1.0+0	1.0+2	Expt	DOE-NDC-19		155	580	RPI	Maguire+CM REL U235.NDG.EXPT TBD.
U	235	NU(BAR)	5.3+5		Theo	DOE-NDC-19		80	580	LAS	Madland+NU CALC CFD EXPT DATA.NDG.
U	235	NU(BAR)	5.0+2	1.0+7	Expt	DOE-NDC-19		134	580	ORL	Gwin+REL CF-252.CFD OTHS.NDG.
U	235	F NEUT DELAY	1.0+6	1.4+7	Theo	DOE-NDC-19		80	580	LAS	England+THR E ALSO.SPEC CALC TBC.NDG

Element S	A	Quantity	Energy (eV) Min	Max	Type	Documentation Ref Vol	Page	Date	Lab	Comments
U	235	SPECT FISS N	5.5+5		Expt	DOE-NDC-19	9	580	ANL	Smith+TOF.REL CF252.PROMPT NS.GRPH.
U	235	SPECT FISS N	5.3+5		Theo	DOE-NDC-19	80	580	LAS	Madland+PROMPT SPEC.GRPH.CFD OTH.
U	235	FISS PROD G	Maxw		Expt	DOE-NDC-19	134	580	ORL	Dickens+DECAY HEAT.NDG.TBP NSE.
U	235	FISS PROD B	Maxw		Expt	DOE-NDC-19	134	580	ORL	Dickens+DECAY HEAT.NDG.TBP NSE.
U	236	SPECT N,GAMM	NDG		Expt	DOE-NDC-19	30	580	BNL	Casten+AVG RES CAPT SPEC.NDG.
U	236	FISSION	3.0+6	5.0+6	Comp	DOE-NDC-19	113	580	NBS	Behrens.57 ISOTOPES.NF VS A.TBP ANS.
U	236	F NEUT DELAY	1.0+6	1.4+7	Theo	DOE-NDC-19	80	580	LAS	England+SPEC CALC TBC.NDG.
U	237	FISSION	3.0+6	5.0+6	Comp	DOE-NDC-19	113	580	NBS	Behrens.57 ISOTOPES.NF VS A.TBP ANS.
U	238	TOTAL XSECT	4.0+4	4.8+6	Expt	DOE-NDC-19	4	580	ANL	Poenitz+NDG.SEE 79 KNOX.TBP NSE.
U	238	TOTAL XSECT	4.0+4	4.8+6	Expt	DOE-NDC-19	4	580	ANL	Poenitz+NDG.SEE 79 KNOX.TBP NSE.
U	238	DIFF INELAST		2.0+5	Expt	DOE-NDC-19	105	580	LTI	Traegde+RING GEOM MEAS.NDG.
U	238	DIFF INELAST	7.0+5	2.0+6	Expt	DOE-NDC-19	103	580	LTI	Beghian+TOF.FROM DNG DATA.NDG.
U	238	DIFF INELAST	9.0+5	1.4+6	Expt	DOE-NDC-19	104	580	LTI	Kegel+TOF.SPEC GRPH.15 KEV RESLN.TBC
U	238	DIFF INELAST	1.5+6		Theo	DOE-NDC-19	106	580	LTI	Kegel.COMPUTER SIMULATED SPEC.GRPH.
U	238	DIFF INELAST	8.2+4		Expt	DOE-NDC-19	134	580	ORL	Hill+DETECTOR USED.NDG.
U	238	DIFF INELAST	8.2+4		Expt	DOE-NDC-19	131	580	ORL	Winters+CS AT 82 KEV DETERMINED.NDG.
U	238	N,GAMMA	2.5-2		Expt	DOE-NDC-19	6	580	ANL	Poenitz+ACT.REL U235,AU197.CS GVN
U	238	N,GAMMA	3.0+4	3.0+6	Expt	DOE-NDC-19	6	580	ANL	Poenitz+ACT.REL U235,AU197.CFD.NDG.
U	238	N,GAMMA	Fast		Expt	DOE-NDC-19	124	580	NBS	Gilliam.ISNF.U238NG/U235NF RATIO GVN
U	238	SPECT N,GAMM	2.0+3	2.4+4	Expt	DOE-NDC-19	19	580	BNL	Stelts+51 DRVD FROM CAPT SPEC.NDG.
U	238	FISSION	1.4+7		Expt	DOE-NDC-19	111	580	MHG	Mahdavi+MEAS TBD.NDG.
U	238	FISSION	3.0+6	5.0+6	Comp	DOE-NDC-19	113	580	NBS	Behrens.57 ISOTOPES.NF VS A.TBP ANS.
U	238	F NEUT DELAY	1.0+6	1.4+7	Theo	DOE-NDC-19	80	580	LAS	England+2 ES.NDG.SPEC CALC TBC.NDG
U	238	F NEUT DELAY	NDG		Exth	DOE-NDC-19	101	580	LRL	Waldo+BETA-DELAY YLDS MEAS,CALC.TBL
U	238	STRNGTH FUNC	2.0+3	2.4+4	Expt	DOE-NDC-19	19	580	BNL	Stelts+51 DRVD FROM CAPT SPEC.NDG.
U	239	FISSION	3.0+6	5.0+6	Comp	DOE-NDC-19	113	580	NBS	Behrens.57 ISOTOPES.NF VS A.TBP ANS.
NP	233	FISSION	3.0+6	5.0+6	Comp	DOE-NDC-19	114	580	NBS	Behrens.57 ISOTOPES.NF VS A.TBP ANS.

Element S	A	Quantity	Energy (eV) Min	Max	Type	Documentation Ref	Vol Page	Date	Lab	Comments
NP	234	FISSION	3.0+6	5.0+6	Comp	DOE-NDC-19	114	580	NBS	Behrens.57 ISOTOPES.NF VS A.TBP ANS.
NP	235	FISSION	3.0+6	5.0+6	Comp	DOE-NDC-19	114	580	NBS	Behrens.57 ISOTOPES.NF VS A.TBP ANS.
NP	236	FISSION	2.5-2		Expt	DOE-NDC-19	9	580	ANL	Gindler.THR FISS CS GVN.
NP	236	FISSION	3.0+6	5.0+6	Comp	DOE-NDC-19	114	580	NBS	Behrens.57 ISOTOPES.NF VS A.TBP ANS.
NP	236	FISS YIELD	2.5-2		Expt	DOE-NDC-19	9	580	ANL	Gindler+TBL PCT FISS YLDS.
NP	237	N,GAMMA	1.0-2	3.0+2	Expt	DOE-NDC-19	132	580	ORL	Dabbs+PRELIM DATA.NDG.TBP.
NP	237	FISSION	7.7+5	9.6+5	Expt	DOE-NDC-19	109	580	MHG	Grady+2ES.PRELIM CS GVN.ANAL TBC.
NP	237	FISSION	1.4+7		Expt	DOE-NDC-19	111	580	MHG	Mahdavi+MEAS TBD.NDG.
NP	237	FISSION	1.0+6	2.0+7	Expt	DOE-NDC-19	112	580	NBS	Wasson+TOF.NDG.
NP	237	FISSION	3.0+6	5.0+6	Comp	DOE-NDC-19	114	580	NBS	Behrens.57 ISOTOPES.NF VS A.TBP ANS.
NP	237	F NEUT DELAY	1.0+6	1.4+7	Theo	DOE-NDC-19	80	580	LAS	England+SPEC CALC TBC.NDG.
NP	237	F NEUT DELAY	NDG		Exth	DOE-NDC-19	101	580	LRL	Waldo+BETA-DELAY YLDS MEAS,CALC.TBL
NP	237	FISS YIELD	NDG		Expt	DOE-NDC-19	109	580	MHG	Grady+ANISOTROPY MEAS TBD.NDG.
NP	237	RESON PARAM	1.0-2	1.0+2	Expt	DOE-NDC-19	132	580	ORL	Dabbs+PRELIM DATA.NDG.TBP.
NP	238	FISSION	3.0+6	5.0+6	Comp	DOE-NDC-19	114	580	NBS	Behrens.57 ISOTOPES.NF VS A.TBP ANS.
PU	236	FISSION	3.0+6	5.0+6	Comp	DOE-NDC-19	114	580	NBS	Behrens.57 ISOTOPES.NF VS A.TBP ANS.
PU	237	FISSION	3.0+6	5.0+6	Comp	DOE-NDC-19	114	580	NBS	Behrens.57 ISOTOPES.NF VS A.TBP ANS.
PU	238	FISSION	3.0+6	5.0+6	Comp	DOE-NDC-19	114	580	NBS	Behrens.57 ISOTOPES.NF VS A.TBP ANS.
PU	238	F NEUT DELAY	NDG		Exth	DOE-NDC-19	101	580	LRL	Waldo+BETA-DELAY YLDS MEAS,CALC.TBL
PU	239	TOTAL XSECT	4.0+4	4.8+6	Expt	DOE-NDC-19	4	580	ANL	Poenitz+NDG.SEE 79 KNOX.TBP NSE.
PU	239	FISSION	1.4+7		Expt	DOE-NDC-19	111	580	MHG	Mahdavi+MEAS TBD.NDG.
PU	239	FISSION	3.0+6	5.0+6	Comp	DOE-NDC-19	114	580	NBS	Behrens.57 ISOTOPES.NF VS A.TBP ANS.
PU	239	F NEUT DELAY	1.0+6	1.4+7	Theo	DOE-NDC-19	80	580	LAS	England+THR E ALSO.SPEC CALC TBC.NDG
PU	239	F NEUT DELAY	NDG		Exth	DOE-NDC-19	101	580	LRL	Waldo+BETA-DELAY YLDS MEAS,CALC.TBL
PU	239	SPECT FISS N	5.5+5		Expt	DOE-NDC-19	9	580	ANL	Smith+TOF.REL CF252.PROMPT NS.GRPH.
PU	239	FISS PROD G	Maxw		Expt	DOE-NDC-19	134	580	ORL	Dickens+NDG.SEE ORNL-NUREG-66.
PU	239	FISS PROD G	Maxw		Expt	DOE-NDC-19	82	580	ORL	Schenter+SPEC MEAS 2-14,000 SECS.NDG

Element S	A	Quantity	Energy (eV) Min	Max	Type	Documentation Ref	Vol	Page	Date	Lab	Comments
PU	239	FISS PROD B	Maxw		Expt	DOE-NDC-19		134	580	ORL	Dickens+NDG.SEE ORNL-NUREG-66.
PU	239	FISS PROD B	Maxw		Expt	DOE-NDC-19		82	580	ORL	Schenter+SPEC MEAS 2-14,000 SECS.NDG
PU	240	TOTAL XSECT	4.0+4	4.8+6	Expt	DOE-NDC-19		4	580	ANL	Poenitz+NDG.SEE 79 KNOX.TBP NSE.
PU	240	DIFF INELAST	1.5+6	2.0+6	Expt	DOE-NDC-19		5	580	ANL	Guenther+NDG.ANAL TBD.
PU	240	DIFF INELAST	1.5+6	2.0+6	Expt	DOE-NDC-19		5	580	ANL	Guenther+NDG.ANAL TBD.
PU	240	FISSION	3.0+6	5.0+6	Comp	DOE-NDC-19		114	580	NBS	Behrens.57 ISOTOPES.NF VS A.TBP ANS.
PU	240	FISSION	Fiss		Expt	DOE-NDC-19		124	580	NBS	Gilliam+SPEC AVG CS RATIO WITH U-235
PU	240	F NEUT DELAY	1.0+6	1.4+7	Theo	DOE-NDC-19		80	580	LAS	England+SPEC CALC TBC.NDG.
PU	240	SPECT FISS N	8.5+5		Expt	DOE-NDC-19		9	580	ANL	Smith+TOF.REL CF252.PROMPT NS.GRPH.
PU	241	FISSION	3.0+6	5.0+6	Comp	DOE-NDC-19		114	580	NBS	Behrens.57 ISOTOPES.NF VS A.TBP ANS.
PU	241	F NEUT DELAY	1.0+6	1.4+7	Theo	DOE-NDC-19		80	580	LAS	.EQUIVALENT TO DOE-NDC-19 MAY,1980.
PU	241	F NEUT DELAY	1.0+6	1.4+7	Theo	DOE-NDC-19		80	580	LAS	England+SPEC CALC TBC.NDG.
PU	241	F NEUT DELAY	NDG		Exth	DOE-NDC-19		101	580	LRL	Waldo+BETA-DELAY YLDS MEAS,CALC.TBL
PU	242	FISSION	3.0+6	5.0+6	Comp	DOE-NDC-19		114	580	NBS	Behrens.57 ISOTOPES.NF VS A.TBP ANS.
PU	242	F NEUT DELAY	1.0+6	1.4+7	Theo	DOE-NDC-19		80	580	LAS	.EQUIVALENT TO DOE-NDC-19 MAY,1980.
PU	242	F NEUT DELAY	1.0+6	1.4+7	Theo	DOE-NDC-19		80	580	LAS	England+SPEC CALC TBC.NDG.
PU	242	F NEUT DELAY	NDG		Exth	DOE-NDC-19		101	580	LRL	Waldo+BETA-DELAY YLDS MEAS,CALC.TBL.
PU	244	SPECT N,GAMM	NDG		Expt	DOE-NDC-19		30	580	BNL	Casten+AVG RES CAPT SPEC.NDG.
PU	244	FISSION	3.0+6	5.0+6	Comp	DOE-NDC-19		114	580	NBS	Behrens.57 ISOTOPES.NF VS A.TBP ANS.
AM	238	FISSION	3.0+6	5.0+6	Comp	DOE-NDC-19		114	580	NBS	Behrens.57 ISOTOPES.NF VS A.TBP ANS.
AM	239	FISSION	3.0+6	5.0+6	Comp	DOE-NDC-19		114	580	NBS	Behrens.57 ISOTOPES.NF VS A.TBP ANS.
AM	240	FISSION	3.0+6	5.0+6	Comp	DOE-NDC-19		114	580	NBS	Behrens.57 ISOTOPES.NF VS A.TBP ANS.
AM	241	FISSION	3.0+6	5.0+6	Comp	DOE-NDC-19		114	580	NBS	Behrens+57 ISOTOPES.NF VS A.TBP ANS.
AM	241	F NEUT DELAY	NDG		Exth	DOE-NDC-19		101	580	LRL	Waldo+BETA-DELAY YLDS MEAS,CALC.TBL.
AM	242	FISSION	3.0+6	5.0+6	Comp	DOE-NDC-19		114	580	NBS	Behrens.57 ISOTOPES.NF VS A.TBP ANS.
AM	242	FISSION	NDG		Expt	DOE-NDC-19		132	580	ORL	Dabbs+CS MEAS.NDG
AM	242	NU(BAR)	1.0+4	2.0+7	Expt	DOE-NDC-19		94	580	LRL	Howe+PRELIM RESULTS.GRPH.

Element S	A	Quantity	Energy (eV) Min	Max	Type	Documentation Ref	Vol	Page	Date	Lab	Comments
AM	242	F NEUT DELAY	NDG		Exth	DOE-NDC-19		101	580	LRL	Waldo+BETA-DELAY YLDS MEAS,CALC.TBL.
AM	243	N,GAMMA	NDG		Expt	DOE-NDC-19		132	580	ORL	Dabbs+CS REMEASUREMENT TBD.NDG.
AM	243	FISSION	3.0+6	5.0+6	Comp	DOE-NDC-19		114	580	NBS	Behrens+57 ISOTOPES.NF VS A.TBP ANS.
CM	240	FISSION	3.0+6	5.0+6	Comp	DOE-NDC-19		114	580	NBS	Behrens.57 ISOTOPES.NF VS A.TBP ANS.
CM	241	FISSION	3.0+6	5.0+6	Comp	DOE-NDC-19		114	580	NBS	Behrens.57 ISOTOPES.NF VS A.TBP ANS.
CM	242	FISSION	3.0+6	5.0+6	Comp	DOE-NDC-19		114	580	NBS	Behrens+57 ISOTOPES.NF VS A.TBP ANS.
CM	242	NU(BAR)	NDG		Expt	DOE-NDC-19		132	580	ORL	Dabbs+NU DETERMINED.NDG.
CM	243	FISSION	3.0+6	5.0+6	Comp	DOE-NDC-19		114	580	NBS	Behrens+57 ISOTOPES.NF VS A.TBP ANS.
CM	244	FISSION	3.0+6	5.0+6	Comp	DOE-NDC-19		114	580	NBS	Behrens+57 ISOTOPES.NF VS A.TBP ANS.
CM	244	FISSION	1.0+0	1.0+2	Expt	DOE-NDC-19		155	580	RPI	Maguire+REL U235.NDG.EXPT TBD
CM	244	FISSION	NDG		Expt	DOE-NDC-19		132	580	RPI	Dabbs+ORL/RPI EXPT TBD.NDG.
CM	245	FISSION	1.0-3	2.0+7	Expt	DOE-NDC-19		94	580	LRL	White+REL U235.GRPH.RES PAR ANAL.
CM	245	FISSION	3.0+6	5.0+6	Comp	DOE-NDC-19		114	580	NBS	Behrens+57 ISOTOPES.NF VS A.TBP ANS.
CM	245	NU(BAR)	1.0+4	2.0+7	Expt	DOE-NDC-19		94	580	LRL	Howe+PRELIM RESULTS.NDG
CM	245	F NEUT DELAY	NDG		Exth	DOE-NDC-19		101	580	LRL	Waldo+BETA-DELAY YLDS MEAS,CALC.TBL.
CM	245	FISS PROD G	Maxw		Expt	DOE-NDC-19		133	580	ORL	Dabbs+G SPEC 1 MIN-50 DAYS.NDG
CM	245	FISS YIELD	Maxw		Expt	DOE-NDC-19		133	580	ORL	Dabbs+GREATER THAN 80 ISOTOPES.NDG
CM	245	RESON PARAM	1.0-3	3.2+1	Expt	DOE-NDC-19		94	580	LRL	White+PRELIM ANAL.AWG WF GVN.
CM	245	STRNGTH FUNC	0.0+0	3.2+1	Expt	DOE-NDC-19		94	580	LRL	White+PRELIM STF GVN
CM	246	FISSION	3.0+6	5.0+6	Comp	DOE-NDC-19		114	580	NBS	Behrens+57 ISOTOPES.NF VS A.TBP ANS.
CM	246	FISSION	1.0+0	1.0+2	Expt	DOE-NDC-19		155	580	RPI	Maguire+REL U235.NDG.EXPT TBD
CM	246	FISSION	NDG		Expt	DOE-NDC-19		132	580	RPI	Dabbs+ORL/RPI EXPT TBD.NDG.
CM	246	FISS YIELD	Spon		Expt	DOE-NDC-19		9	580	ANL	Gindler+TBL PCT FISS YLDS.
CM	248	FISSION	1.0+0	1.0+2	Expt	DOE-NDC-19		155	580	RPI	Maguire+REL U235.NDG.EXPT TBD
CM	248	FISSION	NDG		Expt	DOE-NDC-19		132	580	RPI	Dabbs+ORL/RPI EXPT TBD.NDG.
BK	244	FISSION	3.0+6	5.0+6	Comp	DOE-NDC-19		114	580	NBS	Behrens+57 ISOTOPES.NF VS A.TBP ANS.
BK	245	FISSION	3.0+6	5.0+6	Comp	DOE-NDC-19		114	580	NBS	Behrens+57 ISOTOPES.NF VS A.TBP ANS.

Element S	A	Quantity	Energy (eV) Min	Max	Type	Documentation Ref	Vol	Page	Date	Lab	Comments
BK	246	FISSION	3.0+6	5.0+6	Comp	DOE-NDC-19		114	580	NBS	Behrens+57 ISOTOPES.NF VS A.TBP ANS.
BK	247	FISSION	3.0+6	5.0+6	Comp	DOE-NDC-19		114	580	NBS	Behrens+57 ISOTOPES.NF VS A.TBP ANS.
BK	248	FISSION	3.0+6	5.0+6	Comp	DOE-NDC-19		114	580	NBS	Behrens+57 ISOTOPES.NF VS A.TBP ANS.
BK	249	FISSION	3.0+6	5.0+6	Comp	DOE-NDC-19		114	580	NBS	Behrens+57 ISOTOPES.NF VS A.TBP ANS.
CF	249	TOTAL XSECT	NDG		Expt	DOE-NDC-19		132	580	ORL	Dabbs+TRNS.RES PAR ANAL.NDG
CF	249	FISSION	Spon		Comp	DOE-NDC-19		114	580	NBS	Behrens+57 ISOTOPES.NF VS A.TBP ANS.
CF	249	FISSION	NDG		Expt	DOE-NDC-19		132	580	ORL	Dabbs+CS REMEASURED.NDG.
CF	249	F NEUT DELAY	NDG		Exth	DOE-NDC-19		101	580	LRL	Waldo+BETA-DELAY YLDS MEAS,CALC.TBL.
CF	249	FISS PROD G	Maxw		Expt	DOE-NDC-19		133	580	ORL	Dabbs+MEASUREMENT IN PROGRESS.NDG.
CF	249	FISS YIELD	Maxw		Expt	DOE-NDC-19		133	580	ORL	Dabbs+MEASUREMENT IN PROGRESS.NDG.
CF	249	RESON PARAM	NDG		Expt	DOE-NDC-19		132	580	ORL	Dabbs+TRNS.RES PAR ANAL.NDG
CF	252	NU(BAR)	Spon		Expt	DOE-NDC-19		57	580	INL	Smith+ANAL TBC.PRELIM VAL GVN.
CF	252	F NEUT DELAY	Spon		Theo	DOE-NDC-19		80	580	LAS	.EQUIVALENT TO DOE-NDC-19 MAY,1980.
CF	252	F NEUT DELAY	Spon		Theo	DOE-NDC-19		80	580	LAS	England+SPEC CALC TBC.NDG.
ES	249	FISSION	3.0+6	5.0+6	Comp	DOE-NDC-19		114	580	NBS	Behrens+57 ISOTOPES.NF VS A.TBP ANS.
ES	250	FISSION	3.0+6	5.0+6	Comp	DOE-NDC-19		114	580	NBS	Behrens+57 ISOTOPES.NF VS A.TBP ANS.
MA	NY	FISSION	3.0+6	5.0+6	Comp	DOE-NDC-19		113	580	NBS	Behrens.57 ISOTOPES.NF CS VS A.GRPH.

CHARGED PARTICLE DATA

Li-6(p,He3)He-4 sigma(E)								
LAS	Eval	Prog	DOE-NDC-19	74	80	1.0-1	2.5+0	Hale+ CURV. R-MATRIX. CFD ELWYN+
LAS	Eval	Prog	DOE-NDC-19	74	80	1.0-4	5.0+0	Hale+ NDG. R-MATRIX. ENDF-LIKE FORMAT.
Li-6(p,He3)He-4 sigma(E)								
LAS	Eval	Prog	DOE-NDC-19	74	80	1.0-1	2.5+0	Hale+ CURV. R-MATRIX. CFD ELWYN+
LAS	Eval	Prog	DOE-NDC-19	74	80	1.0-4	5.0+0	Hale+ NDG. R-MATRIX. ENDF-LIKE FORMAT.
C-12(p,x)C-11 sigma(E)								
BNL	Eval	Prog	DOE-NDC-19	40	80	TR	+2	. NNDC. WORK BEGUN.
C-13(p,n)N-13 sigma(E)								
BNL	Eval	Prog	DOE-NDC-19	40	80	TR	+2	. NNDC. WORK BEGUN.
Se-76(p,n)Br-76 sigma(E)								
LRL	Expt	Prog	DOE-NDC-19	87	80	1.9+1	2.5+1	Wong+ NDG.
Se-80(p,n)Br-80 sigma(E)								
LRL	Expt	Prog	DOE-NDC-19	87	80	1.9+1	2.5+1	Wong+ NDG.
Se-82(p,n)Br-82 sigma(E)								
LRL	Expt	Prog	DOE-NDC-19	87	80	1.9+1	2.5+1	Wong+ NDG.
Sr-88(p,n)Y-88 partial sigma(E)								
LRL	Expt	Prog	DOE-NDC-19	85	80	5.8+0	1.1+1	Grimes+ CURV. INTAD. 3 STATES.
Mo-92(p,x)gamma sigma(E)								
LRL	Expt	Prog	DOE-NDC-19	87	80	3.0+0	+1	Dietrich+ NDG.
Mo-96(p,x)gamma sigma(E)								
LRL	Expt	Prog	DOE-NDC-19	87	80	3.0+0	+1	Dietrich+ NDG.
Mo-100(p,x)gamma sigma(E)								
LRL	Expt	Prog	DOE-NDC-19	87	80	3.0+0	+1	Dietrich+ NDG.
H-2(d,p)H-3 sigma(E)								
LAS	Eval	Prog	DOE-NDC-19	72	80	NDG		Hale+ NDG. R-MATRIX ANALYSIS.
LAS	Expt	Prog	DOE-NDC-19	70	80	4.0-2	1.2-1	Brown+ NDG. PRELIMINARY WORK.
H-2(d,p)H-3 sigma(E)								
LAS	Eval	Prog	DOE-NDC-19	72	80	NDG		Hale+ NDG. R-MATRIX ANALYSIS.
LAS	Expt	Prog	DOE-NDC-19	70	80	4.0-2	1.2-1	Brown+ NDG. PRELIMINARY WORK.
H-2(d,n)He-3 sigma(E)								
LAS	Eval	Prog	DOE-NDC-19	72	80	NDG		Hale+ NDG. R-MATRIX ANALYSIS.
H-2(d,n)He-3 sigma(E) x factor								
LAS	Eval	Prog	DOE-NDC-19	74	80	0.0+0	5.0-2	Hale+ CURV. S-FACTOR.
H-3(d,n)He-4 sigma(E)								
LAS	Eval	Prog	DOE-NDC-19	74	80	1.0-4	5.0+0	Hale+ NDG. R-MATRIX. ENDF-LIKE FORMAT.
H-3(d,n)He-4 sigma(E) x factor								
LAS	Eval	Prog	DOE-NDC-19	74	80	0.0+0	3.5-2	Hale+ CURV. S-FACTOR.
He-3(d,p)He-4 sigma(E)								
LAS	Eval	Prog	DOE-NDC-19	74	80	1.0-4	5.0+0	Hale+ NDG. R-MATRIX. ENDF-LIKE FORMAT.

```
H-3(t,2n)He-4   sigma(E)
   LAS  Eval  Prog  DOE-NDC-19  74      80  1.0-4 5.0+0  Hale+ NDG. R-MATRIX. ENDF-LIKE FORMAT.

Li-6(He3,p+alpha)He-4   partial sigma(E)
   ANL  Expt  Prog  DOE-NDC-19   6      80  5.0-1 1.8+0  Elwyn+ NDG. ALSO DIFFERENTIAL DATA.

Li-6(He3,p+alpha)He-4   partial sigma(E) x factor
   ANL  Expt  Prog  DOE-NDC-19   6      80  5.0-1 1.8+0  Elwyn+ NDG. ALSO DIFFERENTIAL DATA.

O-18(alpha,x)n   sigma(E)
   WAU  Expt  Prog  DOE-NDC-19 179      80  3.0+0 9.0+0  Grant+ CURV. PRELIMINARY.
```

ARGONNE NATIONAL LABORATORY

A. NEUTRON PHYSICS

1. Neutron Total and Scattering Cross Sections of ^{6}Li in the Few MeV Region (P. Guenther, A. Smith and J. Whalen)

Neutron total cross sections of ^{6}Li were measured from ~0.5 to ~4.8 MeV at intervals of $\lesssim$10 keV. Neutron differential elastic-scattering cross sections were measured from 1.5 to 4.0 MeV at $\gtrsim$10 scattering angles and at incident-neutron intervals of $\lesssim$100 keV. Neutron differential inelastic-scattering cross sections were measured in the incident-energy range 3.5 to 4.0 MeV. The experimental results were extended to lower energies using measured neutron total and scattering cross sections recently reported elsewhere by the authors. The composite experimental data (total cross sections from 0.1-4.8 MeV and scattering cross sections from 0.22-4.0 MeV) were interpreted in terms of a simple two-level R-matrix model which describes the observed cross sections and implied the reaction cross section in unobserved channels; notably the (n,α)t reaction (Q = 4.783 MeV). The experimental and calculational results were compared with previously reported results as summarized in the ENDF/B-V evaluated nuclear data file. The results are in press (ANL/NDM-52).

2. Fast-neutron Total and Scattering Cross Sections of the Structural Materials (P. Guenther, A. Smith and J. Whalen)

a. Elemental Chromium

Broad resolution neutron total and differential elastic and inelastic scattering cross sections have been measured from 1.5 to 4.0 MeV in steps of 50 keV. Illustrative results are shown in Figs. 1 and 2. These data form a suitable basis for an optical-statistical model analysis. Preliminary interpretations within this framework indicate that a simple spherical model is descriptive of the measured values. The measured neutron total and the elastic-scattering cross sections are reasonably represented by the ENDF/B-V evaluated file. However, these are significant discrepancies between measured and evaluated inelastic neutron scattering cross sections.

b. Elemental Nickel

Complimenting previously reported studies of fast-neutron total and scattering cross sections of ^{60}Ni,[1] similar measurements have

[1] A. Smith et al., Argonne National Laboratory Report, ANL/NDM-44 (1979).

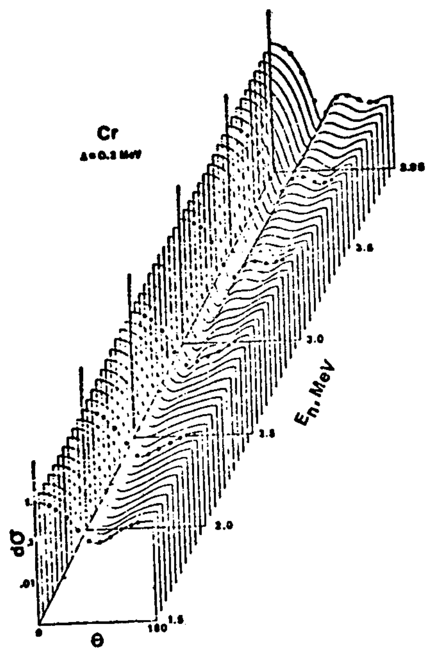

Fig. 1. 200-keV-averaged differential-elastic cross-sections of elemental chromium. The curves are Legendre-polynomial least-squares fits to the experimental data which are indicated by solid circles (dσ in b/sr, θ in lab-degrees).

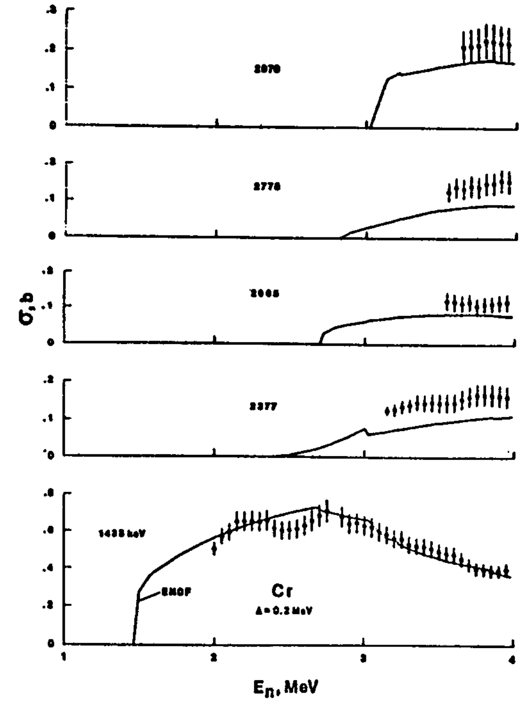

Fig. 2. 200 keV-averaged, angle integrated inelastic cross sections of elemental chromium. Data are indicated by solid circles. The curves are taken from the ENDF/B file.

been initiated for elemental nickel and ^{58}Ni over the energy range 1.0-5.0 MeV. Particular attention is given to accuracies and sample size effects. The energy-averaged neutron total-cross-section results have been completed and are very consistent with the previously reported model based upon ^{60}Ni results.[2] The ultimate objective of the elemental nickel inelastic neutron scattering cross section to 5% accuracy from 1.0-5.0 MeV should be realized from this set of measurements.

c. Copper

Broad resolution neutron total and scattering cross sections have been measured between 1.5 and 4.0 MeV in incident neutron energy intervals of 50 keV. The interpretation of the data is in progress.

---

2 A. Smith et al., Argonne National Laboratory Report, ANL/NDM-44 (1979).

3. Total Neutron Cross Sections in the Fission Product Mass Region
(W. P. Poenitz, J. F. Whalen, A. B. Smith and P. Guenther)

Accurate total-neutron-cross-section data are needed in the fission product mass region in order to establish reliable optical model parameter sets to be used in nuclear model calculations of capture cross sections. A perusal of existing data reveals a substantial lack of such data and/or the existence of discrepancies. Measurements were carried out in the energy range from 50 keV to 4.5 MeV for Y, Zr, Mo, Cd, Sn, Te, Ag, Nb, Rh, Pd, In, and Sb. These data await corrections for resonance self-shielding and will then be used together with scattering data for establishing optical model parameters.

4. Capture Cross Sections of Fission Product Nuclei
(W. P. Poenitz)

Measurements of the fast-neutron capture cross sections of elemental rhodium, palladium, neodymium, and samarium were carried out in the energy range from 0.5-4.0 MeV. A large liquid scintillator and the time-of-flight technique were used in these measurements. The capture cross section of gold was used as a reference. The capture detection efficiency was in the range of 65-85% and is the major limiting factor for the uncertainty of the data which is ~10-15%. The results are outlined in Fig. 3.

Isotopes of the elements measured in the present work are among the 20 most important fission product nuclei. Data are rare or nonexistent in this energy range and evaluated data sets based upon nuclear model calculations differ substantially, with factors of 5 being common. The present results (see Fig. 3) should provide a useful constraint for the evaluation of these cross sections. Extensive nuclear model calculations were carried out with the nuclear model code ABAREX. Parameter dependence was investigated and it was concluded that optical model parameters are insufficiently established in this mass region due to a lack of accurate total neutron cross sections and scattering data.

A paper dealing with the above was contributed to the NEANDC Specialists' Meeting on Neutron Cross Sections of Fission Product Nuclei held in Bologna, December 12-14, 1979.

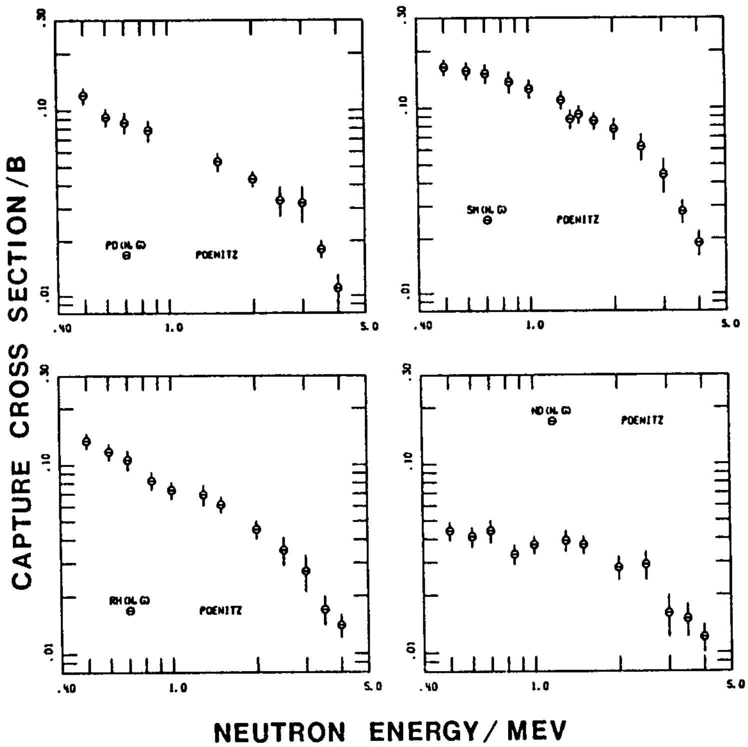

Fig. 3. Measured neutron capture cross sections.

5. Total Neutron Cross Sections of Heavy Isotopes

(W. P. Poenitz, P. Guenther, J. F. Whalen, and A. B. Smith)

Measurements of the total neutron cross sections of ^{181}Ta, ^{197}Au, ^{232}Th, ^{233}U, ^{235}U, ^{238}U, ^{239}Pu and ^{240}Pu between 40 keV and 4.8 MeV were reported at the Conference on Nuclear Cross Sections and Technology held at Knoxville in September 1979. These measurements were supplemented with measurements for samples of varying thicknesses for ^{181}Ta and ^{238}U. The purpose of these additional measurements was to verify the correction for resonance-self-shielding which was obtained with a Monte Carlo Code developed in the context of these measurements. The measured values of the effective total neutron cross section agreed very well with the calculated dependence on the sample thickness for these two materials. An even more rigorous check was made with measurements of W-samples of varying thicknesses for which the calculated correction factors are substantially larger than for the isotopes measured in the present work. These additional measurements suggest that the systematic uncertainty of the correction does not exceed 10% of the size of the correction, thus contributes less than 1% to the uncertainties of the measured cross section values.

A publication was prepared and will be submitted to Nuclear Science and Engineering. Final data values will be transmitted to the National Nuclear Data Center.

Similar measurements were completed for the even isotopes of tungsten at energies of less than 1.0 MeV. At these lower energies the effects of resonance self-shielding on the broad-resolution measured values for the tungsten isotopes can be very significant.

6. Measured and Evaluated Neutron Cross Sections of Elemental Bismuth (A. Smith, P. Guenther, R. Howerton, D. Smith and J. Whalen)

Neutron total cross sections of elemental bismuth were measured with broad resolutions from 1.2 to 4.5 MeV to accuracies of $\approx$1%. Neutron-differential-elastic-scattering cross sections of bismuth were measured from 1.5 to 4.0 MeV at incident neutron energy intervals of $\lesssim$0.2 MeV over the scattered-neutron angular range $\approx$20-160 deg. Differential neutron cross sections for the excitation of observed states in bismuth at 895 ± 12, 1606 ± 14, 2590 ± 15, 2762 ± 29, 3022 ± 21 and 3144 ± 15 KeV were determined at incident neutron energies up to 4.0 MeV. An optical-statistical model was deduced from the measured values. This model, the present experimental results and information available elsewhere in the literature were used to construct a comprehensive evaluated nuclear data file for elemental bismuth in the ENDF format. The evaluated file is particularly suited to the neutronic needs of the fusion-fission hybrid designer.

7. Fast-neutron Scattering Cross Sections of ^{232}Th, ^{233}U and ^{240}Pu (P. Guenther and A. Smith)

Measurements have been made at 1.5, 2.0 and 2.5 MeV resolving a number inelastically scattered neutron groups in addition to the elastically scattered component. The ^{232}Th results supplement those previously obtained at this laboratory over a number of years. The ^{233}U and ^{240}Pu results are the first of a new measurement program which is notable for the difficult nature of the experimental measurements. The samples are relatively small, highly active and, in the case of ^{240}Pu, represent strong spontaneous fission neutron sources in themselves. Detailed numerical procedures have been developed for handling these unusual complications including interpretation of the effects of the necessary sample containers.

8. Measurements of the $^{238}U(n,\gamma)$ Cross Section at Thermal and Fast Neutron Energies (W. P. Poenitz, L. R. Fawcett, Jr., D. L. Smith and G. J. DiIorio)

The capture cross section of ^{238}U was measured using the activation technique and $^{235}U(n,\gamma)$ and $^{197}An(n,\gamma)$ as reference cross sections. Calculations of capture-to-fission central-core reaction ratios for fast benchmark test facilities, using current evaluated data files, result in higher values than experimentally determined. This situation has prevailed for more than 10 years and has resulted in continuous requests to lower evaluated differential data. Therefore, a major effort was undertaken in this present work to determine the absolute activation of metallic uranium samples. Two prominent γ-transitions in the decay of the ^{239}U daughter nuclide, ^{239}Np, were detected with a Ge(Li) detector. The system was calibrated with several absolutely calibrated α-emitters, ^{243}Am, which decays to ^{239}Np. Various effects caused by γ-absorption in the metallic foils were experimentally determined by four independent techniques which resulted in an agreement of ~±1% for 0.025 cm thick samples.

Cross section measurements were carried out at thermal neutron energy and in the neutron energy range from 30 keV to 3 MeV. A thermal cross section value of 2.699 ± 0.019b was obtained which is somewhat lower than the average of previously measured values but is a good confirmation of the ENDF/B-V value of 2.70b. Agreement was very good between values measured at 30 keV and 500 keV with either reference cross section ($^{235}U(n,f)$ and $^{197}Au(n,\gamma)$) which suggests consistency between these cross sectons in ENDF/B-V. The present results for $^{238}U(n,\gamma)$ are about 4% lower at 30 keV and about the same amount higher above 130 keV, thus a solution of the C/E-problem for central reaction rate ratios cannot be argued from these new differential measurements.

B. CHARGED-PARTICLE REACTIONS

1. The $^{6}Li(^{3}He,p)$ Reaction at Low Energies (A. J. Elwyn, R. E. Holland, C. N. Davids, F. P. Mooring, J. E. Monahan, and W. Ray, Jr.)

Nuclear reactions of ^{3}He with ^{6}Li are important contributors to thermonuclear reaction rates associated with the p-^{6}Li advanced fuel cycle which is being studied[3] in connection with the future

---

[3] See, for example, R. W. Conn and G. W. Shuy, Report #UWFDM-262 (Univ. of Wisconsin, June 1979); and J. Rand McNally, Jr., Proc. of the IEEE Int'l Conf. on Plasma Science (June 1979).

generation of fusion reactors. As part of a continuing program to measure absolute reaction cross sections for light ions with ^{6}Li at low energies, we have recently completed cross section measurements for $^{3}He + ^{6}Li$ T $2^{4}He + p$ at energies between 0.5 and 1.85 MeV. Pulsed ^{3}He beams from the Argonne Dynamitron accelerator along with time-of-flight techniques were used to separately study the yields for outgoing protons and α particles. Differential and total cross sections for protons associated with the ground, 2.94, 16.63, and 16.92 MeV states in ^{8}Be, as well as for the underlying continuum protons that arise from various 3-body breakup mechanisms, were obtained to absolute accuracies of between 10 and 20%. The results represent a much more complete and systematic determination of cross sections in the energy region below 2 MeV than do previously published measurements, and complement the measurements recently reported[4] on the $^{6}Li(p,^{3}He)^{4}He$ reaction. Thermonuclear reaction rates calculated from the measured cross sections suggest that the total reactivity in the p-^{6}Li fuel cycle may be somewhat larger than previous studies have indicated.

2. <u>Cross Section Measurement for the $^{52}Cr(n,p)^{52}V$ Reaction Near Threshold</u> (D. Smith and J. Meadows)

Cross sections for the $^{52}Cr(n,p)^{52}V$ reaction have been measured relative to $^{238}U(n,f)$ using cyclic activation techniques to measure the yield of decay gamma rays from 3.76 m ^{52}V. This work provides cross sections for the energy region from 5.3-9 MeV where none were previously available (see Fig. 4). These data and values from the literature for energies $\gtrsim$14 MeV were used to provide an estimate of the excitation function from threshold to 20 MeV. A value of 1.064 mb for the ^{235}U-fission-spectrum average cross section was calculated using the ENDF/B-V fission spectrum. This appears to be in reasonable agreement with integral data.

3. <u>On the Discrepancy between Differential and Integral Results for the $^{63}Cu(n,\alpha)^{60}Co$ Cross Section</u> (G. Winkler, D. L. Smith and J. W. Meadows)

Recent differential data from Argonne National Laboratory and other results from the literature have been used to provide a new evaluation for the $^{63}Cu(n,\alpha)^{60}Co$ cross section excitation function. This evaluation and the ENDF/B-V ^{235}U fission spectrum where used to calculate an average cross section of 0.507 ± 0.049 mb. The available integral data were re-evaluated and a value of 0.534 ± 0.015 mb was obtained. Since these two values agree within the errors, it appears that the long-standing integral/differential discrepancy for this reaction has been resolved.

---

[4] A. J. Elwyn, R. E. Holland, C. N. Davids, L. Meyer-Schutzmeister, F. P. Mooring, and W. Ray, Jr., Phys. Rev. C <u>20</u>, 1984 (1979).

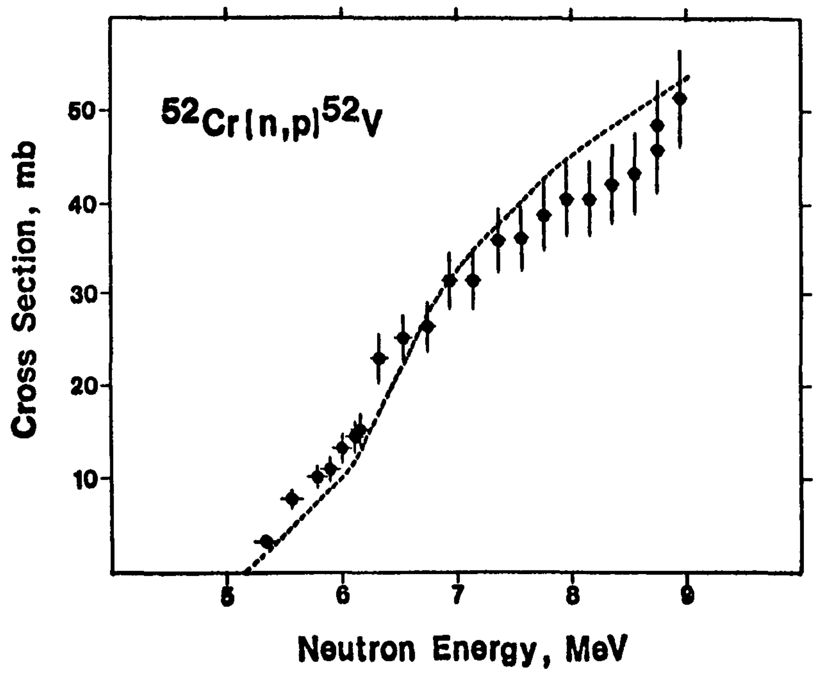

Fig. 4. Cross Section for the $^{52}Cr(n,p)^{52}V$ Reaction.

4. Activation Cross Sections of $^{66}Zn(n,p)^{66}Cu$ (D. L. Smith and J. W. Meadows)

Cross sections for the $^{66}Zn(n,p)^{66}Cu$ reaction has been measured in the energy range 4.2-10 MeV using activation techniques. The spectrum average cross section for the ^{235}U fission spectrum was calculated using the ENDF/B-V spectrum and reasonable extrapolations of the excitation function to higher and lower energies. The energy range of these measurements provides for ~87% of the response in a ^{235}U fission spectrum and there are no other data below 13 MeV. A comparison with experimental integral measurements is shown below.

Kobayashi and Kimura[5]	0.534 ± 0.038
Rau[6]	0.56 ± 0.034
Pfrepper and Raitschev[7]	0.96 ± 0.04
Nasyrov[8]	0.037 ± 0.13
This exp.	0.907

5 K. Kobayashi and I. Kimura, Nucl. Sci. & Tech. (Japan) 13, 531(1976).
6 Gert Rau, Nukleonik 9, 228(1967).
7 G. Pfrepper and C. Raitschev, Radiochimica Acta 23, 127(1976).
8 F. Nasyrov, Soviet Atomic Energy 25, 1251(1968).

C. ACTINIDE FISSION AND DECAY PROPERTIES

1. Fission Cross Sections of ^{230}Th and ^{232}Th Relative to Those of ^{235}U (J. W. Meadows)

The fission cross sections of ^{230}Th and ^{232}Th have been measured relative to ^{235}U from near threshold to near 10 MeV. The weight of the uranium deposit was based on low geometry alpha counting and earlier specific activity measurements of a ^{234}U-^{235}U mixture containing 1% ^{234}U. The weights of the thorium samples were determined by mass spectrometric isotopic dilution analyses. Generally the systematic errors are ~1% and the combined systematic and statistical errors are typically 1.5%. The results are shown in Figs. 5 and 6. The ^{232}Th results are in fair agreement with the ratios calculated from ENDF/B-V cross sections for energies below 2 MeV but are larger by several percent at energies above 2 MeV.

2. Fission Product Yields for Spontaneous Fission of ^{246}Cm and Thermal-Neutron-Induced Fission of ^{229}Th and ^{236}Np (J. E. Gindler, L. E. Glendenin and D. J. Henderson)

Yields of 17 fission product masses were determined for spontaneous fission of ^{246}Cm. Yields of ~40 masses each were determined for thermal-neutron-induced fission of ^{229}Th and ^{236}Np (long-lived). Cumulative fission product yields were measured by γ-ray spectrometry of catcher foils that had been placed in intimate contact with target foils during irradiation and by chemical separation of some fission product elements followed by beta counting. The fission-yield data including their errors (1σ) are given in Table 1. The fission cross section for long-lived ^{236}Np with thermal neutron was evaluated to be $(2.54 \pm 0.46) \times 10^3$ barns.

3. Prompt-Fission-Neutron Spectra of ^{233}U, ^{235}U, ^{239}Pu and ^{240}Pu Relative to that of ^{252}Cf (A. Smith, P. Guenther, G. Winkler and R. McKnight)

The prompt-neutron-induced-fission spectra of ^{233}U, ^{235}U, ^{239}Pu and ^{240}Pu were measured relative to the prompt-spontaneous-fission-neutron spectrum of ^{252}Cf. The fission of ^{233}U, ^{235}U, and ^{239}Pu is induced by $\approx$550 keV neutrons and that of ^{240}Pu by $\approx$850 keV neutrons. The emitted fission neutrons are observed over the energy range $\lesssim$0.5-10.0 MeV using time-of-flight techniques. Analysis of the measured values indicates that the average-fission-neutron energies are -123 ± 30 (^{233}U), -157 ± 24 (^{235}U), -76 ± 29 (^{239}Pu) and -46 ± 29 (^{240}Pu) keV relative to that of ^{252}Cf. The measured ratio values are illustrated in Fig. 7. The experimental results are compared with

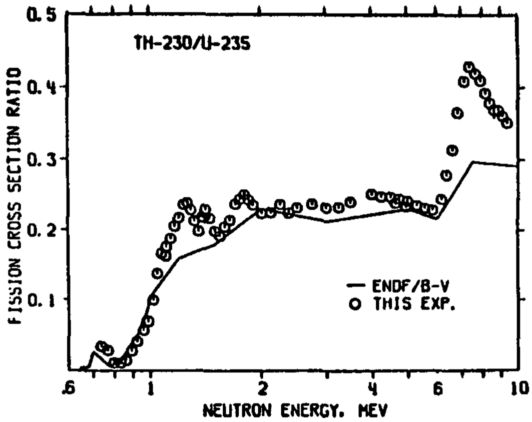

Fig. 5. The $^{230}Th/^{235}U$ Fission-cross-section ratio.

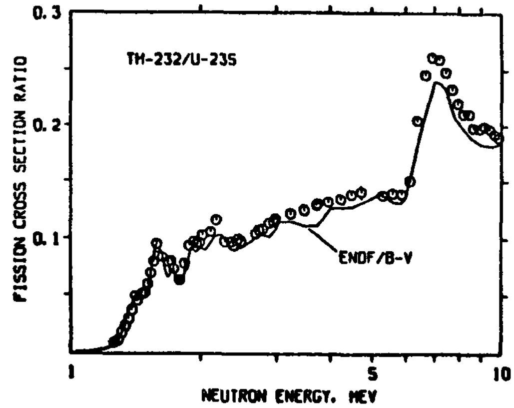

Fig. 6. The $^{232}Th/^{235}U$ Fission-cross-section ratio.

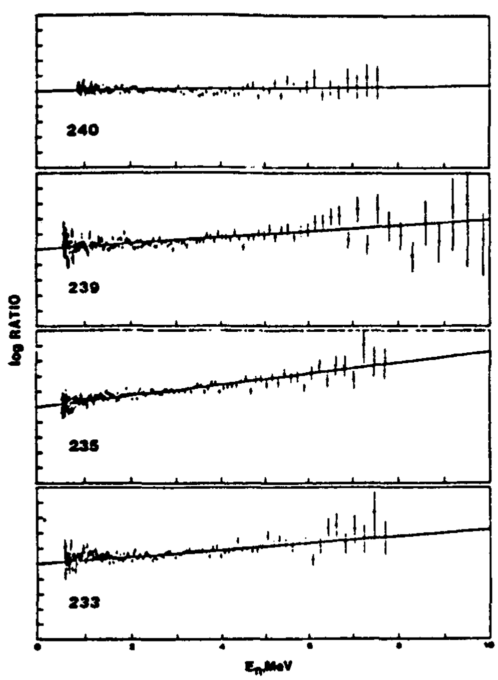

Fig. 7. Spontaneous fission-neutron-spectrum of ^{252}Cf relative to the neutron-induced-fission-neutron-spectra of a number of actinides.

Table 1. Percentage Fission Yields for Several Fissioning Systems

Fission Product	^{229}Th(n,f)	^{236}Np(n,f)	^{246}Cm(sf)
As-77	0.021 ± 0.003	-	-
As-78	0.32 ± 0.06	-	-
Se-83g[a]	2.54 ± 0.33	-	-
Br-83	-	0.35 ± 0.05	-
Br-84g[a]	10.01 ± 0.72	0.53 ± 0.09	-
Kr-85m[a]	9.22 ± 0.30	1.05 ± 0.05	-
Kr-87	7.21 ± 0.33	1.92 ± 0.19	-
Kr-88	7.51 ± 0.30	2.37 ± 0.19	-
Sr-91	6.35 ± 0.20	4.94 ± 0.33	-
Sr-92	5.40 ± 0.62	4.82 ± 0.58	-
Y-93	5.11 ± 0.20	5.45 ± 0.52	-
Y-94	4.51 ± 0.43	-	-
Zr-95	2.77 ± 0.08	6.48 ± 0.52	1.99 ± 0.28
Zr-97	0.73 ± 0.03	6.60 ± 0.25	2.37 ± 0.29
Mo-99	0.15 ± 0.01	6.44 ± 0.28	4.24 ± 0.36
Ru-103	0.026 ± 0.004	5.08 ± 0.25	6.86 ± 0.60
Tc-104	-	2.84 ± 0.35	-
Ru-105	0.013 ± 0.002	2.30 ± 0.09	6.82 ± 0.96
Pd-109	0.012 ± 0.002	0.17 ± 0.03	
Ag-111	0.023 ± 0.003	0.041 ± 0.006	4.64 ± 1.97
Pd-112	0.020 ± 0.003	0.028 ± 0.005	4.05 ± 0.54
Cd-115g[a]	0.021 ± 0.003	0.048 ± 0.008	-
Sn-121g[a]	0.0073 ± 0.001	0.036 ± 0.006	-
Sn-125g[a]	0.0030 ± 0.0005	0.042 ± 0.008	-
Sb-127	0.0092 ± 0.002	0.39 ± 0.04	-
Sb-129	0.084 ± 0.015	1.36 ± 0.15	-
I-131	0.56 ± 0.02	3.99 ± 0.30	3.39 ± 0.29
Te-131m[a]	-	0.68 ± 0.30	-
Te-132	1.19 ± 0.04	4.97 ± 0.23	4.68 ± 0.38
I-133	2.95 ± 0.09	6.13 ± 0.33	5.81 ± 0.53
Te-133m[a]	-	1.82 ± 0.11	-
Te-134	5.46 ± 0.43	5.06 ± 0.46	-
I-134[b]	-	3.8 ± 1.2	-
I-135	5.06 ± 0.16	6.31 ± 0.40	6.31 ± 0.63
Ba-139	-	6.90 ± 0.53	-
Ba-140	8.57 ± 0.25	6.28 ± 0.25	6.54 ± 0.65
Ce-141	7.51 ± 0.38	6.23 ± 0.37	5.47 ± 0.56
La-142	7.28 ± 0.25	4.88 ± 0.23	5.74 ± 1.41
Ce-143	8.22 ± 0.25	4.68 ± 0.21	5.46 ± 0.56
Ce-144	9.39 ± 1.06		5.19 ± 0.91
Nd-147	2.40 ± 0.07	1.56 ± 0.07	2.62 ± 0.24
Nd-149	0.65 > 0.03	1.11 ± 0.06	-
Pm-151	-	0.54 ± 0.03	-
Pm-153	-	0.26 ± 0.05	-
Sm-156	-	0.041 ± 0.004	-

[a] Isomer yield
[b] Independent yield

those of ENDF/B-IV-V and the implications on common integral parameters examined. This assessment raises some significant questions as to the accuracy of measured and/or evaluated prompt-fission-neutron spectra.

4. Precision Measurement of Intensities of Alpha Groups in the Decay of Actinide Nuclei (I. Ahmad)

Our program on the measurement of α-transition intensities of actinide nuclei is part of the IAEA coordinated Research Program on Transactinium Decay Data. Precision measurement of intensities of α-groups in the decay of ^{238}Pu and ^{240}Pu have been made and experiments to measure intensities of ^{239}Pu and ^{242}Pu α-groups are in progress. Isotopically pure samples for these measurements were prepared by the Argonne electromagnetic isotope separator and α-particle spectra were measured with high-resolution Au-Si surface-barrier detectors. Results of our measurements will be presented by C. W. Reich at the June IAEA meeting in Vienna.

5. Decay Properties of 2.22-h ^{250}Es (I. Ahmad and R. J. Sjoblom)

The decay scheme of 2.22-h ^{250}Es has been investigated by measuring gamma ray and conversion electron spectra of mass-separated sources. Intensities of gamma-rays in per cent per electron capture decay have been obtained.

6. Nuclear Structure Theory of the Actinide Elements (R. Chasman)

A large-scale theoretical treatment that incorporates octupole and quadrupole particle-hole modes, together with pairing in the residual interaction, is being developed. In this approach, these particle-hole modes are treated on an equal footing with pairing in a non-perturbative way. A product form of the pairing interaction that avoids the shortcomings of monopole and quadrupole pairing, has been incorporated into this treatment. The method has recently been extended to include odd-mass nuclides.

This model is being used to develop a description of nuclear states in the light actinide region ($225 \leq A \leq 235$). In this region the $K\pi = 0^-$ octupole mode is very important, as signified by the low-lying 0^- state in this region. The coupling of this mode to single-particle states is being investigated. It appears to give rise to large shifts in the single-particle spectrum. The question of which nuclides in this region are most likely to have permanent octupole deformations, with the associated parity doublets, is being investigated.

7. The Half-Life of ^{230}Th (J. W. Meadows, R. J. Armani, E. L. Callis and A. M. Essling)

The specific activity method was used to measure the ^{230}Th half-life. Measurements were made with four isotopic mixtures of ^{230}Th and ^{232}Th ranging from 0.383 to 99.52% ^{230}Th. Sample weights were determined by mass spectrometric isotopic dilution analysis. Alpha counting was done in a low geometry counter whose geometry factor was calculated from precisely measured dimensions. The ^{230}Th half-life was determined to be 75381 ± 295 years.

D. PHOTO-NUCLEAR PHYSICS

1. Photodisintegration of the Deuteron (R. J. Holt, H. E. Jackson R. D. McKeown, J. R. Specht and K. E. Stephenson)

The deuteron is the simplest nuclear system for the study of the meson exchange and virtual isobar effects. Theoretical predictions indicate that the angular distribution of photoneutrons near threshold should be sensitive to final state interactions and momentum dependent effects in the n-n potential. Furthermore, the measurement at Mainz of the D(γ,p) reaction at 0° were in disagreement with all theoretical predictions at moderate photon energies. Thus, it is essential to have accurate measurements of the angular distribution of photoneutrons from the D(γ,p) reaction from threshold to 20 MeV. Relative angular distribution measurements at 45°, 90°, 135° and 155° from threshold to E_{γ} ~20 MeV are in progress. In order to ensure that the desired accuracy ($\lesssim$3%) is achieved a number of preliminary experiments have been carried out to study the magnitude of systematic errors. In particular, the problem of multiple neutron scattering in the target was studied in great detail. Measurements of the angular distributions are expected to be completed later during this year.

2. Photoneutron Studies of E1, M1 and E2 Excitations in ^{13}C (R. J. Holt, R. M. Laszewski, H. E. Jackson, J. E. Monahan and J. R. Specht)

The angular distribution for the $^{13}C(\gamma,n_0)^{12}C$ reaction was observed in the energy region 6.5 to 9.3 MeV and at angles of 90° and 135°. The photoneutron measurements were analyzed in terms of a multilevel R-matrix formalism. The $^{12}C(n,n)^{12}C$ reaction channel was explicitly included in this analysis. The effects of potential capture were directly observed in the photoneutron spectra. The ground-state radiative widths for resonances in this energy region were deduced from the R-matrix interpretation of the results. The E1 excitations at 7.69 and 8.19 MeV were found to be in good agreement with the predictions of the weak-coupling model.

3. Doorway Resonances in ^{29}Si (R. J. Holt, H. E. Jackson and J. R. Specht)

Since the discovery of doorway states in ^{29}Si, the theoretical advances in describing the ^{28}Si + n system have become more sophisticated. In the most recent theory the ^{28}Si(n,γ)^{29}Si reaction was described with the formalism of Boridy and Mahaux by construction of particle-vibration basis states. These theories indicate that there may be a substantial amount of radiative strength for doorway resonances above the present experimental observations. New (γ,n) work will be performed which makes use of the 25-m neutron flight paths and the newly installed multi-directional electron transport system. A $^{29}SiO_2$ quartz sample is currently being fabricated for this work.

4. Isospin Splitting of the Giant Dipole Resonance in ^{60}Ni (T. J. Bowles, R. J. Holt, H. E. Jackson, R. D. McKeown, A. M. Nathan and J. R. Specht)

The question of isospin splitting of the giant dipole resonance in non self-conjugate nuclei has long been an issue in photonuclear physics. Although there are a number of theoretical calculations which predict the amount of splitting and the relative strength of the two components $T_<$ and $T_>$, the experimental information is very sketchy.

The photoneutron reaction is a selective probe for isospin splitting. For example, in a (γ,n_0) reaction only photoneutrons from the $T_<$ component are allowed by the isospin selection rules; whereas in (p,γ) reactions both components can be excited.

In the present work we have observed the cross section at 90° for the ^{60}Ni(γ,n_0) reaction for the first time. The 25-m flight paths and high-current pico second pulse made it possible to achieve sufficient energy resolution to identify ground-state photoneutron transitions. The first results indicate only one broad peak in the (γ,n_0) cross section which is consistent with isospin-splitting of the giant dipole resonance. This work will be completed later this year.

5. Scattering-Matrix Elements for Nuclear Reactions Involving Photons (J. E. Monahan, R. J. Holt and R. M. Laszewski)

The transformation of scattering-matrix elements from a representation appropriate for particle channels to one that describes photon channels is rederived. Previous derivations have ignored an ambiguity in the relative phase of the vector potential for magnetic and electric multipole radiation. The resultant ambiguity in the S-matrix transformation seems to be a source of confusion about the relative phases of the various terms that contribute to the polarization of particles produced in photonuclear reactions.

6. Photon Scattering by the Giant Dipole Resonance (T. J. Bowles, R. J. Holt, H. E. Jackson, K. M. Laszewski, R. D. McKeown, A. M. Nathan, J. R. Specht and R. Starr)

The elastic and inelastic scattering of nearly monochromatic photons from ^{52}Cr, Fe, ^{60}Ni, ^{92}Ni and ^{96}Mo were studied in the energy region of the giant dipole resonance. The central goal of this work was to investigate the coupling of two dynamic collective modes in nuclei, i.e. the coupling of the giant dipole vibration to collective surface vibrations. The inelastic photon scattering provides a sensitive and direct probe of this coupling.

Experimentally, the photon beam was provided by the University of Illinois tagged-photon facility associated with the MUSL-2 electron accelerator. The scattered photons were detected in a state-of-the-art high-resolution NaI spectrometer. Calculations performed in the framework of a dynamic collective model indicate that this particular model for the coupling is able to account for the qualitative features of the data.

E. ACCELERATOR DEVELOPMENT

1. Status of the Argonne Superconducting Linac Project (L. M. Bollinger)

At the present time, the superconducting-linac heavy-ion energy booster under development at Argonne is being employed almost routinely to accelerate beams for use in nuclear-physics research. Twelve resonators have been installed, four more will be added during 1980, and the eight final resonators of the booster will be added in 1981.

The most energetic beam accelerated to date is ^{32}S at 232 MeV, which is approximately equivalent to the performance of a tandem with 16.8 MV on the terminal and two strippers. The upper energy limit is being extended steadily.

After more than 3000 hours of beam time, the performance of the superconducting linac has proved to be remarkably stable and reliable. For example, most of the six resonators installed in January 1979 are still operating with essentially the same Q values and accelerating fields as initially. An indication of the reliability of the system is the fact that, once the machine is put into operation, it has not been necessary to have operators on hand. Rather, users of the machine monitor the linac operation and even change the beam energy, as required.

Originally the linac was operated by means of manual controls, but computer control will soon be the standard mode of operation. All the experience to date indicates that computer-controlled operations will be substantially more efficient and reliable.

BROOKHAVEN NATIONAL LABORATORY

A. NEUTRON CROSS SECTIONS

1. The Capture of 24 keV Neutrons and Stellar Nucleosynthesis

(T. J. Bradley, F. Parsa (New Jersey Institute of Technology), M. L. Stelts, and R. E. Chrien)

The neutron capture cross sections of a number of isotopes have been measured by activation in the 24 keV neutron beam at the HFBR. The isotopes measured were ^{112}Sn, ^{130}Ba, ^{146}Nd, ^{148}Nd, ^{186}W, ^{190}Os, and ^{192}Os. Some of these are relatively low abundance isotopes on the neutron deficient side of the valley of stability. The reliability of the technique was checked by the ^{186}W measurement. The relevance of these results to stellar nucleosynthesis lies in the relatively close proximity of the mean energy of the flux available through an Fe/S filter (24 keV) and the energy corresponding to stellar temperatures, ∿30 keV.

The intensity available with the Fe/S filter at BNL is about 4×10^7 n/sec in a beam of about 8 cm^2.[1] This flux is adequate for activation of even relatively low abundance isotopes such as ^{130}Ba. The measurements were done relative to ^{197}Au whose average cross section over the iron window is known to be 620±3 mb. Samples were prepared in sandwiches of 0.2 gm/cm^2 of Au and ∿/gm/cm^2 of the unknown placed between two sheets of 0.022 gm/cm^2 of Cd, to minimize the effect of thermalized, room return, neutrons.

After irradiation intervals of approximately 1 day the samples were placed in a fixed geometry about 12 cm away from a 10% efficiency Ge(Li) detector. Calibration of the detector efficiency was dependent on ^{226}Ra and ^{182}Ta sources. Irradiations were typically for 24 hours and counting times ranged from a few hours for ^{148}Nd to two weeks for ^{112}Sn.

Figure A-1 shows a typical spectrum, that of neodymium after irradiation, with a dispersion of 0.5 keV/ch. The need for high resolution is apparent from the numerous decay lines seen in the spectrum.

The well known cross section of ^{186}W (250 mb)[2] was in good agreement with our results (247±12), giving confidence in the techniques.

Most compilations of cross sections for stellar nucleosynthesis are done at 30 keV, so it was necessary to extrapolate our results to the energy. To do this we calculated the 24 keV cross sections from the relation,

$$\sigma = 2\pi^2\gamma^2 \sum_{\ell,J} gJ\ (\langle\Gamma_n\rangle/D_J)\ (\langle\Gamma_\gamma\rangle/\langle\Gamma\rangle)F$$

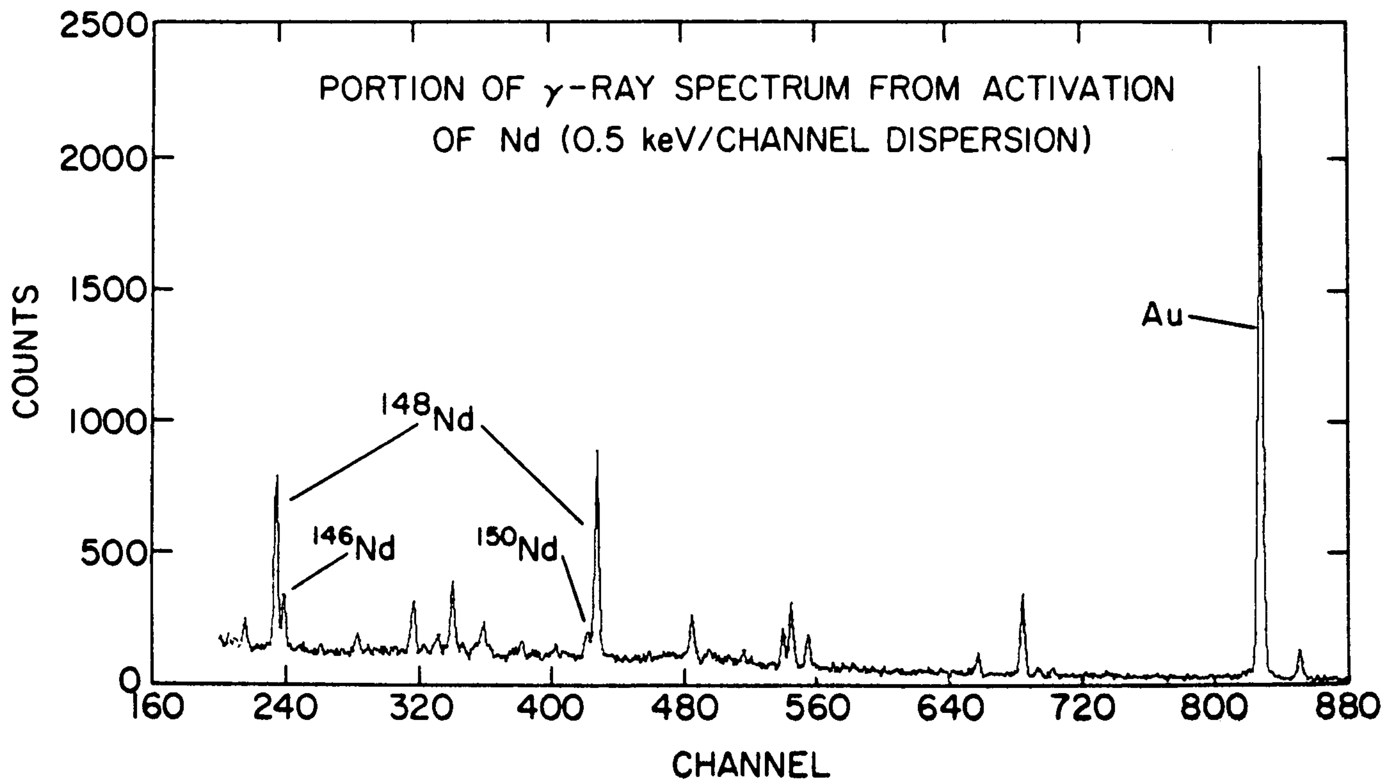

Figure A-1   A portion of the activation spectrum of Nd at 24.3 keV.

where F is Lynn's fluctuation factor. We varied parameters D_J to achieve agreement and then calculated the 30 keV cross section from the same parameters. While the cross sections at 24 keV are directly measured over the ∿2 keV wide window, the extrapolated cross sections will be subjected to additional averaging error, dependent on the number of resonances appearing in that window. This fluctuation error is not included in the table.

Table A-1

Capture Cross Sections Determined in This Experiment

Nuclide	Measured Cross Section at 24 keV	Corrected Cross Sections at 30 keV	Previous Value
^{112}Sn	228±25	202	180†
^{130}Ba	755±54	715	2000†
^{146}Nd	88±6	75	110±25
^{148}Na	127±8	99.4	110±20
^{186}W	247±12	221	220±20
^{190}Os	359±38	320	230
^{192}Os	156±16	144	200

2. S- and P-Wave Neutron Strength Functions Derived from Resonance-Averaged Capture (M. L. Stelts and R. E. Chrien)

In the previous DOE-NDC report, we described a new method of measuring S- and P-wave strength functions from the relative population of final states of given spin and parity by primary transitions following neutron capture. The population depends upon the relative admixture of partial waves and can be calculated given the knowledge of average E-1

† Semi-emperical estimates due to Allen *et al.*[3]

1 R. C. Greenwood and R. E. Chrien, Nucl. Instr. & Meth. 138, 125 (1976).

2 BNL 325, Vol. 2C, Supplement #2 (1966).

3 Allen, Gibbons and Macklin, Adv. in Nucl. Phys. 4 205 (1971).

and M-1 photon strengths.

A computer code, SPARC, has been written to calculate the relative intensities to all final states populated by dipole transitions, and spectra from 24.3 keV and 2 keV neutron capture in the HFBR ^{56}Fe-S filtered beam and scandium beam, respectively, have been analyzed for a number of cases, including ^{167}Er, ^{154}Sm, and ^{238}U targets.

An example of the agreement between measurement and calculation is given by the ^{167}Er case, as shown in Figure A-2. Here the relative populations of the accessible final states are shown for 2 and 24 keV, with the observed populations compared to the calculations from the SPARC code. One notes that the intensities change significantly for certain states in going from 2 to 24 keV, and this reflects the different proportion of ℓ=0 and ℓ=1 components in the beam. The change is particularly spectacular for the higher spin states, as, for example, the 6^+ and 6^- states. For the figure, the following parameters were assumed: Γ_γ=87 meV, $\bar{D}_{obs}$=4eV, and $\langle\Gamma_n^o\rangle/\bar{D}/_{\ell=0}=1.8\pm0.2\times10^{-4}$. From these parameters, all taken from BNL-325, one can deduce the value:

$$\langle\Gamma_n^1\rangle/D = 1.38 \pm 0.10 \times 10^{-4}$$

relative to the assumed value of $\langle\Gamma_n^o\rangle/D$. The p-wave strength function had not been previously measured for ^{167}Er, but the above value is consistent with systematics in this mass region.

For ^{154}Sm, we find

$$\langle\Gamma_n^1\rangle = 2.1 \pm 0.7 \times 10^{-4}$$

relative to a value of $1.8\pm0.5\times10^{-4}$ for $\langle\Gamma_n^o\rangle/D$, from BNL-325.

A closer examination of the above cases shows that the agreement between calculation and experiment for the primary γ-ray intensities is poorest for the higher spin states. There has been noticed, moreover, a systematic tendency for high spin states to be populated more strongly than might be expected, considering only ℓ=0 and ℓ=1 waves. It is tempting to explain this observation by including an ℓ=2 component. A case in point is ^{238}U, where the population of the 5/2 gs$^+$ states of ^{239}U at 2 keV, and of the $5/2^-$ state (E_{ex}=539 keV) at E_n=24 keV are much larger than expected. Adding an E-2 component to the photon strength function would enhance the $5/2^+$ intensity at 2 keV, while the ℓ=2, D wave, component would enhance the $5/2^-$ state through an E-1, $3/2^+$, $5/2^+ \rightarrow 5/2^-$ transition. The former adjustment would require an enhancement of about 5 over the single particle E-2 estimate. For the latter case, the required D-wave component would be of the order of six times the S-wave strength function. While these seem to be rather large enhancement factors, the results are still too tentative for definite interpretation.

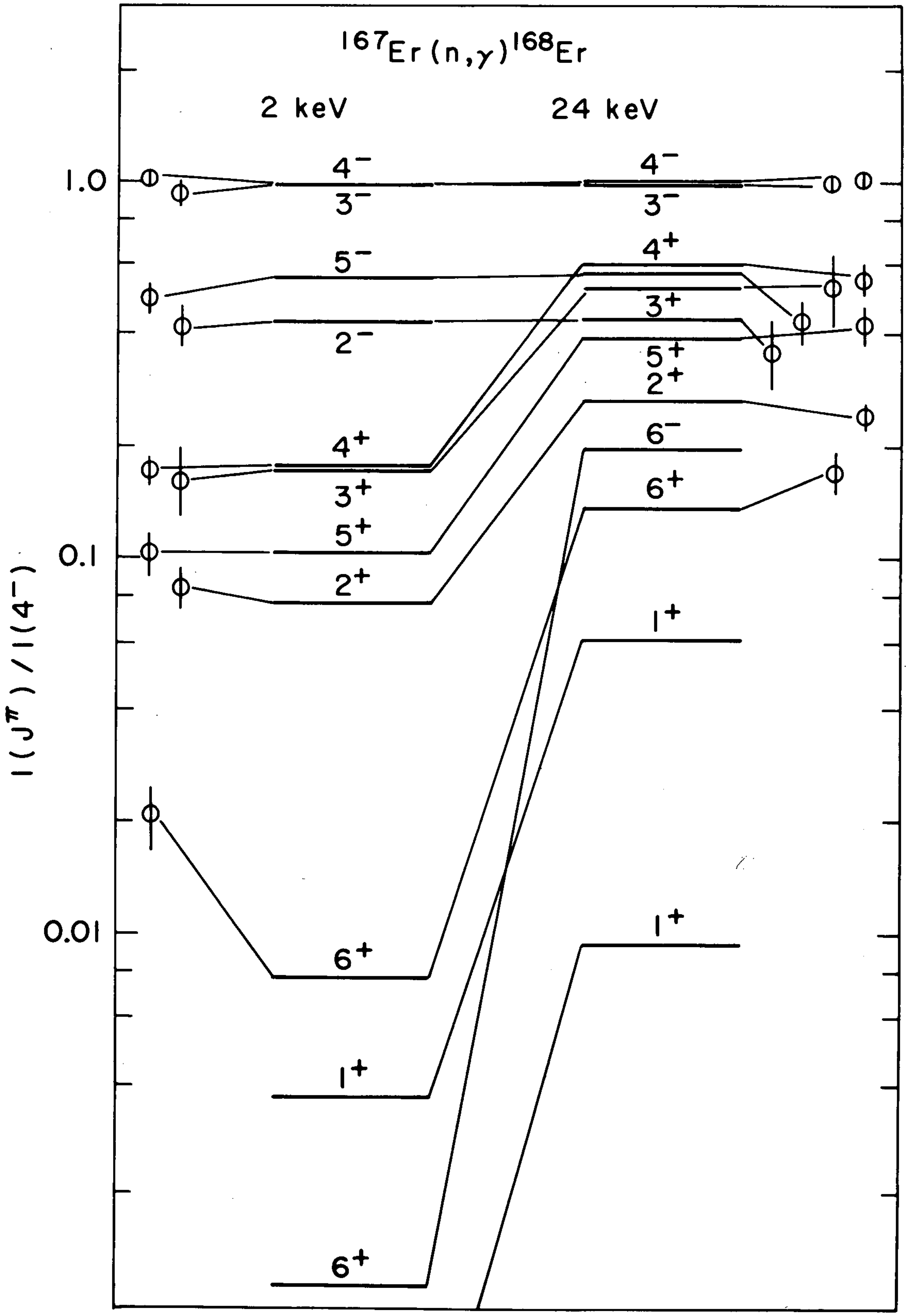

Figure A-2 The population of various final states of ^{168}Er at 2 and 24 keV, compared to calculation.

They are suggestive, however, and we plan for further experiments to define these elusive quantities.

3. Doppler Broadening in Silver Samples (H. I. Liou, R. E. Chrien, and R. Moreh†)

The analysis of the data on the broadening of the 16.3 eV capture resonance of ^{107}Ag has been completed. The effective temperatures T', defined by Lamb theory in the weak binding approximation, have been measured and the DeBye temperature, θ_D, extracted for the cases of metallic Ag, AgCl, and Ag_2O at T=294°K, 77.2°K, and 4.07°K.

Examples of the excellent quality of the least-square fits to the resolution broadened Doppler shape are given in the figures, which show Ag at room temperature and AgCl at 4°. The statistical uncertainties are less than the size of the plotted points. We used known values of Γ_γ, $g\Gamma n$, g, and resolution width ΔE, to extract the best fit values of Δ/Γ and T', from the data. The results are displayed in the table. In all cases the X^2/f quality was of the order of unity.

Table A-3

T' and Deduced θ_D Values

	T=294		77.2		4.066	
	T'	θ_D	T'	θ_D	T'	θ_D
Ag metal	303	226	108±6	229±25	82±7	219±19
AgCl	318±7	379±57	107±6	225±25	64±6	171±16
Ag_2O	306±7	267±83	123±7	285±25	66±10	176±27

As expected, the θ_D for metallic silver is invariant, following Debye theory. For the components, the θ_D is not constant, indicating Debye's theory is not followed exactly. The θ_D for Ag metal is in excellent agreement with previous calorimetric and neutron scattering data. The AgCl results are also consistent with calorimetric, elastic constants, and neutron scattering data at 77° and 4°. The θ_D value for HgCl at room temperature, however, appears to be anomalously high. For Ag_2O, the high result at T=77° appears to be especially interesting; however we are unaware of any previous measurements for Ag_2O.

† Not at University of Illinois.

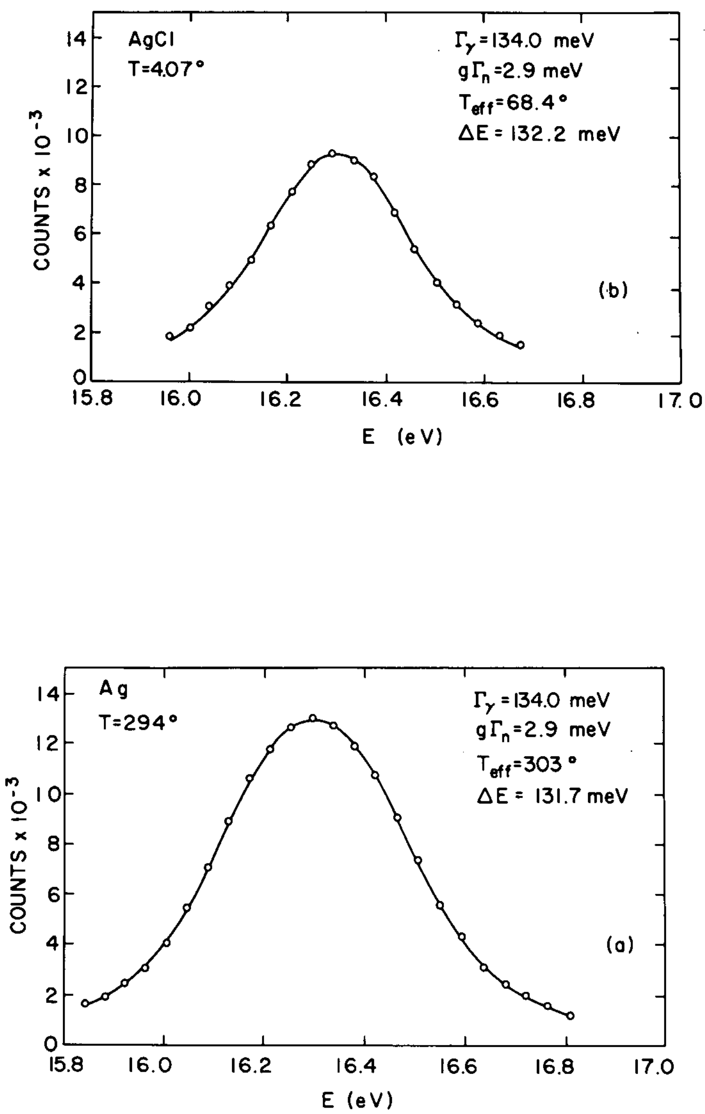

Figure A-3 Least squares fits to the Doppler and resolution-broadened resonance yields for the (n,γ) reaction on ^{167}Ag at the 16 volts resonance.

4. Photon and Neutron Strength Function for the $^{87}Sr(n,\gamma)^{58}Sr$ Reaction (M. L. Stelts and R. E. Chrien, BNL; J. Becker and R. Sullivan, LLL; J. C. Browne, LASL)

The spectral data from the capture of neutrons by ^{87}Sr is needed to understand the systematics of neutron and photon strength functions for the A∿80 region. Extraction of the strength functions requires knowledge of the excitation energies, spins and parities of levels in ^{88}Sr. The relatively low initial state level densities, high binding energy and high capture state spin give rise to a rather high multiplicity for cascade gamma-rays and a mixture of rather strong primary and secondary γ-rays at similar energies.

Measurements were first made in 1975 at BNL with the Fast Chopper (for discrete resonance data) and with the 'tailored' beam facility at 2- and 24-keV (for averaged capture) with single Ge(Lc) detectors. The average capture measurements allow one to make a clear distinction between primary and secondary γ-rays. A careful analysis of these data led us to the following conclusions: a) the initial state averaging for the 'tailored' beam measurement was insufficient to determine the final state spins and parities, and b) the final state level scheme (constructed with Ritz combination and intensity balances) was subject to considerable uncertainty.

With the assistance of the Livermore group, a sample of enriched ^{87}Sr was procured. The response function of the BNL-HFBR pair spectrometer was carefully measured with mono-energetic γ-ray sources: $^{1}H(n,\gamma)$; ^{228}Th, PuBe, $Pu^{13}C$, and $^{207}Pb(n,\gamma)$. The Sr spectra were measured at thermal, 2- and 24-keV with the 'tailored' beam. The response function is being extracted at Livermore to provide the gross γ-ray spectrum above 1.5 MeV γ-ray energy. The data are also in the process of analysis at BNL for discrete γ-ray lines. The simple response and high resolution of the pair-spectrometer has resolved several previous discrepancies in the previous measurements.

Spectra have also been measured at each of the three neutron energies with the pair-spectrometer operated in the singles mode to extract better low energy secondary data. Most recently some 38 million γ-γ coincidence events have been taken. This will enable us to resolve problems with multiple placement γ-rays under Ritz-combinations and construct a reliable level scheme for ^{88}Sr. Analysis is still in progress.

B. NUCLEAR STRUCTURE STUDIES WITH NEUTRONS

1. Systematic Determination of the Pairing Gap for Even-Even Nuclides (M. L. Stelts and R. J. Casten)

It is well known from the mass formulas that even-even nuclei tend to have pairing energy gaps about 2 MeV wide for medium to heavy mass numbers. States below this gap have a collective nature, while above the gap particle-hole excitations are possible. The onset of these excitations will be reflected in a rather sudden increase in the level density, mitigated only by the Fermi distribution.

The resonance-averaged capture techniques populate rather evenly all final states in a given spin-parity range, subject to the degree of averaging combined with the properties of the chi-square distribution class. The guarantee that all levels in the range will be populated, independent of nuclear structure properties, ensures that the sharp change in density above the gap can be observed rather cleanly.

This observation is illustrated in Figure B-1, for the case $^{195}Pt(n,\gamma)^{196}Pt$. The sharp change is clearly evident in the cumulative plot of observed levels against excitation energy. For comparison is plotted the values of $2\Delta n$ and $2\Delta p$, respectively, taken from the mass compilation of Wapstra and Bos. The prediction of the semi-empirical mass formula seem to be well borne out.

The preliminary results of our survey is contained in the following table, which lists E_D (experimentally observed break) vs E_S (theory), which is given by $E_D = 2\Delta o$, where Δo is the lesser of the pairing energy for neutrons or protons, P_N or P_P.

$$P_N(Z,N) = 1/4\ (-Sn(Z,N-1)+2Sn(Z,N)-S_n(Z,N+1)$$

$$P_P(Z,N) = 1/4\ (-Sp(Z-1,N)+2Sp(Z,N)-Sp(Z+1,N))$$

Table B-1

	Es(exp)	E_D(theory)
^{148}Sm	1.90 MeV	2.03 MeV
^{150}Sm	2.01	2.25
^{190}Os	1.89	1.95
^{196}Pt	1.78	1.94

The effect of blocking, which is not taken into account in the simple, first-order calculation given above, is expected to lower the gap energy by about 5%. We plan to continue these measurements to

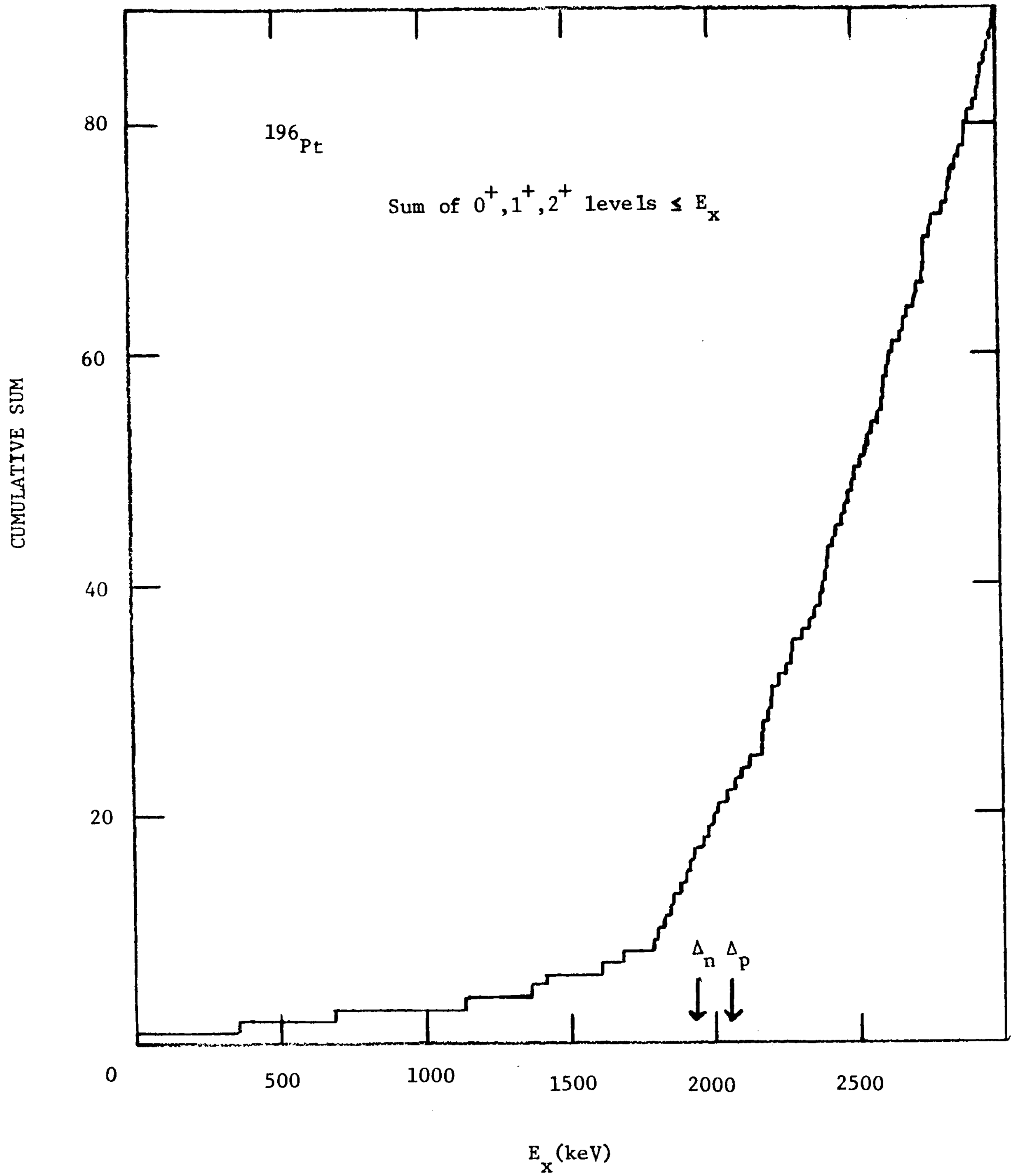

Figure B-1 Cumulative level plot of final states in ^{196}Pt populated by ^{195}Pt(n,γ)^{196}Pt with 24 keV neutrons.

include more nuclei, and to refine the theoretical calculations to try better to fit the experimental results.

2. Resonance Capture γ-rays from Se Isotopes (C. Engler, H. Liou, and R. E. Chrien)

Resonance captures for Se isotopes were measured at the 48 m station of our fast chopper time-of-flight system. A natural sample of Se metal powder having 3.63 gm/cm^2 was used. The data analysis has been essentially finished. The numbers of the primary capture γ-rays identified for each measured resonance and having their intensities extracted, are as follows: 13 and 3 for 27.1 eV and 271.5 eV in ^{75}Se(CN); 3 for 377.0 eV in ^{77}Se(CN); 1.4 and 4 for 112.0 eV, 211.6 eV and 340.8 eV in ^{78}Se(CN); 2 for 1970 eV in ^{81}Se(CN). Assuming only E1 transition γ-rays detected, we infer that the spin and parity for the final states of the observed transitions are ($1/2^-$ $3/2^-$) in 27.1 and 271.5 eV resonances of ^{75}Se(CN), (0^+1^+) in 211.6 eV resonance on ($J^\pi=0^-$) of ^{78}Se(CN), and ($0^+1^+2^+$) in 34.8 eV resonance ($J^\pi=1^-$) of ^{75}Se(CN). The absolute intensities of primary γ-ray were obtained by a comparison with Au capture γ-rays in 4.91 eV resonance. It is of particular interest that the 7733.85 keV transition to 293.21 keV level in ^{75}Se has anomalously large intensity of 14.2% for 27.1 eV resonance and 12.9% for 271.5 eV resonance. The same γ-ray in thermal capture has even a stronger intensity of 22%. This could not quantitatively count either as statistical fluctuation or as direct reaction in valence model.

A thermal capture experiment of Se was also performed with our filtered beam facility, using a natural sample of 8.684 gm and 3.18 x 3.18 cm. The three crystal high resolution spectrometer supressed continuous Compton background as well as the full energy and single escape peaks. A total of 182 γ-rays between 4.3 and 10.5 MeV were identified with improved energies and intensities. Out of them there are 46 newly discovered lines due to either ^{76}Se or ^{77}Se capture. In addition, a low energy measurement found 202 secondary γ-rays between 0.3 and 2.0 MeV. Most of them have clear isotopic identification, and have their energies and intensities accurately determined. Neutron binding energies for various isotopes were deduced from an investigation of many well-established γ-ray cascades. The results are Q(keV) =8027.49$\pm$0.39, 7418.80$\pm$0.23, 10497.78$\pm$0.32, and 6701.06$\pm$0.56 for ^{75,77,78,81}Se(CN) respectively. The γ-ray intensities were normalized to the known gold thermal capture lines. The strong 9883.27 keV primary transition (I=7.3%) in ^{78}Se(CN) to a 2^+ state at 613.8 keV, indicates that the thermal capture of ^{77}Se has a substantial contribution from a J=1 bound state. Since E1 transition is dominant in Se capture, a maximum likelihood method was adopted to obtain the E1 photon strength functions for ^{75,77,78}Se(CN); $k(10^{-9}MeV^{-3})$=1.4$\pm$0.6, 1.2$\pm$0.4 and 1.7$\pm$0.5 for the Single Particle Model, and $k(10^{-9}MeV^{-5})$=5.6$\pm$2.6, 7.1$\pm$2.3 and 6.6$\pm$2.1 for the Giant Dipole Resonance Model, respectively.

3. Resonance Capture of Rb Isotopes (G. Engler, H. I. Liou, and R. E. Chrien)

Substantial data of both high and low energy γ-ray spectra for Rb(n,γ) reaction have been taken using a natural Rb_2CO_3 sample. The resonance capture was carried out at 48 m station of our time-of-flight system, and the thermal capture at 22 m station. Several neutron resonances in $^{85,87}Rb$ below 2 keV can be used to extract nuclear level structure information. We are particularly interested in the photon strength functions. The data are being processed.

A uniform metal plate of potassium (15.2x15.2x0.635 cm) has been used as a target to measure resonance and thermal capture. Both high and low energy γ-ray data were taken, and their preliminary analysis has been done. The main interest is for the 1.111 keV resonance in ^{39}K. After a subtraction of background lines four primary transitions, populated at 24.5, 800-1, 1958.3 and 2260.3 keV states, were identified. Two primary γ-rays of 4647.5 and 7800.6 keV have also been found in the ^{39}K 3.2777 keV resonance capture.

4. Captive in ^{52}Cr (J. Kopecky, ECN, and R. E. Chrien, H. I. Liou, BNL)

Neutron capture γ-ray measurements have been performed upon a natural sample of Cr at 48 m station. The experiments are due to a joint effort of BNL with ECN, Petten (The Netherlands) laboratory. Twenty-six primary γ-rays were observed from the 1626 eV p-resonance of ^{52}Cr. Twenty-four of them were assigned to a level scheme, and the spin-parity of this resonance was determined as $3/2^-$. A separate thermal measurement at Petten with an enriched (99.9%) isotopes showed that the neutron separation energy of ^{53}Cr is 7939.1±0.2 keV. The high (n,γ)-(d,p) correlation found for thermal capture is absent for the p-resonance, however the γ-ray intensities from thermal and resonance capture are correlated with $p=0.86^{+0.06}_{-0.11}$. The results were recently published at Nucl. Phys. A334 (1980), 35-44.

5. The $^{45}Se(n,\gamma)^{46}Se$ Reaction (H. I. Liou, R. E. Chrien, BNL; J. Kopecky, J. A. Konter, ECN)

The study of $^{45}Sc(n,\gamma)$ reaction represents a cooperative work of BNL with ECN, Petten. Primary and secondary γ-rays were measured at four resonances (460.6, 1060.4, 3290 and 4330 eV). High accuracy measurements near the thermal region (0.14-7.65 eV) resulted in an improved set of primary γ-ray energies and level energies above 1 MeV. We obtain a neutron binding energy $B_n(^{45}Sc)=8760.5(2)$ keV. Absolute intensities of γ-rays were derived by comparison to the 4.91 eV resonance capture in gold. E1 and M1 radiation strengths were observed to be about equal. No correlation of any kind was observed. The primary

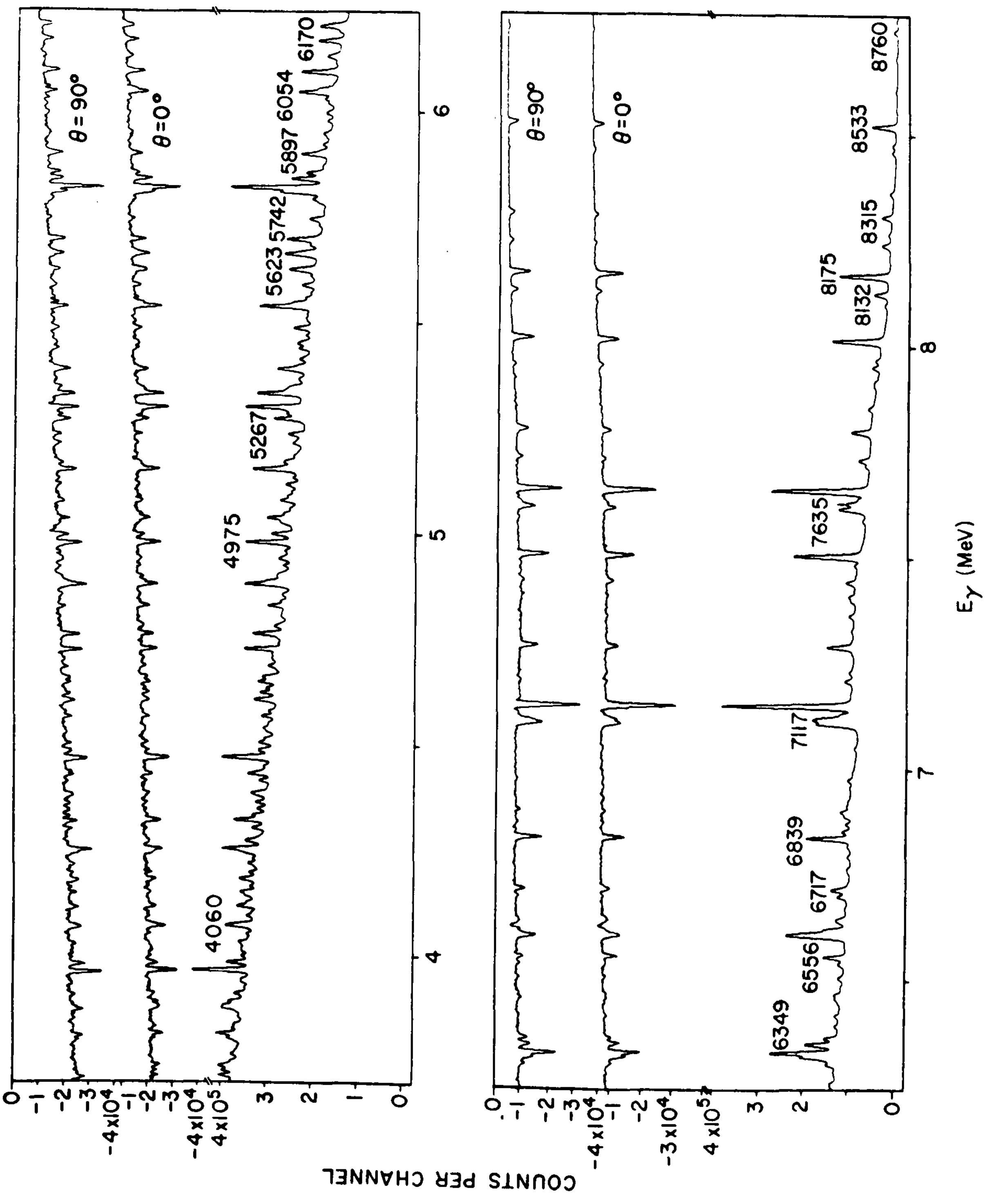

Figure B-2 Spectra obtained for polarized neutron capture on a polarized target of ^{45}Se at thermal neutron energies.

γ-ray spectrum following the capture of polarized neutrons in oriented and unoriented ^{45}Sc nuclei was studied. The final results will be published at Nucl. Phys. A. From the polarized neutron polarized target spectra, an example of which is shown in Figure B-2, information on spin assignments can be obtained. A combined χ^2-analysis of these two experiments resulted in 21 unique spin assignments and many spin restrictions. The fraction of spin $J=3^-$ in thermal capture was determined to be $(92\pm5)\%$.

6. Tests of the Interacting Boson Approximation (R. F. Casten, D. D. Warner, M. L. Stelts, W. R. Kane and Grenoble Collaborators)

Recent studies carried on at BNL and Grenoble have culminated in an extensive test of the IBA model in the Pt-Os region, including the discovery of the O(6) limit in ^{196}Pt and of the O(6) to rotor transition. Experimental studies of a number of nuclei were performed. To finish the experimental study of ^{190}Os, average resonance capture experiments have been performed. The results verified the completeness of the earlier level scheme. The calculations of the O(6) to rotor transition led to a number of unambiguous model predictions for thus far unknown experimental quantities. Several new experiments were started to supply these numbers. These include a more extensive study of transitions in ^{192}Os using double neutron capture and the GAMS spectrometer in Grenoble in order to establish the decay of excited 0^+ states, and a search for E0 transitions from 0^+ levels in ^{188}Os and ^{196}Pt with the BILL spectrometer at Institut Laue Langevin (ILL) in Grenoble.

The theoretical microscopic refinements of the IBA currently underway lead to predictions of other regions of the O(6) symmetry besides ^{196}Pt. One of these regions centers on the Xe-Ba nuclei, and two studies, of levels in ^{132}Xe and ^{136}Ba, are underway. The ^{132}Xe experiment involves the construction of gaseous in-pile targets for use at the ILL and serious target construction problems still remain to be solved. The ^{136}Ba experiment is nearly completed. Another study involved the measurement of average resonance capture spectra of ^{168}Er, to complement extensive ILL data. A thorough level scheme was developed for this well deformed and presumably well behaved nucleus extending beyond 2.5 MeV: it is one of the most complete schemes in existence. It will be used to test several nuclear models including the IBA, in particular the properties and couplings of the f boson, and the possible involvement of the g boson in that model.

In the past year Iachello and co-workers have developed an IBA model of odd nuclei. A study of the level scheme of ^{109}Pd was completed this year and included the discovery, for the first time, of the complete set of low spin levels associated with a unique parity orbit. Normally, only high spin unique parity levels are known, through heavy ion reactions. These are usually interpreted with the particle-rotor model. A more sensitive test, however, occurs for the low spin states of the same parentage. In ^{109}Pd it was found that the particle-rotor model failed to account for the data. Calculations with the IBA, however, succeeded rather well and provided the first sensitive test of the model for odd mass nuclei. A new study of ^{103}Ru was then started to further test the model; average resonance capture studies were completed at BNL and conversion electron studies at the ILL are underway.

One new prediction of the odd mass IBA is the existence of supersymmetries in certain odd nuclei in regions where the even core nucleus has one of the three special IBA limits. The A$\sim$190 regions offers an excellent testing ground since the even nuclei strongly resemble the 0(6) limit. Studies of ^{193,195}Pt are therefore underway as part of an ILL-BNL collaboration involving several (n,γ) techniques. The data collection phase is nearly completed. Level scheme construction and model calculations are planned.

Since the odd nuclei in both the A$\sim$100 and A$\sim$190 regions are transitional in character one might also expect an intermediate coupling model to offer an alternate useful theoretical approach. This idea is indeed reinforced by inspection of the detailed IBA wave functions for ^{109}Pd. Therefore one aim of these studies of odd mass nuclei is also the comparison of Nilsson, intermediate coupling and IBA models and the study of the interrelationships between these models.

7. Studies of Actinide Nuclides (BNL-Grenoble Collaboration)

The systematic behavior of levels in the odd-mass actinides has been the subject of a BNL-Grenoble-Livermore collaboration initiated a few years ago. Levels in ^{231}Th and ^{245}Pu were studied as part of this collaboration. The levels of ^{237}U up to 1 MeV have been studied, and the various bands built upon Nilsson single particle levels have been classified. This nucleus yielded interesting information on the decay of K=1/2 bands in terms of an expanded two-term form for the Alaga rules. The result leads to a value of zero for an important ratio of matrix elements involved in the theory of rotational nuclei. The reactions ^{231}Pa (n,γ) and ^{235}U(n,γ) lead to even mass actinides. The levels of ^{236}U have been difficult to study because of the competition from fission. The fission-to-capture ratio in ^{235}U has been enhanced by spreading the sample on the periphery of a disk, and viewing only a small part of the disk with a detector. The rotating disk intercepts the neutron beam near its periphery. The long-lived fission product activity is distributed over the disk while the prompt γ-rays are seen only near the detector. The relative enhancement of γ lines permits them to be distinguished from fission product activities. A study of ^{231}Pa(n,γ) supplies information not only on ^{232}Pa levels, but also on ^{233}U and ^{234}U formed by successive neutron capture in a high neutron flux. These experiments have been done partly at BNL and partly at Grenoble.

C. DEVELOPMENT IN SUPPORT OF FACILITIES

1. TRISTAN Construction and Development (R. E. Chrien, R. Gill, M. Shmid, and M. L. Stelts, and TRISTAN Users)

The TRISTAN on-line mass separator became operational in 1966 at Ames and over the intervening years produced numerous studies primarily of Kr and Xe nuclei and their daughters. With the decision to relocate the facility to BNL, came a unique opportunity to make major changes which will extend the range of nuclei available for study, improve the operating performance of the separator, and augment the data acquisition and reduction capabilities of the system. Since TRISTAN at the HFBR will be a national facility involving numerous groups of non-BNL users it was necessary to provide facilities to accommodate a greater variety of experiments than at Ames and to modify the separator control system to simplify operation by visitors.

The arrangement of the mass separator at the HFBR is shown in C-1. The major components of the separator with the exception of the ion source remain the same as they were in Ames. Several modifications were made in the layout geometry and ion beam optics in order to eliminate a 100^{o} electrostatic sector which was a necessary though troublesome component of the Ames system, and to permit installation of the optimum shielding configuration. In order to leave room for a second mass line for future experiments the distance between the collector box and the switching magnet has been increased. This necessitated introducing an additional electrostatic quadrupole singlet upstream from the switching magnet.

The improved ion optics system has performed as expected. The elimination of the electrostatic sector used at Ames has made alignment of the ion source and focusing elements possible. Operation of the system is much simpler as the einzel and quadrupole lens potentials do not usually require adjustment. Qualitatively, the focus appears to be better than that available at the Ames facility. A stable, well focused ion beam has been obtained through the switching magnet and on to the tape collector.

A major improvement to TRISTAN has been the incorporation of a FEBIAD-type ion source (forced electron bombardment--induced arc discharge) similar to the design of Kirchner and Roeckl.[1] The new ion source is shown in Fig. C-2. This ion source can be operated in the oscillating electron mode with the end cap at ground potential or in the direct-arc discharge mode with the end cap at anode potential. The former condition maximizes efficiency while the latter produces the best ion optics. Use of an intermediate end cap potential should permit selection of an optimum condition for operation. External Helmholtz coils generate an axial magnetic field to increase electron path length and thus ionization efficiency.

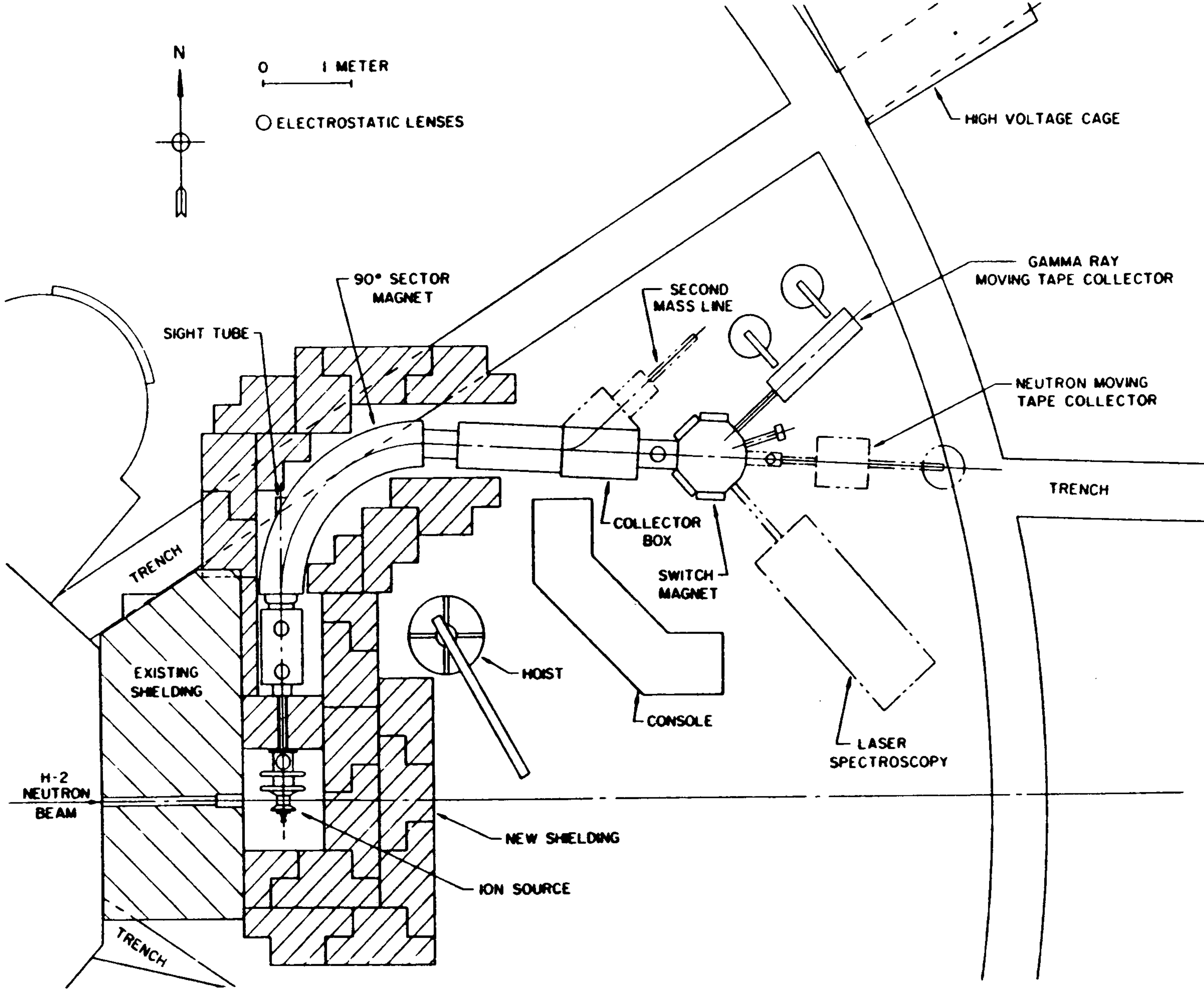

Figure C-1 Layout at the HFBR.

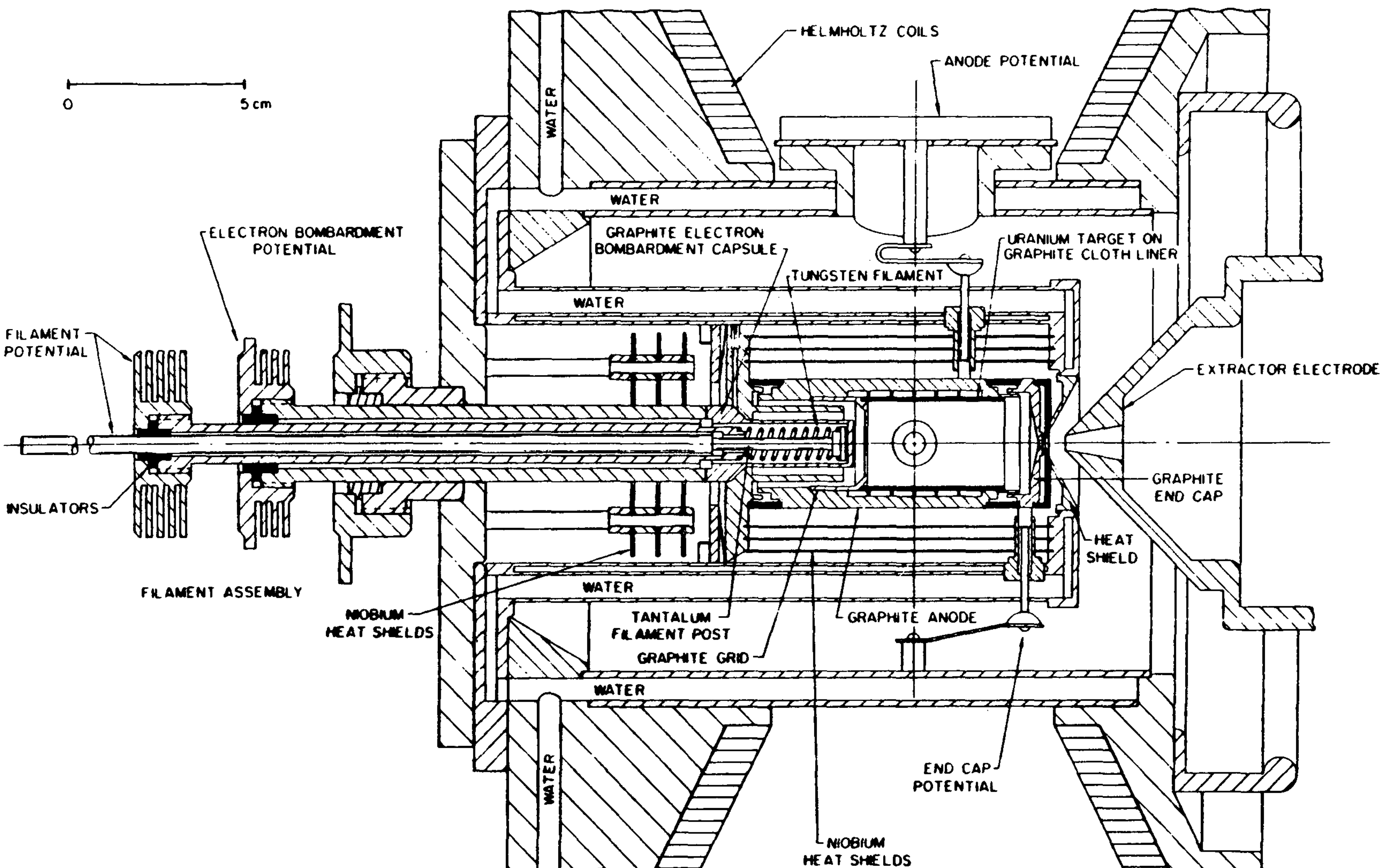

Figure C-2 The FEBIAD ion source used at TRISTAN.

Modifications to the FEBIAD source, which had been designed at Ames, have been made to improve reliability, stability, and lifetime. Initially we observed large oscillations in the anode and electron bombardment currents. These have been brought under control by providing better venting of the capsule and larger filament to capsule spacing. The lifetime has been extended from a few hours to lengths suitable for practical use by using materials near the filament and capsule which are more suited to high temperature operation and by reducing the length of the filament to prevent sagging. These changes, along with changes in the anode and end cap connectors, have greatly improved the reliability of the ion source.

The TRISTAN ion source operates in the temperature range of 1500-1800°C at a power load of about 1.5 kw. It is expected that at these temperatures approximately 20 of the more volatile elements ranging from Zn through La will be available either as direct fission products or from decay of parent nuclides. As experience with the new ion source is gained, efforts will be made to increase the operating temperature in order to reduce holdup time.

The more refractory transition elements and lanthanides are not likely to be extracted with significant yield even at higher temperatures. In order to address this difficult problem an ion source development program is being conceived at Brookhaven. Initial ion source target development will be done on the ISTU (Ion Source Testing Unit) which has been transferred from Ames. This system consists of an ion source housing, lens box with focusing elements, a 90° sector magnet and a collector box at the focal plane.

A second version of the improved FEBIAD source is being constructed as a backup to the present source. Furthermore, a surface ionization source, which is especially suitable for the alkaline metals, such as cesium and rubidium, is being designed.

Removal of the H-2 colliminator for TRISTAN experiments is now possible due to construction of a cask and colliminator modifications. The colliminator can be removed safely and easily to give maximum neutron flux for TRISTAN experiments and it can be replaced to provide the desired appature for the fast chopper time-of-flight experimental program.

2. The Data Acquisition and Analysis System for Nuclear Physics Research at the HFBR (M. L. Stelts, V. Manzella, R. Chrien and H. Liou)

During 1979 the old SDS-910 data acquisition system which had operated continuously since 1962 was replaced by a new system using two

[1] R. Kirchner and E. Roeckl, Nucl. Instr. Meth. 127, 307 (1979).

PDP-11 computers.

The old system served the 'tailored' beam and fast chopper experiments. The arrival of 'TRISTAN' mandated a system which could accommodate several additional data acquisition channels and which could easily be adapted to new experimental configurations. There were several constraints on the system design. With limited manpower, engineering support and budget it was necessary to use commercially available hardware and software as much as possible. To support a variety of experiments it was necessary to allow easy, flexible interfacing of many different experimental devices. An immediate data analysis facility was necessary to monitor the experimental data.

These criteria were satisfied with the following devices. A PDP-11/20 with an RT-11 operating system, disks and two magnetic tape drives were available. To interface the experimental data, a CAMAC system was connected to the unibus through a fast 4096 word microprocessor (MBD). The PDP-11/20 serves as master controller while the MBD serves the experimental devices. Experimental devices could either be directly inserted in CAMAC crates or fed through simple level translators which adapt the digital signal levels to CAMAC input registers. An external memory consisting of 10^6-16 bit words for necessary storage of spectra completes the hardware for data acquisition. The configuration is shown in Figure C-3.

The data analysis portion of the system consists of a PDP-11/34 computer with a floating point processor, extended instruction set and 108K of memory, disk drives, two magnetic tape units, a VT55 display terminal, a printing terminal and a verrsatec printer plotter. The configuration is shown in Figure C-4.

Both the data acquisition and analysis programs are written as much as possible in FORTRAN, and are compatible with the DEC-supplied RT-11 monitor. Only when there is a specific need (necessitated by considerations of speed or device handling) are machine language programs used. Since novice users will be operating the systems, format-free input routines with consistency checks were developed to minimize operator errors.

The actual data acquisition is handled by the MBD microprogrammed brand driver. It has eight priority interrupt channels which contain coding used for servicing a specific experiment on each channel. These channels are activated or deactivated by the PDP-11/20. The code for the MBD is written in macro language which is assembled by the RT-11 MACRO assembler. The action taken by the MBD code depends on the application but typically services devices, increments spectra in the megaword memory and, where appropriate, transfers buffers of event mode discriptors to the PDP-11/20 for further sorting or transfer to magnetic tape. The data acquisition program has the ability to control experiments, display data, transfer spectra to tape, and do some simple calculations.

The data analysis programs in the PDP-11/34 have a similar modular structure and similar input routines. A much more extensive set of programs to manipulate spectra, display, list and plot is available. Event mode tapes can be scanned to generate appropriate spectra. An interactive peak fitting program is being developed.

The following data acquisition channels have been implemented:

PHA	A simple interface for high resolution 8192 channel singles spectra.
FB	An interface for high resolution ADC with routing bits, dedicated to the 'filtered beam' experiment.
FC	A two parameter (pulse height - neutron time-of-flight) experiment to service the fast chopper experiment.
GG	A three parameter (time-pulse height-pulse height) interface for measuring γ-γ coincidence spectra events from up to 8 detectors. The interface is sufficiently powerful to eliminate the need for most external logic circuits to define events.
MS	A 4-channel multi-scale interface that can measure multi scale spectra with a minimum channel width of 1/64 sec.
GMS	A multi-spectrum vs. time channel which measures 4096 channel spectra as a function of time after start. Thirty-two spectra are available, with a minimum time channel width of 1/8 second.
INTERLOCKS	A channel is used to read a 24 bit interlock panel and 16 scalers at a rate of 1/sec. The scalers are divided for use among the various experiments.
CONTROL	One channel is used for start up and control.

The system has been operating reliably for the past 8 months. It can handle events (in the current configuration) at a rate of about 10K/sec. It has been relatively easy to add new experimental configurations as needed. The data analysis system allows rapid interaction with experiment. When the interactive peak fitting routines are complete, the process of data analysis should be greatly expedited. By careful use of existing components, a minimum of specialized interfacing and careful modular programming, a versatile system has been designed and implemented that meets the current data acquisition needs of this facility.

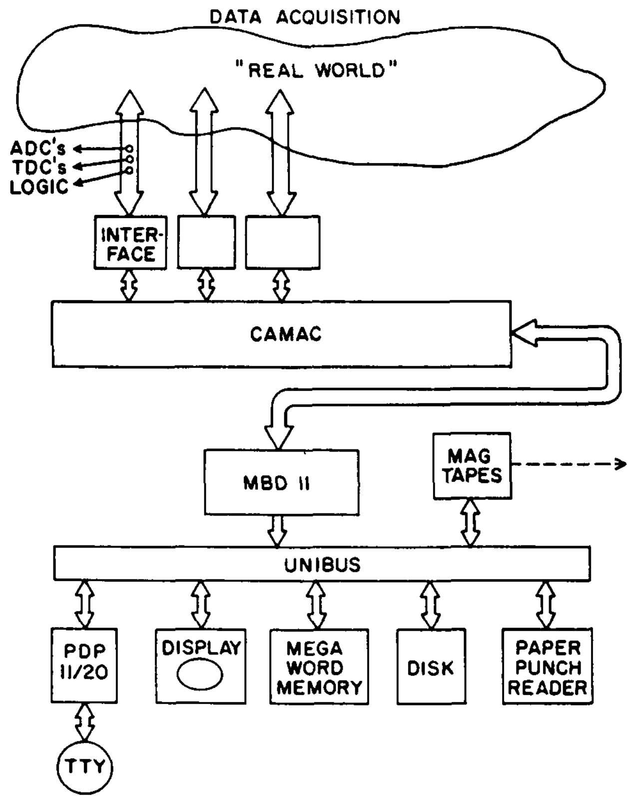

Figure C-3 The configuration for the HFBR nuclear measurements computer system.

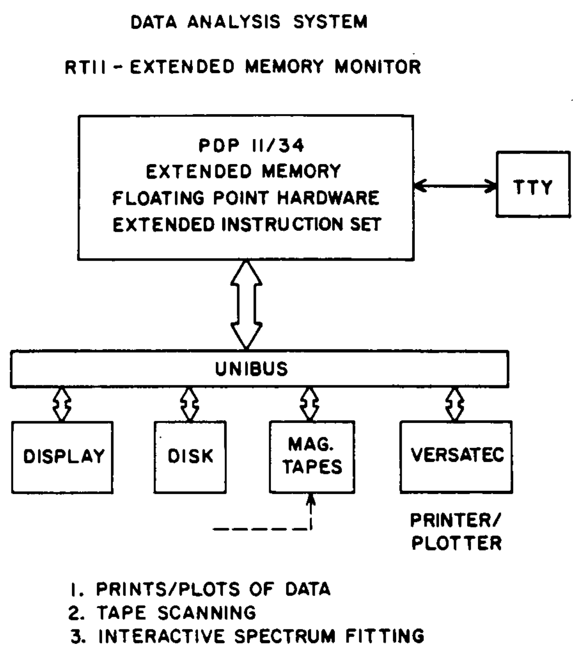

Figure C-4 The analysis computer for HFBR nuclear measurements.

D. NATIONAL NUCLEAR DATA CENTER

1. Data Evaluation

The fourth edition of BNL-325, Vol. 1 Resonance Parameters will be published in two parts. Part I, Z=60, and Part 2, Z=61-100. It is anticipated that the first part will be completed by July 1980 and the second part in February 1981. The recommended resonance parameters are based on experimental data stored in the CSISRS library. A computer program retrieves the data from the library, transforms it into a standard form (such as $g\Gamma_n$ values), groups the data according to resonance energy and $g\Gamma_n$ values, then extracts a weighted and unweighted average with internal and external errors.

The NNDC has begun an evaluation effort on the excitation functions for the production of medical radionuclides. The effort is currently concentrating on the standard reaction $^{12}C(p,x)^{11}C$, the $^{12}C(p,n)^{13}N$ reaction, and other reactions which produce ^{11}C, ^{13}N, ^{15}O. Except for the standard reaction, the incident particles and energies will be restricted to those available on small medical cyclotrons. Since $^{12}C(p,x)^{11}C$ is a standard from about 50 MeV to several hundred GeV and the last evaluation of this standard was performed in 1963, the Center will attempt to evaluate this standard over the entire energy range.

The Center is also planning to produce a charged-particle "Barn" book by late 1982. The publication will consist of experimental cross-section data on the hydrogen-isotope neutron source reactions, other reactions of interest to fusion, and medical radioisotope production. The book will also contain evaluated curves where these are available and "eye-guides" or "mini-evaluations" in the other cases.

In the area of nuclear structure and decay data (NSDD), mass chain evaluations for A=112, 139, and 145 have been completed. NNDC continues to coordinate the U.S. Nuclear Data efforts in this area.

2. Data Libraries

The normal CINDA compilation activity has been continued. Four special indices were prepared for inclusion in the Proceedings of the Nuclear Cross Section Technology Conference, the Capture Gamma-Ray Symposium at Brookhaven, the Meeting on Higher Pu and Am Isotopes for Reactor Applications, and the 1980 DOE-NDC Status Report.

NNDC has assumed full responsibility for entering Area 1 entries into the CINDA master file, and regular exchanges have been initiated with NEA-DB in the new exchange format. Current coverage has been transmitted to NEA-DB for inclusion in CINDA 80, now in press.

In the period March 1979-February 1980, 11 neutron data transmission tapes were sent out containing 116 new entries and 132 updated entries. Our first charged-particle transmission tape was sent out in October and contained 39 entries. The total number of experimental data points currently in the CSISRS data library are about 2.3 million for neutron data, 15,000 for charged particle data, and 20,000 for photonuclear data.

New computation-oriented retrieval formats have been developed for cross sections and resonance parameters, and are now in use. An attempt has been made to coordinate our retrieval format development with that of NEA-DB. The development of a format for fission product yields is now in progress, along with the development of a code package for CSISRS users.

The General Purpose File for ENDF/B has been released. The ENDF/B-V Activation File has been released and the Gas Production File is expected by May 1980. ENDF/B-V data files for cross-section standards, dosimetry, and actinides are available for unrestricted distribution. The fission product file which will also have general availability is expected to be ready for release by May 1980. All materials have passed extensive computer checking and review by experienced evaluators. The files are now being tested against benchmark experiments.

Work is in progress toward defining a more general ENDF format to handle non-neutron projectile as well as other additional reaction properties. Further tests on the format are in progress to test its practicability.

The bibliographic compilation of "integral" charged-particle nuclear data has continued. The third edition of the Bibliography of Integral Charged-Particle Nuclear Data (BNL-NCS-50640, Third Edition) has been published. This edition covers the literature from January 1, 1976, through January 31, 1979. The next edition of the bibliography will go to press by March 31, 1980.

The Center continues to receive and incorporate into the CSISRS data library experimental charged-particle nuclear data compiled by the Karlsruhe Charged Particle Data Group and the Kurchatov Institute and experimental and evaluated data compiled by the Nuclear Data Section, IAEA, Vienna.

The NNDC has been compiling both "differential" and "integral" experimental data on charged-particle-induced neutron source reactions. In addition, work has started on the compilation of "integral" data relevant to radioisotope production.

In addition to the CSISRS data library, the Center has copies of three other charged-particle nuclear data libraries and provides retrievals from these libraries. The libraries are the Oak Ridge Charged Particle Data Group experimental data file, the Lawrence Livermore experimental data file (target and incident $A \leq 4$), and portions of the Los Alamos evaluated data file on fusion-related reactions.

Nuclear structure information at the Center has been updated by revisions of the RECENT REFERENCES and ENDF files prepared by the Oak Ridge Nuclear Data Project. The Center offers retrieval services from these files.

3. DOE-NDC Secretariat

NNDC continues to perform secretariat functions for DOE-NDC. Document distribution lists for the Committee have been maintained and corrections supplied to NEANDC and INDC where required.

DOE/NDC 15U	Reports to the DOE Nuclear Data Committee, April 1979. (BNL-NCS-26133)
DOE/NDC 16U	A Compilation of Requests for Nuclear Data, April 1979. (BNL-NCS-26783)
DOE/NDC 17L	Summary of the Meeting of the DOE Nuclear Data Committee, April 1979. (BNL-NCS-26157)

NNDC
Request Statistics
January 1, 1979 to December 31, 1979

1. Requests

a)	Number of persons requesting information	1,129
b)	Number of requests	5,124

2. Origin of Requests

a)	Government Agencies	55
b)	Educational Institutions	216
c)	Industry	251
d)	Foreign	284
e)	National Laboratories	333

3. Mode of Response (may be more than one mode per request)

a)	Magnetic Tapes/Disk Files	363
	Total Number of Files on Magnetic Tape/Disk	1,722
b)	Computer Listing	423
c)	Cards	6
d)	Plots	222
e)	Documentation	2,296
f)	Telephone	32
g)	Microfiche	344
h)	Letters	52

PACIFIC NORTHWEST LABORATORY

A. DELAYED NEUTRON STUDIES WITH AN ON-LINE MASS SPECTROMETER

1. Energy Spectra of Delayed Neutrons from Separated Precursors (P. L. Reeder and R. A. Warner)

The energy spectra of delayed neutrons from the precursors $^{93,94,95}Rb$ and ^{143}Cs were measured by use of a ^{3}He neutron spectrometer. The precursors were obtained from the on-line mass spectrometer facility SOLAR. The spectral data were corrected for background, detector response, thermal neutrons, gamma pile-up and detector efficiency. An error analysis was carried through for each step in the data analysis. Spectral data for the same precursors were provided by two other laboratories[1,2] so a detailed comparison could be made. Much of the peak structure and overall intensity trends are reproduced in all three data sets. However, the published Studsvik data below 200 keV generally have higher intensities than the data from the other two laboratories. A reanalysis of the Studsvik data now gives spectra in better agreement with the data from Mainz and the present work.[2] The delayed neutron spectra from individual precursors measured by use of ^{3}He neutron spectrometers at different laboratories are now in reasonable agreement with each other. However, other techniques such as proton-recoil or time-of-flight should also be used to verify the delayed neutron energy spectra. The present results have been accepted for publication.[3]

---

[1]K. L. Kratz, University of Mainz (private communication).

[2]G. Rudstam, Studsvik Science Research Laboratory (private communication).

[3]P. L. Reeder and R. A. Warner, "Energy Spectra of Delayed Neutrons from Separated Precursors - ^{93}Rb, ^{94}Rb, ^{95}Rb, ^{143}Cs". Nucl. Sci. Eng. (to be published).

2. Delayed Neutron Yields, Average Energies and Emission Probabilities (P. L. Reeder and R. A. Warner)

We have previously published our measurements of delayed neutron average energies and emission probabilities for separated Br, Rb, Cs and I precursors.[1,2,3] These experiments were done at the SOLAR on-line mass spectrometer facility with the use of a high efficiency neutron counter (SNC). The SNC has now been moved to the TRISTAN isotope separator facility at Brookhaven National Laboratory where it will be used for similar measurements on the approximately 50 precursors expected from that facility.

The first experiments at TRISTAN will survey the counting rates of each precursor. The average neutron energies will be determined by the ratio of counts in the three rings of counter tubes in the SNC. The second series of experiments will be the measurement of neutron emission probabilities with the use of a beta counter inside the SNC to determine the number of precursor atoms in the sample. If sufficient intensities of very neutron rich precursors are available, the SNC counter will be used to search for beta-delayed two neutron emission.

B. ENERGY SPECTRA OF NEUTRONS FROM PHOTONEUTRON SOURCES (P. L. Reeder and R. A. Warner)

The SNC has been calibrated for efficiency as a function of neutron energy by the use of monoenergetic neutrons from photoneutron sources. The neutron spectra from such sources consist of a single peak plus a low energy tail due to multiple scatterings of neutrons within the source. For our calibration purposes it is necessary to know the average energy of the neutrons from the particular size and shape source actually used. We have therefore measured the energy spectra of neutrons from our ^{24}Na +Be and ^{24}Na + D_2O sources by use of a ^{3}He ionization

---

[1]P. L. Reeder, J. F. Wright and L. J. Alquist, Phys. Rev. C 15, 2098 (1977).

[2]P. L. Reeder, J. F. Wright and L. J. Alquist Phys. Rev. C 15, 2108 (1977).

[3]P. L. Reeder and R. A. Warner, Proceedings of the Consultants' Meeting on Delayed Neutron Properties, Vienna, 26-30 March 1979, International Atomic Energy Agency, INDC (NDS)-107/G+Special.

chamber neutron spectrometer. Techniques were developed to remove the effect of intense gamma-ray distortion of the data. The data were also corrected for detector response and detector efficiency. The final spectra are in good agreement with calculated spectra based on Monte Carlo techniques. The peak energy for the ^{24}Na + Be source is 968 keV as expected and the average energy is about 800 keV. For $^{24}Na + D_2O$ the peak energy is 265 keV and the average energy is about 200 keV.

IDAHO NATIONAL ENGINEERING LABORATORY

A. NUCLEAR-STRUCTURE AND DECAY-DATA EVALUATION ACTIVITIES

1. Mass-chain evaluations for the Nuclear Data Sheets (R. L. Bunting, M. A. Lee, C. W. Reich)

Through our participation in the International Nuclear-Structure and Decay-Data Evaluation Network, which has as its objective the establishment and maintenance of a four-year cycle time for the Nuclear Data Sheets, we have the responsibility for the ten mass chains in the region $153 \leq A \leq 162$. The first completed mass-chain evaluation has now been published [Nuclear Data Sheets 27, No. 1, 155 (1979)]. The work on A=158 has been completed; and resultant evaluation is presently in the review process. Presently being evaluated are data on the A=157 and 153 mass chains, with the former scheduled for completion this Spring and the latter in the Fall. In keeping with our philosophy of evaluating A-chains in approximate order of decreasing age, the next two chains to be evaluated will be those for A=160 and 161.

2. Decay-data evaluation for ENDF/B (C. W. Reich, R. L. Bunting)

As a part of our involvement in the work of CSEWG, we have the prime responsibility within the US for the preparation of sets of evaluated radioactive-nuclide decay data for inclusion in the data file ENDF/B. These evaluated decay data will form a part of the nuclear data contained in the Fission-Product File, the Actinide File and Activation File of ENDF/B, Version V. For the Fission-Product File, we have prepared evaluated decay-data sets for 318 nuclides (including isomeric states). These data have been sent out for review and comment. The results of this evaluation process are presently being examined. For the Activation File, evaluated decay data for 69 nuclides have been prepared. The evaluation work is presently completed, but the review process has not yet ended. For the Actinide File, our decay-data evaluations involved 61 nuclides. Subsequent to the issuance of the Version-V Actinide File, a request was made to expand the coverage of this file to include all the nuclides in the decay chains of the "important" actinide isotopes. This evaluation effort is presently underway, and it is presently planned to issue these additional evaluations in the form of a MOD. Forty-two nuclides are involved in this additional evaluation effort. They are the following:

Tl:	207, 209	Ac:	225, 227, 228
Pb:	209, 210, 211, 214	Th:	227, 229, 234
Bi:	210, 211, 213, 214, 215	Pa:	234, 234m
Po:	210, 211, 213, 214, 215, 218	U:	240
At:	217, 218, 219	Np:	240, 240m
Rn:	217, 219, 222	Pu:	245

Fr: 221, 223 Am: 245
Ra: 223, 225, 226, 228

B. APPLICATIONS OF NUCLEAR-DECAY AND γ-SPECTROSCOPIC DATA

1. Gamma-ray emission probabilities and half-life of ^{139}Ba[1] (R. J Gehrke)

Because of the high yield (6.6%) of mass 139 in the thermal-neutron induced fission of ^{235}U, the nuclides in the ^{139}Xe→ ^{139}Cs→ ^{139}Ba→ ^{139}La decay chain are important for many reactor-related problems. At present, γ-ray emission probabilities (i.e., absolute intensities) for the ^{139}Xe and ^{139}Cs parents are based on that of the radiation from ^{139}Ba decay; and these data for ^{139}Ba were determined indirectly from the measured β^- transition intensities to the ^{139}La levels. Unfortunately, the reported values for the intensity of the β^- branch to the 165-keV level of ^{139}La, 26±6%,[2] 32%[3] and 21±5%,[4] exhibit large differences and have large uncertainties. In order to improve our knowledge of the γ-ray emission probabilities of the mass-139 isotopes in general, and of ^{139}Ba in particular, we have remeasured the γ-ray emission probabilities of the 165- and 1420-keV γ rays by 4π β-γ coincidence counting and spectrometric techniques. These values were determined to be (23.76±0.25) and (0.261±0.005) γ rays per 100 disintegrations, respectively. The half-life of ^{139}Ba was measured to be (83.06 ±0.28) minutes.

---

[1] R. J. Gehrke, Int. J. Appl. Radiat. Isotopes 31, 37 (1980).

[2] W. H. Kelly, G. B. Beard, W. B. Chaffee and J. M. Gonser, Nucl. Phys. 19, 79 (1960).

[3] B. S. Dzhelepov, L. K. Peker and V. O. Sergeev Skhemy raspada radioaktivnykh yader (Decay Schemes of Radioactive Nuclei), AN SSSR (1963); R. B. Bagzhanov, D. A. Gladyshev, Kh. M. Sadykov and K. T. Teshabaev, Yadernaya Fizika 4, 1097 (1966); (English translation), Soviet J. Nucl. Phys. 4, 789 (1967).

[4] J. W. Sunier and J. Berthier, Nucl. Phys. A124, 673 (1969).

2. Absolute intensities of the γ rays emitted in the decay of ^{145}Pr[1] (R. J. Gehrke, J. D. Baker)

The only measurement of the absolute γ-ray intensities from the ^{145}Pr decay is that of Bullock and Large[2] which gave I_γ(72 keV)=0.20%. Furthermore, no uncertainty was given for this value. In the more recent evaluation given in the Nuclear Data Sheets,[3] the 72-keV γ-ray intensity from Ref. 2 was arbitrarily assigned a 20% uncertainty. Because of this unsatisfactory situation regarding this important datum, we have measured the absolute intensity of the 748-keV γ ray emitted in the decay of ^{145}Pr by 4π β-γ coincidence counting and Ge(Li) spectrometric techniques. A value of (0.525 ± 0.009) γ rays per 100 decays was found for this quantity. Relative intensities for 13 of the γ rays from ^{145}Pr were measured and are reported in Table B-1. The ^{145}Pr half-life was determined to be (5.984 ± 0.010)h.

TABLE B-1. Relative intensities of the more intense γ rays from the ^{145}Pr decay.

E_γ(keV)	Relative Intensity[a]
72	49.8 $\pm$2.6
352[b]	8.8 $\pm$0.2
492	4.80$\pm$0.12
623	4.54$\pm$0.12
657	12.2 $\pm$0.2
675	97.9 $\pm$1.4
784	100.0
848	13.8 $\pm$0.3
920	27.8 $\pm$0.5
978	48.8 $\pm$0.9
1051	33.4 $\pm$0.6
1150	37.0 $\pm$0.8
1161[b]	4.35$\pm$0.12

[a]For absolute γ-ray intensities (in %) multiply intensities by 0.00525 ± 0.00009.

[b]Peak is a doublet. Intensity is that of the doublet.

[1]R. J. Gehrke and J. D. Baker, Accepted for publication in Intern. J. of Appl. Radiat. and Isotopes.

[2]R. J. Bullock and N. R. Large, Radiochim. Acta 6, 201 (1966).

[3]T. W. Burrows, Nuclear Data Sheets 12, 203 (1974).

3. Emission probability of the 453-keV γ ray emitted in the decay of ^{146}Pr (R. J. Gehrke, J. D. Baker)

The only direct measurement of the absolute intensities (emission probabilities) of the γ rays from the decay of ^{146}Pr is that reported by Daniels et al.[1] for the 453-keV γ ray. From their measurement, the intensity of the β^- branch to the ^{146}Nd ground state was determined to be 40%. The individual β^- branches were also measured by Daniels et al. using a trans-stilbene detector. Unfortunately, the deduced intensity of the β^- branch to the ^{146}Nd ground state (the value was not quoted) was reported[1] as not being as large as would be required by the γ-ray intensity data.

In an evaluation of the mass-146 decay chain, Burrows[2] reiterated this apparent conflict pertaining to the intensity of the ground-state β^- branch and chose not to quote any absolute γ-ray intensities for the ^{146}Pr decay.

Because of the resulting confusion pertaining to the absolute intensities of the γ rays emitted in the decay of ^{146}Pr, we have chosen, as a part of our program to measure the γ-ray emission probabilities of selected fission-product isotopes, to remeasure the emission probability of the 453-keV γ ray. This γ ray represents the transition from the first excited state to the ground state of ^{146}Nd and is the most intense γ-ray transition in the ^{146}Pr decay. Using 4π β-γ coincidence counting techniques, we measured the emission probability of the 453-keV γ ray to be (48.0 ± 1.5) γ rays per 100 decays. The ^{146}Pr half-life was also remeasured and a value of (24.15 ± 0.18) min was obtained.

---

[1] W. R. Daniels, F. O. Lawrence and D. C. Hoffman, Nucl. Phys. A118, 467 (1968).

[2] T. W. Burrows, Nucl. Data Sheets 14, 413 (1975).

4. γ-ray energies for ^{40}K and ^{108m}Ag decay and the ^{226}Ra decay chain[1] (R. G. Helmer, R. J. Gehrke, R. C. Greenwood)

The energies of γ rays from the long-lived sources of ^{40}K(1.28×10^9y), ^{108m}Ag(127y) and ^{226}Ra(1.60×10^3y) have been measured to provide new calibration lines for Ge semiconductor detectors. The energies were determined by measurement of energy differences relative to known lines and computation of crossover energies from known cascade energies. On the new energy scale based on a ^{198}Au energy of 411.80441(108) keV,[2] energy values obtained are: for ^{40}K, 1460.830(5) keV; and for ^{108m}Ag, 433.936(4), 614.281(4) and 722.929(4) keV. Values for thirteen γ rays in the ^{226}Ra decay chain from 609 to 2447 keV are also given in Ref. 1.

---

[1] R. G. Helmer, R. J. Gehrke and R. C. Greenwood, Nucl. Instr. and Methods 166, 547 (1979).

[2] E. G. Kessler, R. D. Deslattes, A. Henins and W. C. Sauder, Phys. Rev. Lett. 40, 171 (1978).

5. Gamma-ray energies from the $^{14}N(n,\gamma)$ and $^{23}Na(n,\gamma)$ reaction [R. C. Greenwood, R. E. Chrien (BNL)]

Precise values for the energies of the γ rays emitted in the $^{14}N(n,\gamma)$ reaction with slow neutrons have been obtained from spectral measurements using Ge semiconductor detectors. The approach which was used in the analysis of the data involved normalization of the $^{14}N(n,\gamma)$ reaction γ-ray energies to our most recent value for the neutron binding energy of ^{15}N [$S_n(^{15}N)=10833.297 \pm 0.038$ keV]. This was accomplished through measurement of energy differences between the 5.2- and 5.5-MeV cascade γ rays, followed by general GAUSS V energy fitting procedures to obtain other γ-ray energies. From this approach the $^{14}N(n,\gamma)$ reaction γ-ray energies shown in Table B-2 together with the ^{15}N excitation energies shown in Table B-3 were obtained. Measurement uncertainties in these data were as small as 6 ppm. Selected energies of γ rays emitted in the $^{23}Na(n,\gamma)$ reaction were then obtained from spectra measured with mixed N and Na targets. From these data, based upon cascade sums, we obtain a value of $S_n(^{24}Na)=6959.426 \pm 0.076$ keV.

TABLE B-2. γ-ray energies from the $^{14}N(n,\gamma)^{15}N$ reaction with slow neutrons.

γ-ray energy (keV)	uncertainty[a] (eV)	γ-ray energy (keV)	uncertainty[a] (eV)
1678.260	59	4508.665	53
1681.589	228	5269.122	35
1884.820	47	5297.795	35
1999.729	77	5533.401	35
2520.281	101	5562.073	35
2830.745	87	6322.474	60
3531.964	87	7298.980	90
3677.748	57	8310.218	104
3855.604	74	9149.068[b]	201
3884.280	74	10829.101	38

[a] The reference uncertainty was taken to be that of $S_n(^{15}N)$, i.e., 2.7 ppm.

[b] Measured γ-ray energy, probably a doublet with contributions from de-excitation of both the 9151- and 9154-keV states to the ground state.

TABLE B-3. Excitation energies of the ^{15}N levels populated in the $^{14}N(n,\gamma)^{15}N$ reaction with slow neutrons.

Level energy (keV)	Uncertainty[a] (eV)	Level energy (keV)	Uncertainty (eV)
0		7300.886	90
5270.116	35	8312.689	104
5298.800	35	9151.607	203
6323.904	60	9154.936	71
7155.064	59	10833.279	38

[a]The reference uncertainty was taken to be that of $S_n(^{15}N)$, i.e., 2.7 ppm.

C. NUCLEAR LEVEL-SCHEMES STUDIES

1. Levels in ^{152}Sm from the $^{151}Sm(n,\gamma)$ reaction (R. C. Greenwood)

Analysis of our $^{151}Sm(n,\gamma)$ reaction data is currently underway. Based on the completed analysis of the primary capture γ-ray spectral data the following preliminary value was determined for the neutron binding energy of ^{152}Sm: $S_n(^{152}Sm)=8260.066\pm0.074$ keV. Analysis of the secondary capture γ-ray spectral data, to provide information on the de-excitation properties of the lower-lying excited states in ^{152}Sm, is continuing.

2. Levels in ^{157}Gd from the decay of ^{157}Eu (R. C. Greenwood)

High-purity samples of 15-hr ^{157}Eu were obtained by direct collection of fission products from the 2-100μg ^{252}Cf spontaneous-fission sources, extraction of the Eu fraction using ion exchange with a high-pressure liquid chromatograph, followed by mass separation. Based on singles counting, some 75 γ rays could be associated with the decay of ^{157}Eu. Gamma-gamma coincidence experiments are currently underway to aid in the placing of these γ rays into a consistent ^{157}Gd level scheme. The study of this decay scheme is a companion effort to our earlier measurements of the $^{156}Gd(n,\gamma)$ reaction γ-ray spectra with 2- and 24-keV neutrons.

D. AUTOMATED FAST-RADIOCHEMISTRY FACILITY FOR THE STUDY OF FISSION PRODUCT RADIONUCLIDES

1. Rapid Separation of Individual Rare-Earth Elements from Fission Products (J. D. Baker, R. J. Gehrke, R. C. Greenwood, D. H. Meikrantz)

A microprocessor-controlled radiochemical separation system has been developed to rapidly separate rare-earth elements from gross fission products obtained from an "open" source of ^{252}Cf. The system is composed of two high-performance liquid-chromatography columns coupled in series by a stream-splitting injection valve. The first column separates the rare-earth group by extraction chromatography using dihexyldiethylcarbamylmethylenephosphonate (DHDECMP) adsorbed on Vydac C_8 resin. The second column isolates the individual rare-earth elements by cation exchange using Aminex A-9 resin with α-hydroxyisobutyric acid (α-HIBA) as the eluent. With this system, fission-product rare-earth isotopes with half-lives as short as three minutes have been studied.

2. A New Isotope ^{158}Sm; Comments on the Decay of ^{157}Sm[1] (J. D. Baker, R. J. Gehrke, R. C. Greenwood, D. H. Meikrantz, V. J. Novick)

One of the first results from the rapid rare-earth separation system was the discovery and subsequent study of a new isotope, ^{158}Sm. The ^{158}Sm was produced as a fission product from a spontaneously fissioning ^{252}Cf source. Twenty-seven γ rays have been assigned to this activity, which decays with a half-life of (5.51 ± 0.09) min. The ^{158}Sm assignment is based upon the radiochemical separation of the samarium fraction from the rare-earth fission products and the observation of the grow-in of the 45.9-min ^{158}Eu daughter from the 5-min parent. The emission probability of the 324-keV γ ray from the decay of ^{158}Sm was determined from grow-in of the ^{158}Eu daughter to be 10.6 ± 1.2 γ rays per 100 decays. Several new γ rays have been identified by half-life as belonging to the decay of ^{157}Sm. The γ-ray energies and relative intensities for ^{157}Sm and ^{158}Sm are reported in Table D-1.

---

[1] J. D. Baker, R. J. Gehrke, R. C. Greenwood, D. H. Meikrantz and V. J. Novick, accepted for publication in J. Inorg. and Nucl. Chem.

3. An automated system for selective fission-product separations applied to the studies of $^{113-115}Pd$ (D. H. Meikrantz, R. J. Gehrke, L. D. McIsaac, J. D. Baker, R. C. Greenwood)

A solvent-solvent extraction regimen has been automated by the use of annular centrifugal contactors. A series of valves and switches operated under microcomputer control manage each of the classical chemical separation steps. This system has been applied to the separation of radiopalladium from mixed fission products generated by a ^{252}Cf spontaneous-fission source. A helium-jet transport system delivered the ^{252}Cf fission products to an on-line collection device which was also under microcomputer control. In addition to the sample collection, other automated steps include dissolution, acidity adjustments, oxime complexation of the palladium feed to the centrifugal

TABLE D-1. Energies and relative intensities of the γ rays observed in the decay of ^{158}Sm and ^{157}Sm

^{158}Sm		^{157}Sm	
γ-ray energy (keV)[a]	Relative Intensity	γ-ray energy (keV)[a]	Relative Intensity
100.2	43.8±2.5	59.7	1.6±0.2
108.7	11.0±1.3	76.7	3.3±0.4
132.3	6.9±1.0	121.0	10.3±0.9
149.0	46.5±3.0	186.0	2.4±0.2
177.7	37.4±2.0	190[b]	2.3±0.4
189.4	143 ±9	196.3	38. ±3.
190.7	39 ±4	197.7	100
224.1	80 ±4	216	
226.6	49 ±4	238	
229.7	63 ±4	253	
283.0	6.6±0.6	255	0.8±0.2
285.4	15.9±1.9	263.1	2.6±0.2
299.7	19.8±2.1	275.8	2.3±0.3
321.3	78 ±4	317.5	3.0±0.3
324.5	100 ±5	394.1	18.7±1.4
326.8	19.4±1.3	472.4	1.5±0.3
338.6	35 ±3	716.1	1.4±0.2
361.7	62 ±4	823	
363.6	117 ±7	1027	
376.5	5.0±0.4	1154	
551.2	28.5±1.9	1377.0	1.1±0.2
791.4	15.5±1.1	1386.1	1.9±0.2
988		1463.0	5.4±1.2
1162.9	11.4±0.6		
1209.9	8.3±1.2		
1343.3	7.8±0.6		
1448.5	3.4±0.3		

[a] Uncertainties in the gamma-ray energies are typically ±0.3 keV. For those gamma rays given to the nearest keV the uncertainties in the energy are ±1 keV.

[b] This line is masked by the 190.7-keV gamma ray in ^{158}Sm.

contactors and subsequent collection of the desired output stream. The three centrifugal contactors were connected in series and provided one stage each of extraction, scrub and strip. The total time required for each palladium separation was ∿150 seconds. Decay curves of the γ rays emitted from the short half-life Pd-Ag decay chains were measured.

Additional counts were made of the chemically separated Ag daughter activities and, when possible, the decay curves of these γ rays were also measured for the purpose of isotopic identification. The half-lives of the short half-life Pd isotopes were determined to be ^{113}Pd (1.4 min), ^{114}Pd (2.4 min) and ^{115}Pd (46 sec). A tentative list of the Pd assignments and their γ-ray energies and relative intensities is given in Table D-2. Prior to these studies, no γ radiation had been reported in the decay of these three activities.

TABLE D-2. Gamma-ray assignments, energies and relative intensities for the decays of $^{113-115}$Pd

^{113}Pd		^{114}Pd		^{115}Pd	
E_γ(keV)[a]	I_γ(rel)[b]	E_γ(keV)[a]	I_γ(rel)[b]	E_γ(keV)[a]	I_γ(rel)[b]
95.9	99	126.6	92	125.4	66
222.1	60	136.7	18	255.4	64
482.8	39	232.0	100	342.7	100
644.0	100	250.0	15		
		358.6	24		

[a]uncertainty (1σ) is ±0.2 keV

[b]uncertainty (1σ) is 15%

E. INTEGRAL REACTION-RATE AND-CROSS SECTION MEASUREMENTS

1. Capture and fission cross sections for actinides (R. A. Anderl, Y. D. Harker, N. C. Schroeder)

In progress are measurements of the integral cross sections important to the production of ^{233}U and to the production and depletion of plutonium, americium and curium in advanced reactor systems. Summarized in Table E-1 are the integral reaction rates and cross sections obtained to date for selected actinide samples irradiated in the fast neutron zone of the Coupled Fast Reactivity Measurements Facility (CFRMF) operated at a power level of 100 kW. All measurements were made by the gamma spectrometric method with the exception of those for the production cross section of ^{242}Cm from capture in ^{241}Am. The latter measurements are based on extensive quantitative chemical separations and isotope dilution alpha spectrometry. Details of these measurements were reported earlier.[1,2]

In FY80 additional measurements of the ^{242}Cm production cross section will be made and the cross section for production of ^{244}Cm via capture in ^{243}Am will be measured. Because of sample-definition problems associated with the earlier ^{242}Pu experiments the ^{242}Pu capture and fission cross sections will be remeasured.

TABLE E-1. Integral reaction rates and cross sections for actinides in the CFRMF.

Reaction	Reaction Rate $(rps/a)X10^{13}$	Integral Cross Section (mb)
$^{232}Th(n,\gamma)$	2.55 $\pm$.07	291 $\pm$ 9
$^{232}Th(n,f)$	.172$\pm$.008	20 $\pm$ 1
$^{242}Pu(n,\gamma)$	1.3 $\pm$.2	150 $\pm$23
$^{242}Pu(n,f)$	4.8 $\pm$.5	560 $\pm$56
$^{241}Am(n,\gamma)\rightarrow^{242}Cm$	9.12 $\pm$.23	1.03$\pm$ .04
$^{243}Am(n,\gamma)\rightarrow^{244g}Am$	.856$\pm$.021	97 $\pm$3
$^{243}Am(n,f)$	3.07 $\pm$.08	352 $\pm$11

[1] R. A. Anderl and Y. D. Harker, "Measurement of the Integral Capture and Fission Cross Sections for ^{232}Th in the CFRMF," Proceedings of the International Conference on Nuclear Cross Sections for Technology, Oct. 22-26, 1979, Knoxville, Tennessee.

[2] Y. D. Harker, R. A. Anderl, E. H. Turk and N. C. Schroeder, "Integral Measurements for Actinides in the CFRMF," Proceedings of the International Conference on Nuclear Cross Sections for Technology, Oct. 22-26, 1979, Knoxville, Tennessee.

2. Capture cross sections for fission products (R. A. Anderl, Y. D. Harker)

Our program to provide integral cross sections of interest to the development of fast reactor systems has included measurements in the CFRMF and in EBR-II. All earlier fission-product capture measurements made in the CFRMF were re-evaluated and re-analyzed. Current decay data (ENDF/B-V) and a consistent flux normalization scheme were applied to all measurements. A review paper[1] summarizing these re-evaluated data and including comparisons to ENDF/B-derived integrals was prepared.

Analyses were completed for the reaction-rate measurements of highly enriched isotopes of neodymium, samarium and europium irradiated in EBR-II. Preliminary results were given in the last two USNDC reports.

The HEDL maximum-likelihood analysis code, FERRET,[2] was used to make a "least-squares adjustment" of the ENDF/B-IV rare-earth cross sections based on the measured dosimeter and fission-product reaction rates. Preliminary results reported to date[3] indicate a need for a significant upward adjustment of the capture cross sections for ^{143}Nd, ^{145}Nd, ^{147}Sm and ^{149}Sm. The adjustments are consistent with more recent measured differential data. A journal publication on this work is being prepared.

---

[1] Y. D. Harker and R. A. Anderl, "Integral Cross-Section Measurements on Fission Products in Fast Neutron Fields," Proceedings of the NEANDC Specialist's Meeting on Neutron Cross Sections of Fission-Product Nuclei, Dec. 12-14, 1979, Bologna, Italy.

[2] F. Schmittroth, "FERRET Data Analysis Code," HEDL-TME 79-40 (September, 1979)

[3] R. A. Anderl, Y. D. Harker and F. Schmittroth (HEDL), "Neodymium, Samarium and Europium Capture Cross Section Adjustments Based on EBR-II Integral Data," Proceedings of the International Conference on Nuclear Cross Sections for Technology, Oct. 22-26, 1979, Knoxville, Tennessee.

F. THE ^{252}Cf $\bar{\nu}$ PROBLEM

1. Measurement of $\bar{\nu}$ for ^{252}Cf (J. R. Smith, S. D. Reeder (ENICO), R. J. Gehrke)

The experiment to measure the number of neutrons per fission ($\bar{\nu}$) for ^{252}Cf is nearly complete. Four ^{252}Cf foils, each mounted in an NBS double fission chamber, were used in the measurement. All were calibrated by neutron-fission coincidence counting and by 2π counting. Two of the foils, being mounted on $250 \mu g/cm^2$ Ni backing, were also calibrated by counting coincidences between fission-fragment pairs. The three calibration methods were in good agreement as to the fission rate, but the neutron-fission coincidence technique proved to be by far the most accurate, consistent, and independent of the effects of self-transfer of the ^{252}Cf deposit

The relative activities of the ^{252}Cf foils covered a range of about 10:1, yet the ratios as determined by fission calibration closely match the ratios of activity induced in the manganese bath. This consistency suggests that coincidence and dead-time corrections were correctly applied.

In addition to neutron yield measurements at a fixed concentration, a dilution experiment was performed. Measurements of the activity produced by three ^{252}Cf sources have been made at six $MnSO_4$

concentrations. The resulting data will allow the derivation of a value of the hydrogen-to-manganese cross section.

At the present stage of analysis, which includes a superficial analysis of some of the dilution data, it appears that the final ^{252}Cf $\bar{\nu}$ value will be near 3.77. Final analysis requires both the completion of some manganese-bath calculations being performed by Goldstein and Chen, and the emergence of an improved value for the absorption cross section of sulfur. The current uncertainty in this cross section reflects an error of nearly a quarter per cent into the manganese bath measurements. This is the largest single error in the $\bar{\nu}$ experiment.

2. <u>The absorption cross section of sulfur</u> (J. R. Smith)

The accuracy of manganese bath measurements of neutron source strength in general, and of ^{252}Cf $\bar{\nu}$ in particular, depends of course upon the accuracy with which the several corrections can be assessed. The sulfur thermal neutron absorption cross section has recently been demonstrated to represent one of the largest residual uncertainties in the manganese-bath method. The current 6% error estimate for the sulfur cross section imposes an uncertainty of nearly a quarter per cent upon any manganese bath measurement of a neutron source strength. Yet, an examination of the cross-section measurements suggest that the uncertainty might be considerably more than 6%. These measurements were typically made about 30 years ago. Accuracy of measurement is made more difficult by the facts that the absorption cross section is low and it does not lead to a radioactive reaction product. Moreover, the fact that the absorption cross section is smaller than the scattering may have had an undetermined effect on the reactivity measurements.

For the final resolution of the ^{252}Cf $\bar{\nu}$ discrepancy, it is essential that the uncertainty in the sulfur cross section be reduced. Measurements to an accuracy approaching 1%, by two independent methods, will be required.

---

[1] J. R. Smith, "Status of the Quest for ^{252}Cf $\bar{\nu}$," EPRI NP-1258 (December, 1979). See also "The ^{252}Cf $\bar{\nu}$ Discrepancy and the Sulfur Discrepancy," Bull. Am. Phys. Soc. <u>24</u>, 883 (1979).

IOWA STATE UNIVERSITY, AMES LABORATORY

A. DECAY STUDIES OF GASEOUS FISSION PRODUCTS AND THEIR DAUGHTERS

Prior to 1976 most of the studies of the decays of fission products at the TRISTAN on-line mass separator facility were confined to the rare gases Kr and Xe and their daughters. Most of this material has been presented in past contributions to the Nuclear Data Committee.

1. Decays of Mass-Separated ^{139}Xe and ^{139}Cs (M. A. Lee and W. L. Talbert, Jr.)

The study of the decay of ^{139}Xe and ^{139}Cs to levels in ^{139}Cs and ^{139}Ba respectively is complete and has been published.[1] Ge(Li) γ-ray singles and γ-γ coincidence measurements were carried out. For the decay of ^{139}Xe, 213 of 230 observed γ-ray transitions have been placed in a level scheme for ^{139}Cs with 55 excited states. For the decay of ^{139}Cs, 167 of 179 observed γ-ray transitions have been placed in a level scheme for ^{139}Ba with 59 excited states. The Q values for the β decays of ^{139}Xe and ^{139}Cs were determined from Ge(Li) plastic scintillator coincidence measurements as 5.02 ± 0.06 and 4.29 ± 0.07 MeV respectively. Ground state β feeding was deduced for both decays.

2. The Decay of ^{90}Kr (C. L. Duke, W. L. Talbert, Jr., F. K. Wohn, J. K. Halbig, and K. Bonde Nielsen)

This material was discussed in detail in last years report and has now been published[2] in Phys. Rev. C.

B. DECAY STUDIES OF NON-GASEOUS FISSION PRODUCTS WITH AN IN-BEAM ION SOURCE

In late 1976 decay studies of the non-gaseous fission products Zn, Ga, Ag, Cd, and In was initiated at the Ames Laboratory Research Reactor. The program of measurements continued until December 1977 at which time the Ames Laboratory Research Reactor was permanently shut down.

1. Decay of Mass-Separated ^{78}Zn (F. K. Wohn, John C. Hill, and D. A. Lewis)

The decay of ^{78}Zn to levels in ^{78}Ga was studied. The half-life

---

[1] M. A. Lee and W. L. Talbert, Jr., Phys. Rev. C 21, 328 (1980).

[2] C. L. Duke, W. L. Talbert, Jr., F. K. Wohn, J. K. Halbig, and K. Bonde Nielsen, Phys. Rev. C 19, 2322 (1979).

of ^{78}Zn was measured to be 1.47±0.15s. A total of 57 γ-ray transitions were placed in a level scheme for ^{78}Ga consisting of 19 excited states. This material has been submitted for publication to Phys. Rev. C.

2. Decay of Mass-Separated ^{78}Ga (D. A. Lewis, John C. Hill, and F. K. Wohn)

The decay of ^{78}Ga to levels in even-even ^{78}Ge was studied. The half-life of ^{78}Ga was measured to be 5.49±0.25s. A total of 45 γ-ray transitions were placed in a level scheme for ^{78}Ge consisting of 19 excited states. This material has been submitted for publication to Phys. Rev. C. Based on our level scheme the Q_β for ^{78}Ga decay measured by Aleklett et al.[3] to be 8.14±0.16 MeV was reevaluated by us to be 7.89±0.16 MeV.

3. Decay of ^{120}Ag and ^{120m}Ag (T. K. Li, C. M. McCullagh, and John C. Hill)

The decay of the two isomers of ^{120}Ag was studied. The low spin ^{120}Ag has a possible J^π of 3^+ and its half-life was measured to be 1.36±0.04s. The high spin ^{120m}Ag has a possible J^π of 6^- and its half-life was measured to be 0.32±0.02s. For both decays a total of 50 γ-ray transitions were placed in level schemes containing a total of 20 excited states in ^{120}Cd. This material has been submitted for publication to Phys. Rev. C.

C. TRISTAN II AT THE BROOKHAVEN HIGH FLUX BEAM REACTOR (HFBR)

After the Ames Laboratory Research Reactor was shut down in December 1977 the TRISTAN II mass separator was moved to the HFBR at Brookhaven National Laboratory. The first beam of stable isotopes was obtained in the Fall of 1979 and the first experiments will begin in the Spring of 1980. The TRISTAN II facility will employ a FEBIAD ion source which will enable us to study a wide variety of non-gaseous fission products similar to those studied with TRISTAN II at Ames. The FEBIAD design should result in longer and more stable operation and possibly higher temperatures which should produce enhanced yields of the very short-lived fission products.

Additional improvements at Brookhaven will result from the fact that the neutron fluxes available on target are up to a factor of 50 higher than those available at Ames. Also a PDP-11 based data acquisition and

---

[3]K. Aleklett, E. Lund, G. Nyman, and G. Rudstam, Nucl. Phys. A285, 1 (1977).

analysis system will enable us to carry out many measurements simultaneously.

A number of different types of measurements are planned for TRISTAN II at the HFBR. They include conventional decay studies using γ-ray spectroscopy, Q_β measurements with intrinsic Ge detectors, γ-γ angular correlation measurements, and several types of measurements on delayed neutrons. An ion source development program will have as its goal the development of an ion source that can produce beams of all of the fission products.

A. PROTON STRENGTH FUNCTIONS (Flynn, Gabbard, Hershberger)

This project deals with high precision, high accuracy measurements and analyses of proton scattering (p,p) and (p,n) reactions. Uncertainties in the measured cross sections must be $\lesssim 2\%$, because the strength functions only appear after dividing the rapidly varying proton absorption cross sections by the equally rapidly varying Coulomb penetrabilities. These measurements are made near and below the Coulomb barrier. Accurate measurements of total (p,n) cross sections were reported for Zr and Mo isotopes for incident proton energies from 1.7 to 6.7 MeV.[1] These were then analyzed, together with (p,p) scattering cross sections, to reveal the potential parameters which would describe the scattering and absorption. The strength functions enables one to see the absorption-broadened potential or size resonances, specifically the tail of the s-wave resonance and the p-wave resonances. Accurate measurements of the resonance properties give powerful constraints on nucleon scattering fields.

The first result ascertained was that the "anomalous" A dependence of the proton absorptive potential W_D reported by Johnson et al.[2] was confirmed in this work, over part of the A-range included in the earlier analyses. The absorptive potential strength showed a large peak for A $\sim$ 105. Some parameter ambiguity could result from incompleteness of the data set of high accuracy cross sections. Thus for ^{92,94}Zr high precision (p,p) scattering cross sections have been measured[3] and included in the analysis. Another possible source of confusion could arise from the fact that states of two different i-spin, $T^> = T_0+1$ and $T^< = T_0-1$, are excited, where T_0 is the target i-spin. Is the scattering potential the same in these two states, and does the presence of scattering in both of them effect the determination of W obtained from a single scattering channel analysis? To test this possibility the (p,p) and (p,n) cross sections were carefully analyzed in coupled-channel formalism, which explicitly couples states of the two i-spins using the Lane formalism and the $T \cdot t$ coupling potential. The real potential strengths for each partial wave (ℓ) were adjusted to fix isobaric analog

---

[1] D.S. Flynn, R.L. Hershberger, and F. Gabbard, Phys. Rev. C 20, 1700 (1979).

[2] C.H. Johnson, J.K. Bair, C.M. Jones, S.K. Penny, and D.W. Smith, Phys. Rev. C 15, 196 (1977).

[3] R. Schrils, D.S. Flynn, R.L. Hershberger, and F. Gabbard, Phys. Rev. C 20, 1706 (1979).

resonances at their measured energies,[3] and thus were slightly ℓ-dependent. This explicit coupled-channels analysis was compared[3] to the conventional single-channel analysis for $^{92,94}Zr$. The average of the real potentials for different ℓ-values from the explicitly T-dependent analysis was negligibly different from that of the single-channel or conventional analysis, indicating, as we expected, that away from analog resonances the background cross section was quite dominated by the $T^<$ states. The narrow widths of the analog resonances is consistent with the lack of influence of $T^>$ contributions, and further the potential needed for the resonances is just that needed for the $T^<$ states. The absorptive potential W_D was the same as determined from both analyses. Finally, high precision and high accuracy measurements and analyses were completed[4] for (p,p) and (p,n) cross sections in ^{107}Ag, ^{109}Ag and ^{115}In. Here also the anomalous A-dependence of W_D near A ~ 105 is confirmed. In the Ag isotopes the analog resonances are shifted to higher proton energies, making it easier to discern the effect of the W_D-spread size resonances.[4]

Plans now call for further work A ~ 103-110 to define the A-dependence of W_D more carefully just at its maximum strength. More importantly, perhaps, coupled-channels analyses of (p,p) and (p,n) cross sections which couple target ground-states to excited states will be made, starting from potentials which are appropriate for neutron scattering in this mass region. These analyses will test two questions:

1) Is the behavior of W_D clearly inconsistent with implications of the Lane model, when neutron and proton potentials are compared?

2) Is the apparent increase of absorption near A ~ 105 real, in that it expresses increased coupling between scattering from target ground and excited states, increased coupling for nuclei well between subshell and shell closures occurring for Z ≃ 40, N = 50 and Z = 50?

B. NEUTRON SCATTERING

1. Large Deformation Effects. (Mirzaa, McEllistrem, Weil, Hanly)

Measurements of neutron scattering cross sections for 2.5 MeV neutrons incident on five even-A Nd isotopes has been completed, data reduced and final sample-size dependent corrections completed to arrive at corrected scattering cross sections. Differential cross sections for elastic and inelastic scattering were completed for isotopes from semimagic ^{142}Nd to permanently deformed ^{150}Nd. A comparison of the elastic scattering for all five is shown in Fig. 1 where the

---

4 R.L. Hershberger, D.S. Flynn, F. Gabbard, and C.H. Johnson, to be published in The Physical Review C.

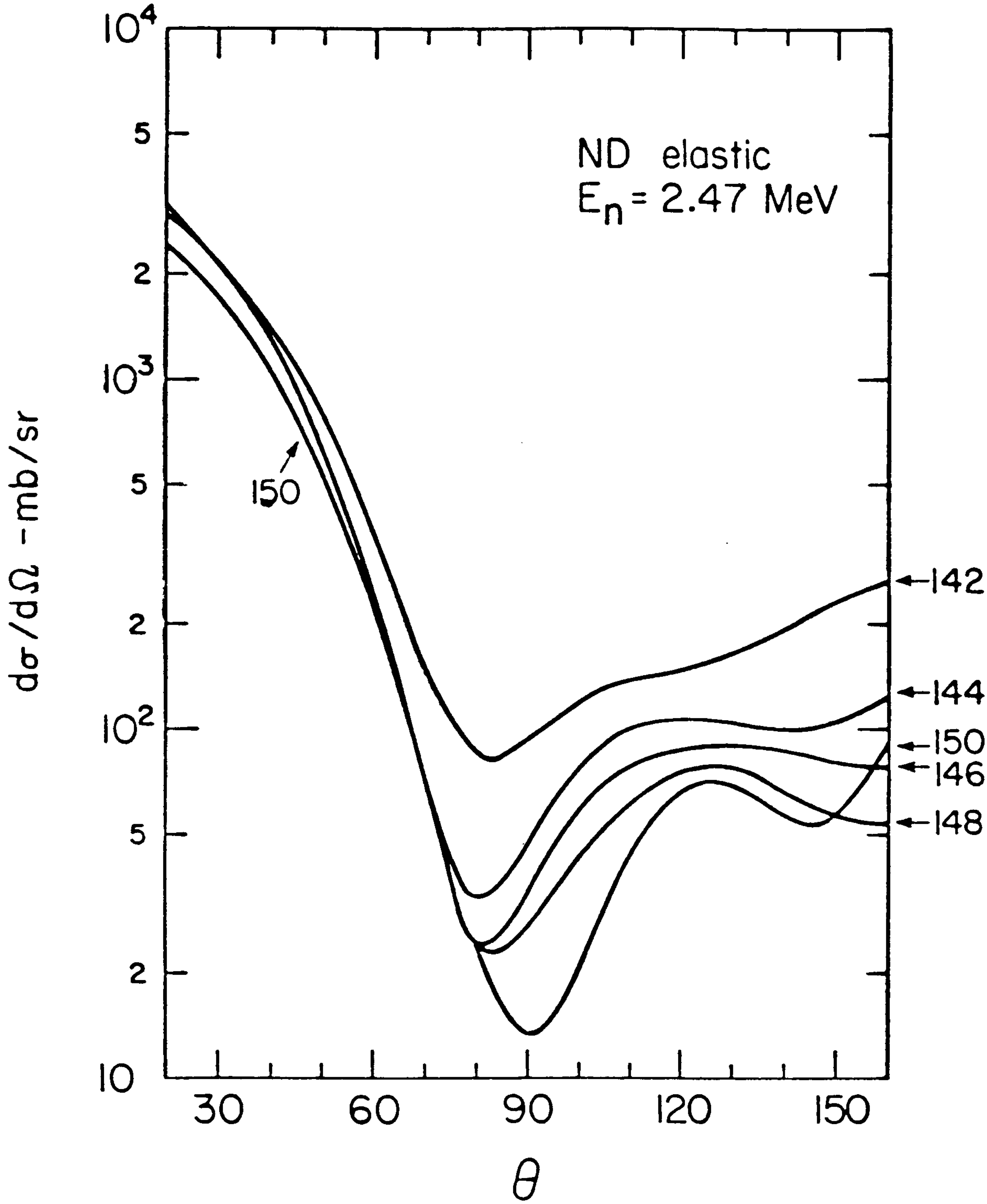

ND elastic
E_n = 2.47 MeV
10^4
5
2
10^3
5
2
10^2
5
2
10
30
60
90
120
150
$d\sigma/d\Omega$ -mb/sr
θ
150
142
144
150
146
148

Fig. B-1

effects of strong coupling between elastic and inelastic scattering channels is especially evident at large angles, near and beyond 70°. The sharp reduction of cross sections between ^{142}Nd and ^{144}Nd shows only the effects of increased competition between elastic and inelastic scattering in ^{144}Nd, where many more levels can be excited than in ^{142}Nd. Thus the compound-elastic scattering (σ_{CE}) is strongly reduced in ^{144}Nd. This reduction in σ_{CE} continues as more neutrons, and thus more open excited levels, are added in going to ^{148}Nd. But the change from isotope to isotope becomes less pronounced as neutrons and σ_{CE} becomes small enough that further reductions in it become less important.

The large decrease in large angle scattering cross sections in going from ^{148}Nd to ^{150}Nd reflects the sudden onset of large deformation effects, something which had previously been observed[5] in scattering from the Sm isotopes, ^{148,150,152}Sm. Now the strength of such effects is confirmed in the scattering from the Nd isotopes. Shown in Figs. 2 and 3 are analyses of scattering for spherical ^{142}Nd, where a single channel analysis is appropriate, and for deformed ^{150}Nd, where even a coupled-channels analysis, using collective excitation models, seems insufficient to provide a good representation of the measurements. The sensitivity of the scattering to deformations at these low energies seems so great that deficiencies of simple collective excitation models with surface excitation form-factors seem to become evident. This deficiency seemed also to be present in our earlier analysis[5] for scattering from ^{152}Sm.

To be able to compare deformation effects in scattering from the isotopes ^{150}Nd and ^{152}Sm, and for spectroscopic information, a separate (n,n'γ) study of the two nuclei was completed.[6] This study showed band structures for the two nuclei strikingly similar, with almost the same level spacings for ground-state, γ-, and β-vibrational bands. The E2 decay rates of excited levels were also quite the same in the two nuclei,[6,7] and even the degree of mixing of the γ-band and β-band into the ground-state band was the same for both.[6] In spite of the fact that no significant spectroscopic differences were found between them, the γ-band is quite a bit more strongly excited in neutron scattering from ^{150}Nd than from ^{152}Sm, and the elastic scattering is also noticeably different for the two nuclei. Considerable additional work is planned

---

[5] D.F. Coope, S.N. Tripathi, M.C. Schell, J.L. Weil, and M.T. McEllistrem, Phys. Rev. C 16, 2223 (1977).

[6] S.N. Tripathi, D.F. Coope, M.C. Schell, and M.T. McEllistrem, to be published in The Physical Review C.

[7] S.W. Yates, Noah R. Johnson, L.L. Riedinger, and A.C. Kahler, Phys. Rev. C 17, 634 (1978).

to interpret neutron scattering at these low energies from these nuclei, using approaches which transcend simple collective excitation models. It appears now that neutron scattering may show a sensitivity to properties of target nuclei which cannot be seen by examining levels and decay schemes.

The path toward future use of neutron scattering to elucidate the dynamical behavior of target nuclei may be exemplified by work in progress with the Pt isotopes, a collaboration between Professor Steve Yates of our Chemistry Department and our nuclear research group. Although we work together on all aspects of the Pt study, Steve takes principal responsibility for level and decay scheme studies while we take responsibility for scattering measurements and interpretation. First efforts to describe work at 2.5 MeV incident has provided a successful description of the scattering for ^{194}Pt. This coupled-channels description includes the 0^+, 2^+, and 4^+ levels of the ground-state band, as well as the 2^+_γ, 3^+_γ levels. The model is not a simple collective excitation picture, but is based on structural details from the study of levels and decays, Coulomb-excitation measurements, and even theoretical models of the ^{194}Pt levels. In other words, it's a detailed matching of nuclear structure properties obtained using several tools to neutron scattering. Such a detailed matching of structure to scattering seems to work, at least for ^{194}Pt, but the results are preliminary. It's perhaps worth noting that the collective excitations in ^{194}Pt are much weaker than those in ^{150}Nd and ^{152}Sm.

All of the studies of collective excitations in neutron scattering discussed above deal with E2 excitations. To see if E1 excitations would influence neutron scattering strengths, cross sections were measured for inelastic scattering to ~6 levels with $J^\pi = 1^-$ in ^{208}Pb. These levels had had their E1 strengths determined in resonance photon scattering. In spite of the fact that the collective 1^- strengths of these levels varied by more than a factor of 10, they were all excited with the same strength in neutron scattering, for an incident energy of 7 MeV. It is not a very sensitive test of possible E1 influences on neutron scattering, because the collective widths of all of these levels are small, but the lack of any observed influence would suggest that neutron scattering reflects E1 excitations weakly or not at all.

2. Levels and Transitions - A $\simeq$ 100 Region. (Fenyes, Kern)

We have been pursuing detailed nuclear structure studies in nuclei with A ~ 90 - 100 for several years, since elucidation of the progression of these structures as nucleons are added to them gives insight into the particle, particle-hole, and particle-particle excitations which may be associated with a transition from rigid spherical nuclei to soft, deformable nuclei and hence to deformed structures. Since the early 1970s, for example, many have argued that ^{100}Mo, the most neutron rich of the stable isotopes, is deformed or nearly deformed. This argument followed partly from quasi-particle phonon interaction models, which predicted ^{100}Mo to be in a shape transitional region. The argument that ^{100}Mo is highly deformable or deformed also arises because of the sudden drop in excitation energy of the first excited 2^+ state compared to other Mo isotopes, together with the strong E2 decay of that state. However, earlier neutron scattering studies of the Mo isotopes done here revealed nothing even remotely like the scattering effects we now see at either end of the rare earth region, in the shape transitional nuclei.

Studies of γ-ray multipolarities have just been completed[8] for odd-odd nuclei ranging from ^{92}Nb to ^{98}Tc. Were deformation effects to be growing progressively to a shape-transition near ^{98}Tc one would expect dominance of M1 decays for a single particle-particle configuration, perhaps appropriate for ^{92}Nb, but strong growth of E2 strength as configurations became more complex, near ^{98}Tc. But this is not what emerged.[8] Instead M1 decay dominates throughout the whole range of nuclei, as strongly dominant for ^{96}Tc and ^{98}Tc as for ^{92}Nb. Deformation effects must arise much later.

3. Neutron Scattering, Spherical Nuclei. (Harper, Weil)

The study of neutron scattering from five even-A Sn isotopes from 1.0 to 4.0 MeV is being analyzed in a coupled-channels analysis treating the excited 2^+ states as vibrational excitations. The scattering is also being analyzed in a conventional single-channel model. The differences between the results from the two analyses can give us insight into the role of vibrational excitations in the dynamics of those nuclei.

In the deformed rare earths and shape transitional nuclei near $A \sim 150$ and $A \sim 190$, measurements of scattering cross sections for collective excitations is continuing, as well as coupled-channels analyses using collective excitation models based on a description of the excited levels in a nuclear model. Realistic descriptions for these nuclei are obtained with an anharmonic vibrator model, as well as other models. The implications of these models is being put into the description of scattering to the excited states of the nuclei modelled. The level and decay schemes of ^{194}Pt and ^{198}Pt are being carefully studied using $(n,n'\gamma)$ techniques to provide information about the structure of these nuclei.

---

[8] D.E. Miracle and B.D. Kern, Nuclear Physics A 320, 353 (1979).

4. Future Nuclear Structure Studies. (McEllistrem, Hanly, Mirzaa, Weil)

The studies of ^{194}Pt, ^{198}Pt have been mentioned above. Soon we expect to begin structure studies on ^{192}Os, which is even closer to the shape transition, from prolate to oblate shapes, than the Pt nuclei we are now studying. Because of the continuing interest in the development toward nuclear softness as A progresses from 90 toward 100, we are studying the levels and decay scheme of ^{96}Nb, at the suggestion of Dr. Tibor Fenyes, who is a collaborator in our laboratory from Hungary. Early studies by Dr. Fenyes' group at Debrecen, Hungary found a pronounced shift in energies of low-lying levels of ^{96}Nb compared to other odd-odd nuclei in that mass region, which could reflect $d_{5/2}$ subshell closure at 56 neutrons. The level and decay schemes of ^{96}Nb are being more extensively studied here, with a view to understanding particle configurations which are important for nuclei beyond A = 96.

LOS ALAMOS SCIENTIFIC LABORATORY

A. NUCLEAR DATA MEASUREMENT

1. Neutron Total Cross Section for Tritium (Seagrave)

A paper on this subject with T. W. Phillips and B. L. Berman of LLL has been accepted for publication by Physical Review C.

This experiment employed 200 000 Ci of tritium gas at high pressure in one of three sample cells housed in an evacuated sample-changer device, all constructed at LASL. The experimental runs were conducted at the LINAC at LLL.

The experiment measured the neutron total cross section for tritium over a wider range (50 keV - 100 MeV) and with higher accuracy ($\pm$ 0.5% over the central range) than has heretofore been achieved for any nuclide.

The results are in quite good agreement with a prediction from the p-^{3}He R-matrix analysis of G. Hale and D. Dodder at LASL (see Sec. B-1) with the Coulomb force "turned off," except for the details of a newly-observed minimum present in both the measurement and the calculation near 500 keV neutron energy.

2. The Zero Energy Cross Section and Scattering Lengths for Tritium (Seagrave)

The implications of the possibility of extrapolating the total cross section to zero energy were recognized, and a paper to Physics Letters B has been submitted with T. W. Phillips and B. L. Berman of LLL to point out the consequences: 1) superseding of earlier erroneous total cross-section data, and 2) the inference of more precise values of the n-^{3}H scattering lengths than have been available previously using thermal neutron techniques. A quadratic extrapolation-to-zero-energy yields a zero-energy cross section of 1.70 $\pm$ 0.03 b, while a linear extrapolation yields 1.69 $\pm$ 0.02 b. Final extrapolation will be based on the Hale-Dodder analysis including the present data.

With a constraint based on recent theoretical estimates, more precise values of the scattering lengths can be inferred from the present results that are consistent with, but independent of, the existing coherent scattering length measurement. A long-standing discrepancy has been resolved by this work.

3. Deuterium and ^{12}C Thermal (n,γ) Cross Sections (Bendt, Jurney)

In order to resolve discrepancies in the earlier reported values of $\sigma(n,\gamma)$ for ^{2}D and to confirm a more recent value[1] determined by beta-counting of the tritium produced in a long reactor irradiation, we have determined the intensity of the 6.2-MeV gamma from D capture relative to that of the 4.9-MeV gamma from ^{12}C capture in a small sample of CD_2. The carbon capture cross section was determined from a separate measurement using a target of CH_2.

Preliminary inspection of the data yields a value for the deuterium capture cross section in agreement with that of Merritt et al.

4. Low-Energy Cross-Section Project (Brown, Jarmie, Hardekopf, Correll, Ohlsen)

The goal of the project is to measure cross sections for interactions between the hydrogen isotopes in the bombarding energy range 10-120 keV. Such cross sections are fundamental to the operation of future controlled fusion systems. Most of the apparatus for the measurements has been assembled and is operating well; this apparatus includes the low-energy accelerator and beam transport system, the cryogenically pumped windowless gas target, the beam calorimeters, and the particle-detection and computerized data-acquisition systems.

Currently, tests are being carried out under full operating conditions by taking preliminary data on the D(d,p)T reaction. So far, 6 angular distributions from 40 to 118 keV have been measured, but the absolute scale has not yet been calibrated to better than about 15%. The scale calibration uses p + D elastic scattering at 10-MeV proton bombarding energy, and a more accurate calibration is now in progress.

5. Neutron Emission Data (Drake, Lisowski, Drosg)

We have measured the neutron emission spectra for some elements that are important to the fusion reactor program, such as $^{6,7}Li$, $^{10,11}B$, and carbon. Targets of these elements were bombarded with neutrons of 6, 10, and 14 MeV and the energy and angular distributions of the emergent neutrons were measured. Figures A-1 and A-2, taken from a forthcoming Los Alamos report, show angular distributions of the elastically scattered neutrons from ^{6}Li and ^{7}Li as well as resolvable inelastic scattering for incident neutrons of 9.83 MeV. Some points

---

[1]J. S. Merritt, J. G. V. Taylor, and A. W. Boyd, Nucl. Sci. Eng. 3, 195 (1968).

taken from earlier data from other laboratories are shown for comparison. Numerical tabulations of the ^{6}Li and ^{7}Li data for incident neutrons of 5.96 or 9.83 MeV can be found in the report.

In measuring these cross sections for low energy neutrons, it was necessary to have a counter whose efficiency was well characterized. Because the pulse height bias must be low, part of the counting efficiency is due to neutron interactions with carbon within the counter. These interactions tend to make the efficiency curve bumpy rather than smooth as one would expect considering only (n-p) scattering. Figure A-3, taken from LA-7987-MS, shows our efficiency curve with these bumps which can cause variations up to 10%.

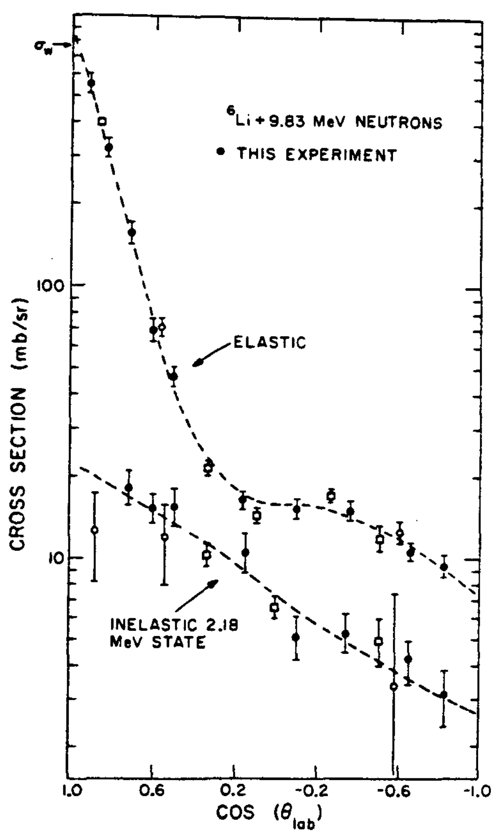

Fig. A-1. Angular distributions of the elastic and inelastic (E^* = 2.18 MeV) scattering cross sections for ^{6}Li bombarded by 9.83 MeV neutrons.

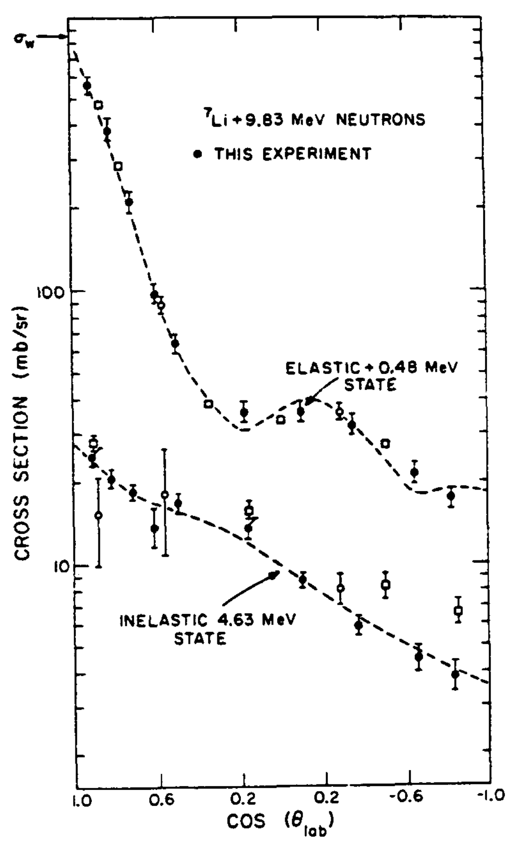

Fig. A-2. Angular distributions of the elastic + 0.48 MeV state and the inelastic (E^* = 4.63 MeV) scattering cross sections for ^{7}Li + 9.83 MeV neutrons.

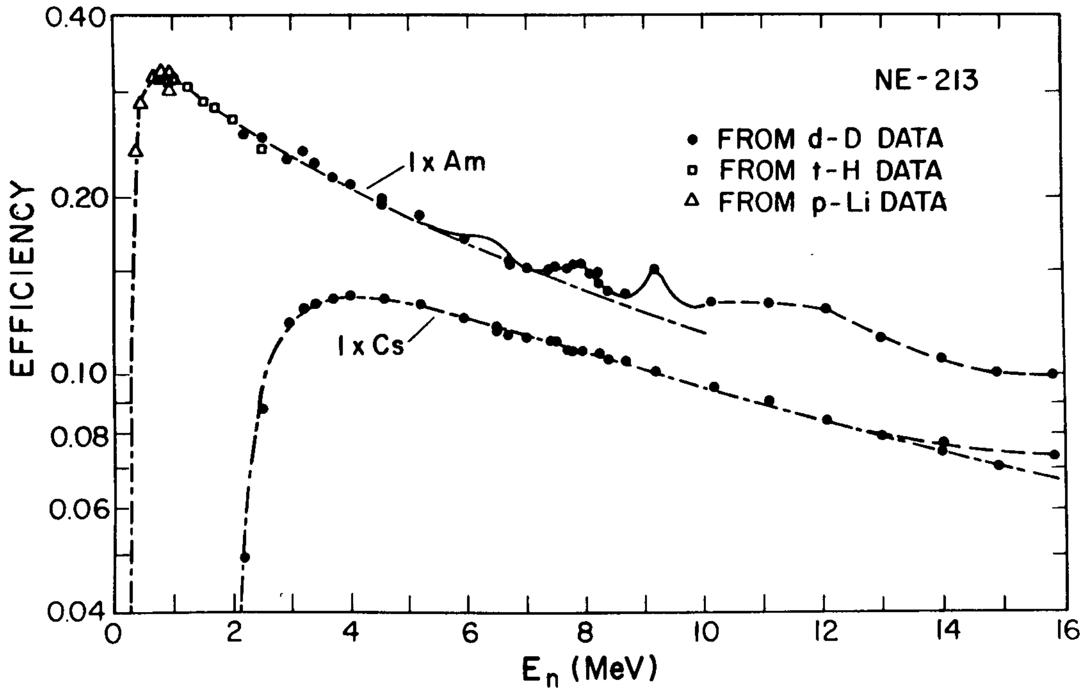

Fig. A-3. Relative efficiency for a neutron bias of 300 keV and 2 MeV.

B. NUCLEAR DATA EVALUATION

1. Charge-Independent Analysis of the Four-Nucleon System (Hale, Dodder)

Our charge-independent R-matrix description of reactions in the four-nucleon system has generally been quite consistent with new experimental results. Scattering lengths for n-^{3}He calculated from the analysis give a coherent value in excellent agreement with a new measurement by Kaiser et al.[1] Similar predictions for n-T appeared not to agree particularly well with low-energy extrapolations of the cross section based on earlier measurements but are in good agreement with precise new total cross-section measurements from a Livermore-Los Alamos collaboration[2] (see Sec. A-1), as shown in Fig. B-1.

---

[1] H. Kaiser, H. Rauch, G. Badurek, W. Bauspiese, and U. Bonse, "Measurement of Coherent Neutron Scattering Lengths of Gases," Z. Physik A291, 231 (1979).

[2] T. W. Phillips, B. L. Berman, and J. D. Seagrave, "Neutron Total Cross for Tritium," submitted to Phys. Rev. C (1980).

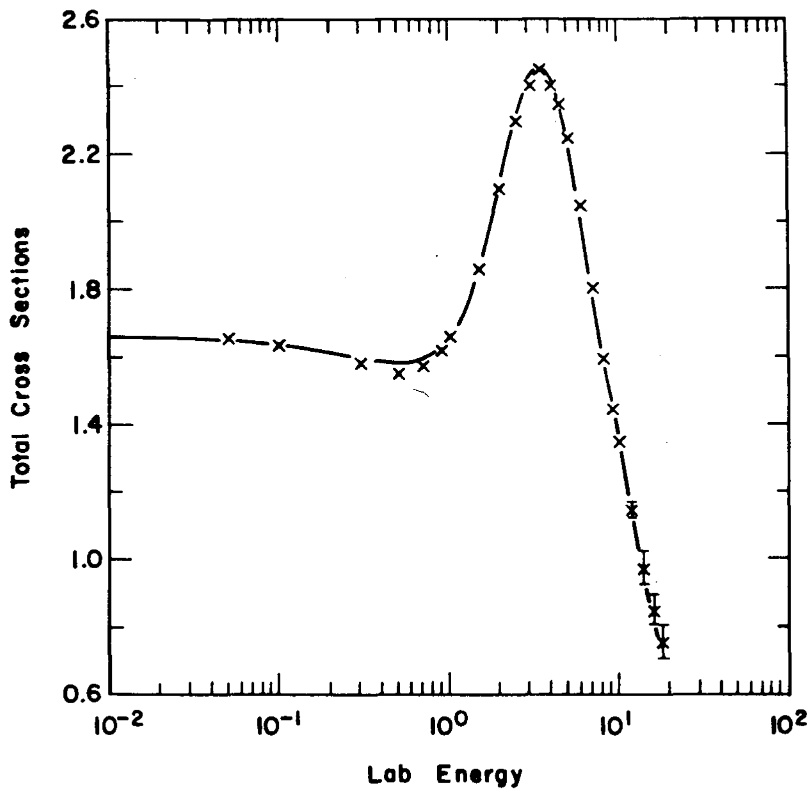

Fig. B-1. Comparison of n-T total cross sections predicted from p-^{3}He R-matrix parameters with points representative of new measurements by Phillips et al.

The calculations shown in this figure are obtained by simply turning off the external Coulomb interaction and shifting the E_λ's of the p-^{3}He R-matrix parameters to account for the absence of internal Coulomb energy in ^{4}H. Thus, the agreement of the prediction with the data is a measure of the macroscopic charge symmetry of nuclear forces, although the comparison is clouded by the simplicity of the correction made for Coulomb effects.

A promising explanation for the puzzling differences in the two branches of the d + d reaction seems to result from allowing a small amount of isospin mixing consistent with internal Coulomb interactions. These small admixtures are able to account for most of the 15-20% differences seen in the D(d,n) and D(d,p) cross sections and polarizations in the few-hundred keV range. We are currently considering these effects at higher energies where large differences between the two branches have also been observed in recent measurements made with polarized deuterons.

2. Low-Energy Behavior of Fusion Cross Sections (Hale, Dodder)

We have been studying the low-energy behavior of fusion cross sections by removing penetrability and 1/E factors from our R-matrix calculations of the cross sections. The remaining quantity, sometimes called the "astrophysical S-function," is often taken to be constant at low energies for purposes of extrapolating the cross section.

We have found significant energy dependence in the behavior of the S-function at low energies for some of the important fusion reactions as illustrated in Fig. B-2 for $T(d,n)^4He$ and in Fig. B-3 for $D(d,n)^3He$. Our calculated S-function for T(d,n) changes by 40% in the 0-30 keV range, clearly disagreeing with the assumption of Arnold et al.[1] in reporting their cross-section values that the S-function is constant below 20 keV (dashed line) and more in agreement with their actual measurements. The 14% change in the D(d,n) S-function at energies below 50 keV is also consistent with measurements.[1] In both cases, the energy dependence of the S-function comes mainly from large s-wave resonances located near [although in the D(d,n) case it is several MeV away] the deuteron threshold.

3. Charged-Particle Fusion Data File (Hale)

Cross sections for many of the important fusion reactions, calculated from our R-matrix analyses of light systems, have been collected in a file having ENDF-like format. Cross sections are tabulated on an average range of laboratory energies from 100 eV to 5 MeV for the reactions $T(d,n)^4He$, $T(t,2n)^4He$, $^3He(d,p)^4He$, $^6Li(p,^3He)^4He$, and $^{11}B(p,3\alpha)$ (this last evaluation is not yet based on our R-matrix analysis). Maxwellian-averaged reaction rates calculated from these cross sections are also available in an ENDF-like format for temperatures kT = 200 eV to 1 MeV.

The most recent measurements for these reactions are the $^6Li(p,^3He)^4He$ data of Elwyn et al.[2] Figure B-4 shows a comparison of the $^6Li(p,^3He)^4He$ cross sections in the file with Elwyn's results. The agreement is quite good, although the Elwyn data were not available at the time the analysis was performed.

---

[1] W. R. Arnold, J. A. Phillips, G. A. Sawyer, E. J. Stovall, Jr., and J. L. Tuck, "Cross Sections for the Reactions D(d,p)T, $D(d,n)He^3$, $T(d,n)He^4$, and $He^3(d,p)He^4$ below 120 keV," Phys. Rev. 93, 483 (1954).

[2] A. J. Elwyn, R. E. Holland, C. N. Davids, L. Mayer-Schutzmeister, F. P. Mooring, and W. Ray, Jr., "Cross Sections for the $^6Li(p,^3He)^4He$ Reaction at Energies Between 0.1 and 3.0 MeV," submitted to Phys. Rev. C (1980).

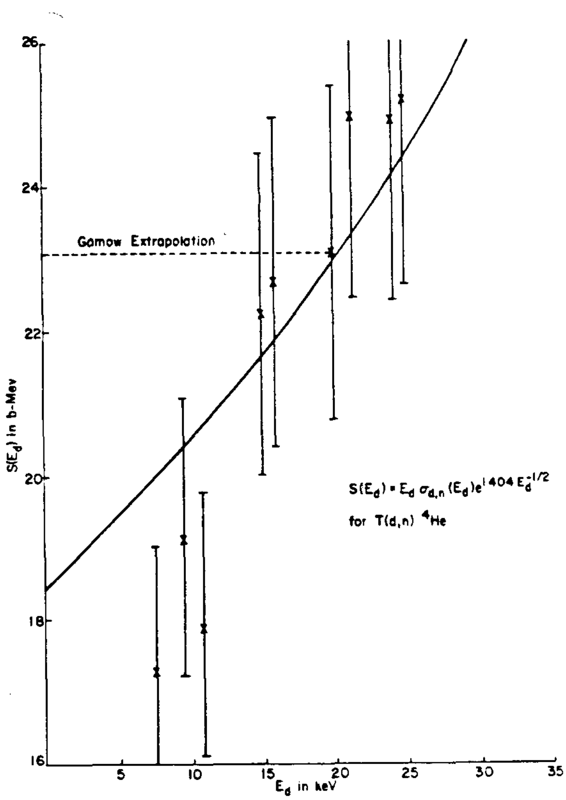

Fig. B-2. Calculated S-function for the $T(d,n)^4He$ reaction compared to the measurements and Gamow extrapolation of Arnold et al. at energies below 30 keV.

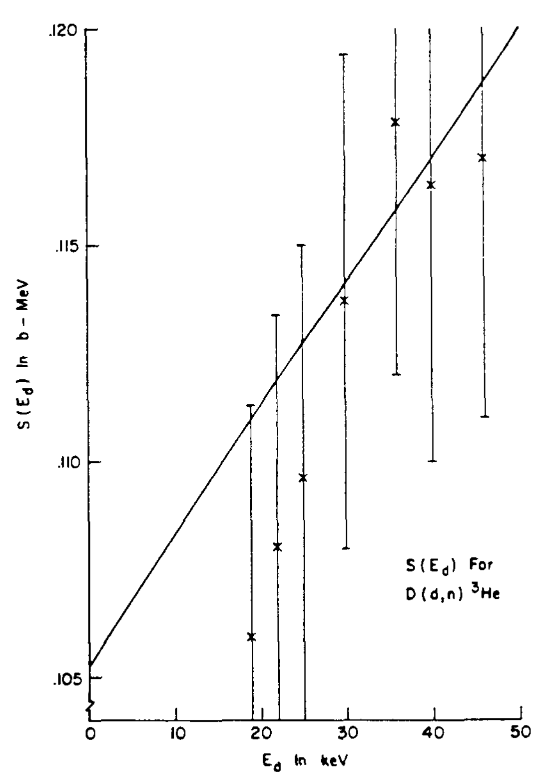

Fig. B-3. Calculated S-function for the $D(d,n)^3He$ reaction at energies below 50 keV compared to measurements by Arnold et al. which have been corrected for changes in the assumed D(d,n) angular distributions.

We plan to extend the contents of the file to include cross sections for the d + d reactions and for several charged-particle elastic scattering processes in the near future.

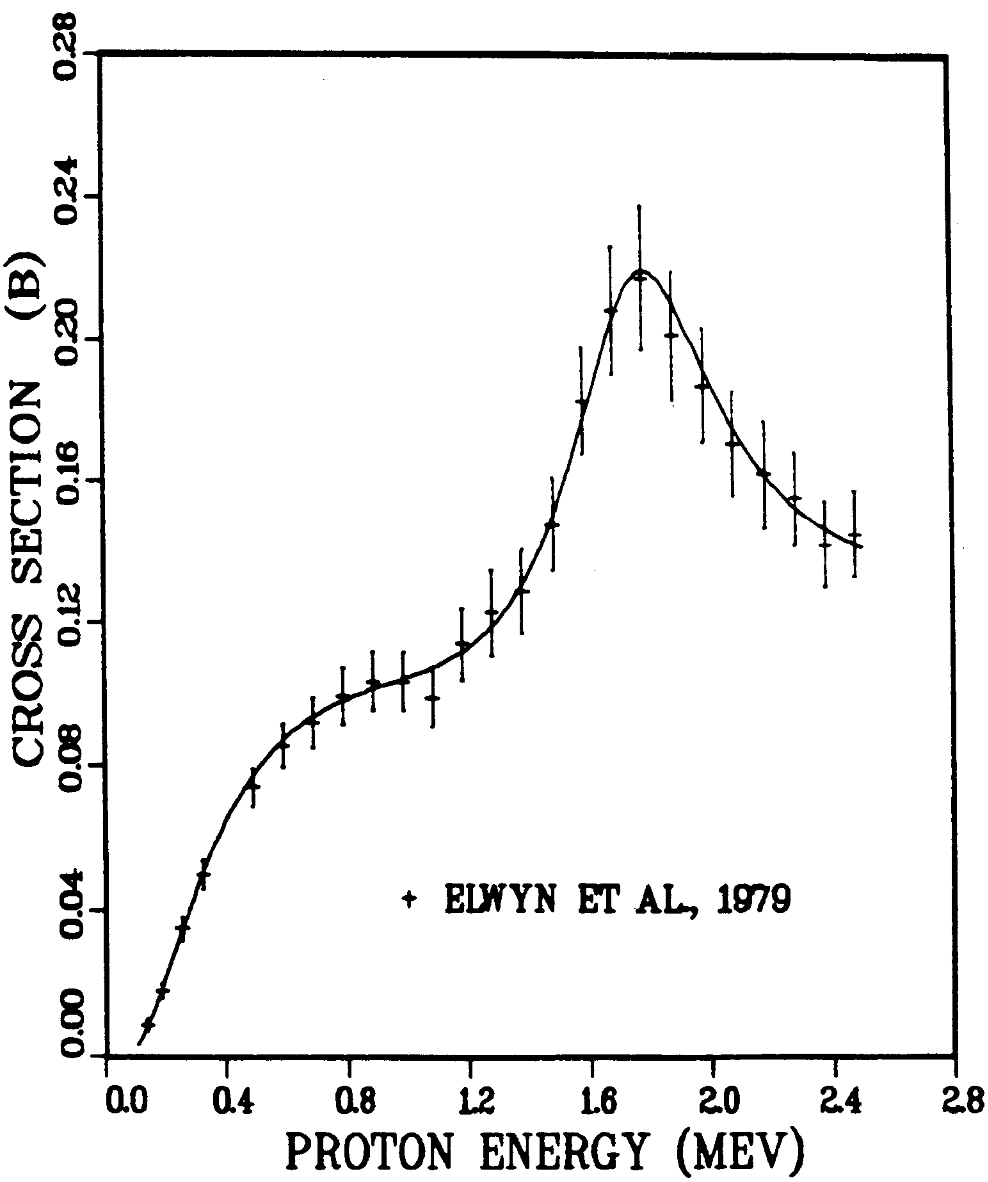

Fig. B-4. Calculated $^{6}Li(p,^{3}He)^{4}He$ cross sections tabulated in the Fusion Data File compared with recent measurements of Elwyn et al. The curve is a prediction, since the Elwyn measurements were not available at the time the analysis was performed.

4. Production of Noble-Gas Isotopes by Nuclear Reactions in the Moon (Reedy)

Cross sections were evaluated or estimated for the production of the isotopes of the noble gases helium, neon, argon, krypton, and xenon by energetic cosmic-ray particles reacting with target elements commonly found in lunar rocks.[1,2] Production rates for these nuclides in lunar rocks were calculated using these cross sections and the Reedy-Arnold model for the fluxes of cosmic-ray particles in the moon. Generally the calculated rates agreed quite well with measured concentrations of cosmogenic noble gases in lunar rocks. The worst agreement is for ^{130}Xe, which is under-calculated by about 40%. Because the agreements for ^{129}Xe and ^{131}Xe are quite good, the source of this discrepancy probably is not the cross sections for the production of ^{130}Xe by energetic protons. It is believed that the $^{130}Ba(n,p)$ reaction, not used in the calculations, has a high cross section (peak value of hundreds of millibarns) and produces a large fraction of lunar cosmogenic ^{130}Xe. During the summer of 1980, we expect to irradiate barium with 14.7-MeV neutrons and to measure mass spectrometrically the xenon produced by $^{130}Ba(n,p)$ and other reactions.

5. Calculation of Neutron Reactions on Iron Between 3 and 40 MeV (Arthur, Young)

Neutron nuclear data needs for the Fusion Materials Irradiation Test Facility (FMIT) extend up to energies around 40 MeV, a region where very few experimental data are available and reliance must be placed upon nuclear-model calculations of the desired cross sections. We have completed calculations[3] of all major neutron cross sections, particle and gamma-ray spectra, and secondary neutron angular distributions for ^{54}Fe and ^{56}Fe between 3 and 40 MeV. We used the Hauser-Feshbach, preequilibrium, and DWBA models, which describe the major reaction mechanisms for neutron-induced reactions in this mass and energy

---

[1] C. M. Hohenberg et al., "Comparisons Between Observed and Predicted Cosmogenic Noble Gases in Lunar Samples," in Proc. of the Ninth Lunar and Planetary Science Conference (Pergamon Press, Elmsford, NY, 1978), pp. 2311-2344 (LA-UR-78-1730).

[2] S. Regnier et al., "Predicted Versus Observed Cosmic-Ray-Produced Noble Gases in Lunar Samples: Improved Kr Production Ratios," in Proc. of the Tenth Lunar and Planetary Science Conference (Pergamon Press, Elmsford, NY, 1979) pp. 1565-1586 (LA-UR-79-1582).

[3] E. D. Arthur and P. G. Young, "Calculation of Neutron Cross Sections on Iron between 3 and 40 MeV," Intnl. Conf. on Nuclear Cross Sections for Technology, Knoxville, TN (Oct. 1979).

region. An important portion of the analysis was the determination, in a consistent manner, of input parameters applicable over the entire range of the calculation through analysis of various types of experimental data, both for neutron and charged-particle induced reactions. Comparisons of calculated cross sections and spectra to data available for neutron reactions between 3 and 22 MeV showed generally good agreement confirming the applicability of the input parameters employed. Comparisons were also made to proton-induced reaction data up to 40 MeV to further test parameters and models at higher incident energies. Figure B-5 illustrates a portion of the calculated results for neutron reactions of ^{56}Fe between 10 and 40 MeV. At higher incident energies, it was necessary in our Hauser-Feshbach and preequilibrium calculations to include complicated decay chains involving 80 compound nuclei and 25 reaction types to properly compute gamma-ray production spectra and cross sections such as that for (n,2np) (sum of contributions from n,npn + n,2np + n,p2n reactions), which dominate above 30 MeV.

6. Neutronics Properties for a "Typical" Fission Product (Arthur, Foster)

We are calculating cross-section sets between 0.001 and 20 MeV for "typical" products of neutron-induced fission of ^{235}U and ^{239}Pu appropriate to times before the first beta decay. We approximate such a typical fission product by a weighted average of individual nuclides chosen from the yield curves appropriate to each case. The calculations are done using the statistical-model code COMNUC at low energies and the preequilibrium-statistical-model code GNASH at higher energies.[1] Since the appropriate nuclides are quite neutron-rich, we have given special attention to determining systematic properties for each element over as wide a range of neutron numbers as possible, using simultaneous fits to total cross sections and resonance data. In order to determine gamma-ray transmission coefficients we are using gamma-strength functions taken from fits to neutron capture cross sections of stable nuclides throughout the mass regions A = 79 to 99 and A = 112 to 138. Wherever necessary, we extrapolate nuclear masses using the Garvey-Kelson relations. Our angular distributions are based on calculated transitions to known discrete levels, supplemented by the Kalbach-Mann prescription for continuum transitions. We have ignored charged-particle competition because of the scarcity of data in the neutron-rich region.

---

[1] C. I. Baxman and P. G. Young, "Applied Nuclear Data Research and Development, April 1-June 30, 1979," Los Alamos Scientific Laboratory report LA-8036-PR (1979), p.8.

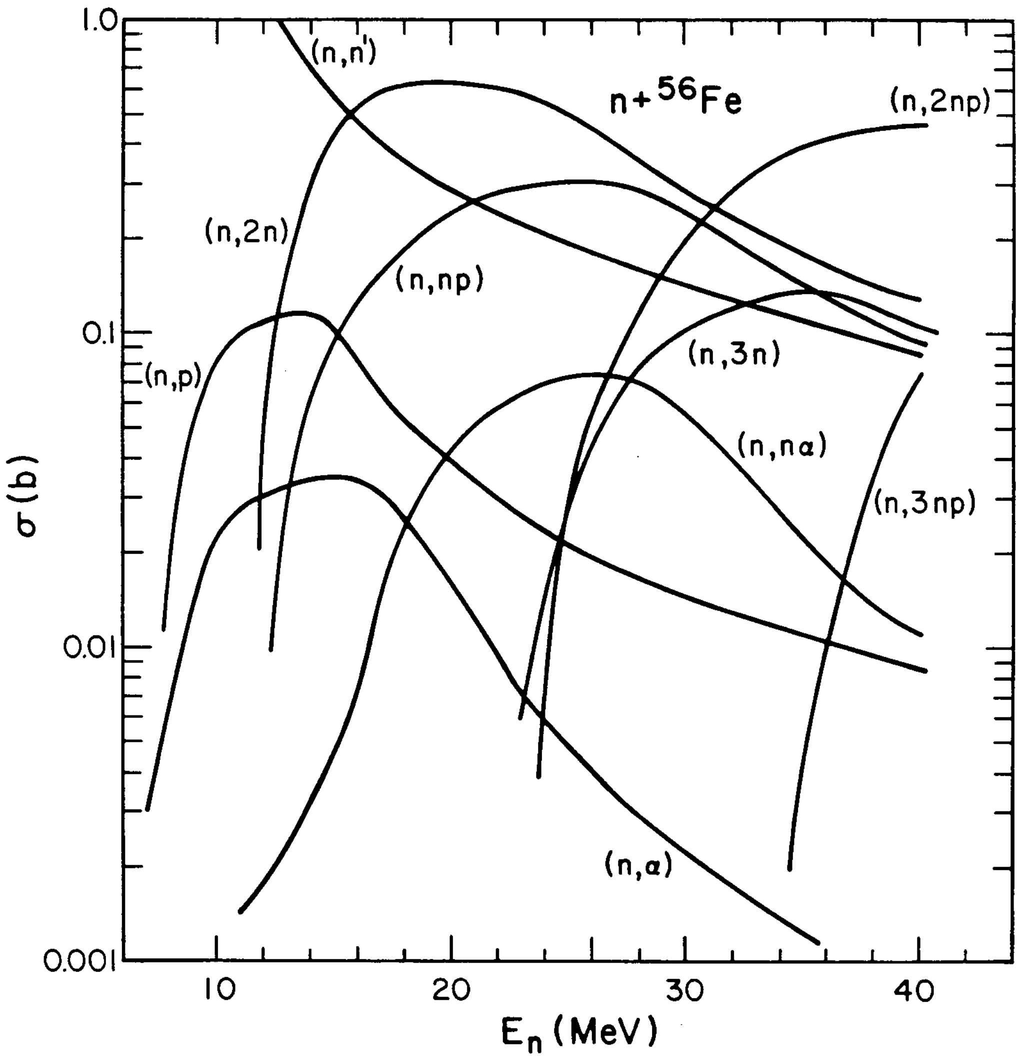

Fig. B-5. Calculated n + ^{56}Fe cross sections in the energy range between between 10 and 40 MeV.

7. Calculation of Prompt Fission Neutron Spectra (Madland, Nix)

Work has been completed on a new calculation of the prompt fission neutron spectrum as a function of both the fissioning nucleus and its excitation energy.[1-3] The calculation is based upon standard nuclear-evaporation theory and accounts for the physical effects of (1) the distribution of fission-fragment residual nuclear temperature and (2) the energy dependence of the cross section for the inverse process of compound-nucleus formation. Using a residual nuclear temperature distribution based upon the Fermi-gas model, calculations have been performed for two different assumptions concerning the cross section for compound-nucleus formation. A constant cross section yields a closed expression for the neutron energy spectrum, while an energy-dependent cross section, calculated with the optical model, yields a numerical integral expression. Results obtained for the two assumptions agree well with experimental data although there is a clear preference for the energy-dependent cross-section calculations. An example is shown in Fig. B-6 for the fission of ^{235}U by 0.53-MeV neutrons.

The formalism for the calculations has also been used to calculate the average number of prompt neutrons per fission, $\bar{\nu}_p$, as a function of fissioning nucleus and excitation energy (incident neutron energy). Calculations have been compared to experimental $\bar{\nu}_p$ data from six actinides with good agreement in each case.

8. Delayed Neutrons (England, Schenter, Schmittroth)

Sufficient neutron emission probabilities spectra and fission yield data now exist to permit accurate calculations of the aggregate spectra and the average delayed neutrons per fission ($\bar{\nu}_d$). This has been done for 11 fissionable nuclides at 1 to 3 incident neutron energies. The spectra for 24 precursors have been used to determine aggregate shapes, and 105 precursors were used to determine the average $\bar{\nu}_d$.

---

[1] D. G. Madland and J. R. Nix, "Calculation of Prompt Fission Neutron Spectra," Trans. Am. Nucl. Soc. 32, 726 (1979).

[2] D. G. Madland and J. R. Nix, "Calculation of Prompt Fission Neutron Spectra," Bull. Am. Phys. Soc. 24, 885 (1979).

[3] D. G. Madland and J. R. Nix, "Calculation of Prompt Fission Neutron Spectra," Intrnl. Conf. on Nuclear Cross Sections for Technology, Knoxville (Oct. 1979).

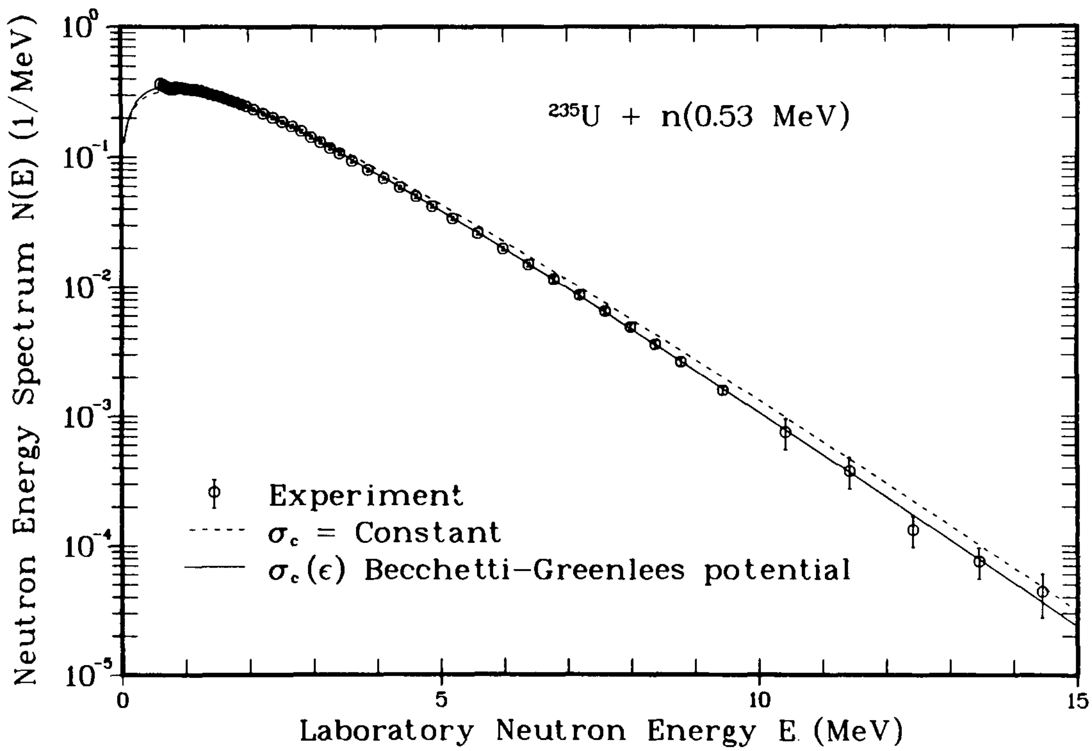

Fig. B-6. Comparison of calculated and experimental prompt fission neutron spectra for the fission of ^{235}U induced by 0.53-MeV neutrons. The experimental data are those of Johansson and Holmqvist [Nucl. Sci. Eng. 62, 695 (1977)].

Some improvements in data are necessary for $\bar{\nu}_d$, but the spectra appear to be a definite improvement over current evaluations. The spectral work is still in progress, but current $\bar{\nu}_d$ calculations have been reported.[1]

---

[1] T. R. England, R. E. Schenter, and F. Schmittroth, "Delayed Neutron Calculations Using ENDF/B-V Data," Intnl. Conf. on Nuclear Cross Sections for Technology, Knoxville (Oct. 1979).

9. Fission Product Cross Sections (Schenter, England)

The status of cross-section evaluations for 196 products along with preliminary evaluations to illustrate the generalized least-squares method now in use was reported in Ref. 1. Evaluations for all nuclides are not yet complete.

10. ^{239}Pu Delayed Beta and Gamma Spectra (England, Dickens)

Plutonium-239 samples were irradiated for 1 to 100 seconds in the fast pneumatic-tube facility at the Oak Ridge Research Reactor. The resulting beta and gamma spectra were measured for times after fission between 2 and 14 000 seconds. Extensive graphical comparisons of these benchmark data with spectra computed with the CINDER-10 code system and the ENDF/B-IV data base are available in Ref. 2 at 47 decay times.

---

[1]R. E. Schenter and T. R. England, "ENDF/B-5 Fission Product Cross Section Evaluations," NEANDC Specialists' Meeting on Neutron Cross Sections of Fission Product Nuclei, Bologna, Italy (Dec. 1979).

[2]J. K. Dickens et al., "Delayed Beta- and Gamma-Ray Production Due to Thermal-Neutron Fission of ^{239}Pu: Tabular and Graphical Spectral Distributions for Times after Fission Between 2 and 14 000 s," Oak Ridge National Laboratory report NUREG/CR-1172 (ORNL/NUREG-66) (January 1980).

A. NUCLEAR DATA APPLICATIONS - MEASUREMENTS

1. Neutron Total Cross Section for Tritium. (Phillips, Berman, and Seagrave*)

We have measured the neutron total cross section for tritium, for incident neutron energies ranging from 60 keV to 80 MeV at the LLL linac, using a high-pressure gas sample and the neutron time-of-flight technique, with an experimental accuracy of better than 0.5% over much of this energy range. Similar measurements on hydrogen and deuterium also were performed.[1,2]

The cross-section data obtained for tritium (Fig. A-1) lead to the following conclusions: (1) the extrapolated zero-energy cross section is found to be 1.70 $\pm$ 0.03 b, in sharp disagreement with previous thermal-energy observations, but in agreement with calculations which also yield the currently-accepted coherent scattering length, 3.73 fm, (2) a minimum in the cross section near 600 keV (with a rise at lower energy) is newly observed, (3) agreement with a prediction from an analysis of p-^{3}He data is within 1% at the resonance peak near 3.5 MeV, but the data differ from this prediction by as much as 6% at lower and higher energies, and (4) the cross section in the heretofore unexplored energy region between 7 and 14 MeV exhibits no structure, thus contradicting the existence of a bound four-neutron state.

2. Photodisintegration of Tritium (Berman, Faul, Meyer, and Olson)

We have measured both the two-body (γ,n) and three-body (γ,2n) photodisintegration cross sections for tritium, for incident photon energies from threshold to $\sim$25 MeV at the LLL linac, using a high-pressure gas sample and monoenergetic photons from the annihilation in flight of fast positrons with photon resolution between 1 and 2%, with an experimental accuracy between 7 and 10%.[3,4] This is the first measurement of

*Los Alamos Scientific Laboratory, Los Alamos, NM 87545.

[1] J. D. Seagrave, B. L. Berman, and T. W. Phillips, Physics Letters B (to be published) and UCRL-83891 (1980).

[2] T. W. Phillips, B. L. Berman, and J. D. Seagrave, UCRL-77783 (1979).

[3] D. D. Faul, B. L. Berman, P. Meyer, and D. L. Olsen, Phys. Rev. Letters 44, 129 (1980).

[4] B. L. Berman, D. D. Faul, P. Meyer, and D. L. Olsen, UCRL-82188 (1979).

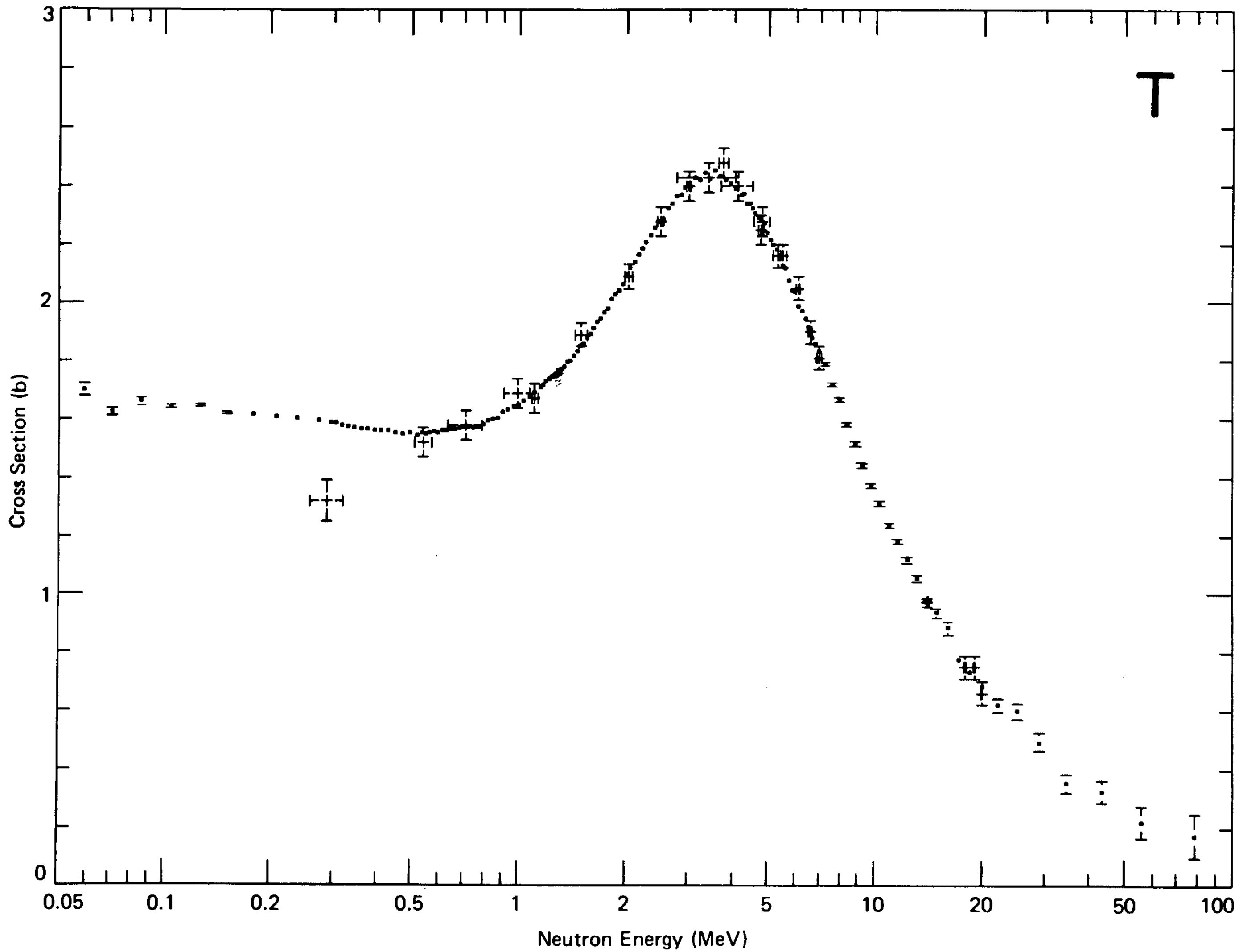

Figure A-1. Total cross section for tritium. The data indicated with crosses are literature values; those with points are present results.

these cross sections across the energy region of their maxima. Similar measurements on deuterium, oxygen, and the helium isotopes also were performed. Presently available calculations for the tritium cross sections are not adequate to explain the measured cross sections.

3. Photoneutron Cross Sections for ^{17}O (Berman, Faul, Meyer, Woodworth, and Jury*)

We have measured the photoneutron [(γ,n) and (γ,2n)] cross sections for ^{17}O from 8 to 40 MeV at the LLL linac, using a water sample and monoenergetic photons from the annihilation in flight of fast positrons with photon resolution between 1 and 2%, with an experimental accuracy of 7%. Similar measurements on ^{13}C and ^{18}O have been reported and published previously; measurements on ^{16}O were performed simultaneously with those on ^{17}O;[5] and others, on ^{15}N, ^{29}Si, and ^{30}Si, will be performed later this year.

4. Measurements of $^{88}Sr(p,n)$ to the Ground State and Low-Lying Excited States of ^{88}Y (Grimes, Poppe, and Wong)

In order to extract the (n,p) cross section for the unstable nuclide ^{88}Y (107 day) we have measured the inverse (p,n) cross section on the stable target ^{88}Sr for proton energies between 5.75 and 11 MeV. Protons from the LLL model-EN tandem Van de Graaff accelerator bombarded a metallic foil target and neutrons were detected using a 16-detector time-of-flight spectrometer. The detectors, NE213 liquid scintillators, spanned angles between 3.5° and 160° and were located at a flight path of 10.5 m. Overall resolution was sufficient to separate the ^{88}Y ground state ($J^{\pi} = 4^-$), the first excited state ($J^{\pi} = 5^-$) at 0.232 MeV, and the second excited state ($J^{\pi} = 1^+$) at 0.393 MeV. Higher unresolved states were also observed. A Legendre polynomial fit was made to the angular distributions and the resulting integrated cross sections are shown in Fig. A-2. From the principle of detailed balance, the inverse cross sections $^{88}Y(n,p)\ ^{88}Sr$(g.s.) may be extracted from these data for the ^{88}Y ground state and the 0.3-ms isomer at 0.393 MeV. The data may also be used as a basis for Hauser-Feshbach calculations which will allow the total (n,p) cross section on the ^{88}Y ground state and important isomers to be estimated.

*Trent University, Peterborough, Ontario, Canada.

[5] J. W. Jury, B. L. Berman, D. D. Faul, P. Meyer, J. G. Woodworth, Phys. Rev. C21, 503 (1980).

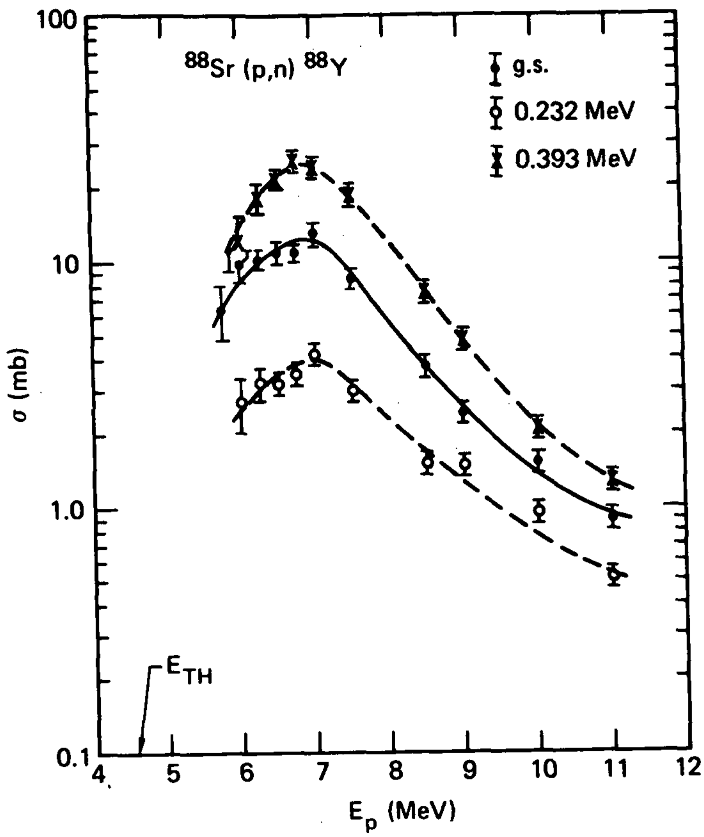

Figure A-2. Angle-integrated cross sections as a function of bombarding energy for the ^{88}Sr(p,n) reaction to the ground state (g.s.) of ^{88}Y and the first two excited states (E_x = 0.232 and 0.393 MeV). The curves serve only to connect the data and guide the eye. The arrow near 4.4 MeV indicates the threshold for the g.s. reaction.

5. Information on Gamma-Ray Strength Functions in the Mass-90 Region from Proton-Induced Reactions (Dietrich, Heikkinen, and Gardner)

In order to understand the systematics of gamma-ray production we have extended our measurements in the mass-90 region to include excitation functions and spectral distributions of gammas produced by proton bombardment of ^{92,96,100}Mo. Data were taken from 3 MeV to energies well above the (p,n) thresholds. Gamma rays were detected with Ge(Li) and anticoincidence-shielded NaI spectrometers. The Ge(Li) detector was used to obtain individual gamma lines from transitions between low-lying states in the compound nucleus and from transitions following the (p,n) and (p,p') reactions where energetically possible. The NaI spectrometer was used to obtain the entire gamma-ray spectrum and the total energy released as gammas. Previous measurements on ^{88}Sr, ^{89}Y, and ^{90}Zr have shown that the excitation functions of individual gamma lines and the total energy released by gammas is reproduced reasonably well by standard Hauser-Feshbach calculations. However, the gamma spectral distributions require a modification of the energy-dependence of the E1 gamma-strength function from the usual Brink-Axel (Lorentzian) form. Such a modification is described elsewhere in this report and is being applied to calculations in the mass-90 region.

6. Studies of (n, charged particle) Reactions with 14-15 MeV Neutrons (Haight, Grimes, and Barschall*)

Materials bombarded by fusion neutrons are altered by nuclear transmutations that produce hydrogen and helium. To assess the potential performance of these materials for fusion reactor application, cross section data are required by the fusion community and the Office of Fusion Energy. Under the sponsorship of the DOE Office of Basic Energy Sciences, we measure these quantities by detecting the charged particles emitted by materials under bombardment by neutrons of 14 to 15 MeV. By also measuring the energy and angular distributions of the charged particles, we are able to test nuclear reaction theories through model calculations and to deduce KERMA factors for consideration of energy deposition by the neutrons.

In the past year we have measured Y, Zr, ^{92,94,95,96}Mo, C, ^{7}Li, and F. Together with our previous data the heavier targets complete most top priority materials for structural application for neutron energies in the 14-15 MeV region. A proton spectrum from ^{94}Mo is shown in Fig. A-3. The lighter targets have been measured at 14 MeV with a conical neutron-producing rotating target. To calibrate the response of the

*University of Wisconsin, Madison, WI 53706.

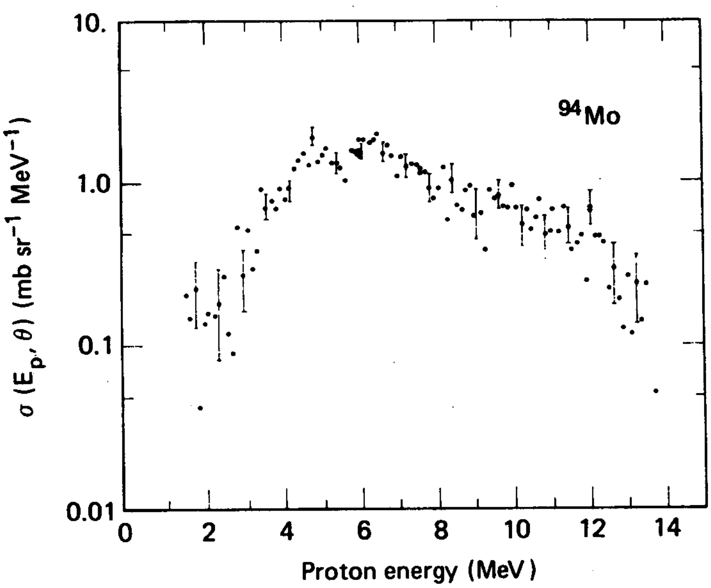

Figure A-3. Spectrum of protons emitted at 90^{o} from ^{94}Mo under bombardment with 15-MeV neutrons.

spectrometer for low-energy alpha particles emitted by the light targets, we have developed a high-pressure thin-window helium gas cell.[6] The n-alpha elastic scattering cross section is taken to be the standard for this calibration.

7. Neutron Total Cross Section Measurements from 2.5 to 60 MeV (Camarda,* Phillips, and White)

Using the Lawrence Livermore Laboratory 100-MeV electron linear accelerator in conjunction with a 250-meter flight path we have measured at the 1-3% level the absolute neutron total cross section of ^{140}Ce and at the 0.3% level the relative cross sections ^{142}Ce/^{140}Ce and ^{141}Pr/^{140}Ce. The samples were in oxide form. For the ^{140}Ce absolute cross section measurement, an H_2O sample with an equivalent amount oxygen formed the open. The effect of the hydrogen was unfolded analytically. For these measurements the neutron-producing target was made of TaBe and the detector consisted of 16 independent plastic scintillators (25cmx25cmx5cm). Optical model calculations are being performed and will be compared with the data.

8. Measurement of the (p,n) Reaction to the Ground- and Excited-Analog States of Se Isotopes (Wong, Pohl, Poppe, and Rhodes)

In recent years we have attempted to deduce neutron scattering by applying the Lane model to measured (p,n) cross sections for charge-exchange to the isobaric analog state of the target nucleus.[7] It was discovered that multi-step processes proceeding through excited states of the target and excited analog states have a pronounced effect on the ground-state transition[8] and must be understood if the Lane model is to be successfully applied. By using a coupled-channel calculation, we are able to reproduce the charge-exchange cross sections to excited analog states using only parameters derived from proton inelastic scattering and results of the ground-state analog measurements.[9] Because of the good agreement between the experiments and calculations, we believe that measurements of (p,n) charge-exchange cross sections will allow us to

---

*Penn State University, Delaware Campus, Media, PA 19063.

[6] R. C. Haight, C. Rambo, J. Cormier, and J. L. Garibaldi, Nucl. Instr. and Meth. 164, 613 (1979).

[7] C. Wong et al., Phys. Rev. C5, 158 (1972); C. Wong et al., Phys. Rev. C7, 1895 (1973); S. M. Grimes et al., Phys. Rev. C11, 158 (1975).

[8] V. A. Madson et al., Phys. Rev. C13, 548 (1976).

[9] C. Wong et al., Phys. Rev. C20, 59 (1979).

deduce both neutron elastic and inelastic scattering. We are continuing to study this hypothesis and recently have completed measurements on the isotopes $^{76,80,82}Se$ for proton energies of 19, 22, and 25 MeV. In this experiment the isobaric analogs of the ground states of the target nuclei were observed as well as the one- and two-phonon excited analogs for the Se isotopes.

9. <u>Level Structure and Octupole Bands in ^{180}W</u> (Mann, Carlson, Lanier, Struble, Buckley, Heikkinen, Proctor, and Singh)

In a study of ^{180}W using the $^{181}Ta(p,2n\gamma)^{180}W$ reaction, we produced states up to I = 12 and were able to establish the details of the $K^{\pi} = 2^-$ octupole band up to the 11^- state.[10] Several other rotational bands were observed, including the previously-studied band built on the metastable $K^{\pi} = 8^-$ state at 1529 keV, the γ-vibrational bands, and a new band built on a K = 5 state at 1639.8 keV. We also observed a state at 1634.6 keV which we tentatively interpreted as the $K^{\pi} = 3^-$ octupole band head, based on its decay properties and on the likely possibility that it is the same state as one observed near 1637 keV in the (d,d') reaction.

A confusing result from this study was our inability to identify the K = 0 and K = 1 components of the octupole vibration. In an attempt to understand this we performed a Hauser-Feshbach calculation using standard proton and neutron optical parameters and γ-ray strength functions.[11] The calculation, which utilized all the known or predicted levels up to 2.5 MeV, gave generally good agreement with our observed γ-ray intensities and indicated that population of the K = 1 octupole band should be easily observable, while population of the K = 0 band would be too weak. We therefore made a further search for the bands using the decay of ^{180}Re.

Rhenium-180 decays to ^{180}W by β emission from the $J^{\pi} = 1^-$ ground state with a Q-value of $\sim$3800 keV. Therefore, we might expect the decay to populate states in ^{180}W having $J^{\pi} = 0^-$ and 1^- (as well as 2^-). In the decay study, we were able to identify states up to 2.9 MeV. None of the states above 1232.7 keV had been observed previously except the one at 1831.7 keV. The states at 1587.25 and 1632.90 keV, and a state at 1693.6 keV observed both in the (p,2nγ) study and in (d,d') excitation, could be the first three members of the $K^{\pi} = 1^-$ octupole band. More speculatively, the state at 1814.9 keV, which agrees very closely in energy with a state seen in (d,d') excitation, could possibly be the I = 3 member of the $J^{\pi} = 0^-$ octupole bands. These conclusions would be consistent with

---

[10] L. G. Mann, J. B. Carlson, R. G. Lanier, G. L. Struble, W. M. Buckley, D. W. Heikkinen, I. D. Proctor, and R. K. Sheline, Phys. Rev. <u>C19</u>, 1191 (1979).

[11] D. G. Gardner, Report No. UCRL-76253, 1975 (unpublished).

the results of the Hauser-Feshbach calculation, i.e., the population of the 1693.6-keV state in the (p,2nγ) experiments agrees well with the predictions for I = 3 member of the $K^{\pi} = 1^{-}$ band.

10. Neutron-Capture Cross Sections for Osmium Isotopes (Berman and Browne*)

We have measured the neutron-capture cross sections for ^{186}Os, ^{187}Os, ^{188}Os, ^{189}Os, ^{190}Os, and ^{192}Os for neutron energies from 0.5 eV to 150 keV at the LLL linac, using powdered-metal samples and the neutron-time-of-flight technique, with an experimental accuracy of 5%.[12] The ratio of the Maxwellian-weighted average cross sections for ^{186}Os and ^{187}Os near 30 keV is a vital parameter for the determination of the duration of nucleosynthesis prior to the formation of the solar system, and thus, for the determination by the nuclear-dating technique of the age of the universe. The present result of $17 \pm 4 \times 10^{9}$ y is in concordance with the values obtained from U-Th dating and from the globular-cluster method, but clearly exceeds the most recent determination of the Hubble time.

11. Pulsed Sphere Tests of the ENDF/B-V Cross Sections for Cu, Nb, ^{232}Th and ^{238}U (Hansen, Wong, Komoto, Pohl, and Howerton)

The time-of-flight measurements of the neutron emission spectra from pulsed spheres of Cu (1.0, 3.0 and 5.0 mfp), Nb (1.0 and 3.0 mfp), ^{232}Th (1.0 mfp), and ^{238}U (1.0 and 3.0 mfp), bombarded with 14-MeV neutrons, were reported in the 1979 Status Report, together with Monte Carlo calculations using the ENDF/B-IV library. These calculations were carried out with TARTNP, a coupled neutron-photon transport code.

For the recent version V of the ENDF/B library, the cross sections for Cu, ^{232}Th and ^{238}U have been reevaluated. (The Nb evaluation is the same in versions IV and V.) We present here a comparison between the above measurements and the TARTNP calculations using the new cross sections.

The measured integrals and the ratios of calculated to measured integrals for the energy intervals 0.8 to 5, 5 to 10, and 10 to 15 MeV are tabulated in Table A-1. The ratios calculated with the ENDF/B-IV library are also given for purposes of comparison between versions IV and V. The comparisons between the measurements and the calculations show that, with the exception of ^{232}Th where an appreciable improvement

---

*Present address: Los Alamos Scientific Laboratory, Los Alamos, NM 87545.

12 A brief description is in: J. C. Browne and B. L. Berman, Nature 262, No. 5565, 197 (1976).

Table A-1. Measured integrals and ratios (RIV, RV) of calculated (ENDF/B-IV, ENDF/B-V) to measured integrals.

Material	E MeV	Exp ±7%	RIV	RV	Exp ±7%	RIV	RV	Exp ±7%	RIV	RV
		1 mfp			3 mfp			5 mfp		
Cu	0.8-5	0.313	0.898	0.895	0.465	0.815	0.802	0.285	0.737	0.723
	5.0-10	0.041	0.610	0.537	0.037	0.514	0.459	0.017	0.588	0.412
	10.0-15	0.642	0.988	0.964	0.236	0.949	0.886	0.082	0.915	0.780
Nb	0.8-5	0.308	0.763	a	0.422	0.628	a			
	5.0-10	0.031	0.581	a	0.033	0.636	a			
	10.0-15	0.707	0.987	a	0.265	0.898	a			
^{232}Th	0.8-5	0.442	1.057	1.048						
	5.0-10	0.039	0.513	1.000						
	10.0-15	0.645	0.974	1.008						
^{238}U	0.8-5	0.670	0.888	0.984	0.803	1.054	1.159			
	5.0-10	0.059	0.780	0.610	0.063	0.825	0.635			
	10.0-15	0.669	0.964	0.967	0.232	1.022	1.052			

a) The ENDF/B-IV and V libraries are identical for Nb.

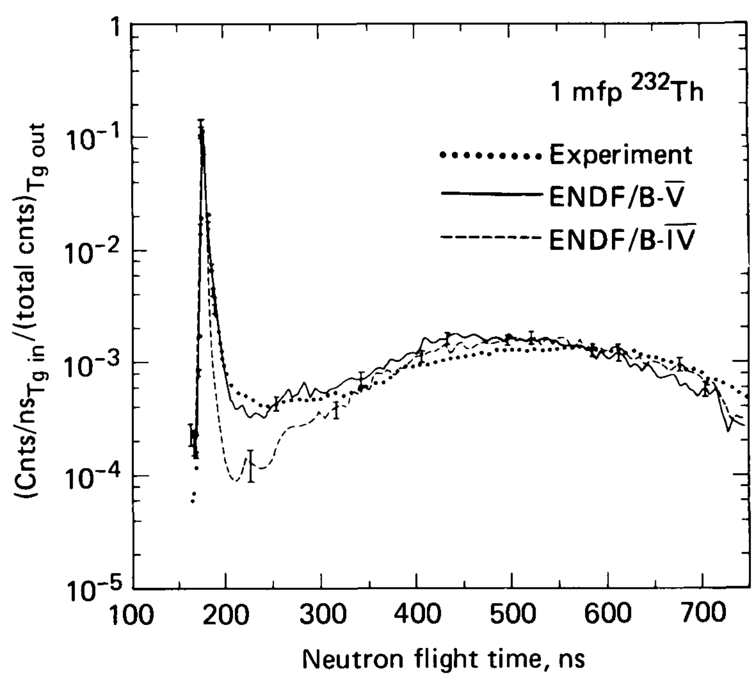

Figure A-4. Neutron emission spectrum measured by time of flight from a 1 mfp ^{232}Th sphere compared with calculations based on the ENDF/B-IV and ENDF/B-V libraries.

in the fit to the measurements has been achieved with the new cross sections (see Fig. A-4), the changes in the cross sections between the B-IV and B-V library do not reduce the discrepancies between measurements and calculations pointed out earlier for version IV of the library. In particular the B-V calculations continue to underestimate the neutron production between 5 and 10 MeV for Cu and ^{238}U. The discrepancies vary from up to 59% for Cu to 37% for ^{238}U.

A detailed discussion of the cross section changes between the two libraries and the reasons for the persistence of the discrepancies is given in Ref. 13.

12. Proton Inelastic Scattering in the Actinide Region (Hansen, Proctor, Madsen, Pohl, and Brown)

Elastic and inelastic proton differential cross sections have been measured for ^{232}Th and ^{238}U at 20 and 26 MeV, using the proton beam from the LLL cyclograaff facility. From these data and nuclear model calculations we hope to understand more fully the corresponding neutron scattering cross sections as well as (p,n) reactions. Proton groups corresponding to levels up to 6^+ in the ground state rotational band of ^{232}Th and up to 8^+ in ^{238}U have been measured with an Enge split-pole spectrograph. The data have been analyzed using coupled-channel calculations for deformed nuclei with the Oregon-State code, updated by Madsen and Brown.

We have studied the sensitivity of the results: (a) to the optitical parameters used in the calculations, (b) to the shape of the nuclear charge distribution (a deformed homogeneous or a deformed Fermi distribution), (c) to the type of coupling assumed among the levels (i.e. quadrupole and/or hexadecapole for the 4^+, 6^+ levels), (d) to the type of expansion (a Taylor power series or a Legendre polynomial) used for the nuclear and Coulomb potentials, and (e) to the magnitude of the deformation parameters, β_N and β_C used for the nuclear and Coulomb potentials.

From the fits to the data we have determined the best choice among conditions b-d, and the best set of optical and deformation parameters. These results will be used in the analysis of the (p,n) cross sections at 26 MeV for ^{232}Th and ^{238}U isobaric analog states. These (p,n) measurements are in progress and the simultaneous analysis of the proton scattering and charge exchange data will allow us to infer neutron in-elastic cross sections for these nuclei.

---

[13] L. F. Hansen et al., Measurements and Calculations of the Neutron Emission Spectra from Materials used in Fusion-Fission Reactors (submitted for publication in Fusion Technology).

13. Fission Cross Section of ^{245}Cm (White, Browne*, Howe, and Landrum)

As part of an ongoing series of measurements in the transplutonium mass region, the neutron-induced fission cross section of ^{245}Cm has been measured from 0.001 eV to 20 MeV using the LLL 100-MeV linac. The sample consisted of 190 μg of enriched (>99%) ^{245}Cm. A sample of ^{235}U was included in the measurement and was used to normalize the ^{245}Cm cross section above 10 keV. Below 10 keV the neutron flux was measured with a lithium glass detector and both the ^{245}Cm and ^{235}U data were reduced to relative cross sections by normalization to the measured flux shape. With the known 2200 m/sec ^{235}U fission cross section, the ratio of ^{245}Cm/^{235}U masses, and relative efficiencies of the fission chambers, the ^{245}Cm data were reduced to absolute cross sections.

Errors (statistical) on the data are approximately 2% near thermal, 1% at 2 MeV and 5% at 14 MeV. The measured thermal fission cross section for ^{245}Cm in this experiment is 2080 barns.

The data were analyzed in the resonance region with a multichannel R-matrix code with least-squares fitting capability. Preliminary resonance parameters have been obtained for levels below 32 eV. Figure A-5 shows fits to the ^{245}Cm fission data from 10 eV to 32 eV. The average fission width is 550 meV and the neutron strength function (1.02 x 10^{-4}) is in reasonable agreement with neighboring nuclei.

14. Fission Neutron Multiplicities for ^{245}Cm, ^{232}Th, and ^{242m}Am(n,f) Reactions (Howe, Browne*, White, Dupzyk, Landrum, and Dougan)

Fission neutron multiplicities have recently been measured for neutrons incident on ^{245}Cm. Neutrons with energies between 10 keV and 20 MeV were produced with the electron linac. Typical uncertainties were 5% at 1 MeV and 25% at 15 MeV. A separate experiment was performed with this same accelerator to measure the neutron multiplicity near thermal energy to an accuracy of 1.7%. Preliminary results from both of these measurements fall below previous thermal values and typical rates of increase with incident neutron energy. To provide further confirmation of these numbers, a future experiment is being planned using a monoenergetic 14-MeV neutron source.

Analysis is complete on the data from ^{232}Th(n,f) neutron multiplicity experiment. Results supplement existing measurements by filling in the unmeasured regions: 4.5-13 MeV, 17-40 MeV, and 1.0-1.2 MeV.

---

*Present address: Los Alamos Scientific Laboratory, Los Alamos, NM 87545.

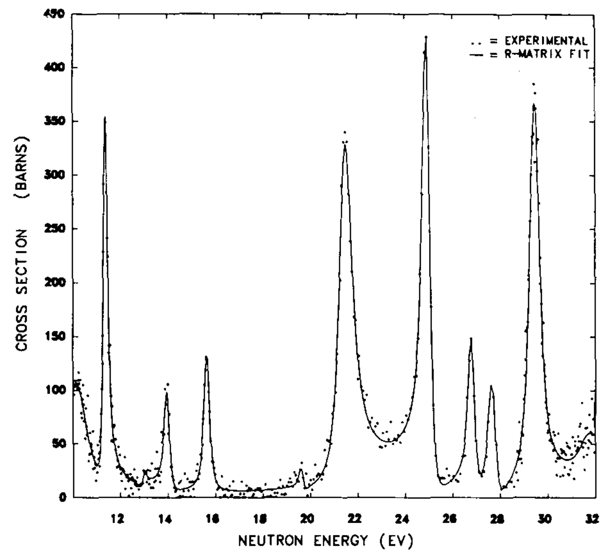

Figure A-5. Fission cross section of ^{245}Cm from 10 to 32 eV.

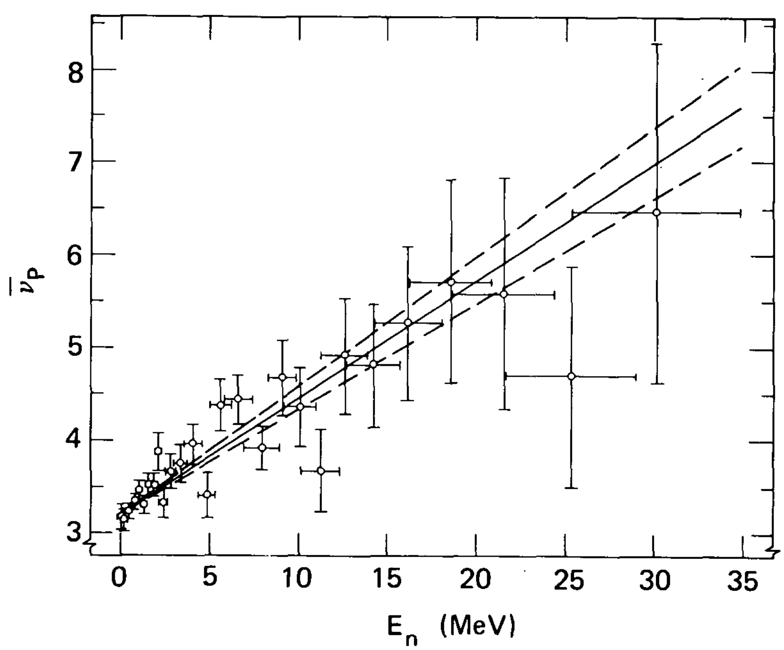

Figure A-6. Fission neutron multiplicity of ^{242m}Am. The solid line represents a bivariant-weighted least-squares fit; the dashed lines indicate a confidence level of one standard deviation.

Previously-observed deviations from linearity below 2 MeV have been confirmed. While no unusual effects were observed near the (n,n'f) threshold, a slight depression in the data does appear between 3 and 4 MeV.

Results from the $^{242m}Am(n,f)$ measurement are shown in Figure A-6.

B. NUCLEAR DATA APPLICATIONS - CALCULATIONS

1. A Study of the E1 Gamma-Ray Strength Function. (Gardner, Gardner, and Dietrich)

Previously, we described systematics for the parameterization of $f_{E1}(E_\gamma)$, the E1 gamma-ray strength function, in terms of the tail of the giant dipole resonance (GDR), which was assumed to be Lorentzian in shape.[14] The parameterization was tested in the mass-90 region by a study of neutron and proton capture cross sections and the resulting capture gamma-ray spectra.[15] We found that the capture cross sections could be predicted fairly well, with perhaps two exceptions, but the calculated gamma-ray spectra were invariably too "soft," i.e., lacking in sufficient strength for the higher energy gamma rays.

It was felt that the problems concerning the spectral shapes might be attributed to the choice of the Lorentz form for the extrapolated tail of the GDR. This past year we have developed an alternate form for the parameterization of the GDR,[16] and are in the process of evaluating it, both in the mass-90 region[17] and also for nuclei from Ta to Au.[16]

The GDR parameterization consists of two parts, the correlation of the GDR parameters of peak energy, width and peak cross section for elements from V to Bi, assuming two overlapping peaks with a separation dependent upon deformation; and the description of the shape of each

---

[14] D. G. Gardner and M. A. Gardner, Neutron Capture Gamma-Ray Spectroscopy, ed. by R. E. Chrien and W. R. Kane, Plenum Press, New York, 1979, pp. 612-614.

[15] M. A. Gardner and D. G. Gardner, Proceedings of an International Conference on Neutron Physics and Nuclear Data for Reactors and Other Applied Purposes, Harwell, Sept., 1978, pp. 1121-1125. D. G. Gardner, F. S. Dietrich, and D. W. Heikkinen, ibid., pp. 1126-1130.

[16] D. G. Gardner and F. S. Dietrich, UCRL-82998, Oct., 1979.

[17] M. A. Gardner and D. G. Gardner, UCRL-82999, Nov., 1979.

peak of the GDR with a Breit-Wigner form, but with an energy-dependent width.

$$\Gamma(E_\gamma) = \Gamma_R \left(\frac{C + E_X}{C + E_R}\right)\left(\frac{E_\gamma^{\,2}}{E_X}\right)\left(\frac{2}{E_X + E_R}\right) \tag{1}$$

Here Γ_R and E_R are the usual GDR width and peak energy, while C and E_X are global constants to be obtained by fitting spectral data. Thus the true damping width, $\Gamma(E_\gamma)$, was allowed to increase with gamma-ray energy until $\Gamma(E_\gamma) = \Gamma_R$, at which point the width was held constant for all higher energies.

An example of the new functional form is illustrated in Fig. B-1 in the case of $^{93}Nb(n,\gamma)$. The two energy-dependent Breit-Wigner (EDBW) curves represent different choices for the constant C in Eq. 1. Both EDBW curves produce "harder" gamma-ray spectra than the Lorentz curve. The results of our preliminary study show that the same values for the two constants, C and E_X, produce acceptable fits for both neutron capture cross sections and capture gamma-ray spectra, both in the mass-90 region and also in the Ta-Au mass region, and, in addition, produce agreement with the photonuclear data at higher gamma-ray energies.

2. Nuclear Level Densities (Grimes, Bloom, and Dalton*)

The Fermi-gas model is the most extensively used approach to nuclear level densities. A more fundamental approach, however, would be to calculate the level densities from the two-body force. Not only would the connection between the force and level densities be explicit, but for practical calculations one could avoid empirical adjustments that the Fermi-gas model requires to account for shell effects.

We are investigating the calculation of nuclear level densities from the two-body force through the theory of spectral distributions. The level distribution in a finite basis is assumed to be Gaussian and can be characterized in terms of the total number of states, the average energy of the states ($\langle H \rangle$) and the average energy squared of the states ($\langle H^2 \rangle$). Comparison of such an expansion with the eigenvalues obtained

*Ames Laboratory, USDOE, Ames, Iowa 50011.

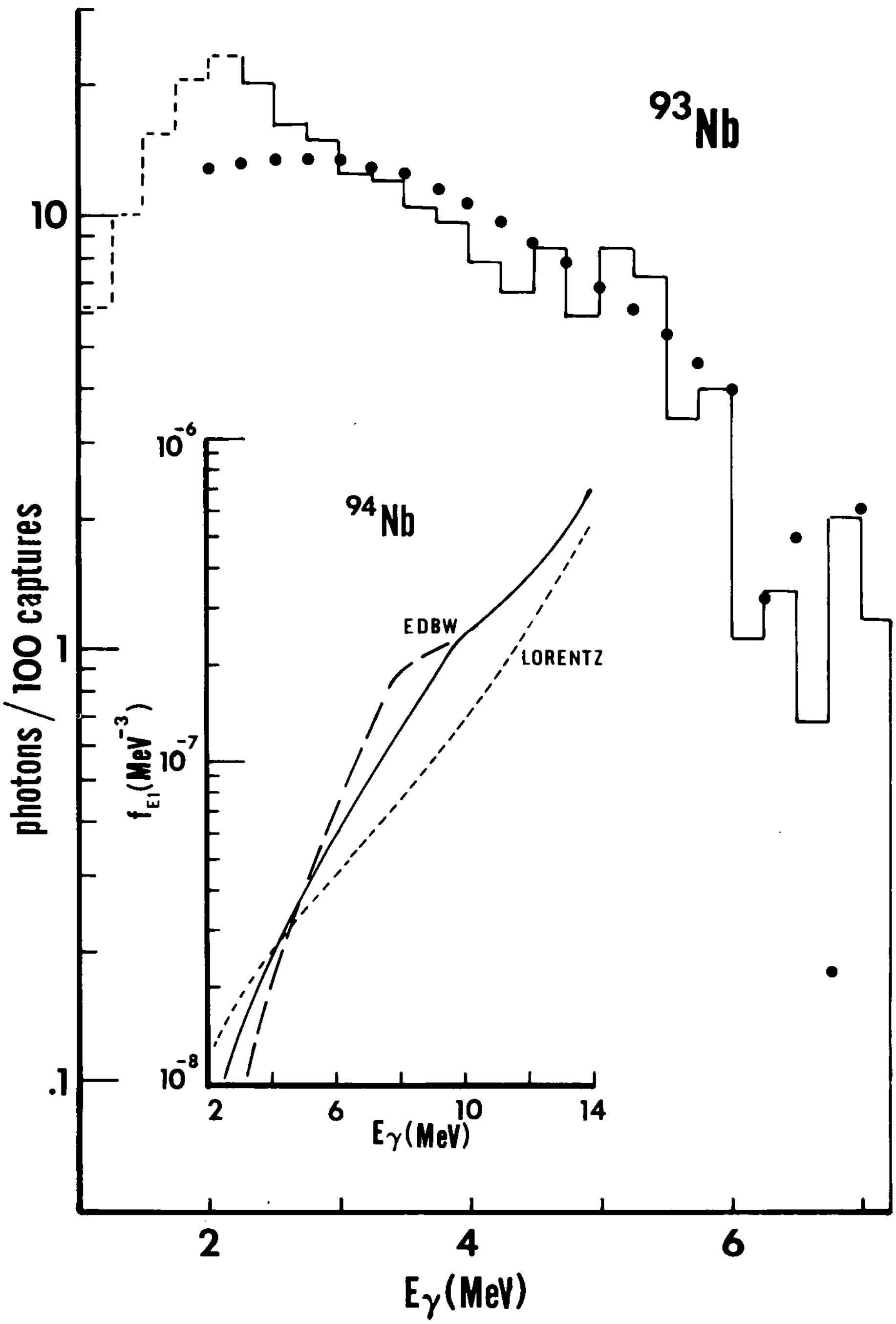

Figure B-1. Comparison of measured thermal neutron capture gamma-ray spectrum for ^{93}Nb (histogram) with that calculated with the double-peak, EDBW model (solid circles). (Data source: V. J. Orphan et al., AD-717 (1970).) Insert compares f_{E1}'s for ^{94}Nb: Lorentz form (short-dashed curve), EDBW model (solid curve), and EDBW model with an extreme parameter set (long-dashed curve).

from diagonalization showed good agreement.[18] In more recent work[19] we found that the spectral distribution calculations compared fairly well with experimental data, but that terms additional to the Gaussian were needed to obtain the spin cutoff parameters. Work is presently under way to expand the capability of the level density codes to allow the calculation of third and higher moments of the Hamiltonian.

C. NUCLEAR DATA FOR REACTOR SAFETY

1. Determination of Properties of Short-Lived Fission Products (Meyer, Henry, and Lien)

Decay data on short-lived fission products are required to resolve a number of problems associated with the design and operation of both thermal and fast reactors. Existing reactors cannot exceed power levels which are determined by the amount of heat generated in the core following a loss-of-coolant accident. This decay heat is produced by fission products and can be measured on a case-by-case basis or calculated using summation calculations. These calculations depend on existing data bases. In a program supported by DOE/BES we are measuring the decay properties of critical short-lived fission products in order to upgrade the ENDF/B data base. Existing plants must also carefully monitor effluents and the production of poisons (neutron absorbers) in the reactor core. Both these procedures depend on an accurate fission product data base. Finally the properties of the short-lived fission products which are beta-delayed neutron emitters must be known to predict the kinetic behavior of thermal and fast reactors. Our program is directed toward the measurement of the total decay energies, γ-ray spectra, beta-delayed-neutron spectra, and the average β- and γ-energy releases from these isotopes. Isolation of individual nuclides is performed with rapid automated radiochemical separation procedures because these techniques yield isotopes of elements not available with the purely physical separation systems currently being used.

We have completed detailed experiments aimed at the determination of absolute intensities of γ rays associated with the antimony fission products. Of particular importance is ^{133}Sb in which we discovered the unexpectedly large population of the daughter ^{133}Te isomer. Of the 168 γ rays we observed in the ^{133}Sb decay only those with intensities of five percent or greater are listed in Table C-1.

---

[18] K. F. Ratcliff, Phys. Rev. C3, 117 (1971).

[19] S. M. Grimes, C. H. Poppe, C. Wong, and B. J. Dalton, Phys. Rev. C18, 1100 (1978).

Table C-1. Absolute Intensities of γ rays above 5% absolute intensity for ^{133}Sb decay.

E_γ keV	I_γ per cent
817.8 (4)[a,b]	13.0 (1.1)
836.88 (7)	7.9 (1)
1096.22 (3)	100 (3)
1728.59 (7)	6.0 (4)
2416.2 (8)	6.0 (1.1)
2755 (1)	8.8 (1.4)

[a] Numbers in parenthesis are uncertainties in the last figure(s).

[b] Several γ rays of this energy are observed for antimony.

Table C-2. Comparison of experimental and calculated absolute delayed-neutron yields.

Nuclide	Observed Yield %	Calc. Yield This work %
^{232}Th	5.27 $\pm$ .40	5.24
^{232}U	0.44 $\pm$ .03	0.45
^{233}U	0.74 $\pm$ .04	0.79
^{238}U	4.60 $\pm$ .25	4.43
^{237}Np	1.07 $\pm$ .10	1.04
^{238}Pu	0.46 $\pm$ .07	0.43
^{239}Pu	0.65 $\pm$ .05	0.68
^{241}Pu	1.57 $\pm$ .15	1.57
^{242}Pu	1.97 $\pm$ .233	2.46
^{241}Am	0.51 $\pm$ .06	0.45
^{242m}Am	0.69 $\pm$ .05	0.69
^{245}Cm	0.59 $\pm$ .04	0.75
^{249}Cf	0.27 $\pm$ .02	0.36

2. Fission Products with γ Rays up to 9 MeV and Ge(Li) Detector Calibrations (Henry, Lin, and Meyer)

We have identified and isolated fission products with γ rays of up to 9 MeV, e.g., from the decay of 5-s ^{84}As. In order to determine their relative intensities we have had to recalibrate a large volume Ge(Li) detector against the thermal neutron capture γ rays of chlorine and chromium. The general shape of the efficiency curve to 10 MeV has been questioned in the literature by McCallum and Coote.[20] Our calibration curve is in general agreement with theirs.

3. Time Dependent Beta-Delayed Neutrons from Fissioning Systems (Waldo, Karam,* and Meyer)

We have used a ^{3}He ionization chamber in computer-controlled rapid rabbit transit system to measure the time-dependent β-delayed neutron yields. The time-dependent gross neutron counts were analyzed in a least-squares manner to obtain a few (4-6) group analysis. Gross β-delayed neutron yields (relative to ^{235}U) were obtained for ^{232}Th, ^{232}U, ^{233}U, ^{238}U, ^{237}Np, ^{238}Pu, ^{239}Pu, ^{241}Pu, ^{242}Pu, ^{241}Am, ^{242m}Am, ^{245}Cm, and ^{249}Cf. These data were compared with results calculated using a simple Z_p model of the form

$$Z_p = 0.4153\Delta - 1.19 + 0.167 \left(236 - 92\frac{\Delta_c}{Z_c}\right) \quad \Delta < 116$$

$$Z_p = 0.4153\Delta - 3.43 + 0.243 \left(236 - 92\frac{\Delta_c}{Z_c}\right) \quad \Delta > 116$$

where Δ_c and Z_c are the composite mass and charge of the fissioning nuclide and Δ is the mass of the fission product in question. The results from our calculations and experiments are compared in Table C-2.

D. FISSION PHYSICS

1. Fission Barriers of Rotating Nuclei (Mustafa, Baisden, and Chandra)

We have calculated fission barriers of beta-stable nuclei as a function of angular momentum in a modified rotating liquid-drop model

---

*Georgia Institute of Technology, Atlanta, GA.

20 G. J. McCallum and G. E. Coote, Nucl. Instr. & Methods 124, 309 (1975).

(MRLDM).[21] The calculation covered the mass range from 20 to 260 and the angular momentum range from zero to the limiting value, at which point the fission barrier disappears. The model used in the calculation is macroscopic (no shell effects) and it is similar to the rotating liquid-drop model (RLDM) of Cohen, Plasil, and Swiatecki.[22] Unlike RLDM, our model incorporates the finite range of nuclear force and the diffuse nuclear surface, as in the Yukawa-plus exponential model of Krappe, Nix, and Sierk.[23]

The calculated fission barriers have been compared with the predictions of RLDM. In general, the fission barriers in our model are lower than those of RLDM, and we have found up to 25 per cent difference in the predictions of the two models. These predictions can be tested by heavy-ion reaction studies and utilized in a statistical-model calculation of the deexcitation of a compound nucleus by particle emission and fission.

E. DATA EVALUATION AND COMPILATION

1. Evaluation of Neutron Interactions with ^{209}Bi (Howerton and Smith*)

Neutron interactions with ^{209}Bi have been evaluated from $E_n = 10^{-11}$ to 20 MeV in response to requests from the magnetic fusion energy community. The evaluated data, in ENDF/B format, are available from the National Nuclear Data Center.

2. Atlas of Photoneutron Cross Sections (Berman)

A supplement to the Bicentennial Edition of the Atlas of the Photoneutron Cross Sections Obtained with Monoenergetic Photons, including recent data on ^{13}C, ^{18}O, ^{55}Mn, ^{59}Co, $^{186,188,189,190,192}Os$, ^{232}Th, and $^{235,236,238}U$, was issued in 1979 (UCRL-78482 Supp.) A new edition, including more recent data on ^{3}H, ^{3}He, ^{4}He, and ^{17}O, and expanded to include graphs of the running sums of the integrated cross sections and their first and second moments, is in preparation and will be published in Atomic Data and Nuclear Data Tables.

---

*Argonne National Laboratory, Argonne, IL 60439.

21 P. A. Baisden, M. G. Mustafa, and H. Chandra, Bull. Am. Phys. Soc. (Series II), 24, 815 (1979).

22 S. Cohen, F. Plasil, and W. J. Swiatecki, Ann. Phys. (N.Y.) 82, 557 (1974).

23 H. J. Krappe, J. R. Nix, and A. J. Sierk, Phys. Rev. C20, 992 (1979).

A. NEUTRON PHYSICS

1. Neutron Inelastic Scattering Cross Sections for ^{232}Th and ^{238}U Obtained from (n,n'γ) Measurements

(L.E. Beghian, G.H.R. Kegel, G.P. Couchell, J.J. Egan, A. Mittler, D.J. Pullen, W.A. Schier, J.D. Menachery and A.T.Y. Wang)

Inelastic Cross sections in ^{232}Th and ^{238}U have been obtained for states in the excitation energy range 0.7 - 2.0 MeV. The level cross sections have been inferred from 125° gamma-ray production measurements which employed a Ge(Li) spectrometer in conjunction with time-of-flight techniques and Compton suppression via a NaI(Tℓ) annulus.[1,2] The data have been corrected for the finite sample effects of neutron attenuation and multiple scattering, as well as gamma-ray attenuation, using the codes NEVES and PENHA which were developed at this laboratory by G.H.R. Kegel to deal with our disk scatterer geometries. Corrections were also applied to the data for internal conversion and for the variation of the incident fluence over the sample.

Inelastic scattering from states in the region of excitation near 1 MeV and above is an important process which contributes to the shape of the low energy spectrum in fast reactors. The high level density in this region of excitation makes direct observation by (n,n') very difficult. The excellent energy resolution attainable in gamma-ray spectroscopy makes this technique very attractive. However, direct neutron measurements must be made in order to resolve problems which may arise in inferring level cross sections from gamma-ray measurements. In particular we are looking into the effects of electric monopole transitions, weak branching and internal conversion.

---

[1] J.J. Egan, J.D. Menachery, G.H.R. Kegel and D.J. Pullen, "Proceedings of the International Conference on Nuclear Cross Sections for Technology", Knoxville, 1979 (to be published).

[2] A. Mittler, G.P. Couchell, W.A. Schier, S. Ashar, J.H. Chang and A.T.Y. Wang. "Proceedings of the International Conference on Nuclear Cross Sections for Technology" Knoxville, 1979 (to be published).

2. Uranium and Thorium (n,n') (G.H.R. Kegel, G.P. Couchell, J.J. Egan, A. Mittler, D.J. Pullen, W.A. Schier, J.D. Menachery, J.H. Chang and J.C. Shao*)

Work is in progress on (n,n') measurements for states in ^{232}Th and ^{238}U above the ground state rotational band. Using disk scatterers and the time-of-flight technique we have been able to achieve an overall energy resolution of 15 keV optimized for the detection of neutrons of 250-300 keV in energy. This allows us to study the inelastic cross sections by direct neutron measurements as a complement to our (n,n'γ) work. Fig. 1 shows a sample TOF-spectrum for E_n = 1.3 MeV on ^{238}U obtained with our system. Each peak is labeled by the excitation energy of the state in ^{238}U. Peaks labeled by energies in parentheses are

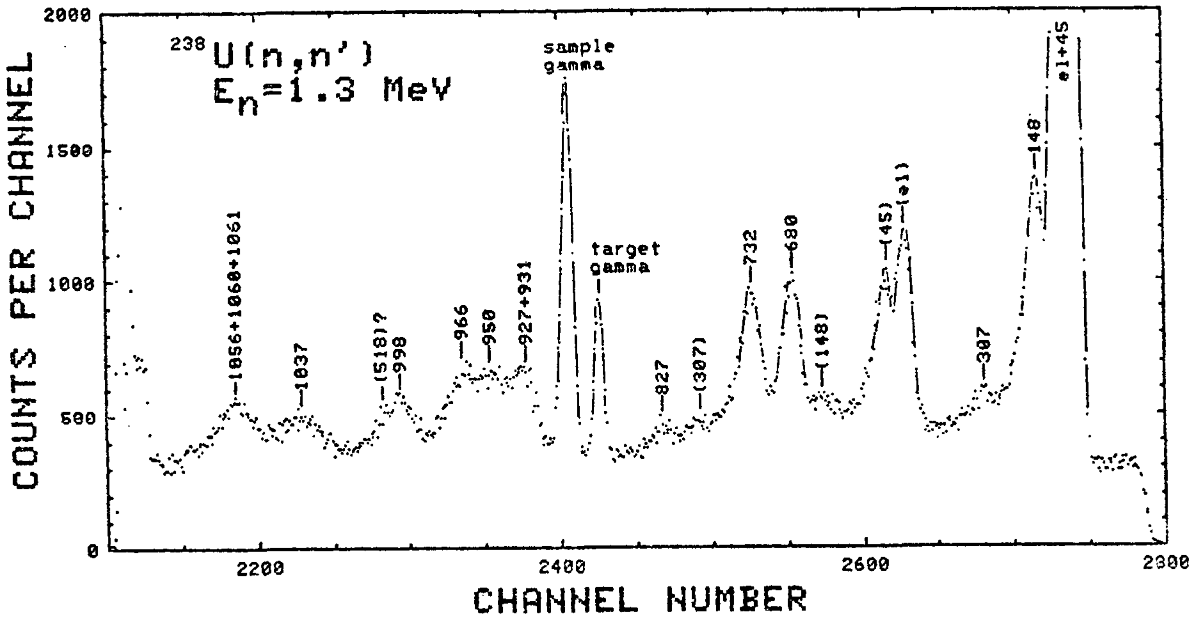

Fig. 1 ^{238}U(n,n') time-of-flight spectrum obtained using ^{7}Li(p,n)^{7}Be neutrons. The peaks are labeled by the corresponding excitation energy (in keV) in ^{238}U. Energies in parentheses indicate peaks arising from the scattering of the second group of neutrons from ^{7}Li(p,n)^{7}Be.

* Visiting Scholar from the People's Republic of China.

"echo" peaks due to the second group of neutrons from the $^7Li(p,n)^7Be$ reaction which was used as a neutron source.

At present we are investigating the 700-1100 keV region of excitation requiring that measurements be made in the 900-1400 keV bombarding energy range. In each case the bombarding energy is carefully chosen so that the resolution of the TOF spectrum is optimized for a particular state (or states) in ^{232}Th or ^{238}U. This will occur about 250 keV above the threshold for the state.

3. E O Transitions in ^{232}Th and ^{238}U (C. Ciarcia, G.P. Couchell, J.J. Egan, J.D. Menachery, A. Mittler and W.A. Schier)

In obtaining cross sections from gamma-ray data care must be taken in accounting for electric monopole transitions. Theoretical considerations as well as experimental measurements of branching ratios[3,4] indicate that EO transitions can be appreciable in actinide nuclei. Branching ratios for $0^+ \rightarrow 0^+$ transitions (in competition with $0^+ \rightarrow 2^+$ transitions) are poorly known in ^{232}Th and ^{238}U, and recent Coulomb excitation measurements[5] suggest possible overestimates in some of the earlier EO determinations. We have estimated EO strengths in these nuclei by comparing cross sections obtained in (n,n'γ) measurements with (n,n') level cross sections determined by the neutron-time-of-flight method. Computer-assisted stripping of the neutron time-of-flight spectra is required to obtain individual level cross sections for most cases of interest. As a rule this method is sensitive to EO branching ratios of 20% or larger.

4. Ring Geometry Measurements of Inelastically Scattered Neutrons from ^{238}U*(45 keV) for Incident Energies, E_n<200 keV K. Traegde, W.A. Schier, G.P. Couchell, G.H.R. Kegel, D.J. Pullen and J. Moyle

Neutrons scattered from the ground state and inelastically scattered from the 45-keV state in ^{238}U have been measured in ring geometry for incident energies, $E_n \leq 200$ keV. The time-of-flight measurement in this "open geometry" method gives adequate time resolution at 50 cm flight paths. To date, a spectrum at E_n = 100 keV still gives a neutron peak corresponding to the inelastically scattered neutrons with good statistics and small background after a partial background subtraction

---

[3] M.R. Smorak, Nuclear Data Sheets 20, 165 (1977).

[4] Y.A. Ellis, Nuclear Data Sheets 21, 549 (1977).

[5] D.K. Olsen et al., ORNL/TM-6832 (1979).

is made with a lead ring. Advantages of a conventional forward geometry ($\theta<90°$) and an innovative back-angle geometry ($\theta>90°$) were investigated through computer simulation. Experimental measurements at even lower neutron energies and in the back-angle geometry are presently under investigation with particular attention be given to target assembly design, lithium target fabrication, background suppression and choice of scintillator.

5. Computer Simulated Time-of-Flight Spectra (G.H.R. Kegel)

We have written the computer code IMBUI to simulate neutron time-of-flight spectra for different experimental conditions. This code includes the effects of neutron target cross sections and kinematics, flight path dispersion caused by the scatterer geometry, energy dispersion introduced through the scatterer kinematics by the finite range of scattering angles, and neutron attenuation. If known, the differential neutron scattering cross section may also be included.

In Fig. 2 is shown a typical simulation spectrum obtained for ^{238}U at a primary neutron energy of 1.5 MeV and for levels in the energy range 1000-1300 keV. The total neutron cross sections for

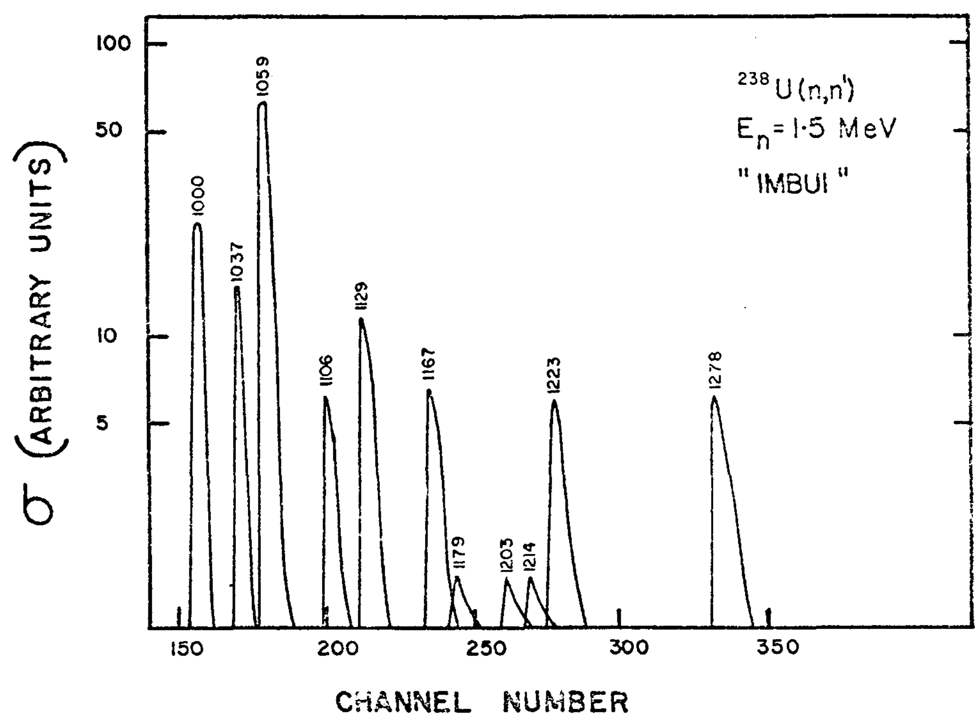

Fig. 2. Simulated neutron time-of-flight spectrum for ^{238}U.

these levels were estimated from our (n,n'γ) data assuming isotropic angular distributions. It is seen that with the factors assumed in this calculation, an apparent resolution of 10 keV is obtained. This would increase to about 15 keV if a 10-keV thick neutron target were used. The effect of flight time resolution is negligible in this case. These considerations show that it should be possible to resolve all neutron groups in this excitation region, with the exception of the 1167/1179-keV doublet and the 1203/1214/1223-keV triplet.

6. <u>Theoretical Calculations of Inelastic Cross Sections in ^{233}Th</u> (E. Sheldon)

The recent cross section data for inelastic scattering of fast neutrons on ^{232}Th at incident energies from 0.8-2.1 MeV populating a variety of excited levels have been compared with the predictions of the compound-nucleus (CN) model using appropriate optical potential parameters.[6] With increasing projectile energy, the CN model progressively falls short of matching the data, due to the onset of direct interaction (DI) contributions and fluctuation interference effects. To allow for the DI contributions, their magnitudes have been evaluated using coupled-equations and direct-interaction programs.

A shortcoming in the theoretical treatment is the use, for pragmatic reasons, of an incoherent sum of CN and DI contributions in order to build the net cross section. This takes no account of the likelihood of CN/DI interference and of the development of "extended Hauser-Feshback" formalisms which offer a unification of the CN and DI approach. Thus, Tepel, Weidenmüller[6,7]

---

6 H.M. Hofmann, J. Richert, J.W. Tepel and H.A. Weidenmüller, "Direct Reactions and Hauser-Feshback Theory", Annals of Physics (N.Y.) 1975, <u>90</u>, 391 & 403.

7 J.W. Tepel, H.M. Hofmann and H.A. Weidenmüller, "Hauser-Feshbach Formulas for Medium and Strong Absorption", Physics Letters 1974, <u>49B</u>, 1.

and others[8,9,10] have succeeded in merging DI with CN amplitudes in a synthesis that has already had important quantitative consequences. From energy-averaged elements of a unitarily-transformed fluctuating part of the scattering S-matrix, a modified "penetrability term", akin to the conventional Hauser-Feshbach factor $\tau \equiv T_a T_b / \Sigma_c T_c$, but uniting CN with DI, can be derived and thence the absolute cross sections determined. This line of attack is now being pursued with the aim of arriving at numerical results which would offer still better agreement with experiment and so provide a means of theoretically predicting statistical cross-section behaviour under circumstances when direct measurements are impractical or unfeasible.

---

[8] M. Kawai, A.K. Kerman and K.W. McVoy, "Modification of Hauser-Feshbach Calculations by Direct-Reaction Channel Cou;ling", Annals of Physics (N.Y.) 1973, 75, 156.

[9] P.A. Mello, "A Statistical Theory of Nuclear Reactions based on a Variational Principle", Physics Letters 1979, 81B, 103.

[10] M.C. Nemes and T.H. Seligman, "Surprisal Approach to Improved Hauser-Feshback Formulae", Physics Letters 1979, 84B, 13.

THE UNIVERSITY OF MICHIGAN
Department of Nuclear Engineering

A. MEASUREMENTS WITH PHOTONEUTRON SOURCES (D. J. Grady, G. T. Baldwin, and G. F. Knoll)

1. Absolute Fission Cross Sections of Np-237

Experimental measurements and preliminary analysis have been completed to support an absolute cross section measurement on Np-237 at two independent energies. The threshold nature of the cross section allowed use of the two highest energies available from our sources at 770 keV (La-Be) and 964 keV (Na-Be). Preliminary values obtained were 1.191 and 1.365 barns, respectively. These values are based on target mass determinations obtained by weighings performed by the supplier of the foils, Oak Ridge National Laboratory. This is the same technique used in our previous target foils of uranium and plutonium, and we have previously obtained independent varification of the target masses using other methods. An attempt to provide a similar independent check on the Np-237 mass determinations using alpha assay techniques has not yet been successful. This work, being conducted at the National Bureau of Standards, is hampered by the deposit thickness required in order to obtain adequate fission rates. The resulting alpha spectra are significantly broadened so that it is difficult to separate various components of the alpha activity. A repeat of this determination will be made shortly using a thinner deposit obtained from the same batch of enriched isotope. A third approach will also be tried in which the target mass will be inferred from a measurement of the activity of Pa-233, the alpha decay daughter in secular equilibrium with the parent Np-237.

In addition to the target mass confirmations, additional work still planned includes a measurement of the fission fragment anisotropy at these energies using the tandem dynamitron at Argonne National Laboratory. These measurements will be similar to those performed earlier on our U-235 and Pu-239 targets. We also plan a recalibration of the Cf-252 neutron reference source used in these measurements once NBS-2 can be obtained on loan from the National Bureau of Standards.

A paper describing these measurements was presented at the International Conference on Cross Sections for Technology held in Knoxville on October 26, 1979.

2. U-233 Absolute Fission Cross Section

The measurements of the absolute fast fission cross sections of U-233 are progressing well. The experimental work has been completed at all five of the photoneutron energies 964, 770, 265, 140, and 23 keV. Track counting is now complete for these runs. The data from these sets of experiments are now being analyzed, and pending accurate cross calibration of the foil masses, cross section values will be forthcoming. The U-233 foils will be sent to NBS for alpha-counting to confirm the gravimetric mass determination. A third independent mass assay may yet be required should the alpha counting be hampered by poor resolution of the U-233 alpha lines from isotopic impurities with high specific activity. We also plan to perform the anisotropy measurements using a smaller third U-233 foil at Argonne National Laboratory, along with the Np-237 anisotropy measurements.

3. In-115 Neutron Capture Cross Section Measurements

Since measurement techniques for both the fission cross sections and the capture cross sections share a significant portion of the source preparation and target irradiation facilities, the high priorities given to the fission measurements have minimized the amount of experimental work on the capture cross sections. However, some experimental progress has been accomplished on various β-γ coincidence techniques, using the 4 $\pi\beta$-γ detector and the 2" x 2" NaI(Tl) scintillation detector. Several experiments were performed to test out the coincidence detection equipment in preparation for the beginning of the capture cross section measurements in the near future.

4. Th-232 Capture Cross Section at 23 keV

An absolute determination of the Th-232(n,γ) cross section at 23 keV is underway. Facilities already available and in use at this laboratory, particularly those for activation, handling and calibration of photoneutron sources, make this an especially appropriate and timely application of resources. We have therefore carried out an initial design of this experiment, and initial measurements are underway.

Part of the demonstration of feasibility for the proposed activation measurement of the Th-232 capture cross section requires estimation of the detection sensitivity for the Pa-233 311 keV decay gamma ray. A fairly small amount of the Pa-233 daughter is produced even after long irradiation, so that sufficient detection efficiency is necessary to ensure acceptable counting statistics and background suppression. An approximate determination of the efficiency and background to be expected for the $4\pi\beta-\gamma$ coincidence system is in progress. Our small N-237 target foil (to be used for the anisotropy measurements) is calculated to have approximately the same amount of Pa-233 activity as anticipated for the thorium irradiation. A Ge(Li) detector has been used for the gamma channel in the $4\pi\beta-\gamma$ coincidence system presently used for the In-115 measurement.

B. <u>FACILITY DEVELOPMENT FOR MEASUREMENTS AT 14 MeV</u>
(M. Mahdavi, D. McKeon, and G. F. Knoll)

We are completing the installation of a 14 MeV neutron generator in a new laboratory that formerly housed the University of Michigan cyclotron. Our intent is to use these facilities for the measurements of absolute cross sections, using both proton recoil monitors and associated particle counting for flux determination. We will begin with a series of fission cross section measurements on U-235, Pu-239, U-233, Np-237, and U-238. Targets used for these measurements will be the same fissile foils used for our previous photoneutron measurements. In this way, we will take advantage of the excellent documentation on their mass that we have gained from their previous use.

A low-mass grid floor has been erected in the laboratory to support the generator and associated equipment. The neutron source is thus located at the approximate midpoint of a large shielded room with nearest surfaces approximately 11 feet from the target. This environment will provide for a very low room return component for the cross section measurements. The 150 kV accelerator has been installed at this location, and is now in the initial phase of testing and check-out.

This program will involve the joint participation of the University of New Mexico, under the supervision of Professor Craig Robertson.

A. NEUTRON PHYSICS

1. ^{237}Np Fission Cross Section Measurements in the MeV Energy Region (A. D. Carlson, B. H. Patrick*)

The measurements of the energy dependence of this cross section have been made from ∿1-20 MeV neutron energy at the 60 m flight path of the NBS neutron time-of-flight facility. The neutron flux was measured with a special annular proton telescope and a fission chamber was used to detect the fission events.

Since the last status report the data from 1-3 MeV has been analyzed and the complete measurement was reported at the Int. Conf. on Nuclear Cross Sections for Technology at Knoxville, TN (Oct. 1979).

2. The Absolute ^{235}U(n,f) Cross Section Measurements at the 3 MV Van de Graaff Laboratory (O. A. Wasson, K. C. Duvall, A. D. Carlson)

The absolute ^{235}U(n,f) cross section covering the 0.2-1.2 MeV energy interval is completed and was reported at the Knoxville Conference (Oct. 1979). Measurements at 14.4 MeV using the ^{3}H(d,n)^{4}He reaction and the associated particle technique as a neutron flux monitor are in progress. Several different neutron flux measuring techniques are planned in order to assess the systematic errors. The mass and uniformity of the ^{235}U deposits are being measured by both α particle decay counting and thermal neutron fission fragment detection. The dimensions of the neutron cone produced from the small angle time-correlated associated particle technique agree with that predicted from the known nuclear scattering and reactions in the neutron producing targets. Lower energy neutron background is measured using pulsed-beam time-of-flight techniques.

3. ^{235}U Mass Measurement Scale (C. D. Bowman, O. A. Wasson)

By 1978 measurements of the ^{235}U(n,f) cross section standard in the higher keV region had progressed to the point that uncertainties in foil mass had become apparently the largest uncertainty (>1% SD) of the

* A.E.R.E. Harwell, England

experiment. Our NBS reference foil mass was considered known to only ± 1.4% (1 SD) and its relation to a number of independent mass scales in the U.S. was not clear. There seemed to be no easy resolution of this problem and an NBS program was therefore proposed for the DOE with two primary thrusts. The first was the re-establishment of a national ^{235}U mass scale using the methods developed for the U.S. actinide half-life program. The second phase involved the generation of a set of foils with a variety of backings and deposit thickness which would be calibrated and maintained by NBS and distributed to users as requested.

Dr. W. Poenitz of the ANL has subsequently undertaken a review of the five U.S. mass scales and the intercomparisons between them. From his work it appears that the existing scales can be readjusted on a rational basis so that foil masses in the country probably are known as well as ±0.5%(1 SD) and perhaps as well as ± 0.3%(1 SD). These adjustments include discarding one of the two ANL mass scales and a change in the NBS scale as a result of more redundancy in our measurements. At this time it appears likely that while a re-establishment of the mass scale could be done to greater accuracy, perhaps to ± 0.2%(1 SD), such work probably is not warranted by cross section measurement needs. Therefore one of the major thrusts of the proposal to DOE probably has been resolved. The remaining foil calibration and dissemination service by NBS is probably still a valid long-term need.

4. Studies of Fission Cross-Section Systematics in the MeV Neutron Energy Range (J. W. Behrens)

An earlier study has shown straightforward systematic behavior as a function of constant proton and neutron number for neutron-induced fission cross sections of the actinide isotopes in the incident-neutron energy range 3-5 MeV.[1] This 1977 study utilized fission cross-section measurements for 26 isotopes of elements ranging from thorium through californium. Since 1977 a number of new measurements have become available. Therefore, the systematics published in Ref. 1 have been re-examined for a total of 57 isotopes of elements ranging from radium through einsteinium and will be presented at the June 1980 ANS meeting in Las Vegas, NV.

In Fig. A-1 a plot of fission cross sections as a function of the atomic mass number of the target nucleus within the incident-neutron energy range of the first fission plateau (3-5 MeV) is shown. The figure also shows that the systematic trends found in Ref. 1 seem to apply over most of the atomic mass range; however, there appears to be a departure

---

[1] J. W. Behrens, Phys. Rev. Lett. 39, 68 (1977).

over the range $144 \leqslant N \leqslant 149$ starting with the curium and berkelium isotopes. Higher accuracy measurements for the curium, berkelium, and californium isotopes are clearly needed to confirm these deviations.

Ultimately, this fission cross-section phenomenology might yield reliable predictions of fission cross sections for actinides which cannot be measured due to either high natural radioactivity or insufficient sample mass and/or purity.[2]

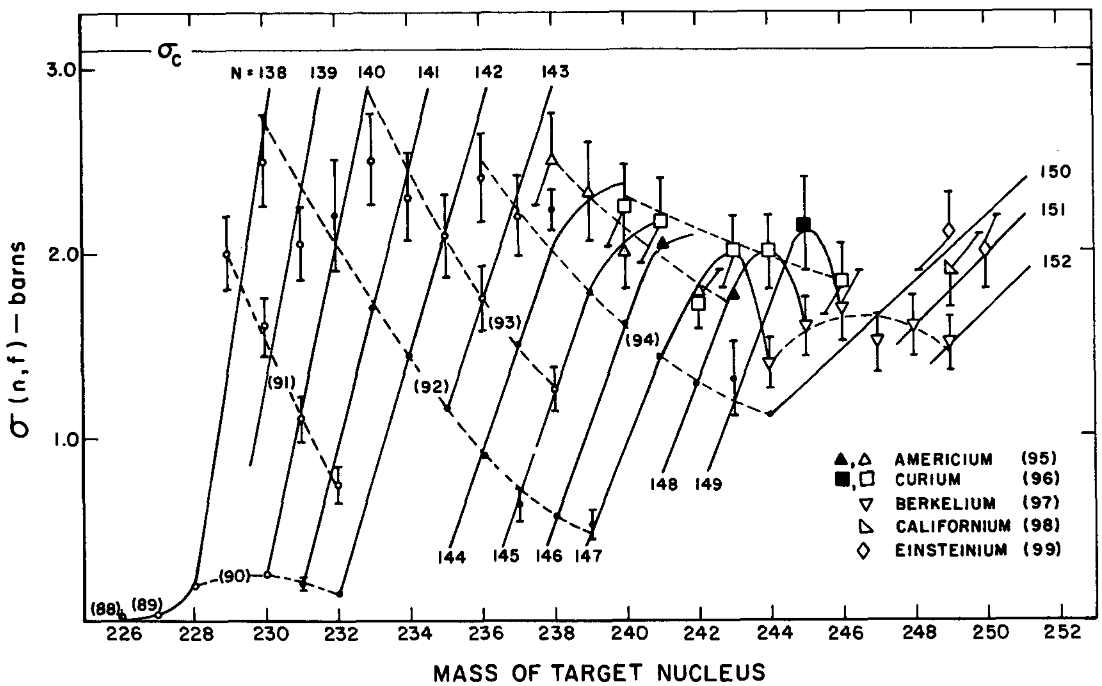

Fig. A-1. Neutron-induced fission cross section as a function of the atomic mass number of the target.

---

[2] J. W. Behrens and R. J. Howerton, Nucl. Sci. Eng. 65, 464 (1978).

5. <u>A Measurement of the Ratio of the $^{10}B(n,\alpha)$ to $^{6}Li(n,\alpha)$ Cross Sections Below 1 keV</u> (J. B. Czirr, A. D. Carlson)

These measurements were initiated in order to determine if problems associated with these standards are the source of a discrepancy in recent measurements[3,4] of the ^{235}U fission cross section. The same Li glass and BF_3 detectors used as flux monitors in the fission experiments were used for these ratio measurements.

The data were obtained at the 20-m flight path using Au, Co, and Na filters for background determination. The results of this investigation are shown in Fig. A-2 and Fig. A-3. These measurements do not explain the discrepancy in the fission measurements. The present data do not agree with the ENDF/B-V ratios below ~20 eV.

The results of this investigation were reported at the Int. Conf. on Nuclear Cross Sections for Technology at Knoxville, TN (Oct. 1979).

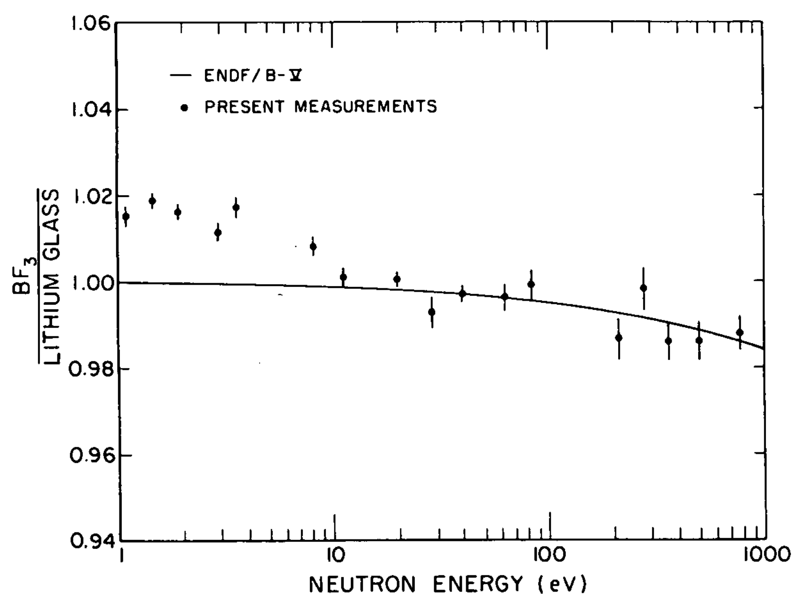

Fig. A-2. The ratio of the (n,α) cross sections of $^{10}BF_3$ and ^{6}Li glass compared to the ratio from ENDF/B-V. The present ratio has been normalized to ENDF/B-V above 20 eV and ENDF/B-V has been normalized to 1.0 at 1 eV.

---

[3] J. B. Czirr and G. W. Carlson, Nucl. Sci. Eng. <u>64</u>, 892 (1977).

[4] Private communication from R. Gwin, Oak Ridge National Laboratory, 1977.

Table C-1. Absolute Intensities of γ rays above 5% absolute intensity for ^{133}Sb decay.

E_γ keV	I_γ per cent
817.8 (4)[a,b]	13.0 (1.1)
836.88 (7)	7.9 (1)
1096.22 (3)	100 (3)
1728.59 (7)	6.0 (4)
2416.2 (8)	6.0 (1.1)
2755 (1)	8.8 (1.4)

[a] Numbers in parenthesis are uncertainties in the last figure(s).

[b] Several γ rays of this energy are observed for antimony.

Table C-2. Comparison of experimental and calculated absolute delayed-neutron yields.

Nuclide	Observed Yield %	Calc. Yield This work %
^{232}Th	5.27 $\pm$ .40	5.24
^{232}U	0.44 $\pm$ .03	0.45
^{233}U	0.74 $\pm$ .04	0.79
^{238}U	4.60 $\pm$ .25	4.43
^{237}Np	1.07 $\pm$ .10	1.04
^{238}Pu	0.46 $\pm$ .07	0.43
^{239}Pu	0.65 $\pm$ .05	0.68
^{241}Pu	1.57 $\pm$ .15	1.57
^{242}Pu	1.97 $\pm$ .233	2.46
^{241}Am	0.51 $\pm$ .06	0.45
^{242m}Am	0.69 $\pm$ .05	0.69
^{245}Cm	0.59 $\pm$ .04	0.75
^{249}Cf	0.27 $\pm$ .02	0.36

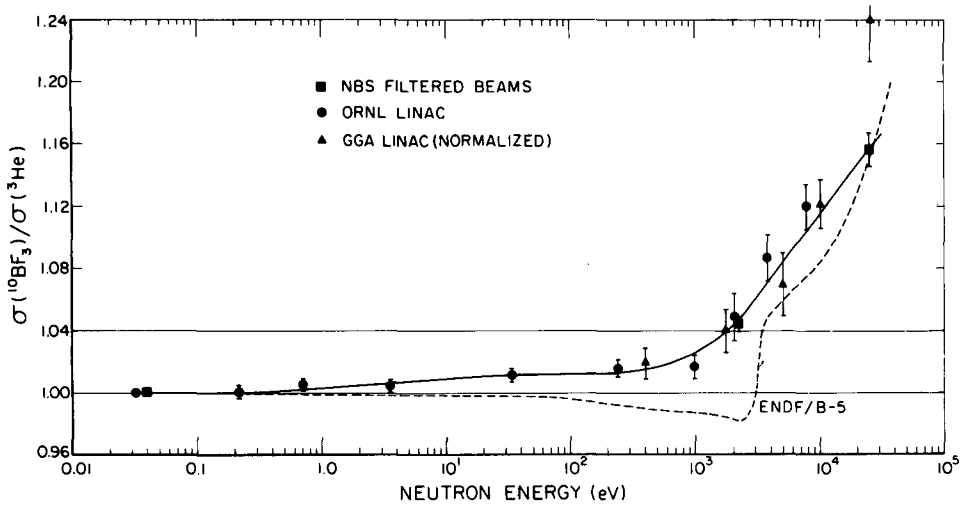

Fig. A-4. The ratio of the (n,α) cross section of $^{10}BF_3$ and the (n,p) cross section of ^3He normalized to 1.0 at 0.025 eV. A few representative points from the GGA Linac unpublished results are included. The solid line is to guide the eye. The dashed line is the ratio from ENDF/B-V.

7. A Comparison of (n,α) Cross Section Measurements for $^{10}BF_3$ and Solid ^{10}B from 0.5 to 1000 eV (A. D. Carlson, C. D. Bowman, R. G. Johnson)

The investigation of an expected deviation from a 1/v cross section for $^{10}BF_3$ is continuing. New measurements of the (n,α) rate for $^{10}BF_3$ compared to solid ^{10}B have been made. For these measurements the energy dependence of the background was determined by using Au, Co, and Na filters. The $^{10}BF_3$ detector was found to be sensitive to background gamma rays. This sensitivity caused an error in our earlier measurements reported in the last status report. The results of the new work are shown in Fig. A-5. Within the accuracy of the measurements, the ratio is constant. These measurements indicate molecular effects probably do not have significant effects on the ^{10}B(n,α) standard implemented using $^{10}BF_3$ in the 0.5 to 10000 eV energy region. This result is not consistent with our present understanding of the physical basis for the expected effect. This work has been reported on at the Int. Conf. on Nuclear Cross Sections for Technology at Knoxville, TN (Oct. 1979). Further work will be done in order to improve our understanding of molecular effects on neutron cross sections.

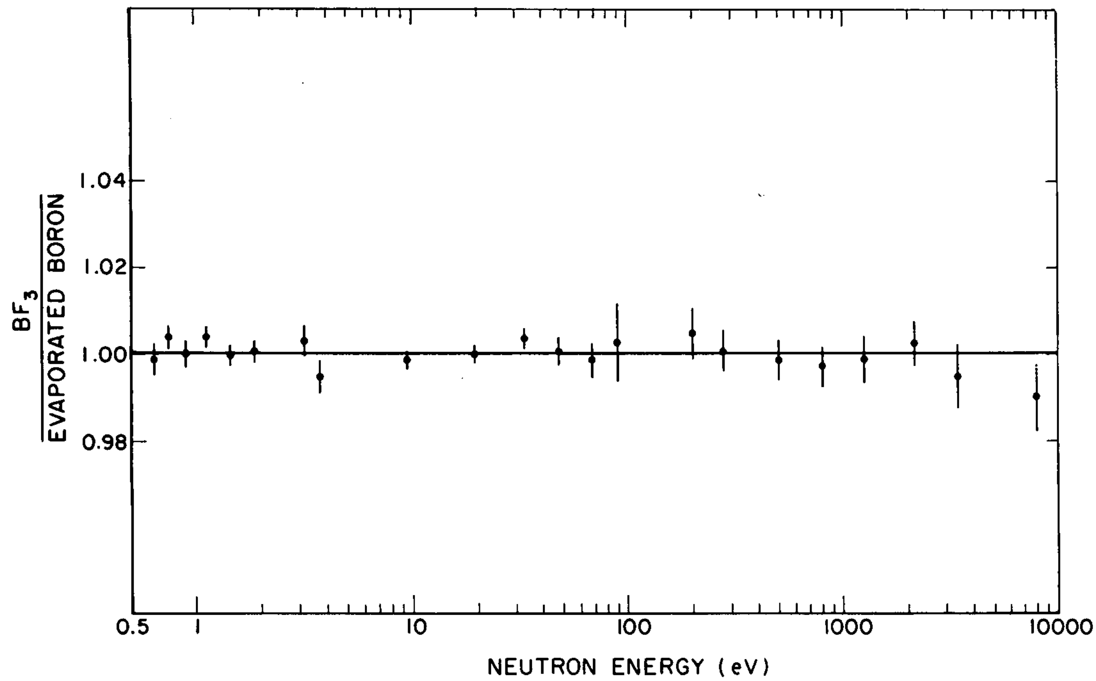

Fig. A-5. The ratio of the (n,α) cross sections of $^{10}BF_3$ and evaporated boron.

8. <u>Neutron Induced De-excitation of the Long-lived 2S Electronic Triplet State in He</u> (C. D. Bowman, R. A. Schrack, M. Danos)

The 2S-triplet state of helium lies at about 20 eV and can easily be excited. The transition to the ground state is strongly forbidden so that the lifetime of this state is determined by wall effect, impurity atoms, etc. and may be as long as a few tenths of a second. A study was undertaken to predict the cross section for de-excitation of this state by neutron inelastic "down" scattering in which the atom ends up in its ground state and the neutron carries away the excitation energy.

The first reaction calculated was that in which the neutron scatters off the ^4He nucleus giving it an impulse which then can induce the transition. For energies below 100 eV, the momentum transfer is so small that the cross section for this process is in the microbarn range and therefore very difficult to detect.

Another de-excitation mechanism was also considered in which the neutron interacts with the electron by virtue of their magnetic moments (paramagnetic scattering). In this case the momentum is transferred directly to the electron rather than to the nucleus. The calculation in first order gives a very small cross section since in this case the momentum transfer is so large. A second order calculation therefore has been initiated in which the electron is excited to a continuum state which subsequently decays to the ground state. For this calculation the energy and momentum transfer can be more consistently matched, with the possibility that cross sections high enough to be measured will be predicted.

This work is part of an NBS effort to better understand interaction at the interface between nuclear and atomic physics and to bring the results to bear on practical problems such as cross section standards, neutron moderation, etc.

9. Resonance Neutron Radiography (J. W. Behrens, R. A. Schrack, C. D. Bowman, A. D. Carlson)

Work continues on the development of resonance neutron radiography techniques at the NBS. The technique might be used in safeguarding nuclear materials and the NBS is receiving support from the Nuclear Regulatory Commission. This method utilizes epithermal neutrons and a position-sensitive proportional counter (PSPC) and has applicability as both a nondestructive evaluation (NDE) and assay (NDA) technique. To demonstrate and test the method a broad energy spectrum of epithermal neutrons and a linear PSPC were used with the time-of-flight technique to determine (1) the distribution and thickness of silver between two silver-brazed metal plates [reported in Ref. 5 and at the Int. Conf. on Nuclear Cross Sections for Technology, Knoxville, TN (Oct. 1979)] and (2) the amount of ^{234}U, ^{235}U, and ^{238}U in a fresh UO_2 nuclear fuel pellet [reported at the Knoxville Conference and at the Conf. on Meas. Technology for Safeguards and Material Control, Kiawah Island, SC (Nov. 1979)]. For (2) the value obtained by neutron radiography for the enrichment was 4.01 ± 0.08 atom % ^{235}U as compared to a chemical assay value supplied by the manufacturer of 3.96 ± 0.005 atom %. The value obtained by neutron radiography is thus about 1% different from the chemical assay value, well within the 2% error quoted for the measurement.

High spatial resolution PSPCs are required to improve the imaging quality and the speed of assaying of the method. High spatial resolution area PSPCs are being developed to replace the linear PSPCs.

---

[5] J. W. Behrens, R. A. Schrack, and C. D. Bowman, "Resonance Neutron Radiography Using a Position-Sensitive Proportional Counter," Trans. Am. Nucl. Soc. 32, 207 (1979).

2. <u>Uranium and Thorium (n,n')</u> (G.H.R. Kegel, G.P. Couchell, J.J. Egan, A. Mittler, D.J. Pullen, W.A. Schier, J.D. Menachery, J.H. Chang and J.C. Shao*)

Work is in progress on (n,n') measurements for states in ^{232}Th and ^{238}U above the ground state rotational band. Using disk scatterers and the time-of-flight technique we have been able to achieve an overall energy resolution of 15 keV optimized for the detection of neutrons of 250-300 keV in energy. This allows us to study the inelastic cross sections by direct neutron measurements as a complement to our (n,n'γ) work. Fig. 1 shows a sample TOF-spectrum for E_n = 1.3 MeV on ^{238}U obtained with our system. Each peak is labeled by the excitation energy of the state in ^{238}U. Peaks labeled by energies in parentheses are

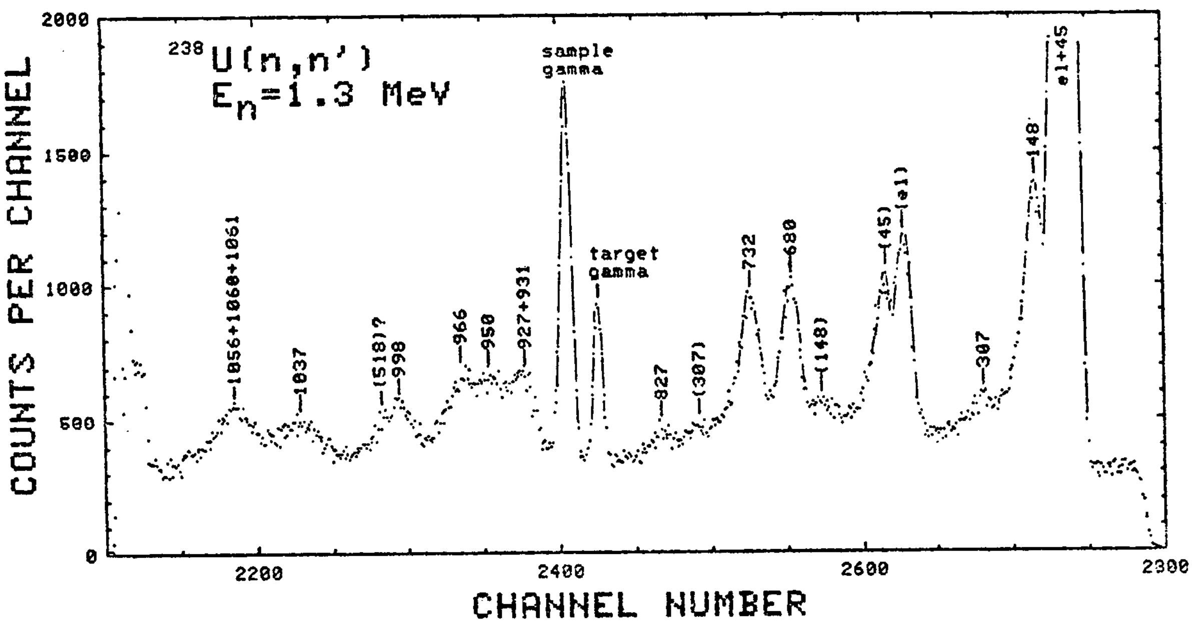

Fig. 1 ^{238}U(n,n') time-of-flight spectrum obtained using ^{7}Li(p,n)^{7}Be neutrons. The peaks are labeled by the corresponding excitation energy (in keV) in ^{238}U. Energies in parentheses indicate peaks arising from the scattering of the second group of neutrons from ^{7}Li(p,n)^{7}Be.

---

* Visiting Scholar from the People's Republic of China.

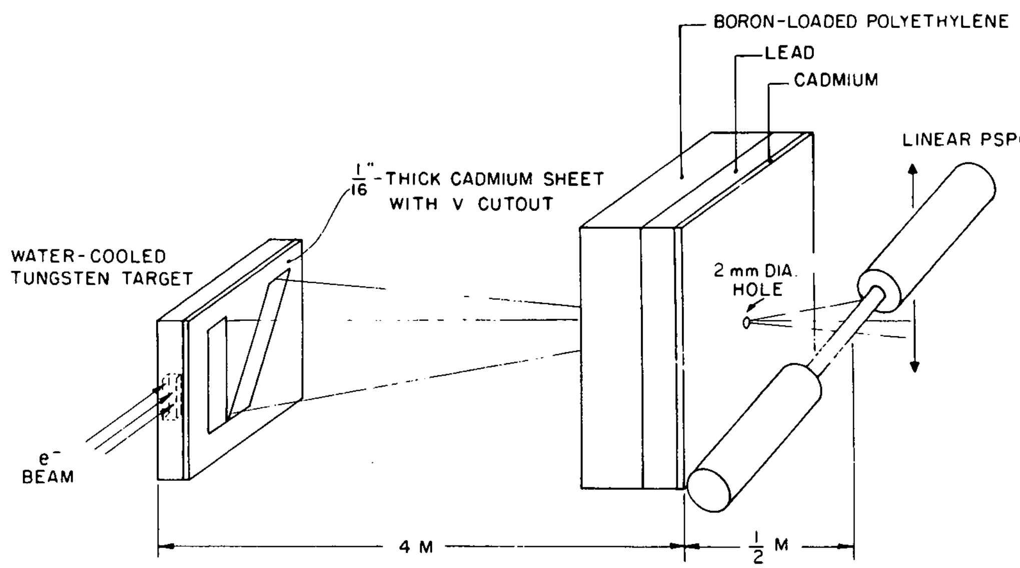

Fig. A-6. Experimental arrangement for neutron pin-hole camera.

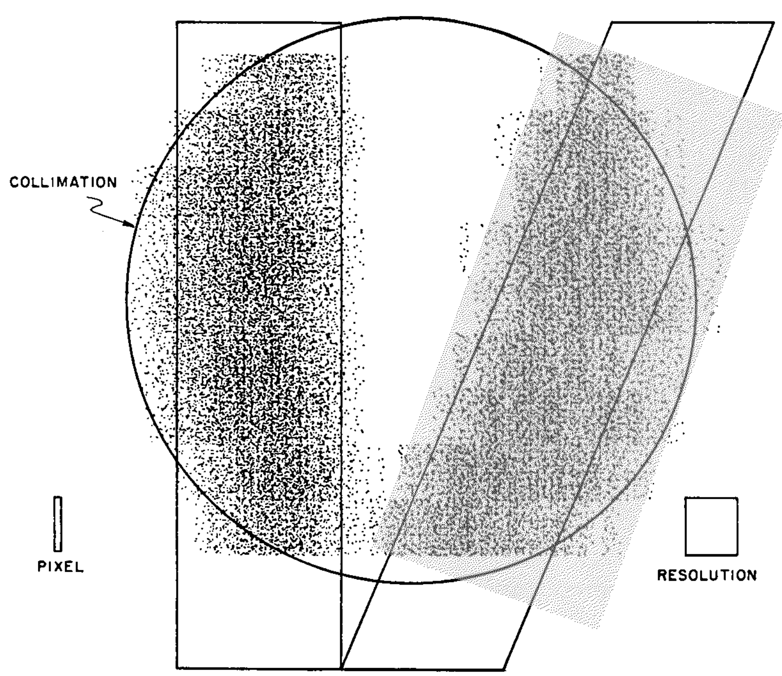

Fig. A-7. Pin-hole camera image of the "V" obtained with low-energy neutrons.

not commercially available. For this reason the NBS, together with Oak Ridge National Laboratory are presently developing suitable high spatial resolution PSPCs. The first area PSPCs contain 3 atm ^3He, 11.5 atm Xe, and 0.5 atm CO_2. The sensitive area is 50X50 mm^2 and the spatial resolution is 1.5X1.5 mm^2. Work continues on improving this design. Position sensing was determined using resistance-capacitance position encoding as described in Ref. 6.

12. Neutron Dosimetry and Instrument Calibrations
(K. C. Duvall, O. A. Wasson, R. B. Schwartz)

Calibration services for the industrial and scientific community have been provided at the 3 MV positive ion Van de Graaff accelerator. The 0.2 to 1.2 MeV standard neutron flux facility has been used to measure the response as a function of energy of several types of personnel dosimeters and neutron monitors. In the upcoming year, we expect this level of facility usage to continue. Calibration services will also continue to be available at the thermal, 2 keV, 24 keV, and 144 keV neutron beams at the NBS reactor facility.

13. Efficient Neutron Production Using Low Energy Electron Beams
(C. D. Bowman)

A comparison of (γ,n) and atomic cross sections shows that neutron production with an electron beam can be as energy efficient with 10 MeV electrons as with the conventionally used 30 to 100 MeV electrons. Neutron production from W using 100 MeV electrons is compared with a thin W converter followed by a deuterium or beryllium containing target using electrons near 10 MeV. The results are shown in Fig. A-7 where neutrons per 1000 MeV of electron energy are plotted against electron energy for several different materials. The dashed line shows the conversion efficiency for W using 100 MeV electrons. It is seen that above 10 MeV a D_2O target will produce half as many neutrons per joule of beam energy as 100 MeV electrons on W. Modern electron accelerator technology allows one to produce high beam current at low energy with a rather modest accelerator. Some advantages of neutron production at lower electron energy are (1) reduced capital for the accelerator, (2) reduced physical space requirements, (3) more reliable accelerator operation, (4) lower maintenance, (5) greatly reduced activation of accelerator and neutron target. The disadvantages are less source brightness and the unavailability of neutrons above about 4 MeV. The concept should permit the implementation of an intense pulsed white neutron source for laboratory or industrial use at a significant reduction in cost over existing accelerators.

---

[6] C. J. Borkowski and M. K. Kopp, Rev. Sci. Instrum. 46, 951 (1975).

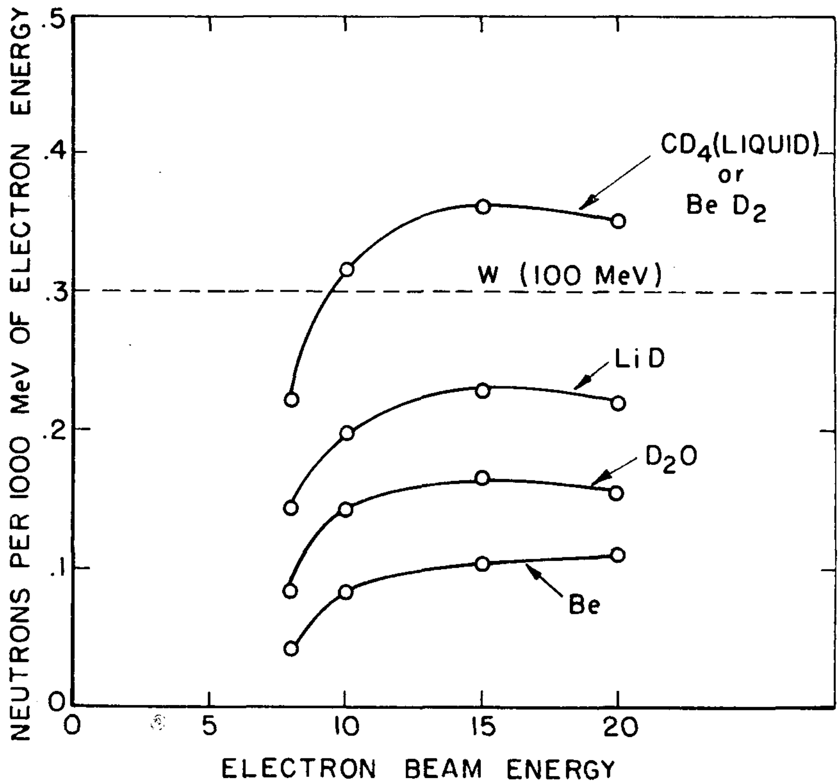

Fig. A-8. Neutron production efficiency for various target materials. A target thick enough to attenuate 5 MeV γ-rays by 1/e is assumed. The dashed line is the efficiency for 100 MeV electrons on tungsten.

14. Spectrum-Averaged Fission Cross Sections for ^{233}U, ^{232}Th, and ^{240}Pu in the Coupled Fast Reactivity Measurements Facility (CFMRF) (D. M. Gilliam, J W Rogers[§])

The CFMRF reactor is a well characterized and well documented benchmark neutron field for reactor fuels dosimetry and reactor materials dosimetry.[7] A 1975 paper[8] by Grundl et al. reported spectrum-averaged fission cross section for ^{238}U, ^{239}Pu, and ^{237}Np relative to the spectrum-averaged fission cross section for ^{235}U. The new data given below are spectrum-averaged fission cross section ratios for ^{233}U, ^{232}Th, and ^{240}Pu relative to the ^{235}U cross section, as before.

The measurements were made by means of double fission-ionization chamber which permitted simultaneous counting of fissions for back-to-back deposits of ^{235}U and one of the other isotopes of interest.

The new results are as follows:

$$\bar{\sigma}_f(^{233}\mathrm{U})/\bar{\sigma}_f(^{235}\mathrm{U}) = 1.56 \pm 3.\%$$

$$\bar{\sigma}_f(^{232}\mathrm{Th})/\bar{\sigma}_f(^{235}\mathrm{U}) = 0.0130 \pm 3.\%$$

$$\bar{\sigma}_f(^{240}\mathrm{Pu})/\bar{\sigma}_f(^{235}\mathrm{U}) = 0.368 \pm 3.\%$$

15. Fast Neutron Capture Cross Section Measurements in the Intermediate-Energy Standard Neutron Field (D. M. Gilliam)

The ^{238}U(n,γ) and ^{197}Au(n,γ) cross sections have been measured in the fast-reactor-like Intermediate-Energy Standard Neutron Field (ISNF). Both measurements involved major collaborative efforts by other laboratories. (Details will be presented in "Interlaboratory Reaction Rate Program 12th Progress Report" available from E. P. Lippincott, HEDL, Westinghouse Hanford Co., P.O. Box 1970, Richland, WA 99352).

---

§ EG&G Idaho, Idaho Falls, ID.

7 J W Rogers, D. A. Millsap, Y. D. Harker, "CFRMF Neutron Field Spectral Characterization," Nuclear Technology, 25, 330 (1975).

8 J. A. Grundl, D. M. Gilliam, N. D. Dudey, R. J. Popek, "Measurement of Absolute Fission Rates," Nuclear Technology, 25, 237 (1975).

The $^{238}U(n,\gamma)$ measurement [relative to $^{235}U(n,f)$] was made in cooperation with D. W. Maddison and S. G. Carpenter of the ANL (Idaho) Applied Physics Division. Activation foils of ^{238}U and ^{235}U were irradiated in the NBS ISNF facility and then shipped to ANL (Idaho) for gamma activity analysis. The result was

$$\bar{\sigma}_\gamma(^{238}U)/\bar{\sigma}_f(^{235}U) = 0.1412 \pm 1.7\%,$$

in good agreement with the calculated value of 0.1410, which was derived from ENDF/B IV cross sections and a 240 group discrete ordinates calculation of the ISNF spectrum.

The $^{197}Au(n,\gamma)$ cross section measurement [again relative to $^{235}U(n,f)$] was made in cooperation with A. Fabry of the Belgian Center for the Study of Nuclear Energy (CEN/SCK), Mol, Belgium. Fabry brought a carefully calibrated NaI spectrometer to NBS for activation analysis of gold foils irradiated in the ISNF. In these irradiations, the ^{235}U fission rate was determined by a fission ionization chamber. The result was

$$\bar{\sigma}_\gamma(^{197}Au)/\bar{\sigma}_f(^{235}U) = 0.248 \pm 2.9\%,$$

in fair agreement with the calculated value of 0.258.

B. FACILITIES

1. The 3 MV Positive Ion Van de Graaff Facility (O. A. Wasson, K. C. Duvall)

During the past year, the vacuum system in the 0° beam line was improved by replacing the oil diffusion pump with a turbo-molecular pump. No oil diffusion pumps remain in the major beam lines. Progress was made in lowering the energy of the deuteron beam in order to increase the yield from the $^{3}H(d,n)^{4}He$ reaction. The lower part of the accelerator column was shorted and an 8-cm extension was inserted on the corona needle control which permitted accelerator control for voltages as low as 325 kV. Deuteron beams with energies of 250 kV were obtained from 500 kV molecular ion beam. Modifications are in progress to establish an additional beam line into the heavily shielded experimental room for studies in neutron dosimetry.

2. Data Acquisition Systems (R. A. Schrack, C. D. Bowman, R. G. Johnson)

Over the last few years the data acquisition systems at NBS have been completely modernized. Three nearly identical systems (one at the Van de Graaff and two at the Linac) are now routinely used for neutron and other nuclear measurements. The basic system consists of a CAMAC front end backed by a Harris DC6024/5 minicomputer with suitable peripheral devices. All three systems can be used for multiparameter experiments using a 5.4 Mbyte (or 10.8 Mbyte) moving head disc for random access storage. In addition, a one million word memory has been acquired which will increase the maximum permissible event rate from 300 s^{-1} to over 10^4 s^{-1}. The software has been specifically designed to permit multiparameter operation. For time-of-flight measurements two EGG TDC-100 time digitizers are available and for PHA data multiple Tracor Northern NS-623 ADC units are available, all interfaced to the CAMAC system. These data acquisition systems have proved to be both powerful and easy to use since their installation.

C. DATA COMPILATION

1. X-Ray and Ionizing Radiation Data Center (J. H. Hubbell)

In addition to completion of a high-energy photon cross section compilation with H. Gimm (MPI, Mainz, Germany) and I. Øverbø (TH, Trondheim, Norway)[9], this Data Center responded to a total of 257 requests for data or information in 1979.

2. Compilation of Data Useful for Germanium-Detector-Efficiency Calibrations (D. D. Hoppes, F. J. Schima)

The results of appropriate half-life and gamma- or x-ray measurements by members of the Alpha-, Beta-, and Gamma-Ray Spectrometry Working Group of the International Committee for Radionuclide Metrology (ICRM) are being collected and tabulated. Uncertainties are to be stated in a consistent and apparent way. Results obtained in the past 10 years by 12 laboratories are currently in hand, together with sufficient detail to allow them to be used in a subsequent evaluation. The compilation will be published as a NBS-ICRM report.

---

[9] J. H. Hubbell, H. A. Gimm, and I. Øverbø, "Pair, Triplet and Total Atomic Cross Sections for 1 MeV-100 GeV Photons in Elements Z=1 to 100," submitted to J. Phys. Chem. Ref. Data.

OAK RIDGE NATIONAL LABORATORY

A. NUCLEAR CROSS SECTIONS FOR TECHNOLOGY CONFERENCE

The Conference on Nuclear Cross Sections for Technology, organized by personnel in the Physics and Engineering Physics Divisions at ORNL, was held in Knoxville, Tennessee, October 22-26, 1979. There were 42 invited speakers and 165 contributed talks at this conference. Abstracts of the papers were published in the September 1979 APS Bulletin. The proceedings, edited jointly by ORNL and NBS, will be published in two volumes in mid-1980.

Following is a list of titles of papers from ORNL presented at the conference. Since the abstracts of these presentations are available in the September 1979 Bulletin of the American Physical Society, they are not reproduced here.

J. K. Dickens, "Fission-Product Decay Heat for Thermal Reactors," p. 862.

D. C. Larson, J. A. Harvey, and N. W. Hill, "Neutron Total Cross Sections of H, C, O, and Fe from 500 keV to 60 MeV," p. 862.

D. C. Larson, "Evaluation of ^{23}Na for ENDF/B-V," p. 863.

C. Y. Fu, D. M. Hetrick, and F. G. Perey, "Simultaneous Evaluation of ^{32}S(n,p), ^{56}Fe(n,p), and ^{63}Cu(n,2n) Cross Sections," p. 863.

D. E. Bartine, "The Use of Thorium in Fast Breeder Reactors," p. 865.

D. T. Ingersoll, R. L. Childs, and F. J. Muckenthaler, "Deep Penetration Integral Experiment for a Thorium Blanket Mockup," p. 865.

J. R. White and D. T. Ingersoll, "Analysis of the Swiss Thorium Blanket Integral Experiments," p. 865.

J. H. Marable, C. R. Weisbin, and G. de Saussure, "Cross Section Adjustment Applied to Estimation of Uncertainty in Breeding Ratio of a Large LMFBR," p. 867.

Y. Yeivin, J. H. Marable, C. R. Weisbin, and J. Wagschal, "An Adjusted Nuclear Data Library for Fast Reactor Core Physics," p. 867.

J. Barhen, W. E. Ford III, R. W. Roussin, J. J. Wagschal, C. R. Weisbin, J. E. White, and R. Q. Wright, "Vitamin E: A Multipurpose ENDF/B-V Coupled Neutron-Gamma Cross Section Library," p. 868.

R. G. Alsmiller, "Shielding of Fusion Reactors," p. 869.

F. S. Alsmiller, R. G. Alsmiller, Jr., T. A. Gabriel, and R. A. Lillie, "Calculated Particle Production Spectra and Multiplicities from Nucleon-Fissile Element Collisions at Medium Energies ($\gtrsim$ 1 GeV)," p. 874.

L. W. Weston, "Evaluation of the Fission and Capture Cross Sections of ^{240}Pu and ^{241}Pu for ENDF/B-V," p. 875.

S. Plattard, G. F. Auchampaugh, N. W. Hill, R. B. Perez, G. de Saussure, and J. A. Harvey, "High Resolution Neutron Fission Cross Section of ^{231}Pa," p. 876.

G. T. Chapman and G. L. Morgan, "Integral Experiments for Fusion Reactor Design: Experimentation," p. 880.

R. T. Santoro, R. G. Alsmiller, Jr., J. M. Barnes, and E. M. Oblow, "Integral Experiments for Fusion Reactor Design: Analysis," p. 880.

D. K. Olsen, G. L. Morgan, and J. W. McConnell, "Measurement of ^{238}U(n,n'γ) and ^{7}Li(n,n'γ) Gamma-Ray Production Cross Sections," p. 882.

J. A. Harvey, Cindy Moore, and N. H. Hill, "Neutron Total Cross Section of ^{233}U from 0.01 to 1.0 eV," p. 882.

R. F. Carlton, J. A. Harvey, M. S. Pandey, N. W. Hill, and R. W. Benjamin, "Neutron Total Cross Section Measurements on ^{249}Cf," p. 882.

R. R. Spencer, "Absolute Measurement of $\bar{\nu}_p$ for ^{252}Cf by the Large Liquid Scintillator Tank Technique," p. 883.

C. Y. Fu, "A Consistent Nuclear Model for Compound and Precompound Reactions with Conservation of Angular Momentum," p. 884.

D. M. Hetrick, D. C. Larson, and C. Y. Fu, "Neutron Emission Spectra induced by 14-MeV Neutrons from the U.S. Evaluated Nuclear Data File (ENDF/B-V) - A Critical Review," p. 884.

C. H. Johnson, J. L. Fowler, N. W. Hill, and J. M. Ortolf, "Measurement of the 2.35-MeV Window in ^{16}O + n," p. 886.

J. W. T. Dabbs, "Neutron Cross Section Measurements at ORELA," p. 888.

J. J. Wagschal, B. L. Broadhead, and R. E. Maerker, "Least Squares Methodology Applied to LWR-PV Damage Dosimetry, Experience and Expectations," p. 888.

B. CROSS SECTION MEASUREMENTS

1. Gamma-Ray Production Data

a. Measurement of the $^{7}Li(n,n'\gamma)^{7}Li^{*}$ (0.478-MeV) Cross Section from 0.5 to 5.0 MeV* (D. K. Olsen, G. L. Morgan,** and J. W. McConnell)

The cross section for the production of 478-keV gamma rays by 0.48- to 5.0-MeV neutrons incident on ^{7}Li has been measured with a 95-cm^3 Ge(Li) detector positioned 20 m from the ORELA white neutron source. The incident neutron flux was measured with a solid-state recoil-proton detector and polyethylene radiator. These results, which are an unambiguous measurement of neutron inelastic scattering to the 478-keV ^{7}Li state, are listed and compared with recent measurements from other workers and the ENDF/B-IV evaluation.

2. Capture Cross Sections

a. Neutron Capture Cross Sections at ORELA (R. L. Macklin, R. R. Winters,† and J. Halperin)

Analyses of the ORELA capture cross section measurements on four isotopes of Ru (including the important fission product 105) have been completed. A paper has been accepted for publication in Nuclear Science and Engineering. A series of capture measurements was made on broad s-wave resonances using ^{6}LH filters to reduce drastically the correction due to scattered neutrons. Capture measurements on rare gases using a thin-walled, stainless steel cell at pressures up to 40 atmospheres were completed for Ne, Ar and ^{86}Kr.

b. Half Life of ^{132}Te‡ (J. K. Dickens)

The half life of ^{132}Te has been measured by γ-ray spectroscopy. γ-ray spectra of fission-product decay following thermal-neutron fission of ^{239}Pu were obtained for decay times between one and thirty days. Decay of the 228.2-keV γ-ray from ^{132}Te was analyzed to obtain the half life of ^{132}Te. The measured ^{132}Te half life was 76.29 ± 0.21 hr. Similar measurements were made for the 140.5-keV γ-ray from decay of ^{99}Mo, the 364.5-keV γ-ray from decay of ^{131}I, and 293.2-keV γ-ray from decay of ^{143}Ce. The half lives obtained were 66.16 ± 0.30 hr for ^{99}Mo, 191.93 ± 1.34 hr for ^{131}I, and 33.31 ± 0.32 hr for ^{143}Ce.

---

*To be published in Nucl. Sci. Eng.
**Los Alamos Scientific Laboratory, Los Alamos, New Mexico.
†Denison University, Granville, Ohio.
‡Radiochem. Radioanal. Letters 39, 107 (1979).

c. The $^{232}Th(n,\gamma)$ Cross Section from 100 eV to 50 keV* (R. B. Perez, G. de Saussure, R. L. Macklin, J. Halperin, and N. W. Hill)

The neutron capture rate in two ^{232}Th samples (0.0008 and 0.0027 atom/b, respectively) were measured with the ORELA time-of-flight facility, over incident neutron energies from 100 eV to 50 keV. Below 4 keV a detailed comparison of the measured capture rates with calculations based on ENDF/B-V suggests that, above 500 eV, the evaluation needs additional work; in particular the resonance neutron widths appear systematically underestimated. From 4 to 10 keV the ^{232}Th cross section has a considerable amount of resonance structure suggesting that an extension of the resolved range above 4 keV would be desirable. The capture cross section derived from our measurement is 10 to 15% larger than that of ENDF/B-V in the range 6 to 10 keV, and about 5% higher in the range 10 to 40 keV. The uncertainty of our average cross section is estimated to rise from 4% at 4 keV to about 15% at 50 keV.

3. Total Cross Sections

a. Neutron Total Cross Sections for H, C, Al, Si, Ca, Cr, Fe, Ni, Cu, Au and Pb from 2 to 80 MeV (D. C. Larson, J. A. Harvey, and N. W. Hill)

We have measured the transmission of neutrons through samples of the above materials, with thicknesses n = 0.15 to 0.41 atoms/barn. The Be block target of ORELA provided the neutrons, which were detected by a NE110 proton recoil detector located 80 m from the source. The data were corrected for deadtime losses and background effects, and converted to cross sections. Our measured hydrogen cross section agrees to better than 1% over the complete energy range with results from recent phase-shift analyses of this cross section. These data are needed for shield design of the Fusion Material Irradiation Test (FMIT) facility.

b. Neutron Total Cross Section of Sulfur: Single-Level to Multilevel to Optical Model (C. H. Johnson and R. R. Winters)

The total cross section of sulfur, which was measured with good resolution at ORELA for 25-1100 keV neutrons, has been analyzed to obtain both single-level parameters and potential phase shifts at each resonance. A well fitting multilevel curve was then created from 25 to 1100 keV by converting in a straightforward manner from single-level to multilevel parameters and by using the potential phase shifts for deducing the effects of levels above and below the 25-1100 keV region. Two good results came out of this study. Firstly, the process of single- to multilevel conversion could possibly improve the efficiency of multilevel

*To be published as an ORNL/TM report.

codes. Secondly, the results yield not only the strength functions but also the real smoothed R-functions, which are to be interpreted by an optical model potential. For sulfur, the real well of the potential is found to be 8 MeV deeper for p-waves than for s-waves.

c. Comparison of Neutron Total Cross Section Measurements with Optical Model Predictions from 2 to 80 MeV* (D. C. Larson, D. M. Hetrick, and J. A. Harvey)

We have recently measured transmission of neutrons through samples of polyethylene, C, O, Al, Si, Ca, Cr, Fe, Ni, Cu, Au and Pb (see Section 3.a). Results from these measurements have been compared with predicted total cross sections obtained from standard optical model parameter sets. In particular, results were obtained for the Becchetti-Greenlees and Wilmore-Hodgson parameter sets, as well as selected "best-fit" sets for some of the materials. Comparison of the predicted total cross section with measured values provides guidance as to the choice of the best set as a function of mass and energy range for use in shielding calculations.

4. Scattering and Reactions

a. ^{238}U Inelastic Scattering at 82 keV* (R. R. Winters,** G. L. Morgan,† R. L. Macklin, D. K. Olsen, J. A. Harvey, and N. W. Hill)

We have measured as a function of angle the ratio of the 2^+ inelastic yield to the elastic yield using 82-keV "window" neutrons produced from the ORELA flux filtered through $\sim$30 cm of iron. The inelastic neutron scattering on ^{238}U is important for fast reactor design, particularly the threshold cross section to the first-excited 2^+ level at 45 keV. Au and ^{238}U samples were employed at an $\sim$9 m flight path. Scattered neutrons were detected 0.406 m from the samples with a NE-110 scintillator viewed by three photomultipliers in coincidence. The yield ratios were determined with the aid of the elastic line shape from the Au sample and have been corrected for the combined effects of elastic anisotropy and multiple scattering. With this ratio and the accurately known total cross section, the inelastic cross section at 82 keV was determined.

---

*Abstract of paper to be presented at the APS Meeting, Washington, D.C., April 28-May 1, 1980.
**Denison University, Granville, Ohio.
†Los Alamos Scientific Laboratory, Los Alamos, New Mexico.

5. Actinides

a. Actinide Neutron Cross Sections Program (J. W. T. Dabbs, C. H. Johnson, L. W. Weston, J. H. Todd, M. L. Williams, J. A. Harvey, J. A. Carter, J. K. Dickens, S. Raman, C. E. Bemis, Jr., J. Halperin, R. L. Macklin, and N. W. Hill)

Fission - A measurement on σ_{nf} (^{242m}Am) was carried out. In this measurement, considerable difficulties with rapid growth of spontaneous fission background in the sample were planned for and overcome. A remeasurement of σ_{nf} (^{249}Cf) was also carried out. A collaborative measurement with Rensselaer Polytechnic Institute on the fission cross sections of ^{244}Cm, ^{246}Cm, and ^{248}Cm is planned for April or May 1980. These measurements will take advantage of the high intensity of the Rensselaer Intense Neutron Spectrometer to overcome the strong spontaneous fission background of these samples. These measurements will provide a check on earlier underground nuclear explosion measurements. A very precise determination of the value of $\bar{\nu}_p$ (^{242}Cm) was obtained in connection with the fission cross section measurements on ^{242m}Am.

Capture - Preliminary data on the ^{237}Np capture cross section from 0.01 to 300 eV have been transmitted to the National Nuclear Data Center. Resonance parameters have been derived to describe data in the resonance region (0.01-100 eV). Publication of these ^{237}Np data should be completed this year. A remeasurement of the capture cross section of ^{243}Am is planned for the latter part of the year.

Total - Resonance analysis of the transmission data from an 85% ^{249}Cf sample using a multilevel R-matrix code was completed. Transmission measurements were made on two sample thicknesses of ^{231}Pa from 0.01-100 eV. The data will be analyzed to obtain resonance parameters. The neutron widths of these low energy resonances are needed to combine with fission data to determine fission widths for the resonances.

Integral Experiments - Last year, irradiated samples of ^{239}Pu (2), ^{240}Pu, and ^{241}Pu were analyzed. We plan to measure other irradiated samples of ^{233}U, ^{235}U, and ^{238}U this year. These samples were irradiated in EBR-II. A "spin-off" of this program has been the establishment of an irradiation program in collaboration with UK. This program will involve irradiations at Dounreay.

Calculation and Analysis - In 1979, sensitivity and uncertainty calculations for one irradiated ^{239}Pu sample were published. We also examined the impact of recent changes in cross sections (e.g., the change from ENDF/B-IV to ENDF/B-V) on selected fuel cycle parameters of a commercial LMFBR model. Beginning in 1980 the calculational program was expanded to a full man year effort on (1) interpretation of results from irradiated samples, (2) an analysis of the effect of cross section uncertainties on power-reactor performance and economics, and (3) an assessment of the effects of cross section measurements made since ENDF/B-IV. A sensitivity analysis approach will be used to find those cross sections which are still lacking, or which are of insufficient accuracy, as a guide to experimenters.

Fission Product Yields - Because of the availability of certain samples two "experiments of opportunity" have been undertaken. These are the determination by γ-ray assay with Ge(Li) detectors of fission product yields for thermal-neutron fission of ^{245}Cm and thermal fission of ^{249}Cf. In the former, γ-ray spectra were obtained for all fission products simultaneously for periods between 1 minute and 150 days following irradiation of the sample. Fission product yields have been determined for >80 isotopes representing 50 mass chains. The measurement on ^{245}Cm is complete and the measurement on ^{249}Cf is in progress.

Actinide Newsletter - The third issue, edited by S. Raman, will appear in early 1980 and has 60 contributions from 25 laboratories in 11 countries. The IAEA Advisory Group on Transactinium Isotope Nuclear Data at its second meeting in Cadarache, France, in May 1979, made a strong recommendation for the continuation of the Actinide Newsletter and for persons working in this field all over the world to make contributions to it. The publication schedule is expected to be one issue per year in the future.

b. The Triple-Humped Fission Barrier of ^{232}Pa* (S. Plattard,** F. G. Auchampaugh,† N. W. Hill, G. de Saussure, R. B. Perez, and J. A. Harvey)

The neutron-induced fission cross section (σ_f) of ^{231}Pa was measured at ORELA from 0.4 eV to 12 MeV at flight paths of 41.68 m for E_n > 0.1 MeV and 18.30 m for E_n < 10 keV. The fission fragments were detected in a sealed gas scintillator loaded with 265 mg of ^{231}Pa and 130 mg of ^{235}U. From 0.15 to 1 MeV σ_f exhibits prominent structures, particularly below 380 keV where two narrow ($\sim$2.6 keV FWHM) and well separated peaks are centered around 156.7 and 173.3 keV respectively. Occurrence of such two resonances with $K^\pi = 3^+$ and 3^- is very likely the signature of a vibrational level (K = 3) trapped in the asymmetrically deformed third well of the ^{232}Pa potential energy surface. In addition, uniformly distributed narrow fission resonances have been observed for the first time above a neutron energy of 1.3 eV. This feature, together with a measured average fission width of 8 μeV for these resonances, indicates

*Abstract of paper to be presented at the APS Meeting, Washington, D.C., April 28-May 1, 1980.
**Bruyères-le-Châtel, France.
†Los Alamos Scientific Laboratory, Los Alamos, New Mexico.

that 1) the first minimum of the ^{232}Pa fission barrier is on the order of, or lower than, the neutron separation energy in ^{232}Pa and 2) the third minimum is rather shallow (0.5 to 1 MeV).

c. Fission-Product Energy Release for Times Following Thermal-Neutron Fission of ^{235}U between 2 and 14000 Seconds* (J. K. Dickens, T. A. Love, J. W. McConnell, and R. W. Peelle)

Fission-product decay energy-release rates have been measured for thermal-neutron fission of ^{235}U. Spectral data were obtained using scintillation spectrometers for beta and gamma rays separately, and were processed to the form of total yield and total energy-release integrals for each set of time-interval parameters. The irradiations were for 1, 10, and 100 sec, and measurements were made covering times following irradiation from 1.7 to 13950 sec. The separate beta- and gamma-ray energy-release data were summed to obtain the total ($\beta + \gamma$) energy-release rates for the cases studied. The data are processed to provide two standard representations of decay energy release, the one following a pulse of fissions, and the other following an infinite period of irradiation. A complete representation of estimated uncertainties is given in the form of a variance-covariance matrix. For the pulse representation of the data, diagonal components correspond to uncertainties in the range 3-4%, with correlation coefficients in the range 0.1 to 0.5. The experimental data are compared with other experimental data. The present results are generally smaller than other data, in some cases by more than the estimated uncertainties.

The present results are smaller than the proposed 1973 ANS Decay-heat Standard by as much as 10% for times-following-fission between 2 and 400 sec, and are also smaller than the presently proposed (1978) ANS Decay-heat Standard by 5 to 8% for the time interval 2-600 sec. The reasons for these differences are discussed, and the importance for analyses using the new standard is presented.

d. Measurement of the Average Number of Prompt Neutrons Emitted per Fission of ^{235}U Relative to ^{252}Cf for the Energy Region 500 eV to 10 MeV** (R. Gwin, R. R. Spencer, R. W. Ingle, J. H. Todd, and H. Weaver)

The average number of prompt neutrons emitted per fission, $\bar{\nu}_p(E)$, has been measured for ^{235}U relative to $\bar{\nu}_p$ for the spontaneous fission of ^{252}Cf over the neutron energy range from 500 eV to 10 MeV. The samples of ^{235}U and ^{252}Cf were contained in fission chambers located in the center of a large liquid scintillator. Fission neutrons were detected by the large liquid scintillator. The present values of $\bar{\nu}_p(E)$

*To be published in Nucl. Sci. Eng.
**Abstract of ORNL/TM-7148, ENDF-289 (January 1980).

for ^{235}U are about 0.8% larger than those measured by Boldeman.[1] In earlier work with the present system, it was noted that Boldeman's value of $\bar{\nu}_p(E)$ for thermal energy neutrons was about 0.8% lower than obtained at ORELA. It is suggested that the thickness of the fission foil used in Boldeman's experiment may cause some of the discrepancy between his and the present values of $\bar{\nu}_p(E)$. For the energy region up to 700 keV, the present values of $\bar{\nu}_p(E)$ for ^{235}U agree, within the uncertainty, with those given in ENDF/B-V. Above 1 MeV the present results for $\bar{\nu}_p(E)$ range about the ENDF/B-V values with differences up to 1.3%.

e. Delayed Beta- and Gamma-Ray Production due to Thermal-Neutron Fission of ^{239}Pu: Tabular and Graphical Spectral Distributions for Times after Fission between 2 and 14000 Sec* (Dickens, England, Love, McConnell, Emery, Northcutt, and Peelle)

Fission-product decay energy-release rates have been measured for thermal-neutron fission of ^{239}Pu. Samples of mass 1 and 5 μg were irradiated for 1 to 100 sec using the fast pneumatic-tube facility at the Oak Ridge Research Reactor. The resulting beta- and gamma-ray emissions were separately counted for times-after-fission between 2 and 14,000 sec, giving spectral distributions $N(E_\gamma)$ vs E_γ and $N(E_\beta)$ vs E_β. The gamma-ray spectra were obtained using a NaI detector, and the beta-ray spectra were obtained using an NE-110 detector with an anticoincidence mantle. The raw data were unfolded to provide spectra distributions of moderate resolution. These distributions are given in graphical and tabular form as differential spectral intensity $I(E)$ (MeV^{-1} $fission^{-1}$) averaged over gamma-ray energy intervals ranging from 10 keV for $E_\gamma < 0.18$ MeV to 100 keV for $E_\gamma > 6.8$ MeV, and beta-ray energy intervals ranging from 20 keV for $E_\beta < 0.25$ MeV to 160 keV for $E_\beta > 6.4$ MeV. Counting-time intervals ranged from 1 sec for times-after-fission (t_w) < 6 sec to 4000 sec for $t_w \sim 10^4$ sec.

For comparisons the graphical representations show calculated spectra obtained using the CINDER-10 summation code and the ENDF/B-IV fission yield and decay scheme data base.

6. Experimental Techniques

a. Majority Logic NE-110 Detector for keV Neutrons** (N. W. Hill, J. A. Harvey, D. J. Horen, G. L. Morgan, and R. W. Winters)

A proton recoil detector for neutrons in the energy range of 5 keV to 1 MeV has been developed whose efficiency is reproducible and

[1]J.W. Boldeman, J. Frehaut, and R.L. Walsh, Nucl. Sci. Eng. 63, 430 (1977).
*Abstract of ORNL/NUREG-66 (January 1980).
**Abstract of paper to be presented at the APS Meeting, Washington, D.C., April 28-May 1, 1980.

stable. A 6 x 6 x 2 cm scintillator with RCA 8850 photomultipliers on three of its faces has been used for total cross section measurements to 5 keV where the efficiency is ∿10%. Each discriminator is biased well below the single photoelectron level; majority logic eliminates phototube noise and requires one or more photoelectrons in at least two tubes. Pulse height measurements of the summed signals have been made from 5 keV to 350 keV using both a continuous neutron beam and Fe window neutrons. The experimental results were compared with Monte Carlo calculations to obtain the absolute neutron detection efficiency of the detector. This detector has been used to determine the inelastic scattering cross section of 82 keV neutrons from ^{238}U.

C. DATA ANALYSES

1. Theoretical Calculations

a. Analysis of ORNL Fusion Reactor Shield Integral Experiments* (Santoro, Alsmiller, Barnes, Chapman, Morgan, Oblow, and Peelle)

The nuclear performance of the blanket and shield in a fusion reactor will have a substantial impact on the overall operation and capital cost of the reactor. It is necessary, therefore, to have experimental verification of the nuclear data and radiation transport methods that will be used to carry out the nuclear design calculations for these assemblies. Integral experiments are being performed at the Oak Ridge National Laboratory to provide the experimental data needed for this verification. The verification will be made by extensive comparisons between calculated results and these experimental data. Measurements of the transport of 14-MeV neutrons through laminated shields containing materials that are anticipated for use in fusion applications and the effect of introducing penetrations in the shields will be made. This paper summarizes the results of measurements and calculations to determine neutron and photon spectra behind laminated shields of varying composition and thickness.

b. Computation of Analytical Bounds for the Cross Section Self-Shielding Factors* (J. Barhen and D. G. Cacuci)

A general methodology for computing strict upper and lower bounds for self-shielding factors has been developed. The complete range of self-shielding factors computed by cross section processing codes was addressed, and ENDF/B specified cross section discontinuities were taken into account. A stand alone code BRINE provides users with a practical tool to check the f-factors.

---

*Abstract of paper presented at the APS Meeting, San Francisco, California, November 11-16, 1979.

2. ENDF/B Related Evaluations

a. Uncertainty Analysis (J. J. Wagschal)

A detailed uncertainty analysis of ^{237}Np, ^{238}U, and ^{239}Pu fission rate ratios to ^{235}U measurements in the NBS ^{252}Cf and ISNF standard neutron fields and of the ^{235}U absolute fission rate in the same ^{252}Cf field are given in refs. 1 and 2. The corresponding covariance matrices were explicitly derived in ref. 1 and are also reported in ref. 2. Calculated fission rate ratios in the ISNF central region, as well as uncertainties in the calculated values, are given in ref. 3. All of these data were used in order to demonstrate the importance of the various covariances in cross-section adjustments[4] and in flux unfolding calculations.[5]

b. An Overview of CSEWG Shielding Benchmark Problems (R. E. Maerker)

The fundamental philosophy behind the choosing of CSEWG shielding benchmarks is that the accuracy of a certain range of cross section data be adequately tested. The benchmarks, therefore, consist of measurements and calculations of these measurements. The term "benchmark candidate" is used to designate any single measurement or any single calculation of a measurement that is documented in an appropriate benchmark format; the term "benchmark" is reserved to designate two or more "benchmark candidates" (for example, a measurement and a calculation of the measurement or two uncorrelated measurements of the same quantity) which together, in the opinion of CSEWG, provide sufficient independent verification as to warrant the benchmark label. At the present time, twelve experiments, along with corresponding calculations of them, have been designated as CSEWG shielding benchmarks.

---

[1] J. J. Wagschal, R. E. Maerker, and D. M. Gilliam, "Covariances of Fission-Integral Measurements at the NBS ^{252}Cf and ISNF Facilities and at the ORNL-PCA Facility," Third ASTM-EURATOM Symposium on Reactor Dosimetry, Ispra (Varese), Italy, October 1-5, 1979.

[2] J. J. Wagschal, R. E. Maerker, and D. M. Gilliam, "Detailed Error Analysis of Average Fission Cross Section Measurements in NBS Standard Neutron Fields," Trans. Am. Nucl. Soc. 33, 823 (1979).

[3] B. L. Broadhead and J. J. Wagschal, "The NBS Intermediate-Energy Standard Neutron Field (ISNF) Revisited," Trans. Am. Nucl. Soc. 33, 848 (1979).

[4] J. J. Wagschal, R. E. Maerker, and B. L. Broadhead, "Cross Section Adjustment: Sensitivity to Uncertainties," Trans. Am. Nucl. Soc. 33, 698 (1979).

[5] J. J. Wagschal, B. L. Broadhead, and R. E. Maerker, "Least Squares Methodology Applied to LWR-PV Damage Dosimetry, Experience and Expectations," APS Int. Conf. Nucl. Cross Sections for Technology, Knoxville, Tennessee, October 22-26, 1979.

c. Processing ENDF/B-V Uncertainty Data into Multigroup Covariance Matrices* (J. D. Smith, H. L. Dodd, F. G. Perey, and C. R. Weisbin)

The purpose of this work is to develop the capability of processing ENDF/B-V uncertainty data into multigroup covariance matrices. These matrices, coupled with conventional sensitivity analysis, allow not only for propagation of uncertainties in basic nuclear data (i.e. ENDF/B-V) to uncertainties in reactor performance parameters such as k-effective and breeding ratio, but also provide valuable feedback to the nuclear data community as to which measurements need further refinement. The capability of processing newly formatted ENDF/B-V data has been developed. Specifically, processing capabilities have been added for new uncertainty relationships, explicit cross reaction and cross material relationships, and derived uncertainties. Capabilities have also been added to produce the off-diagonal submatrices resulting from derived (in the context of summing) uncertainties. Processing uncertainties in the average number of neutrons per fission ($\bar{\nu}$) has also been included. Finally, an important accomplishment of this work has been to separate the uncertainty processing from the cross section processing, originally suggested by LASL, to provide not only for a modular code system, but to reduce computing costs.

d. BAYES: A Generalized Least-Squares Program for Updating Cross Section Evaluations with Correlated Data Sets** (D. M. Hetrick and C. Y. Fu)

The PDP-10 FORTRAN IV computer programs INPUT.F4, BAYES.F4, and OUTPUT.F4, which employ Bayes' theorem (or generalized least-squares) for simultaneous evaluation of reaction cross sections, are described. Evaluations of cross sections and covariances are used as input for incorporating correlated data sets, particularly ratios. These data are read from Evaluated Nuclear Data File (ENDF/B-V) formatted files. Measured data sets, including ratios, and absolute and relative data, are read and combined with the input evaluations via the least-squares technique. The output evaluations have not only adjusted cross sections and covariances, but also cross-reaction covariances. These output data are written into ENDF/B-V format.

3. Validation of ENDF/B Evaluations Through Integral Measurements

a. Sensitivity and Uncertainty Analysis for the Mixed-Oxide Thermal Lattice U-L212 (Childs, de Saussure, Lucius, Drischler, Baker, Marable, and Westfall)

*Abstract of paper presented at the APS Meeting, San Francisco, California, November 11-16, 1979.
**To be published as an ORNL/TM report.

The sensitivities of a mixed oxide (2Wt%PuO_2 - 8% ^{240}Pu) fueled, light water moderated critical lattice experiment carried out at Battelle Northwest Laboratories under EPRI sponsorship have been determined. A two-dimensional diffusion theory analysis was performed and the sensitivity of the eigenvalue (k) and four reaction rate ratios to changes in nuclear data have been determined. The sensitivity analysis capability was extended to include upscattering and multi-dimension ability. A covariance matrix has been developed for ^{239}Pu, and the uncertainty associated with calculated performance parameters due to uncertainties in nuclear data has been obtained. This uncertainty has been found to be comparable in size to experimental or calculational model uncertainties. Sensitivity coefficients have been used to estimate the impact of cross section changes proposed for a preliminary version of the ENDF/B-V library.

A study of the large ^{240}Pu resonance at 1.05 eV indicated the linear perturbation theory not to be adequate for predicting the effect of cross section changes of the magnitude proposed for ENDF/B-V. Similarly a need for a more rigorous treatment of the ^{238}U resonance shielding factor changes has also been indicated.

b. Sensitivity Coefficient Compilation for CSEWG Data Testing Benchmarks* (C. R. Weisbin, J. H. Marable, J. Hardy,** and R. D. McKnight†)

The purpose of this report is to compile and document sensitivity coefficients generated by member laboratories of the Cross Section Evaluation Working Group (CSEWG) in the course of ENDF/B data testing. It is anticipated that this work will be continuously updated as new benchmarks and new types of data are developed. The broad scope of this effort (i.e., sensitivities for fast reactors, thermal reactors, shielding, etc. to many cross section data types) allows only for detailed tabulation of the energy-integrated sensitivity coefficient (i.e., the change in response due to a uniform one percent change in cross section over the entire energy domain), sensitivities to changes in individual resonance parameters, and illustrative examples of energy dependent sensitivity profiles. The entire compilation of energy dependent coefficients is available in a computer-retrievable format along with programs for editing, mode changing, folding with projected changes to the reference data file, and performance parameter uncertainty estimation.

*Abstract of BNL-NCS-24853, ENDF-265.
**Bettis Atomic Power Laboratory, Pittsburgh, Pennsylvania.
†Argonne National Laboratory, Argonne, Illinois.

D. NUCLEAR DATA PROJECT ACTIVITIES - 1979

(S. J. Ball,* Y. A. Ellis, W. B. Ewbank, B. Harmatz, F. W. Hurley,* M. J. Martin,** M. R. McGinnis,* J. T. Miller,* S. Ramavataram,** C. D. Savin,* and M. R. Schmorak)

1. Data Evaluation

As part of the international network for nuclear structure data evaluation, the Nuclear Data Project has continuing responsibility for approximately 100 mass chains in three regions: A = 45-69, 101-118, and 195-up. A total of 19 new mass chains was prepared and published during 1979. Figure D-1 gives the publication status of the mass chains for which NDP is responsible. For comparison, the status of all published mass chains is shown in Fig. 2.

In addition to its evaluation responsibility, NDP is committed to maintaining uniform, high standards for ENSDF (and consequently for Nuclear Data sheets) by providing a thorough review of the first few mass chains prepared by each new evaluator. During 1979, NDP staff reviewed 12 mass chains prepared by new evaluators from seven other data evaluation centers. NDP staff members have also organized training seminars for new data evaluators in order to introduce them to NDP evaluation techniques, analysis programs, and conventions used in ENSDF and Nuclear Data Sheets. At the invitation of the Japanese Nuclear Data Committee, M. J. Martin conducted a training session at JAERI in Tokai-mura, Japan. The session was attended by nine Japanese nuclear structure data evaluators.

2. Evaluated Nuclear Structure Data File

The Evaluated Nuclear Structure Data File (ENSDF), developed and implemented by the NDP, contains a documented summary of the current status of nuclear measurements. The ENSDF now contains 7100 distinct sets of evaluated nuclear information. This includes:

1960 sets of adopted level properties (41,000 nuclear levels)
1980 decay schemes
3310 nuclear reaction data collections, including

250 (n,γ) reactions
230 (d,p) reactions
950 (charged-particle,$xn\gamma$) reactions.

All decay scheme information in ENSDF is now at least as complete as the most recent Nuclear Data Sheets. Normalization information is included wherever available, and details of electron capture and internal

*Technical support staff.
**Part-time assignment to Nuclear Data Project.

conversion have been added systematically, so that complete tables of atomic and nuclear radiations can be assembled for more than 1600 decay schemes.

The ENSDF computer format has been adopted as an international standard for the systematic storage and exchange of nuclear structure data. At six-month intervals NDP has prepared complete copies of ENSDF on magnetic tape for distribution through an international network of data centers.

3. Nuclear Structure References

Nuclear Data Project's Nuclear Structure References (NSR) file contains about 70,000 entries. Approximately 5000 indexed new research works are added each year. About half of the additions are journal publications; the other half consists of reports, conference abstracts, preprints, etc. Each month an SDI (selective dissemination of information) service is provided from new entries to the NSR file. An index to the new literature is published three times per year as "Recent References," which includes both isotope and reaction indexes for both journal and nonjournal literature.

The NSR file is being used as an international standard for the systematic exchange of indexed reference information. Copies of the complete indexed file have been distributed to the international network of data evaluation centers.

4. Publications

The Nuclear Data Project is the editorial and publications office for the journal Nuclear Data Sheets. The NDP prepares camera-ready copy which is sent to Academic Press for publication and distribution. Manuscripts are now being received from several data evaluation centers other than NDP. Thirty percent of the new evaluations published during 1979 were prepared by non-NDP evaluators.

The ENSDF system makes practical the systematic selection and publication of special collections of nuclear structure data for special user groups. In 1979 several such collections were published:

1) All spontaneously fissioning isomeric states[1]

2) Nuclear decay data for selected radionuclides[2]

---

[1]W. B. Ewbank, Y. A. Ellis, and M. R. Schmorak, Nucl. Data Sheets 26, 1 (1979).

[2]M. J. Martin, Ed., Nuclear Decay Data for Selected Radionuclides, Appendix A in National Council on Radiation Protection and Measurements Report NCRP-58 (November 1978).

3) Transactinide nuclear levels with $T_{1/2} \geq 1$ s[1]

4) Strong γ-rays ($I \geq 1\%$) from nuclei with $A \geq 207$[1]

5) Strong α-radiations ($I > 1\%$) from nuclei with $A > 207$[1]

6) Complete atomic and nuclear radiations from over 1500 radionuclides.[2]

---

[1]W. B. Ewbank, in Proceedings, IAEA Advisory Group Meeting on Transactinium Nuclear Data (Cadarache, France, May 1979), to be published.

[2]W. B. Ewbank, Ed., Atomic and Nuclear Radiations from ENSDF/MEDLIST, Oak Ridge National Laboratory Report ORNL-5535, to be published.

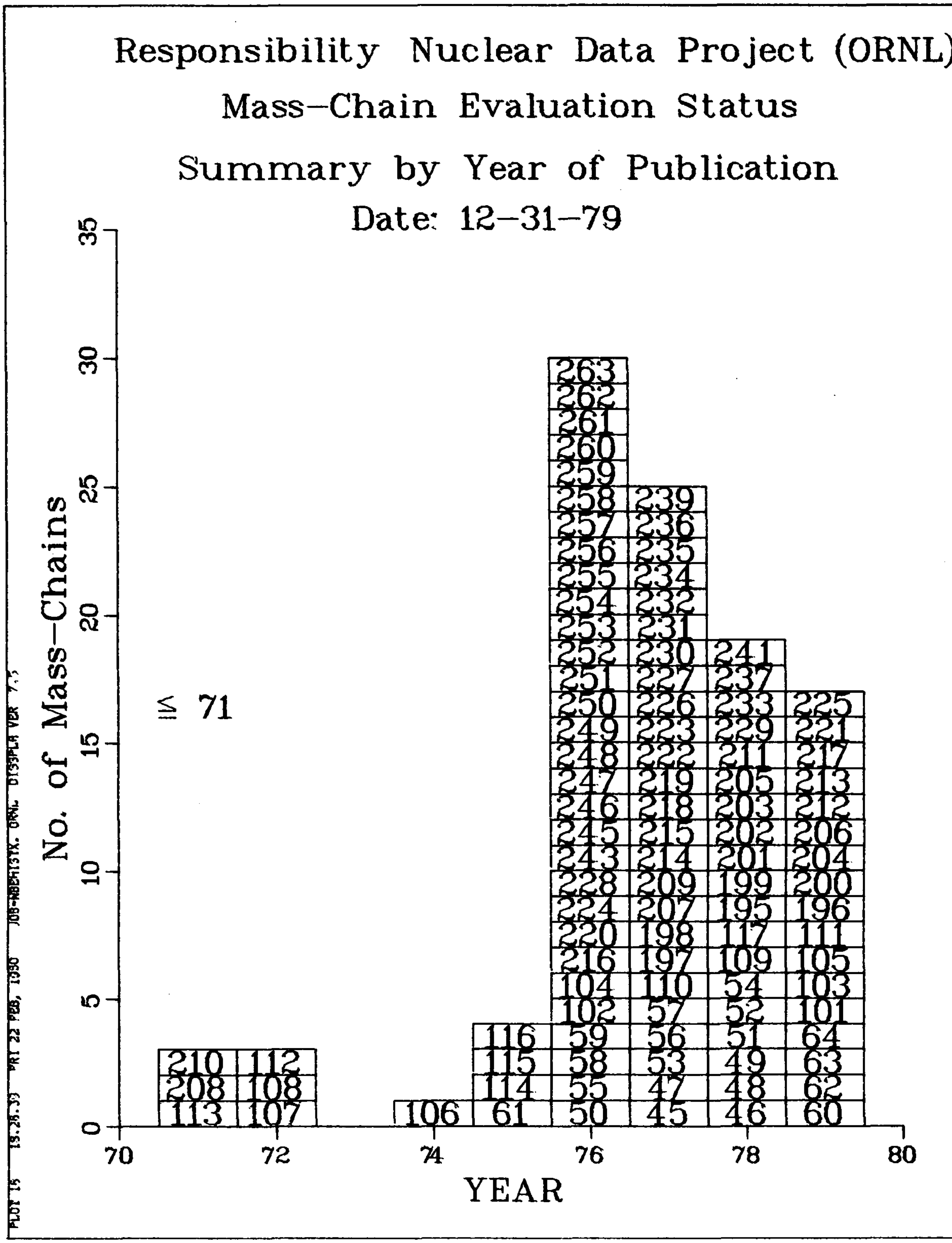

Fig. D-1. Status of mass-chain evaluations in NDP's regions of responsibility.

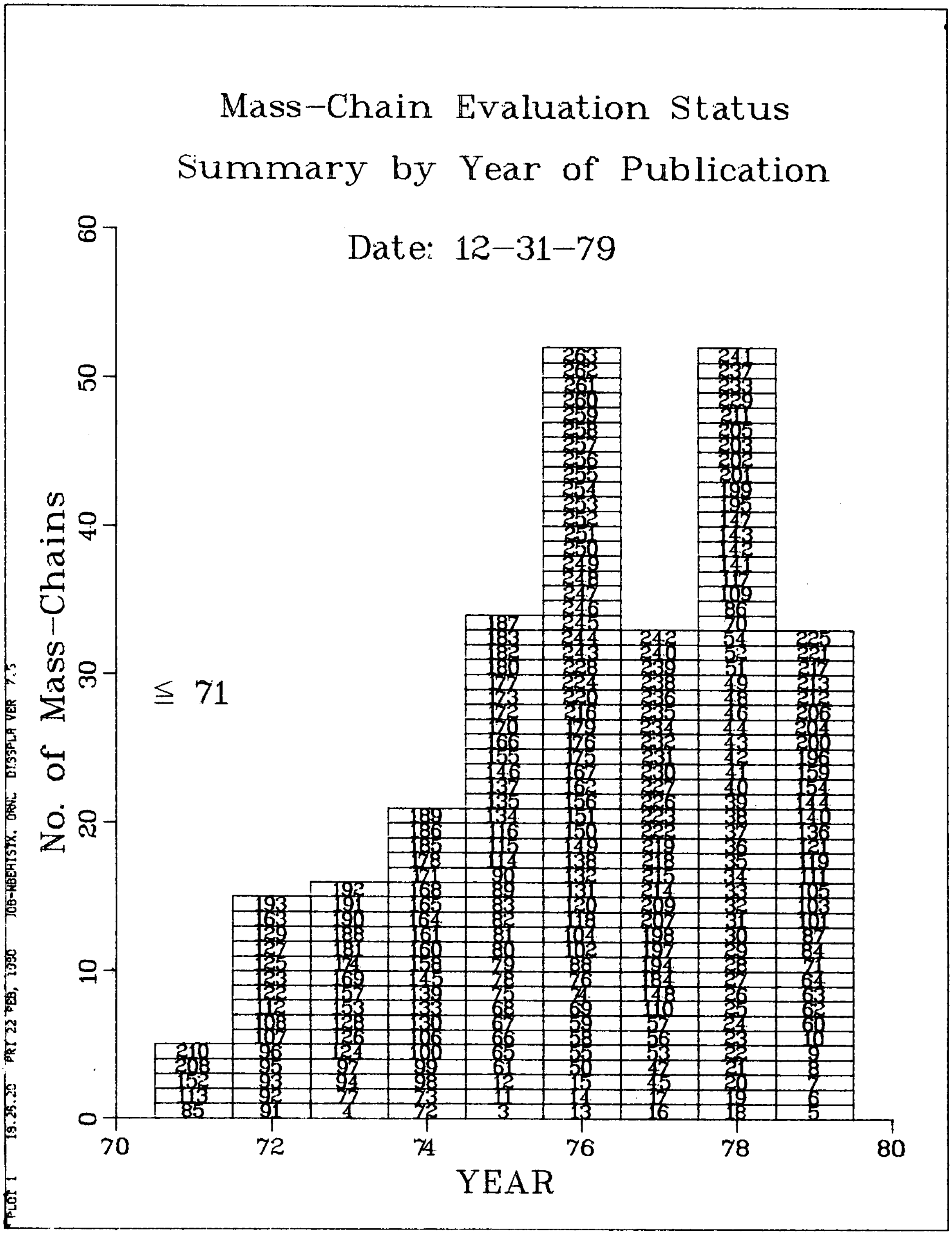

Fig. D-2. Status of all mass-chain evaluations, A   5.

OHIO UNIVERSITY

A. NEUTRON MEASUREMENTS

1. ^{6}Li and ^{7}Li (H. Knox, D. Resler, P. Koehler, R. Lane)

Final analysis of differential elastic scattering data for ^{6}Li and ^{7}Li at 2.3, 2.8, 3.3, 3.8 and 4.08 MeV has been completed. For ^{6}Li, the present results are in good agreement with the earlier work of Knitter et al.[1] at 2.3 and 2.8 MeV and with earlier[2] work at this laboratory at 4.08 MeV. A 6.5 m flight path was used in these measurements to resolve the elastic and first inelastic (Q = -0.478 MeV) neutron groups for ^{7}Li. The analysis of the inelastic data is complete except for final multiple scattering corrections. These data combined with the earlier work of Lane, et al.[3] and previous[2] work at this laboratory provide a data base for both ^{6}Li + n and ^{7}Li + n scattering up to 8 MeV. An R-matrix analysis of the ^{7}Li + n scattering data is described below. For ^{6}Li + n a similar study will begin later this year.

2. ^{11}B and ^{13}C (P. Koehler, D. Resler, R. Lane, H. Knox, G. Randers-Pehrson)

Elastic and inelastic differential cross sections for neutrons scattered from enriched samples of ^{11}B and ^{13}C have been measured. Angular distributions of elastic and inelastic (2.12 MeV level) neutron scattering from ^{11}B were obtained at 7 incident energies between 4.82 and 7.55 MeV. For ^{13}C angular distributions of elastic and inelastic (3.09, 3.68, and 3.85 MeV levels) neutron scattering were obtained at 6 incident energies between 5.70 and 8.25 MeV. These data, together with measurements reported last year[4] complete our initial survey of differential inelastic cross sections for these nuclei. Further ^{13}C measurements are planned for the coming year to map out resonances seen in the initial survey. The ^{11}B measurements may be extended pending an examination of the state of the experimental and theoretical

---

1 Knitter, Budtz-Jorgensen, Mailly and Vogt, Euratom Report EUR-5726e (1977)

2 Knox, White and Lane, Nucl. Sci. Eng. 65, 65 (1978)

3 Lane, Elwyn and Langsdorf, Jr., Phys. Rev. 136, B1710 (1964)

4 Reports to the DOE Nuclear Data Committee, BNL-NCS-26133, p. 184

work for this nucleus. No previous differential elastic or inelastic data above 6.50 MeV have been reported for ^{13}C.

Analysis of these data is currently underway. The second and third inelastic groups from ^{13}C are not well separated, especially at higher energies. A fitting procedure will be used to separate them. A new multiple scattering code is being written to make corrections for both the elastic and discrete inelastic differential cross sections. The program uses both elastic and inelastic energy versus angle differential cross section meshes as input. Time-of-flight spectra for single collisions and for the experimental mock-up are output for up to 20 angle bins.

3. Elastic and Inelastic Scattering of 24 MeV Neutrons from Oxygen Isotopes* (P. Grabmayr, J. Rapaport, R.W. Finlay)

Measurements of elastic and inelastic differential cross sections were obtained for 24 MeV neutrons incident on $^{16,18}O$ by standard time-of-flight techniques. The samples consisted of natural water and water enriched to 95% in ^{18}O and were contained in thin aluminum cans. Inelastic excitation of the first 2^+ and 3^- states were obtained simultaneously with the elastic scattering in each case.

Elastic scattering data were analyzed in terms of a Lane-consistent optical model potential. By extending the analysis to include the neutron scattering data of Meir, et al.[5] at 14 MeV and the proton scattering data of Escudie, et al.[6] at 24.5 MeV, both the energy dependence and the isovector terms of the optical model potential could be well established for this light nucleus.

In addition to the evident practical value of neutron cross sections from common materials, the oxygen isotopes provide a unique testing ground for some interesting questions in nuclear theory. The effects of core polarization on the excitation of the first 2^+ state in ^{18}O have been investigated by a variety of methods including electromagnetic transitions in mirror nuclei[7] and inelastic scattering

---

* Work performed under NSF Grant PHY-78-09911

5 D. Meir et al., Helv. Phys. Acta. 42, 813 (1969)

6 J.L. Escudie et al., Phys. Rev. C10, 1645 (1970)

7 Bernstein, Brown and Madsen, Phys. Rev. Lett. 42, 425 (1979)

of $\pi^{\pm}$ mesons in the region of the (3,3) resonance in π-N system.[8] The present results are in excellent agreement with the electromagnetic results but rather poor agreement with any of the four pion experiments. Additional studies will be required before it can be concluded that the various probes are measuring the same aspect of nuclear structure, but it is encouraging to note that the traditional methods of nuclear spectroscopy are in good agreement.

A complete description of this work is being submitted to Nuclear Physics.

4. Differential Elastic and Inelastic Scattering of Neutrons from ^{58,60}Ni at En = 11 and 24 MeV* (Y. Yamanouti**, J. Rapaport, S.M. Grimes†, V. Kulkarni, R.W. Finlay, D. Bainum‡, P. Grabmayr, G. Randers-Pehrson)

Differential cross sections for the scattering of 11 and 24 MeV neutrons from ^{58,60}Ni were measured as part of a continuing study of nucleon scattering from single-closed-shell nuclei. Measurements were taken every 5° from 15° to 150° using the Ohio University time-of-flight spectrometer. Inelastic excitation of the first 2^+ and 3^- states were measured simultaneously with the elastic scattering in each case.

The deuteron beam from the Ohio University Tandem Van de Graaff accelerator was pulsed, bunched ($\sim$ 700 ps FWHM) and focussed onto a single-entrance-foil gas target. The D(d,n)^{3}He reaction was used to produce 11 MeV neutrons, and the ^{3}H(d,n)^{4}He reaction was used for the 24 MeV experiment.

At 11 MeV scattered neutrons were detected in a conventional 18 cm diameter by 5 cm thick liquid scintillation counter, while at 24 MeV the VLD[9] (Very Large Detector) was used to provide higher detection efficiency at no loss in time-of-flight resolution. Otherwise the details of the two experiments (flight path, scattering

---

* Work performed under NSF Grant PHY-78-09911

** JAERI, Tokai-Mura, Naka-Gun, Ibaraki-Ken, JAPAN

† Lawrence Livermore Laboratory, Livermore, California

‡ Emporia State University, Emporia, Kansas

[8] S. Iverson et al., Phys. Rev. Lett. 40, 17 (1978)
S. Iverson et al., Phys. Lett. 82B, 51 (1979)
J. Jensen et al., Phys. Lett. 77B, 359 (1978)
C. Lunke et al., Phys. Lett. 78B, 201 (1978)

[9] Carlson, Finlay and Bainum, Nucl. Instr. Meth. 147, 353 (1977)

samples, normalization, etc.) were essentially the same. At both 11 and 24 MeV the 3^- states are not resolved from nearby states. At this stage in the analysis it is assumed that the contributions from these adjacent states to the "3^- cross section" are small.

A local optical model potential which included both surface and volume absorption was used for the analysis of the 24 MeV elastic neutron scattering data. Initial parameters were chosen from the global optical model of Rapaport, Kulkarni and Finlay[10] and the search code GENOA[11] was used to obtain best fits to the data. Throughout the searches, the parameters of the spin-orbit term in the potential were divided into isoscalar and isovector components, and the two data sets were simultaneously searched to obtain best-fit values of the isovector potential parameters, which were in good agreement with the global results.

The collective model of inelastic scattering was used both in the Distorted Wave and Coupled Channel Born Approximations in order to extract deformation parameters for the strong one-phonon vibrations in each nucleus. One important goal of this program is to investigate the differing contributions of target protons and neutrons to the strong collective excitation, i.e. to determine the isovector deformation parameters. The present results indicate that the nickel isotopes obey the systematics we have found for other closed-shell nuclei.[12,13] For quadrupole vibrations, the experimental ratio $\beta_{pp'}/\beta_{nn'} = 1.21$ for ^{58}Ni and 1.19 for ^{60}Ni is in very good agreement with theoretical models[14] of core polarization. For octupole vibrations, the experimental ratio is close to unity as might be expected.[15]

A more detailed account of this work will appear in the Proceedings of the International Conference on Neutron Cross Sections for Technology, Knoxville 1979.

---

[10] Rapaport, Kulkarni and Finlay, Nucl. Phys. A330, 15 (1979)

[11] F.G. Perey, private communication

[12] Bainum, Finlay, Rapaport, Hadizadeh, Carlson and Comfort, Nucl. Phys. A311, 492 (1978)

[13] Finlay, Rapaport, Brown, Madsen and Comfort, Phys. Lett 84B, 169 (1979)

[14] Madsen, Brown and Anderson, Phys. Rev. C12, 1205 (1975)

[15] Finlay, Hadizadeh, Rapaport and Bainum, Nucl. Phys. (to be published)

B. R-MATRIX ANALYSES

1. R-Matrix Analysis Code Modifications (D. Resler, H. Knox, G. Randers-Pehrson, P. Koehler, R. Lane, R. White*)

The Ohio University R-Matrix Analysis Program, ORMAP, has undergone several modifications during the past year. The code uses the formalism of Lane and Thomas[16] to calculate the elements of the scattering matrix from the R-matrix and then the formalism of Blatt and Biedenharn[17] to calculate the Legendre polynomial expansion coefficients for elastic neutron scattering from the scattering matrices. With this program either the channel coupling scheme or the j-j coupling scheme for angular momentum can be used. Modifications to the code include removal from the main energy loop of both the transformation from j-j to L-S coupling and the computation of the $\bar{Z}$ coefficients.[17] These modifications have resulted in an order of magnitude decrease in the running time of the program.

A second code using the same formalism as the original has been developed which now allows analysis of both neutron elastic scattering and inelastic scattering data to the first two excited states of the target nucleus. The program allows up to fifteen J^{π} values, four angular momentum channels for each J^{π} for each of the three particle channels, five levels of the same J^{π} and ℓ values up to and including 3.

One further modification is currently underway, namely, the addition of charged particle channels to the code. An R-matrix program used in an earlier[18] analysis of charged particle scattering and reaction data for the ^{8}Be system is operational at this laboratory. The best features of this program and the existing ORMAP code will be combined to provide a single code capable of analyzing neutron differential elastic and inelastic scattering data as well as neutron induced charged particle reaction data.

---

* Lawrence Livermore Laboratory, Livermore, California

16 A.M. Lane and R.G. Thomas, Rev. Mod. Phys. 30, 257 (1958)

17 J.M. Blatt and L.C. Biedenharn, Rev. Mod. Phys. 24, 258 (1952)

18 G. Randers-Pehrson, Ph.D. Dissertation, University of Maryland, 1979

2. Studies of the Structure of ^{8}Li via Neutron Elastic and Inelastic Scattering from ^{7}Li (H. Knox, R. Lane)

Using the new version of ORMAP a comprehensive study of the ^{8}Li system has been undertaken. This study includes the R-matrix analysis of all available ^{7}Li + n differential elastic, differential inelastic (Q = -0.478 MeV and Q = -4.63 MeV) and $^{7}Li(n,n'\gamma)^{7}Li$ (Q = -0.478 MeV) data up to 8 MeV incident neutron energy. Prior to this study seven unbound levels in ^{8}Li had been identified below E_x = 9 MeV with spin and parity assignments made for only two of these levels. From the present work, four additional levels have been identified and J^{π} assignments for these and six of the seven previously identified levels in ^{8}Li have been made. The J^{π} assignments made in the present work are in excellent agreement with the cluster model calculations of Stöwe and Zahn.[19] A final report of this work is currently being prapared for publication.

3. Study of ^{12}B Structure via $^{11}B(n,n)^{11}B$ (R. White*, R. Lane, H. Knox)

Using the code, ORMAP, an R-matrix analysis of ^{11}B + n differential elastic scattering data has been completed. Included in the analysis were differential cross section data at 85 incident energies between $2.6 \leq E_n \leq 8$ MeV measured at this laboratory as well as other elastic scattering data at energies as low as E_n = 0.1 MeV. Very good overall fits to the data were obtained over this wide range of energies and this analysis has led to new assignments to states in ^{12}B up to 10.7 MeV excitation energy. A paper describing this work has been accepted for publication in Nuclear Physics.

4. Study of ^{14}C Structure via $^{13}C(n,n)^{13}C$ (R. Lane, R. White*, G. Auchampaugh**, D. Resler, P. Koehler, H. Knox)

The R-matrix fitting of the elastic scattering of neutrons from ^{13}C has just recently been completed and a manuscript for journal publication is now in preparation. Differential elastic scattering cross sections from 1.25 MeV to $\sim$ 6 MeV neutron energy were measured at 9 angles and reported previously[20] together with a preliminary R-matrix

---

* Lawrence Livermore Laboratory, Livermore, California

** Los Alamos Scientific Laboratory, Los Alamos, New Mexico

[19] H. Stöwe and W. Zahn, Nucl. Phys. A289, 317 (1977)

[20] Lane, White, Knox and Auchampaugh, Bull. Am. Phys. Soc. 23, 501 (1978)

analysis. Subsequently a more complete analysis of these data together with total cross section data of Auchampaugh et al.[21] and Cohn et al.[22] down to ∿ 0.1 MeV was made to obtain one consistent interpretation of states of ^{14}C from the neutron separation energy, E_x = 8.177 MeV to E_x ∿ 13 MeV and including the important 0^- and 1^- bound states contributing strongly to the nonresonant cross section below $E_n \simeq$ 1 MeV. The broad 1^- and 2^- states deduced from this analysis can be readily understood in terms of coupling of $1d_{5/2}$, $1d_{3/2}$, and $2s_{1/2}$ incoming neutrons to the simplest configuration possible for the ground state of ^{13}C, i.e. a $1P_{1/2}$ neutron coupled to a closed ^{12}C core. However, the 1^+ state at E_x = 11.3 is a rather unique state in ^{14}C in that it is the lowest (and so far the only) observed 1^+ state in ^{14}C and can be produced by only a very limited number of configurations. Our R-matrix analysis shows clearly substantial contributions of both $p_{1/2}$ and $p_{3/2}$ neutron amplitudes for coupling to the ground state of ^{13}C. This bears on the model calculations for ^{14}C and in particular on the degree of openness of the ^{12}C core. Contacts with theorists active in this area such as John Millener and Frederica Darema-Rogers of Brookhaven and Michael Micklinghoff of Germany are being pursued.

C. TRIPLET QUADRUPOLE SPECTROMETER

1. Charged Particle Emitted in the Neutron Bombardment of Deuterium* (V. Kulkarni, S.M. Grimes**, J. Rapaport, R.W. Finlay, P. Grabmayr, G. Randers-Pehrson)

Neutron induced break-up of deuteron D(n,p)2n was investigated at En = 11 and 25 MeV, using the recently constructed Quadrupole Triplet Spectrometer at Ohio University. Deuterated polyethlene target was used. Proton spectra with good energy resolution were measured near $\theta p = 0°$ in laboratory to study that kinematical region of the three-body final state. Differential cross sections have been obtained and theoretical calculation using Faddeev three-body formalism is in progress.

---

* Work performed under NSF Grant PHY-78-09911

** Lawrence Livermore Laboratory, Livermore, California

21 Auchampaugh, Plottard, Extermann and Ragan III, Nucl. Sci, Eng. 69, 30 (1979)

22 Cohn, Bair and Willard, Phys. Rev. 122, 534 (1961)

Neutron-deuteron elastic scattering D(n,d)n was also studied using the spectrometer. Deuteron angular distribution was measured from $\Theta d = 0^\circ$ to 45° in 5° steps in laboratory at En = 9 MeV and from 0° to 55° at En = 11 MeV. The cross sections will be compared with the predictions of the three-body calculation.

2. Proton Spectra from ^{58}Ni(n,p) (G. Randers-Pehrson, P. Grabmayr, V. Kulkarni, R. Finlay, J. Rapaport)

Measurements of ^{58}Ni(n,p) have been made at three angles each for 8 and 11 MeV neutrons. These data confirm that the reaction ^{58}Ni(n,n')^{58}Ni*(p) (involving excited states of ^{58}Ni which are below the neutron separation energy) is responsible for the excess of low energy neutrons present at 15 (ref. 23) and 11 MeV because that channel is closed at 8 MeV.

3. Development

a. Software (G. Randers-Pehrson, P. Grabmayr, V. Kulkarni, J. O'Donnell, D. Carter)

An interrupt service routine was written for the OUAL-16K mini-computer to reduce three parameter input data to useful one-dimensional arrays. The energy sum from a detector telescope and the particle time-of-flight are used to calculate $E * \Delta t^2$ which is proportional to mass. We obtain resolution of $\Delta M/M \approx 1/10$ which is useful not only to separate the real events from each other, but for background supression. Digital gates are used to route the energy sum signal to separate arrays for each mass number.

All sprectra from each run are stored on disk by our IBM 1800. Copies are later transmitted over a data link to the University computer center for off-line analysis. The off-line analysis program, which was also completed this year, determines the energy-dependent solid angle and normalization based on measurements of proton spectra from thick polyethylene and thus calculates the doubly-differential cross sections.

---

[23] Grimes, Haight, Alvar, Barschall and Borcheus, Phys. Rev. C19, 2127 (1979)

b. Hardware (G. Randers-Pehrson, P. Grabmayr, V. Kulkarni, S.M. Grimes*)

Since the completion of the spectrometer last year, we have spent a great deal of effort locating and correcting conditions which could potentially distort our data. Such items are installation of means to locate the target ladder precisely and carefully leveling the floor to prevent changes in the magnet focus due to bending the support frame. We have also upgraded the vacuum system to protect our intrinsic germanium detectors and improve the shadow bars.

We have nearly completed construction of a carbon foil plus channel plate device to extend our measurements to lower energies. (We are presently limited to 1.5 MeV protons due to a 30 μm silicon ΔE detector.)

---

* Lawrence Livermore Laboratory, Livermore, California

UNIVERSITY OF PENNSYLVANIA

A. COMPLETED WORK

1. "Energy Levels of Light Nuclei: A = 5-10."

This paper has been published in Nuclear Physics A320 (1979) p. 1-224.

F. Ajzenberg-Selove (and C. L. Busch)

2. "Energy Levels of Light Nuclei: A = 11-12."

This paper will shortly be published in Nuclear Physics A336 (1980) p. 1-154.

F. Ajzenberg-Selove and C. L. Busch

B. WORK IN PROGRESS

A review paper on A = 13-15 is being prepared, to be submitted for publication in September 1980. The first preprint, a preliminary review of A = 13, will be sent out for comments in March 1980. Our work is proceeding on schedule.

F. Ajzenberg-Selove (and E. K. Loomis)

RENSSELAER POLYTECHNIC INSTITUTE

A. NUCLEAR DATA

1. Fission Cross Section Measurements of the Even Curium Isotopes

(H.T. Maguire, Jr., C. Stopa, R.C. Block, J.W.T. Dabbs (ORNL) and R.W. Hoff (LLL))

The neutron-induced fission cross section of ^{244}Cm, ^{246}Cm, and ^{248}Cm from approximately leV to 100eV will be measured using the RINS (Rensselaer Intense Neutron Spectrometer) 75-ton lead slowing down spectrometer. The intense neutron flux obtained with RINS will enable the neutron-induced fission to be comparable to or exceed spontaneous-fission background. The high intensity neutron flux will permit the measurement with only about five microgram quantities of each curium sample. These samples will be prepared at the Nuclear Chemistry Division at Lawrence Livermore Laboratories. A sample of ^{235}U will be prepared at RPI, and its fission cross section will be measured simultaneously with the curium isotopes. The fission cross section of the curium isotope will be normalized to the ^{235}U fission cross section.

The fission chamber design follows that of Dabbs et al.[1] with modifications to accomodate the isotropic neutron flux of RINS. The fission plates (five plate pairs) will be supplied by ORNL. These plate pairs are concentric hemispheres with each sample deposited on about a 4-mm-dia. spot on the inner hemisphere. The plates are held in place by a series of stainless-steel rods with aluminum spacers and teflon insulators. The assembly is contained in an aluminum chamber filled with two atmospheres of pure methane gas. The chamber is now being constructed.

2. Neutron Capture Cross Section of ^{232}Th Below 10eV

(R.L. Little, D.R. Harris and R.C. Block)

The neutron capture cross section of ^{232}Th has been measured at RPI in the energy range .008 $\sim$10eV. Results have been found which differ from previous measurements [1,2] and evaluations [3].

^{232}Th is a radioactive isotope which causes a large natural background from gamma rays emitted by various daughter products. To perform this experiment, it was necessary to carry out a chemical separation to remove the "bothersome" daughter products. The separation procedure

---

[1] Dabbs, Hill, Bemis and Raman, Proc. Conf. on Nucl. Cross Sections and Technol., NBS Spec. Publ. 425, Vol. I, p 81 (1975).

used gave excellent results as the background from radioactive decay was reduced approximately two orders of magnitude. The thorium used for capture measurements was in the form of ThO_2.

Using the 100-MeV electron linear accelerator and the time-of-flight method, a preliminary capture yield was found by measuring capture events in the ^{232}Th inside a 1.25-m-dia. liquid scintillator relative to neutron events in a "black" (for this energy range) $^{10}B_4C$-NaI detector. Results for a preliminary capture yield have been determined from 0.008 eV to 10eV. To convert this preliminary capture yield to the capture cross section, corrections must be made for multiple scattering and self-shielding, and the data will be normalized to the known thermal capture cross section. The RPI results indicate a 1/v capture cross section from 0.1 ∿1.0eV. The departure from 1/v is smaller than has been previously reported[1,2]. The preliminary capture yield also indicates a capture cross section which increases with energy less rapidly than 1/v for neutron energies below ∿0.1eV. Although the mechanism causing this departure from 1/v below ∿0.1eV is not well understood at this time, possible crystal interference patterns in the results have indicated the need for further understanding of molecular and crystal effects in this energy range where the wavelength of the neutron is comparable to the crystal lattice spacing and the neutron energy is less than the atomic binding energy. It is felt that the mechanism causing the departure below 0.1eV will not affect the results at higher energies.

B. INTEGRAL MEASUREMENTS

1. Neutron Spectra Measurements Upon a Spherical Assembly of Thoria

(R.C. Block, M. Becker, D.R. Harris, B.K. Malaviya, S.A. Bokharee,* R.W. Emmett, P.S. Feigenbaum, S.H. Levinson, H.T. Maguire, Jr., (RPI) and S.A. Hayashi, S. Yamamoto (KUR))

A cooperative research program between the Kyoto University Research Reactor Institute (KUR) and the Gaerttner Linac Laboratory at RPI has carried out neutron spectra measurements upon a thoria assembly. The assembly consists of 300 kg of thoria contained in a 0.6-m-dia. stainless steel sphere and is the same assembly reported by Nishihara

---

[1] G. Lundgren, Nukleonik, 11, p 51 (1968).

[2] Chrien,Liou, Kenny, Stelt, Nucl. Sci. Eng., 72, p 202 (1979).

[3] ENDF/B-V, National Nuclear Data Center, Brookhaven National Laboratory, Upton, New York.

* Now at United Engineers & Contractors, Inc., Philadelphia, Pa.

et al.[1] A 1-kw air-cooled spheroidal Ta photoneutron target was developed for use with this assembly. Neutron spectra measurements have been carried out from approximately 1 keV to 15 MeV at radii of 15 and 20 cm with angles of 90^o and 130^o respectively. The high-energy spectra were obtained with a 40-cm-dia.-by-12.5-cm-thick proton recoil detector at 100 meters, and the low-energy spectra were obtained with the 30-cm-dia.-by-5-cm-thick ^{10}B-Vaseline-plus-NaI detector at 32 meters. In order to compare with experiment, spectra are being calculated with the DTF-IV one-dimensional transport code with ENDF/B-V data.

A set of intercomparison DTF-IV calculations with ENDF/B-IV data will be carried out at KUR and RPI to ensure that the codes and data processing are the same at both laboratories.

C. SAFEGUARDS AND FISSILE ASSAY

1. The Applicability of the Lead Slowing Down Spectrometer for Non-Destructive Assay of Commercial-Size Fuel Elements
(F.W. Bornt, Jr., D.R. Harris and R.C. Block)

As the use of nuclear power increases, so will the amounts of fissionable material (^{235}U and ^{239}Pu in particular) increase. This will require improved non-destructive assay (NDA) methods for both fresh and spent fuel which must be able to determine accurately how much and what kind of fissionable material is in the pin or assembly, and must also be relatively tamper-proof. The Lead Slowing Down Spectrometer (LSDS), able to meet these conditions, has been used in the past to assay single fresh fuel pins (Karlsruhe)[1], but no one has ever, to our knowledge, used it for spent fuel assemblies.

At the RPI Gaerttner LINAC Laboratory, there is a 75-ton LSDS which was built as part of a program to develop a system that can assay single spent fuel pins from the Shippingport LWR breeder experiments. Used with a 100-MeV electron linear accelerator, this system produces $\sim 10^{12}$n/sec in 60-nsec bursts at a repetition rate of 400 pps. Based on experiments with single breeder mock-up (BMU) pins, assay accuracies of better than 0.5% are obtained for 50 pins/day and (with appropriate sampling) 0.2% for the E.O.L. core inventory[2]. Again, this is for single spent fuel pins.

We are trying to determine analytically what effect a full size, 17 x 17 commercial PWR assembly would have on this system. Among these

---

[1] Nishihara, et al., J. of Nucl. Sci. and Tech. 14, 426 (1977).

effects are the self-shielding of the inner pins of the assembly by the outer pins as well as the effect of UO_2-Zr "sponge" and are using the 16-group Hansen Roach Cross Sections for a multigroup, multiregion transport calculation. After studying these results and improving our understanding of the effect the fuel has on the LSDS system, we will account for the heterogeneity in the assembly in the next generation computer code.

[1] H. Krinninger, E. Ruppert and M. Siefkes, Nucl. Instr. and Meth. <u>117</u>, (1974).

[2] Private Communication with Dr. R.E. Slovacek.

A. NEUTRON CROSS SECTION EXPERIMENTS

1. Neutron Time of Flight Program - General Status (A. Beyerle, S. G. Glendinning, C. R. Gould, H. H. Hogue,* Sadiq El Kadi, C. E. Nelson, R. Pedroni, F. O. Purser, L. W. Seagondollar, P. Thambidurai, R. L. Walter)

For the last five years TUNL has been involved in an extensive program of neutron elastic and inelastic scattering cross section measurements in support of the U. S. fusion energy program. The measurements were primarily undertaken to address the high priority medium and long range differential nuclear data needs of the Office of Fusion Energy. However, the information gained is also of fundamental interest in terms of optical model parameterizations of nucleon scattering, studies of isospin dependence in nucleon scattering, nuclear level density measurements and studies of pre-equilibrium emission processes.

The early work at TUNL concentrated on measurements of elastic and discrete inelastic neutron scattering cross sections from p-shell nuclei (Li, Be, B, C, O) in the 8 to 15 MeV bombarding energy region. This work was performed with the $D(d,n)^3He$ source reaction and is now essentially completed. Results for Li, B and O scattering are summarized below.

The main thrust of the present program is toward measurements of continuum neutron emission spectra from medium and heavy mass nuclei. This work necessitated installation of a tritium gas target capability, development and calibration of two neutron detection systems operating at low neutron threshold energy (~300 keV) and development of codes for acquiring and correcting continuum neutron scattering data. Progress in these areas and our first experimental results for Fe, Cu, Ni and Pb are discussed below. In support of these continuum measurements we have also undertaken discrete scattering studies with separated ^{54}Fe, ^{56}Fe, ^{63}Cu and ^{65}Cu samples. Much of this current work was reported at the Conference on Nuclear Cross Sections for Technology held at Knoxville in Oct. 22-26 this year and will appear in the Proceedings.

The coordination meeting of representatives of the laboratories currently participating in the Office of Basic Energy Sciences nuclear data procurement program was held in March of this year at TUNL. The progress towards satisfying the nuclear data needs of the fusion energy program was discussed, and plans for future work were outlined by the participating laboratories. This was the second review meeting, the first having been held in Oak Ridge in 1976. The meeting was coordinated by F. Perey and included representatives from Brookhaven, Rockwell, Argonne, Livermore, Hanford, Oak Ridge, Los Alamos, DOE, TUNL and Ohio.

---

*Y-12 plant, Oak Ridge, Tennessee

2. Summary of Recent Facility Improvements

Neutrons for the TOF facilities are produced by bombardment of gas targets by protons or deuterons. Negative hydrogen ions are produced in a direct extraction negative ion source (DENIS II--see Cyclo-Graaff Laboratory layout). The ions are accelerated by the FN tandem electrostatic generator and then deflected 38° into the time-of-flight area. This beam leg extends 25 m and terminates in either a deuterium or tritium gas target. The beam leg contains appropriate valves, focussing lenses, beam-defining slits and vacuum systems. Almost all gaskets are indium. The vacuum systems are part of an over-all safety system that is needed when tritium gas is used in order to prevent unacceptable contamination of personnel and/or equipment.[1]

The cross-section of the tritium target is shown in Fig. A2-1. The

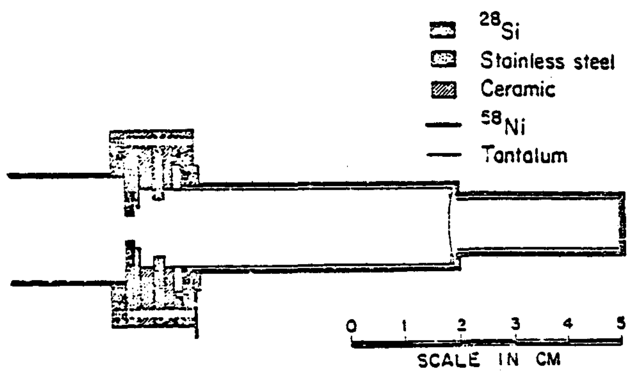

Fig. A2-1. Cross section of the TUNL gas target. The curved foil is 3.5 μm molybdenum. Gas enters cell through tube at bottom of drawing.

tritium, usually at about 2 atm absolute pressure, is separated from the vacuum in the beam leg by foils of about 3.5 μm thickness. In accord with the measurements of Drosg et al.,[2] a ^{28}Si collimator and a ^{58}Ni beam stop are used. The gas filling system for the tritium target permits evacuation of the target to fore-vacuum pressure, filling with helium gas, and filling with tritium. The tritium reservoir is a uranium furnace which can be heated electrically to furnish tritium up to 2 atm absolute pressure. A liquid-nitrogen cooled, activated charcoal trap can also be used to store additional tritium which can be released subsequently to the target if higher pressures are desired. Originally the tritium gas pressure was determined during filling by a small Bourdon gauge and the gauge was monitored by closed circuit television during runs. This gauge has been replaced by a silicon pressure transducer (National

[1] See Triangle Universities Nuclear Laboratory Progress Report for 1977 (TUNL XVI).
[2] M. Drosg and C. F. Auchambaugh, Nuc. Inst. and Meth., 140 (1977) 515

Semiconductor Device LX1704GB). The gas volume of this device is less than that of the Bourdon gauge. Also, instead of having a visual indicator, it puts out a small dc voltage proportional to the absolute pressure. Fig. A2-2 shows the linearity of the

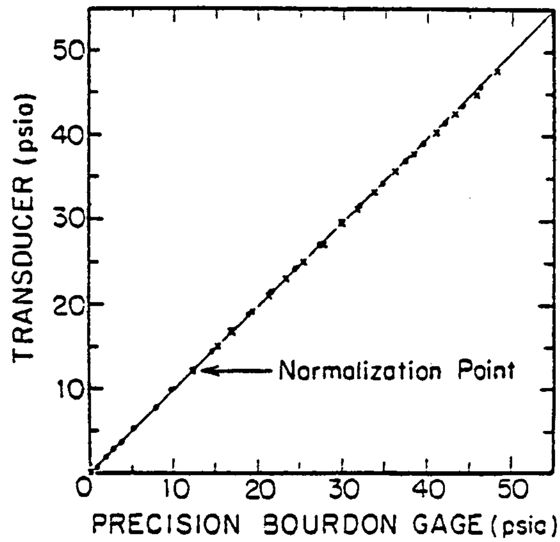

Fig. A2-2. Calibration of silicon pressure transducer against a precision Bourdon gage. The normalization point was 1 atm -- 14.4 psia on both gages.

device as determined by comparison with a precision Bourdon gauge (Wallace and Tieman, Series 1000 Dial Instrument). The dc voltage is used as input to a digital voltmeter near the filling system, another digital voltmeter in the control room and also, in the control room, a strip chart recorder and a D'Arsonval meter containing adjustable upper and lower limit controls. The strip chart recorder gives us continuous "written" record of the target pressure during a run; a particularly informative record if a target foil begins to fail. The limit controls set off an audible alarm if the target pressure varies beyond the adjustable limits. The transducer system has only been used on one 5-day run to date and it functioned as expected. Two worries existed about the system; (a) the hot tritium gas from the furnace might raise the temperature of the transducer above its maximum design operating temperature, and (b) radiation damage might occur. Built into the transducer is a lead which gives voltage variations with temperature variations--2 to 4 mv/°C. As the target was filled, this voltage variation was observed with a separate digital voltmeter. The tritium target was filled several times during the run. In each case, the temperature rise of the transducer was less than 10°C. Also, the pressure readings of the transducer were compared over a wide range of pressures to that of a small Bourdon gauge still in the filling system before and after the run. There is no indication of radiation damage to the transducer. However, since this run was a particularly low current run, a radiation shield will be installed between the transducer and the neutron target before the next run.

Neutrons are detected at this facility by four liquid scintillators. Two of them are used as monitors. One monitor is mounted overhead at a distance of 2 m from the target and an angle of 60° above the beam line. It is in a 350 kg copper shield with a straight aperture directed towards the neutron target. The other monitor has no shield, is portable, and is usually placed at about 4 m from the target along the 0° line. The other two detectors are in massive shields and are used to measure angular distributions of scattered neutrons. Each of them is on its own steel cart which pivots along a line directly below the axis of the scattering samples. Each detector can be located by convenient electric drive at any angle between 0° and 155° from the beam line with a precision of about 0.1°. One detector and its shield has been described[1] earlier. That unit can be moved radially for flight paths of 2.7 m to almost 4 m. The other shielded detector is similar to the first except: (a) it uses a larger scintillator (12.5 cm-diameter, 5 cm-thick), (b) the shield has about 30 cm more material in back of the detector to further reduce background neutrons scattered from the laboratory walls, and (c) the path can be changed from 2.7 m to almost 6 m. Both detectors are used simultaneously. Fig. A2-3 shows a cross-section of the second detector and its shield.

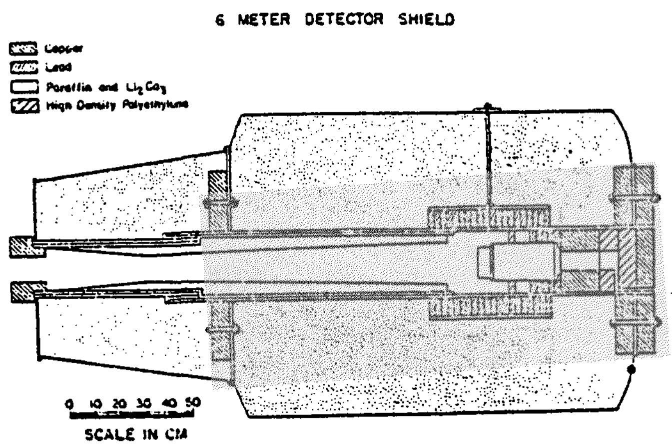

Fig. A2-3. Cross section of the new detector and shield.

---

[1] Glasgow et al., Nat. Bur. Stand. (U.S.) Spec. Publ. 425, 1, 99 (1975)

3. Elastic and Inelastic Scattering of 7- to 14-MeV Neutrons from ^{6}Li and ^{7}Li

This work has been published in Nucl. Sci. and Eng. 69 (1979) 22. The abstract appears below:

"Differential cross sections are reported for the elastic and discrete inelastic scattering of neutrons from ^{6}Li and ^{7}Li. Source neutrons were provided by the $^2H(d,n)^3He$ reaction in the energy range 7 to 14 MeV. Scattered neutrons were detected at a distance of 3.9 m at angles from 25° to 160° in 5° intervals. Total cross sections were obtained for elastic scattering from ^{6}Li and for the sum of elastic and 0.478-MeV state inelastic scattering from ^{7}Li. Inelastic scattering cross sections were obtained for the 2.18-MeV state in ^{6}Li and the 4.63-MeV state in ^{7}Li. The results are compared to ENDF/B-IV predictions and to previous measurements. Inelastic scattering to the 4.63-MeV state in ^{7}Li accounts for less than half of the total tritium production cross section for neutron interactions with ^{7}Li."

4. Elastic Scattering of 8-14 MeV Neutrons from ^{10}B, ^{11}B and ^{16}O

a. Boron Data

Boron data described in earlier reports (TUNL XVII) have been studied using a spherical optical model. Our $^{10}B(n,n)^{10}B$ data when combined with the $^{10}B(p,p)^{10}B$ data of Watson (1969) provide an opportunity to examine the isospin dependence of the model for T(target) = 0. That this dependence should take the form of a correction to the incident energy of the projectile was suggested by Rapaport (1976). An empirical value for this energy correction was calculated by the program GENOA, which fit all the angular distributions for both incident neutrons and protons simultaneously. Our results show an energy reduction of 4.6 ± 1.4 MeV for incident protons as compared with neutrons. The value for the Coulomb correction term in the real well depth would then be $0.66 * Z/(A^{1/3})$.

The ^{11}B data were also included in a search to find a set of global optical model parameters for boron data between 8 and 14 MeV. Our previously reported ^{11}B data were used. Angular distributions which were very near two sharp resonances in the ^{11}B total neutron cross section were omitted from the search. The results of these searches are presented in Table A4-1 and in Figs. A4-1, A4-2, and A4-3.

The ^{11}B data were also suitable for analysis using the coupled-channels optical model of Tamura. In this method, the inelastic data for the state at 4.44 MeV (5/2-) were predicted by assuming that ^{11}B is a permanently deformed nucleus with a quadrupole deformation parameter of 0.037 b. The values for the other

TABLE A4-I

Optical Model Parameters for ^{10}B and ^{11}B

Parameter	^{10}B Data	^{11}B Data	Both Isotopes
V_o (MeV)	48.1 - 0.3 Ecm	45.7 - 0.005 Ecm	45.8 - 0.06 Ecm
r_o (fm)	1.34	1.40	1.37
a_o (fm)	0.55	0.35	0.49
W_d (MeV)	0.16 - 0.78 Ecm	-6.27 + 1.13 Ecm	0.05 + 0.78 Ecm
r_i (fm)	1.41	1.10	1.31
a_i (fm)	0.34	0.50	0.33
V_{so} (MeV)	5.5	5.5	5.5
r_{so} (fm)	1.15	1.15	1.15
a_{so} (fm)	0.57	0.57	0.57
V_c (MeV)	0.66	-	0.66
V_s (MeV)	-	-	24.5
W_s (MeV)	-	-	11.5

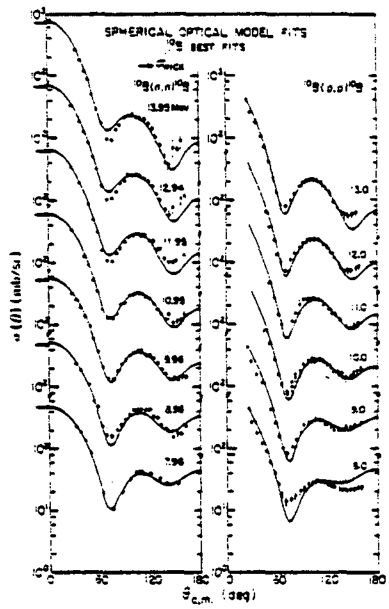

Fig. A4-1. Optical model fits to ^{10}B elastic scattering data.

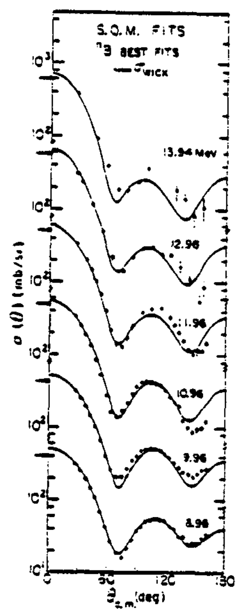

Fig. A4-2. Optical model fits to ^{11}B elastic scattering data.

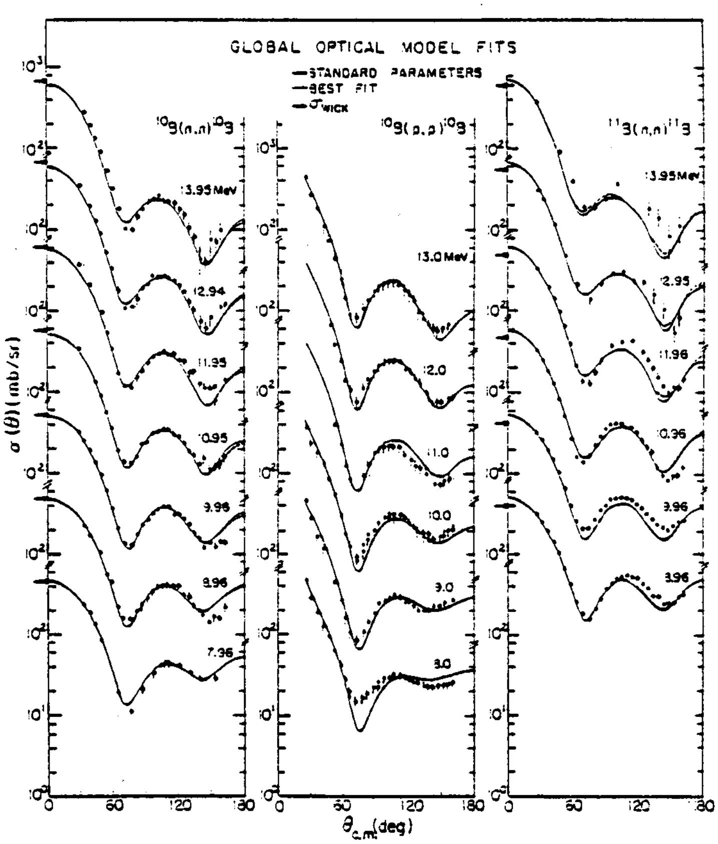

Fig. A4-3. Global optical model fits to ^{10}B and ^{11}B elastic scattering data.

optical model parameters which gave the best fits to the elastic data are shown in Table A4-2 and the fits are shown in Fig. A4-4. The program JUPITOR (Karlsruhe version) was used to perform the calculations.

TABLE A4-2

Coupled - Channels Optical Model Parameters for ^{11}B

Parameter	Coupled - channels Value	S.O.M. Value
V_o (MeV)	71.86 - 2.91 Ecm	45.7 - 0.005 Ecm
r_o (fm)	1.40	1.40
a_o (fm)	0.35	0.35
W_d (MeV)	-3.74 + 0.58 Ecm	-6.27 + 1.13 Ecm
r_i (fm)	1.22	1.11
a_i (fm)	0.35	0.50
V_{so} (MeV)	5.5	5.5
r_{so} (fm)	1.15	1.15
a_{so} (fm)	0.57	0.57
(b)	0.037	

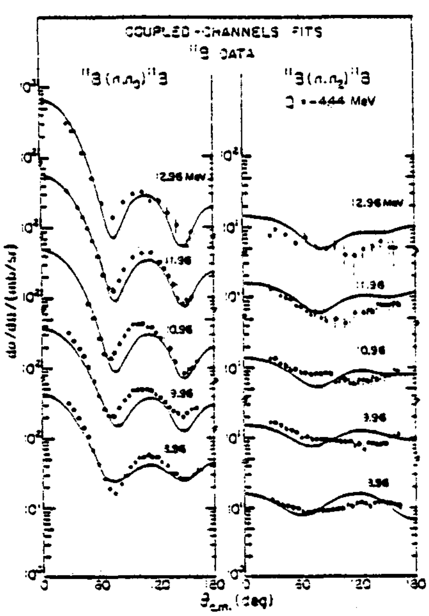

Fig. A4-4. Coupled-Channels optical model fits to ^{11}B data.

b. ^{16}O Data

The $^{16}O(n,n)^{16}O$ data reported earlier have also been studied using a spherical optical model, modified to include the presence of resonances. Background optical model parameters were obtained using the program GENOA to fit angular distributions at 9.21, 10.71, 12.94 and 13.94 MeV which were near minima in the total cross sections. Resonances at Elab = 10.13, 11.15 and 11.54 MeV were included, and tentative assignments of $J^{\pi} = 7/2^{-}, 7/2^{-}$ and $5/2^{+}$ were chosen. Results of these calculations are shown in Table A4-3 and Figs. A4-5 and A4-6.

TABLE A4-3

Optical Model and Resonance Parameters for ^{16}O

Optical Model Parameter	Value		
V_o (MeV)	65.8 - 1.52 Ecm		
r_o (fm)	1.27		
a_o (fm)	0.51		
W_d (MeV)	-0.64 + 0.80 Ecm		
r_i (fm)	1.45		
a_i (fm)	0.24		
V_{so} (MeV)	5.5		
r_{so} (fm)	1.15		
a_{so} (fm)	0.55		
Resonance energy (com)			J
9.51	0.40	0.10	(7/2)-
10.50	0.34	0.14	(5/2)-
10.80	0.18	0.06	(5/2)+

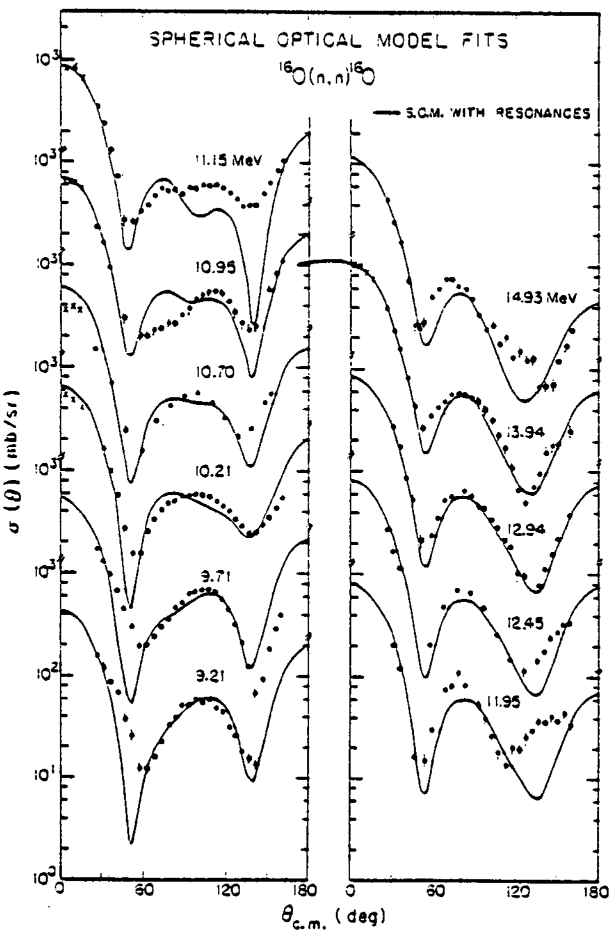

Fig. A4-5. Spherical optical model fits to $^{16}O(n,n)^{16}O$ data.

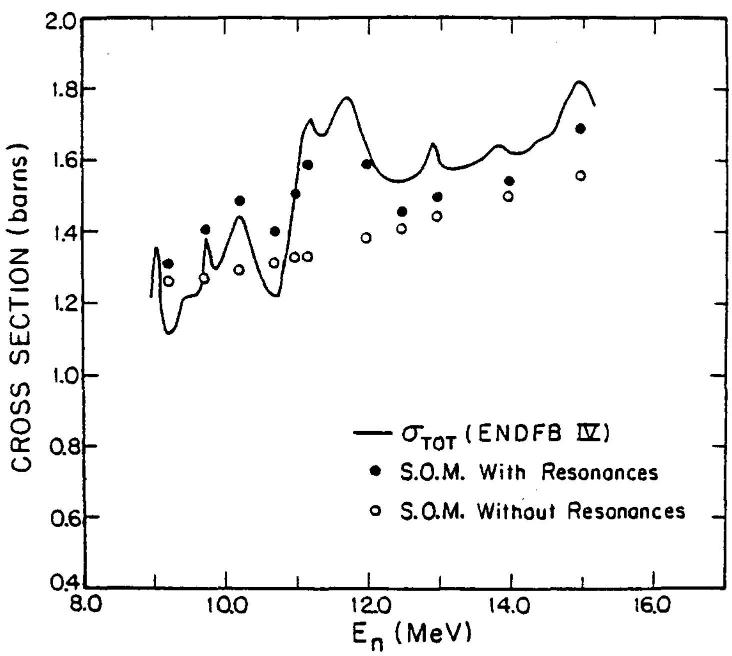

Fig. A4-6. Total cross section predictions for ^{16}O. The circles represent calculations from the S.O.M. background parameters and the dots are ANSPEC calculations.

5. Double Differential Neutron Scattering Cross Sections for Fe, Cu, Ni and Pb between 8 and 12 MeV

In order to complement theoretical predictions of neutron emission cross sections, we have undertaken a program of (n,n') measurements on medium mass to heavy nuclei, with particular emphasis on inelastic scattering to the continuum region. Our first experiments concentrated on neutron emission spectra measurements for natural iron, nickel, copper and lead following 7.5-MeV, 10- and 12-MeV neutron bombardment. Here we review our progress in converting the data to absolute double differential inelastic scattering cross sections.

The proton or deuteron beams were pulsed and bunched into about 2 ns bursts at a repetition rate of 1 MH_Z with typical beam currents on target of 1.5 μA. The neutron flight paths were 2.76 and 3.73 m respectively for the two detectors, permitting detection of neutrons below 300 keV in energy without overlap from previous beam bursts. The neutron detectors were biased near the pulse height minimum between the 26- and 59-keV γ rays from our ^{241}Am source, corresponding to a threshold neutron energy of ~300 keV. The detection efficiency of the scintillators was measured in separate experiments from threshold to ~20 MeV.

The data at 7.5 MeV were taken with the ^{2}H(d,n) reaction. This corresponds to a deuteron energy which is below threshold for deuterium gas breakup and therefore this neutron source is strictly monoenergetic apart from ^{2}H breakup in the cell and entrance foil. At higher energies the D+d gas breakup cross section relative to the monoenergetic cross section rises more rapidly than for the ^{3}H(p,n) reaction. The ^{3}H(p,n) source is a factor of 3 better in this respect than the ^{2}H(d,n) reaction. Therefore, the 10- and 12-MeV data were taken with the ^{3}H(p,n) reaction. Background neutrons from (p,n) reactions in the cell material and beam stop are also present but, as in the case of the D+d experiment, can be taken into account by performing a gas-out measurement. These background contributions were large for the T+p experiments, even with the use of a ^{58}Ni beam dump. For the D+d experiments a tantalum beam dump was used and the backgrounds were much lower. The entrance foil in all experiments was of 3.5 μm molybdenum.

At 7.5 MeV the samples were in the form of small solid cylinders 3.0 cm high and 2.0 cm in diameter. At 10 and 12 MeV hollow cylindrical samples were used of height 4.5 cm, 3.0 cm outside diameter and 1.3 cm inside diameter.

Neutron angular distributions were typically measured at five angles from 40° to 145° at each energy. At each angle four TOF spectra were accumulated. These corresponded to (1) gas in, sample in, (2) gas out, sample in, (3) gas in, sample out, (4) gas out, sample out. Here "gas in" refers to deuterium or tritium gas in the cell. "Gas out" refers to the hydrogen isotope having been removed and replaced by an equal pressure of helium. This simulates energy loss effects. These four spectra were normalized to the integrated charged particle beam on target. Fig. A5-1 shows TOF spectra for the scattering of 10-MeV neutrons from iron at 100°. The neutron elastic scattering peak is visible in about channel 700 only in spectrum 1. The sample out backgrounds in spectra 3 and 4 are relatively flat. The contribution of the (p,n) background in spectrum 2 is structured because of resonances in the elastic scattering cross section of iron. The background associated with (p,n) reactions in the cell material is eliminated by forming the difference (1-3)-(2-4). This is the final TOF spectrum and is shown in Fig. A5-2. Most of the structure between channels 400 and

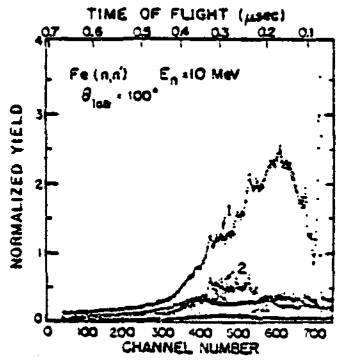

Fig. A5-1. Four neutron scattering spectra.
1) Tritium in cell, sample in place
2) Helium in cell, sample in place
3) Tritium in cell, sample removed
4) Helium in cell, sample removed

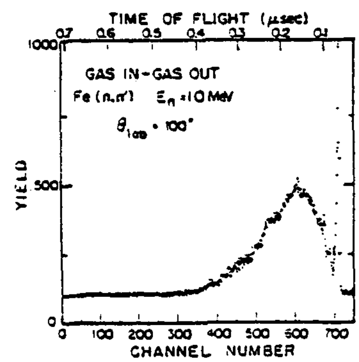

Fig. A5-2. Difference spectrum from Fig. A5-1 (1-3)-(2-4). This spectrum is biased by 100 counts.

550 is removed and the final spectrum is relatively smooth. Scattering of tritium-gas breakup neutrons is still present in this spectrum and is not removed by subtracting the "gas out" spectra. The contribution of these neutrons to the continuum yield is taken into account later in the analysis.

The final time of flight spectra are transformed to energy spectra, folding in the detector efficiency. Figure A5-3 shows energy spectra for iron, nickel, copper and lead scattering at 125° for an incident neutron energy of 12 MeV. These spectra are arbitrarily normalized and are not corrected for attenuation effects or for multiple scattering. The fluctuations below ~2 MeV for the iron and nickel data at 12 MeV are an artifact of the data due to a slight energy shift between the gas-in and gas-out runs. There is some evidence for collective enhancement in the region of the 3^- states of the even-even nuclei.

Fig. A5-4 shows the angular distributions for the scattering of 10-MeV neutrons from iron. The spectral shapes are almost identical apart from the effects of the highly anisotropic elastic scattering peak.

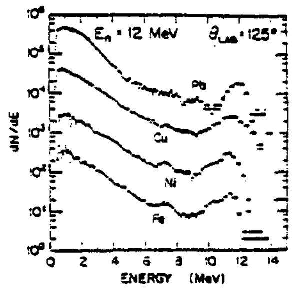

Fig. A5-3. Energy spectra for neutron scattering from Fe, Ni, Cu, Pb at 125° for an incident neutron energy of 12 MeV. The vertical scale is arbitrarily normalized and is in counts per 20 keV energy internal.

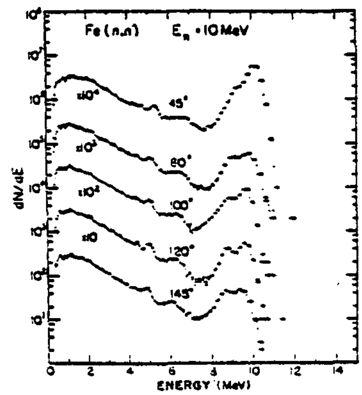

Fig. A5-4. As Fig. A5-3 except Fe scattering at 10 MeV for five different laboratory scattering angles.

6. Multiple Scattering Corrections

Work has continued on development of the Monte Carlo programs for the correction of neutron scattering data. Aimed at producing a realistic simulation of the time-of-flight experiment and data reduction conditions, EFFIGY and EFFIGYC include the effects of finite volume of the neutron production sites, the scattering sample, and the detector, as well as non-zero time and energy resolution. Multiple scattering and attenuation are also calculated. Included are capabilities for multi-element samples of hollow cylindrical shape. Kinematics are calculated to allow for energy loss in light elements and cross section searches have been speeded up. The simulation procedure is outlined in Fig. A6-1. During the past year work to make the programs nearly identical to the user and to simplify operation has neared completion. A detailed description of both codes and their operation should be ready early in 1980.

EFFIGY calculates corrections to angular distributions of up to ten discrete groups. Time-of-flight spectra are generated and windows summed to derive "experimental" angular distributions which are compared to the measured values. Cross section tables are updated and the procedure is repeated iteratively until agreement between experiment and calculation are obtained. For multi-element samples, effects of known cross sections may be removed from the calculation to obtain single element cross sections where levels overlap. An example of the results of these processes is shown in Fig. A6-2 for ^{11}B elastic scattering data. This code has had no major revision in the simulation process for the period of this report and has been used to correct the data for the discrete scattering program.

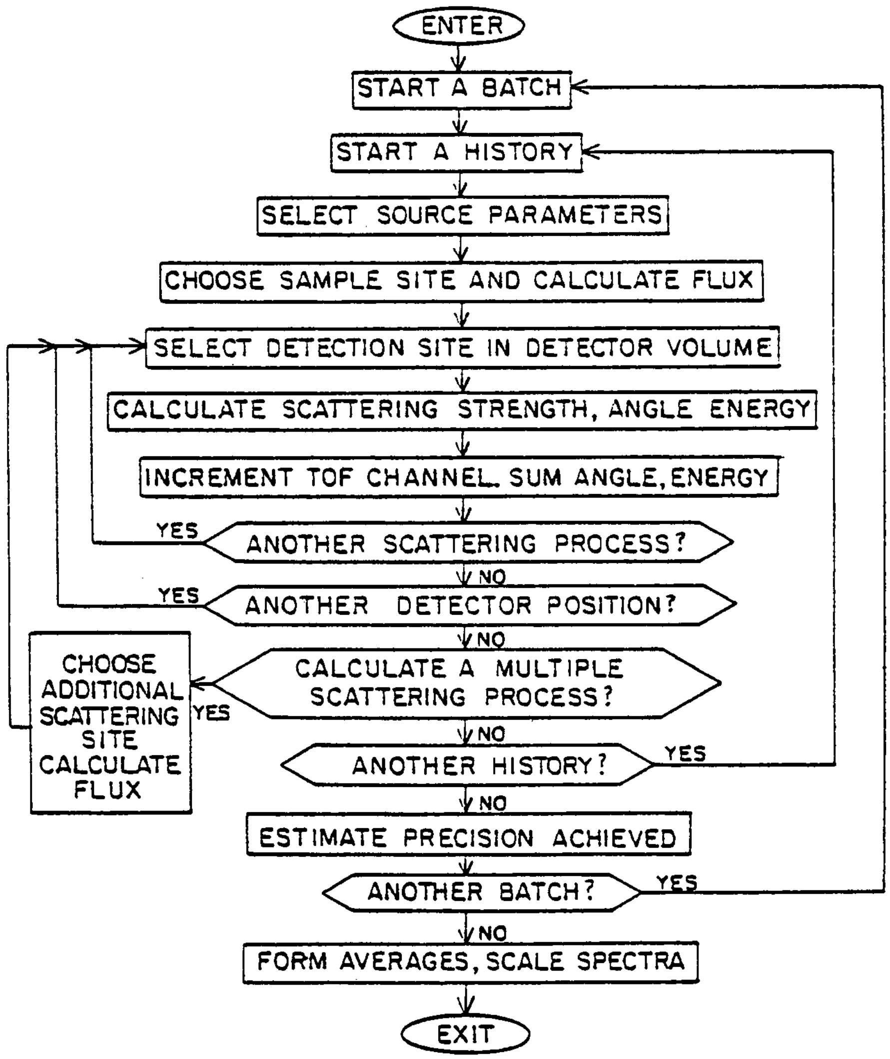

Fig. A6-1. Simulation procedure in multiple-scattering correction code.

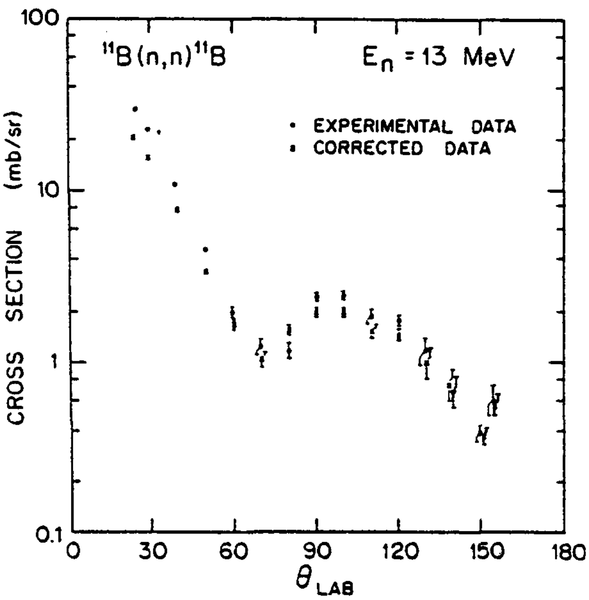

Fig. A6-2. EFFIGYC calculation of time-of-flight spectra compared to experimental spectra for E_n=12 MeV.

EFFIGYC calculates corrections to the energy distributions of continuous neutron emission spectra, including effects of up to ten continuum and discrete processes. Cross sections for 1 unknown continuum process are updated and the effects of 1 known continuum process and up to nine discrete processes may be removed. Any of these processes may overlap the continuum. For source distributions which are not monoenergetic, EFFIGYC calculates the effects of gas breakups and removes this from the cross section. Time-of-flight spectra for up to five angles are compared to experiment and the cross sections tables are updated. EFFIGYC iterates until the calculation agrees with experiment. Fig. A6-3 shows the results of such a calculation. The data are the circles and the line is the result of the calculation.

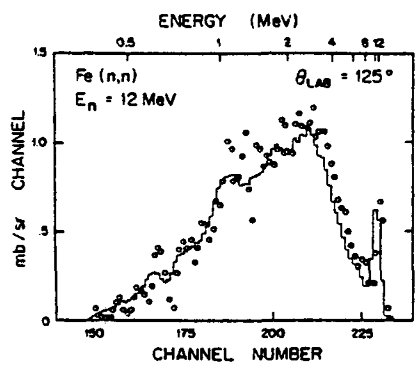

Fig. A6-3. Effect of EFFIGY correction on a typical angular distribution for ^{11}B.

7. Elastic Scattering of 8-, 10- and 12 MeV Neutrons from ^{54}Fe, ^{56}Fe, ^{63}Cu and ^{65}Cu

Angular distributions of elastically scattered neutrons have been obtained at 8.0, 10.0 and 12.0 MeV for greater than 98% pure isotopically enriched samples of ^{54}Fe, ^{56}Fe, ^{63}Cu and ^{65}Cu. Measurements were made in 5° steps from 30° to 155° to a statistical accuracy of about ±3% or better. The $^2H(d,n)^3He$ source reaction was employed, and the overall time resolution was about 3 ns. Data were also obtained at 14.0 MeV, but, because there were difficulties with the neutron monitor detector, the data may need to be remeasured.

The time resolution was not sufficient to separate the first inelastic groups from the elastic group at all angles. The spectra do permit determination of the inelastic cross sections when the elastic-to-inelastic ratio is less than 50:1 at the two lowest energies. This allows a determination of $\sigma(\theta)$ for Fe(n,n') and Cu(n,n') for angles between about 45° and 160° at 8 and 10 MeV. However, to extract the inelastic $\sigma(\theta)$, a gaussian peak fitting routine must be used. The accuracy of the data is deleteriously affected by the use of this procedure and by a tail of unknown origin which begins at the elastic peak and extends under all the inelastic peaks. The uncertainties that will be assigned to the inelastic data are in the range of 10%.

The elastic data were normalized to the yield obtained with a hydrogenous scatterer. This method, coupled to our knowledge of the detector relative efficiencies, i.e., calibrated to about ±3%, should give cross-section determination to a relative accuracy of about 5% and an absolute accuracy of under 8%.

A preliminary analysis of the data was shown at the International Nuclear Cross Section meeting at Knoxville. Fig. A7-1 illustrates the shape of the

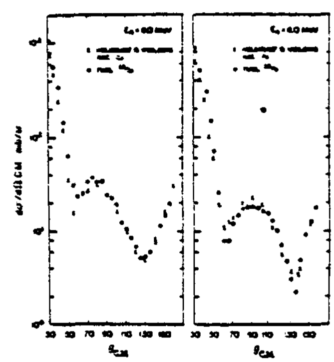

Fig. A7-1. Comparison of present results to previous work.

cross section and how the present data compare to the earlier data of Holmquist and Weilding.[1] Our data have been processed with the multiple scattering code EFFIGY

[1] B. Holmquist and T. Weilding, A. B. Atomenergi, Studsvik, Sweden, Report AE-303 (1967); BNL 400, TID-4500 (1970), EANDC(US)-138 "U".

This program also accounts for geometrical effects and the relative efficiency of the detector. Our corrected data are in good agreement with those of Holmquist and Weilding, except for the forward angles.

Optical model comparisons of the data for all four isotopes were initiated, using our preliminary cross-section values. The results for ^{63}Cu and ^{56}Fe are shown in Figs. A7-2 through A7-5. In Fig. A7-2 and A7-3 the data are compared to the predictions using the Wilmore and Hodgson[1] parameters, after adding the "standard" spin-orbit term of Ref. 2, $V_{so} = 6.2$ MeV, $r_{so} = 1.1$ fm, and $a_{so} = 0.75$ fm. The agreement is already quite good without varying any of the parameters. The neutron optical model set given by Bechetti and Greenlees describes the data poorly.

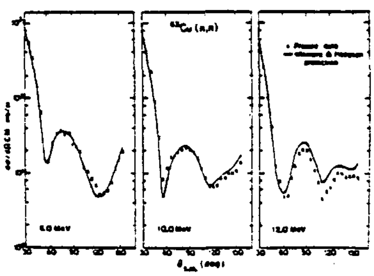

Fig. A7-2. Present results compared to optical model predictions based on Wilmore and Hodgson parameters.

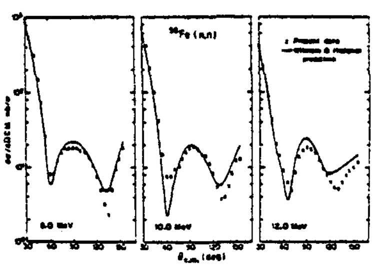

Fig. A7-3. Present results compared to optical model predictions based on Wilmore and Hodgson parameters.

A quick search on the real-well depth and the imaginary-well depth was made using the code GENOA of F. Perey. The search started with the Wilmore-Hodgson set. The results for two isotopes are shown in Figs. A7-4 and A7-5. The ^{63}Cu data are quite well described, but the ^{56}Fe calculations undershoot the data in the first minimum. Compound-nucleus contributions can fill in such minima, but we expect these effects to be small.

Before the data will be published we intend to do the following:

---

[1] D. Wilmore and P. E. Hodgson, Nucl. Phys. 55 (1964) 673

[2] F. D. Bechetti, Jr. and G. W. Greenlees, Polarization Phenomena in Nuclear Reactions, edited by H. H. Barschall and W. Haeberli, The University of Wisconsin Press, p. 682, Madison (1971).

(1) recheck each measurement, carefully evaluating the inelastic contribution to the elastic peak and extracting the best inelastic yield; (2) examine our procedure for assigning errors; (3) conduct compound nucleus calculations to estimate the size of this contribution; (4) carry out a careful systematic global optical model search of the data for these four isotopes.

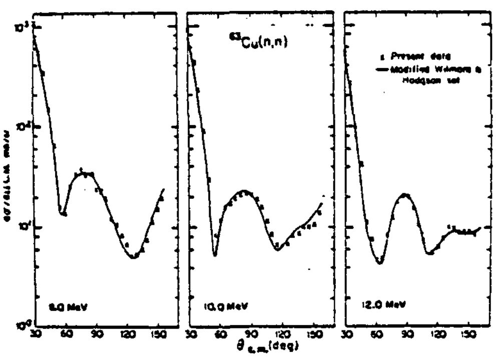

Fig. A7-4. Present results compared to optical model search on V_o and W_o.

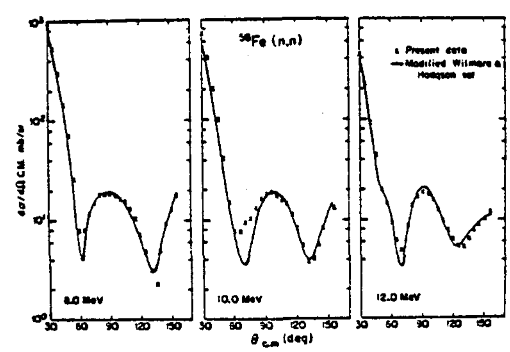

Fig. A7-5. Present results compared to optical model search on V_o and W_o.

A. FAST NEUTRON PHYSICS

1. The n-^{6}Li Interaction below 4 MeV (Y. -H. Chiu and F. W. K. Firk)

We have made refinements to the global analysis of the n-^{6}Li interaction below 4 MeV reported last year. Particular attention has been paid to multiple scattering correction to our polarization measurements. The optimum resonance parameters are given in a paper which has been submitted to Nuclear Physics.

2. Polarization Effects in n-^{209}Bi Scattering below 4 MeV (M. Ahmed and F. W. K. Firk)

We have completed measurements of the asymmetry of polarized neutrons elastically scattered from ^{209}Bi as a continuous function of energy between 2 and 4 MeV. The measured values have been corrected for multiple scattering and finite angular resolution effects in the angular range 3° to 15°. The results are being analyzed using the method of Hogan and Seyler which generalizes the original method of Schwinger. Our measurements of the differential cross section and polarization at wide angles are being used to narrow the range of optical model parameters which are required in the analysis. This part of the project is at an advanced stage.

3. Polarization Effects in n-^{24}Mg, -^{28}Si, and -^{32}S Scattering at Energies between 50 and 500 keV (J. Kruk and F. W. K. Firk)

Previous attempts to study Mott-Schwinger scattering have been carried out at energies above about 500 keV using heavy nuclei. Although the interpretation of the results is in principle straightforward, uncertainties in the purely nuclear part of the scattering amplitude tend to cloud the issue, and have prevented a precise determination of the amplitude associated with the polarizability of the neutron. We have therefore started a series of polarization measurements at lower energies using nuclei with a small number of well-known resonances in order to be able to calculate the nuclear scattering amplitudes exactly. We have already made calculations that show that such studies are feasible in these light nuclei, and have shown that the Mott-Schwinger scattering has a strong energy dependence that will provide information not available in studies in the MeV region.

UNIVERSITY OF WASHINGTON

A. ALPHA IN YIELDS (Patrick J. Grant, Gene L. Woodruff, & David L. Johnson)

A large ($\sim$1.5 m) graphite assembly has been constructed for the measurement of (α,n) yields from low z targets. The assembly contains an array of ten ^{3}He detectors perpendicular to and at varying angles with respect to an incoming accelerator beam tube. The target at the center of the assembly is surrounded by a spherical shell of either Be or Fe in order to flatten the detection efficiency at high energies.

A preliminary set of results for ^{18}O is shown in Fig. A1 together with those reported by Bair & Gomez del Campo[1] and West & Sherwood[2]. The assembly has not yet been calibrated and the results in Fig. 1 are normalized to the Bair volume at 7 MeV. The relative values appear to be in fairly good agreement.

---

[1] J.K. Bair and J. Gomez del Campo, Nuc. Sci. Eng. 21, 18 (1979).

[2] D. West and A.C. Sherwood, Proceedings of Intl. Conf. on Neutron Physics and Nuclear Data for Reactors and Other Applied Purposes, Harwell, U.K. (Sept. 1978).

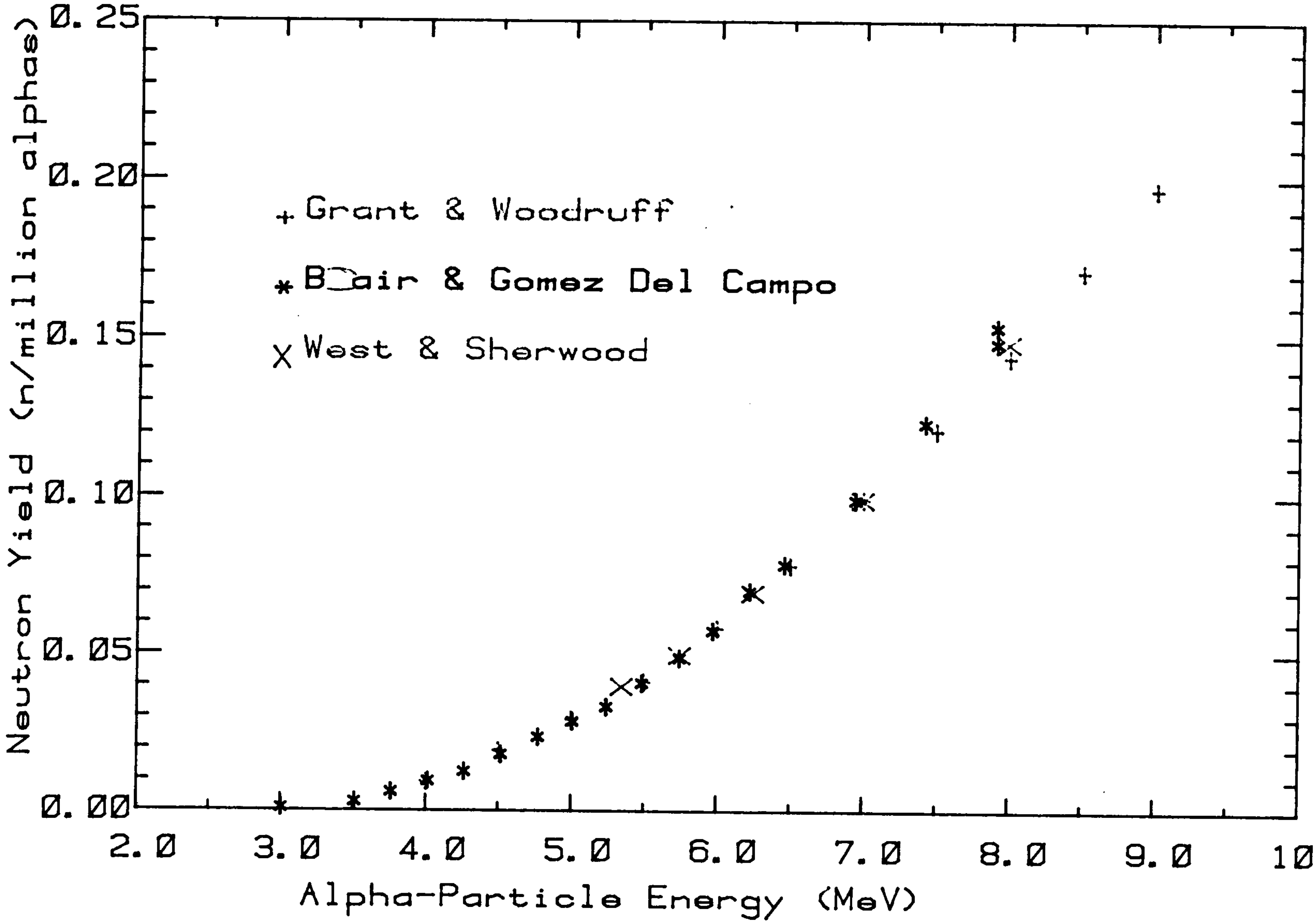

FIGURE A - 1 $^{18}O(\alpha, N)$ YIELDS VS ALPHA ENERGY

A. NEUTRON PHYSICS

1. Helium Generation Cross Sections for 14.8-MeV Neutrons
(D.W. Kneff, B.M. Oliver, M.M. Nakata and Harry Farrar IV)

The fast-neutron-induced helium generation cross sections of several pure elements and isotopes have been measured for the T(d,n) reaction. The present measurements were made by irradiating a capsule containing a large number of samples for 76.7 h, and subsequently analyzing, by high-sensitivity gas mass spectrometry, the total amount of helium generated in each sample.[1] A comprehensive set of foil activation and helium accumulation neutron dosimeters was included to characterize the neutron irradiation environment over the capsule volume. The helium generation measurements were then combined with the neutron fluence data to deduce the cross sections listed in Table 1. These cross sections are total integral helium generation cross sections for the incident neutron energy spectrum, including helium produced from all neutron induced reactions. The average energy of the neutrons incident upon the helium generation materials was calculated to be 14.8 ± 0.1 MeV. The spectrum full-width-at half-maximum was determined to be ∿0.6 MeV.

A detailed three-dimensional neutron fluence map was required for the capsule irradiation volume, because of the steep fluence gradients present. An average map was first constructed using the foil activation counting results. Detailed adjustments were then made to the map using the results from segmented helium accumulation neutron dosimetry rings. The absolute fluence uncertainty for the irradiation capsule volume is estimated to be ±7%. This includes an estimated ±5% relative uncertainty from the map itself, and ±2% and ±4% absolute uncertainties from the radiometric counting results and from the ^{93}Nb(n,2n) cross section (463 ± 19 mb), respectively.

Several materials other than those listed in Table 1 were also irradiated in this experiment, and will be analyzed shortly to determine their helium generation cross sections. These include C, V, Zr, Mo, and the separated isotopes of B, Fe, and Mo. A third T(d,n) experiment, now being prepared for irradiation at the Rotating Target Neutron Source-II (RTNS-II) facility at LLL, will expand this measurement set further to

---

[1] H. Farrar IV, W.N. McElroy, and E.P. Lippincott, Nucl. Tech., 25, 305 (1975).

include Be, O, F, Si, Mn, Co, Sn, W, Pb, and most of the separated isotopes of Ti, Cr, Sn, W, and Pb.

Table 1

Total Helium Generation Cross Sections for $\sim$14.8-MeV Neutrons

Material	Cross Section (mb)		
	Present Work	Previous Experiment[a]	Charged-Particle Measurements[b]
Al	145 ± 10	143 ± 7	121 ± 25
Ti	37 ± 3	38 ± 3	34 ± 7
Cr	34 ± 4	-	38 ± 6
Fe	48 ± 3	48 ± 3	43 ± 7
Ni	100 ± 7	98 ± 6	97 ± 16
^{58}Ni	116 ± 8	-	106 ± 17
^{60}Ni	79 ± 6	-	76 ± 12
^{61}Ni	53 ± 4	-	-
^{62}Ni	18 ± 6	-	-
^{64}Ni	61 ± 4	-	-
Cu	51 ± 3	51 ± 3	42 ± 7
^{63}Cu	67 ± 5	-	56 ± 10
^{65}Cu	17 ± 2	-	13 ± 3
Au	0.72 ± 0.09	24 ± 12[c]	-

[a]H. Farrar IV and D.W. Kneff, Trans. Am. Nucl. Soc., 28, 197 (1978)

[b]S.M. Grimes, R.C. Haight, K.R. Alvar, H.H. Barschall, and R.R. Borchers, Phys. Rev. C, 19, 2127 (1979), and R.C. Haight and S.M. Grimes, UCRL-80235, Lawrence Livermore Laboratory (1977).

[c]High value attributed to helium recoil into the thin gold foil from an adjacent foil.

LAWRENCE BERKELEY LABORATORY

A. ISOTOPES PROJECT

(E. Browne, J. M. Dairiki, R. Firestone, C.M. Lederer, and V.S. Shirley)

The Isotopes Project compiles and evaluates experimental nuclear structure data and develops compilation methodology. Since the completion of the 7th edition of the Table of Isotopes[1] in 1978, the Project has been operating as part of the closely-coordinated U.S. Nuclear Data Network (NDN), organized in 1976. Authorship of Nuclear Data Sheets for the mass regions A = 146-152 and A = 163-194 has been assigned to the Project as a principal responsibility, all mass chains to be updated on a four-year cycle.

The evaluation of nuclear structure data for all nuclei with mass number A = 163 has been completed and will soon be published in Nuclear Data Sheets. The evaluation of data for four more mass chains, A = 190-193, is well underway. In addition, mass chains A = 188, 189, 174, and 169 are scheduled for completion in early 1980.

In 1979, the Isotopes Project produced Nuclear Wallet Cards [2] for the NDN. This 84-page "shirt-pocket" booklet contains tables of nuclear properties, elemental properties and energy conversion factors. The data presented in the nuclear properties table are adopted values from the 7th edition of the Table of Isotopes[1]. Data for each isotope include spin and parity assignment, mass excess, half-life and/or natural abundance (level widths are given for particle-unstable nuclides), and decay mode(s). Included in the elemental properties table are atomic weight, density, melting point, boiling point, and principal oxidation states.

Primary distribution of the Wallet Cards locally and to the nuclear divisions of the APS and ACS (about 4500 copies) was supported by LBL; the National Nuclear Data Center (BNL) serves as the distribution center for additional copies.

A "Table of Nuclides" (an expanded version of the Nuclear Wallet Cards) is being prepared for G. Friedlander and E. Macias, for inclusion in the 2nd edition of the textbook Nuclear and Radiochemistry.

A Radioactivity Handbook for applied users is one of the planned publications of the U.S. Nuclear Data Network. On behalf of the NDN, the Isotopes Project will produce this Handbook with specifications agreeable to members of the international network of nuclear structure and decay data centers. The Handbook will be produced at four-year intervals beginning in 1982. It will contain recommended decay data, taken from the current version of the Evaluated Nuclear Structure Data File (ENSDF). Each mass chain will be referenced to the most recent evaluation in the Nuclear Data Sheets, as the source for further details and references to the original papers.

A description and sample format (Fig. 1) for the Radioactivity Handbook have been prepared by the Isotopes Project, guided by input from U.S. network members. This sample material, intended as a broad outline for the contents and format, has been distributed to all NDN members for comment. Comments from readers of this report would also be appreciated.

References

1 C.M. Lederer and V.S. Shirley, eds; E. Browne, J.M. Dairiki, and R.E. Doebler, principal authors; A.A. Shihab-Eldin, L.J. Jardine, J.K. Tuli, and A.B. Buyrn, authors; Table of Isotopes, Seventh Edition, John Wiley and Sons, Inc., New York (1978).

2. V. S. Shirley and C. M. Lederer, eds; E. Browne, J. M. Dairiki, R. E. Doebler, A.A. Shihab-Eldin, L. J. Jardine, J. K.Tuli, A. B. Buyrn, J. H. H. Chong, and D. P. Kreitz, Nuclear Wallet Cards, produced by the Isotopes Project on behalf of the U. S. Nuclear Data Network (1979).

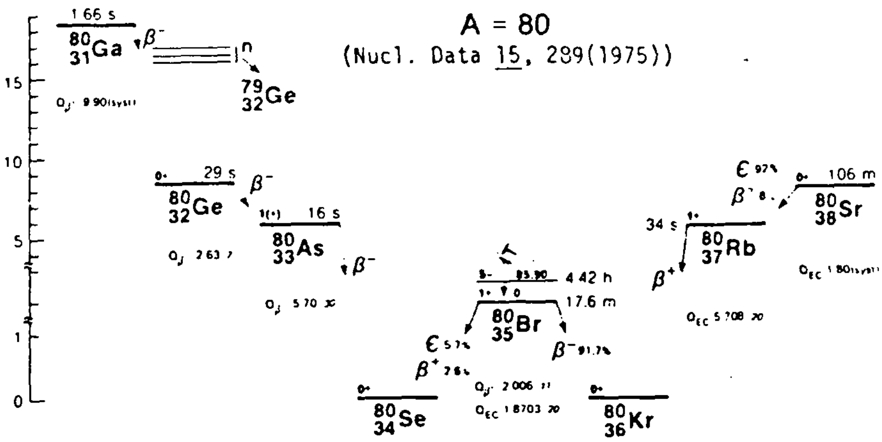

$^{80}_{31}$Ga

$t_{1/2}$: 1.66 *2* s
γ: β^-, β^-n
Δ: -59.53(syst)
Prod: fission

$^{80}_{32}$Ge

$t_{1/2}$: 29 s
γ: β^-
Δ: -69.43 *31*
Prod: fission

γ:

Energy (keV)	Intensity[a] (%)
110.4 *4*	6.0 *3*
265.6 *4*	25
782.3 *4*?	≈0.8
937.2 *4*	4.0 *4*
1014.0 *4*	2.5 *5*
1116.0 *4*	2.6 *4*
1256.1 *4*	3.1 *4*
1564.3 *4*	4.5 *4*

a) Quoted uncertainties refer to relative intensities; 40% additional uncertainty applicable to absolute intensities.

Average energies:
$\langle E_{\gamma+x} \rangle$: 280 *116*

(a)

$^{80}_{33}$As

$t_{1/2}$: 16 s
γ: β^-
Δ: -72.06 *30*
Prod: ^{80}Se(n,p), fission

β^-:

Energy (keV)	Intensity (%)
1970 *300*	0.1
2090 *300*	0.2
2680 *300*	1.0
2860 *300*	0.2
2930 *300*	0.3
3180 *300*	1.2
3390 *300*	7.1
3740 *300*	1.3
3830 *300*	4.2
4220 *300*	0.5
4250 *300*	0.9
5030 *300*	27
5700 *300*	56

γ:

Energy (keV)	Intensity[a] (%)
321.2 *5*?	5.5 *1*[b]
666.2 *2*	42
782.4 *5*	0.80 *17*
908.7 *5*?	0.71 *13*[b]
811.3 *5*	0.46 *17*
861.6 *4*	0.76 *8*
1064.7 *5*	0.13 *4*
1207.2 *2*	4.7 *4*
1294.1 *4*	1.0 *1*
1415.9 *5*	0.08 *4*
1422.7 *5*?	0.04 *4*[b]
1448.8 *5*	1.0 *1*
1633.3 *5*?	1.2 *2*[b]
1645.4 *2*	8.0 *4*
1847.8 *5*	0.9 *2*
1960.1 *5*	0.38 *8*
1968.8 *5*?	0.13 *8*[b]
2156.9 *5*	0.08 *4*
2357.8 *5*	0.9 *2*
2461.3 *5*?	0.2 *1*[b]
2514.0 *5*	0.17 *8*
2598.1 *5*?	0.13 *8*[b]
2774.2 *10*	0.3 *1*
2836.2 *10*	0.25 *8*
2940.3 *10*	0.08 *4*
3024 *2*	0.08 *4*
3060.8 *20*	0.04 *4*

$^{80}_{33}$As (Continued)

a) Quoted uncertainties refer to relative intensities.
b) If isotopic assignment is correct; γ ray could alternatively be assigned to ^{82}As.

Average energies:
$\langle E_{\gamma+x} \rangle$: 643
$\langle E_{e^-} \rangle$: 2308

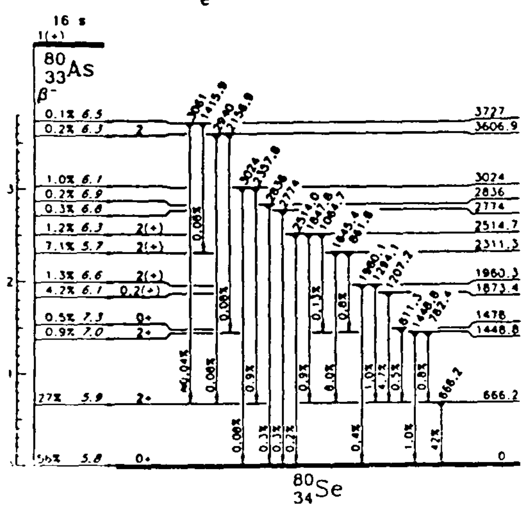

$^{80}_{34}$Se

%: 49.8
Δ: -77.7613 *35*
σ: 0.61 *6* b (to ^{81}Se)
0.07 *2* b (to ^{81m}Se)

Fig. 1 a,b,c. Sample layout for mass chain A = 80, illustrating the proposed format for the Radioactivity Handbook. The Handbook will be ordered by mass number (A) and subordered by atomic number (Z). Each mass chain will consist of a mass-chain decay scheme, tabulated data (with uncertainties) for each isotope, and a decay scheme for each parent isotope.

$^{80}_{35}$Br

$t_{1/2}$: 17.6 m
Decay: β^- 91.7%, ε 5.7 3%, β^+ 2.6 2%
Δ: -75.8910 36
Prod: ^{79}Br(n,γ), daughter ^{80m}Br, ^{79}Br(d,p)

β^-:

Energy (keV)	Intensity (%)
686 11	0.19 2
750 11	0.31 3
1390 11	6.2 6
2006 11	84.9 7

β^+:

Energy (keV)	Intensity (%)
848.3 20	2.6 2

γ:

Energy (keV)	Intensity[a] (%)	Decay mode
616.2 5	6.7	β^-
639.4 2	0.24 2	β^-
666.2 2	1.1 2	$\varepsilon+\beta^+$
677.0 10?	0.008 2	
687.4 10?	0.012 3	
703.8 2	0.19 3	β^-
782.4 5?	≤0.013	$\varepsilon+\beta^+$
811.3 5	0.033 7	$\varepsilon+\beta^+$
1256.1 4	0.067 7	β^-
1338.5 8	0.020 7	β^-
1448.8 5?	≤0.016	$\varepsilon+\beta^+$

a) Quoted uncertainties refer to relative intensities; 9% additional uncertainty applicable to absolute intensities.

Other radiations:

Radiation	Energy (keV)	Intensity (%)
Se Auger-L	1.32	7.0 7
Se Auger-K	9.67	2.2 2
Se LX	1.38	~0.1
Se K_{α_2}X	11.18140 2	0.9 1
Se K_{α_1}X	11.22240 2	1.8 3
Se K_βX	12.5	0.4 1
$\gamma^\pm$		5.2 4

Average energies:
$\langle E_{\gamma+x}\rangle$: 80 25
$\langle E_{e^-}\rangle$: 718 7
$\langle E_{e^+}\rangle$: 368 28

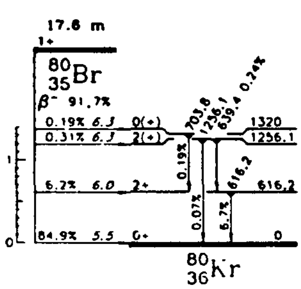

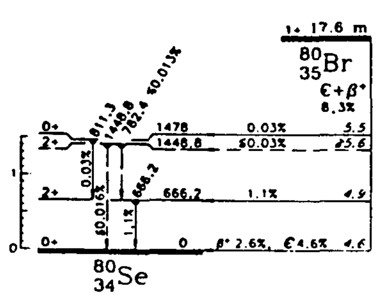

(b)

$^{80m}_{35}$Br

$t_{1/2}$: 4.42 1 h
Decay: IT
Δ: -75.8051 36
Prod: ^{79}Br(n,γ)

γ:

Energy (keV)	Intensity (%)
37.052 2	39.1 8
48.85 3	0.324 6

Other radiations:

Radiation	Energy (keV)	Intensity (%)
Br Auger-L	1.4	176 35
Br Auger-K	10.2	48 5
K-37	23.578	54.0 15
L-37	35.270	6.1 2
K-49	35.38	72.6 26
M-37	36.795	0.95 3
L-49	47.07	22.4 8
M-49	48.59	3.8 2
Br LX	1.48	1.6 4
Br K_{α_2}X	11.87760 2	23.0 20
Br K_{α_1}X	11.92420 2	45 4
Br K_βX	13.3	11.0 14

Average energies:
$\langle E_{\gamma+x}\rangle$: 24 1
$\langle E_{e^-}\rangle$: 62 1

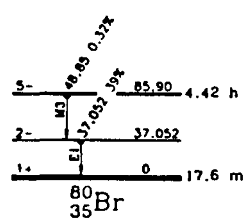

$^{80}_{36}$Kr

%: 2.27 (atmospheric sources; variations reported for meteoritic sources.)
Δ: -77.897 11
σ: 11.5 6 b (to ^{81}Kr)
4.6 7 b (to ^{81m}Kr)

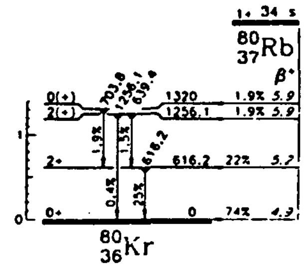

$^{80}_{37}$Rb

$t_{1/2}$: 34 4 s
Decay: β^+
Δ: -72.190 23
Prod: daughter ^{80}Sr, ^{71}Ga(^{12}C,3n)

β^+:

Energy (keV)	Intensity (%)
3366 20	1.9 3
3430 20	1.9 3
4070 20	22 3
4686 20	74 3

γ:

Energy (keV)	Intensity[a] (%)
616.2 5	25
639.4 2	1.5 2
703.8 2	1.9 2
1256.1 4	0.42 6

a) Quoted uncertainties refer to relative intensities; 12% additional uncertainty applicable to absolute intensities.

Other radiations:

Radiation	Energy (keV)	Intensity (%)
$\gamma^\pm$		200

Average energies:
$\langle E_{\gamma+x}\rangle$: 1204 188
$\langle E_{e^+}\rangle$: 2072 14

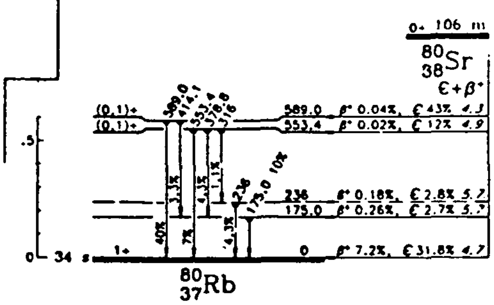

$^{80}_{38}$Sr

$t_{1/2}$: 106.3 15 m
Decay: ε 92%, β^+ 8%
Δ: -70.39(syst)
Prod: ^{14}N on Ga, ^{65}Cu(^{20}Ne,5n)^{80}Y(ε+β^+)

(Continued)

$^{80}_{38}Sr$ (Continued)

β^+:

Energy[a] (keV)	Intensity (%)
189	0.04
225	0.02
542	0.18
603	0.26
778	7.2

a) Based on systematic decay energy.

γ:

Energy (keV)	Intensity[a] (%)
175.0 *5*	10.4 *10*
235.9 *8*	4.3 *4*
316.0 *15*	1.1 *1*
378.8 *5*	4.3 *4*
414.1 *5*	3.3 *3*
553.4 *5*	7.0 *7*
589.0 *5*	40

a) Quoted uncertainties refer to relative intensities; 20% additional uncertainty applicable to absolute intensities.

Other radiations:

Radiation	Energy (keV)	Intensity (%)
Rb Auger-L	1.68	100 *3*
Rb Auger-K	11.4	27 *1*
Rb LX	1.69	1.0 *3*
Rb $K_{\alpha_2}X$	13.33580 *2*	15.7 *6*
Rb $K_{\alpha_1}X$	13.39530 *2*	30.4 *10*
Rb $K_\beta X$	15	7.9 *5*
$\gamma^\pm$		16

Average energies:

$\langle E_{\gamma+x}\rangle$: 425 *94*

(c) $\langle E_{e^+}\rangle$: 198

B. RANGE AND STOPPING POWER TABLES FOR 0.2 to 12.5 MeV/NUCLEON HEAVY IONS

G.U. Rattazzi, R. P. Schmitt, G.J. Wozniak, and L.G. Moretto)

With the advent of accelerators capable of producing beams of particles from throughout the periodic table, there is a growing need for accurate range-energy data. In addition, there is also a strong need for empirical or semi-empirical formulae which reproduce the experimental data over broad ranges of energy and of atomic numbers of both the incident heavy ion and stopping medium. Such relationships would be very useful for correcting the energies of heavy fragments producedin deep-inelastic collisions for energy losses in the target and in the entrance windows of heavy-ion gas telescopes. Furthermore, such a formula would be useful in identifying the atomic numbers of the heavy fragments from their energy loss in ΔE counters. We have attempted to construct such a formula using recent experimental data.[1,2]

Recent stopping power measurements for 0.2-3.5 MeV/nucleon ^{19}F, ^{24}Mg ^{27}Al, ^{32}S and ^{35}Cl in Ti, Fe, Ni, Cu, Ag and Au; and ^{40}Ar, ^{84}Kr, ^{136}Xe, and ^{238}U impinging on C, Al, Ag, Au and Bi have shown significant discrepancies when compared with the calculated values of Northcliffe and Schilling,[3] particularly for light stopping media, heavy projectiles, and low energies. The discrepancy reaches 30 percent for Kr ions degraded by Al and C, the calculated stopping power being too low. Hubert et al.[4] were able to reproduce the experimental data in the energy range 2.5-12 MeV/nucleon for projectiles up to ^{103}Rh. However, their empirical formula gives a discrepancy of up to 100 percent for U impinging on ^{12}C at energies of the order of 1 MeV/A. Since the energy corrections are most important for heavy projectiles impinging on very light materials (polypropylene), we decided to search for a more general formula. Different semi-empirical expressions have been proposed [3,5,6] for the dependence of the effective charge on velocity. Most of them are of the following type:

$$\gamma_1 Z_1 = Z_1 [1 - D \exp (-V/V_0 Z_1{}^{B})] \qquad (1)$$

with $V_0 = e^2/\hbar = 2.188 \times 10^8$ cm/s, where D and B are adjustable parameters. By fitting the experimental data, we obtained the following parameters.

$$\gamma_1 = 1.0 - A(Z_1) \exp (-0.857 V_r) \qquad (2)$$

with

$$A (Z_1) = 1.124 - 0.237 \exp (-0.024 Z_1) \qquad (3)$$

and

$$V_r = V/ (V_0 Z_1{}^{0.645}) \qquad (4)$$

As a starting point we determined a set of effective charge parameters for protons, alphas and heavy ions at the same velocities. We also assumed that: (a) the variation of γ_1 with respect to stopping medium and velocity are independent; (b) the variation of γ_1 vs the velocity is well reproduced by Eq. (2); (c) the effective charge for α's with an energy >3 MeV and protons with energy >200 keV lays between 0.99 and 1.00; and (d) as shown by Ward et al. that[7]

$$(d/E/dx)_\alpha = 4\gamma_a{}^2/\gamma_p{}^2 \; (dE/dx) \; p.$$

Assumption (a) enables us to write the effective charge parameterization as the product of two factors:

$$\gamma_{1,2} = F(Z_1, Z_2) \times \gamma_1$$

By using the assumptions given by Hubert et al., we obtained a fit to the experimental F values with the function:

$$F(Z_1, Z_2) = A_1 + A_2 Z_1 Z_2 + A_3 Z_1/Z_2 + A_4 Z_1^2 Z_2$$

$$= A_5 Z_1^2/Z_2$$

where

$$\begin{aligned} A_1 &= 0.981 \\ A_2 &= -0.239 \times 10^{-4} \\ A_3 &= 0.795 \times 10^{-2} \\ A_4 &= 0.788 \times 10^{-7} \\ A_5 &= 0.103 \times 10^{-3}. \end{aligned}$$

The stopping power $S_{1,2}$ of a given medium 2 and for a given ion 1 was calculated from that of medium 2 for α particles (same E/A value) denoted by $S_{\alpha,2}$ using the following equation:

$$S_{1,2} = S_{\alpha,2} (\gamma_{1,2} A_1)^2 / (\gamma_\alpha Z_\alpha)^2$$

where γ_α was calculated by using assumption (d). The terms $S_{\alpha,2}$ and $S_{p,2}$ were derived from a recent literature search for all available experimental values of stopping powers of ^{4}He and ^{1}H ions in materials. By comparing our tables with the experimental data available we were able to reproduce the experimental data within the experimental errors for heavy ions like Xe and U on light targets like C and Al. In almost all cases the calculated values agree with the experimental data within 10 percent.

References

1. J. S. Forster et al., Nucl. Instrum. Meth. 349, 136 (1976).
2. F. Z. Nickel, Physik 125, 288 (1978).
3. L. C. Northcliffe and R. F. Schilling, Nucl. Data Tables A7, 233 (1970).
4. F. Hubert et al. CEIPN Report no. IN 2P3 (1978).
5. M. Brown and C. D. Moak, Phys. Rev. B6 , 90 (1972).
6. H. D. Betz, Rev. Mod. Phys. 44, 465 (1972).
7. D. Ward et al. AECL Report no. 4914 (1975).
8. J. F. Ziegler, the Stopping and Ranges of Ions in Matter, Vol. 4, (Pergamon Press, 1977).

U.S. GOVERNMENT PRINTING OFFICE: 614-090-#5